VOLUME 101 | SUPPLEMENT 1 | MARCH 2021

LI

LABORATORY INVESTIGATION

THE BASIC AND TRANSLATIONAL PATHOLOGY RESEARCH JOURNAL

ABSTRACTS

GYNECOLOGIC AND OBSTETRIC PATHOLOGY (532-634)

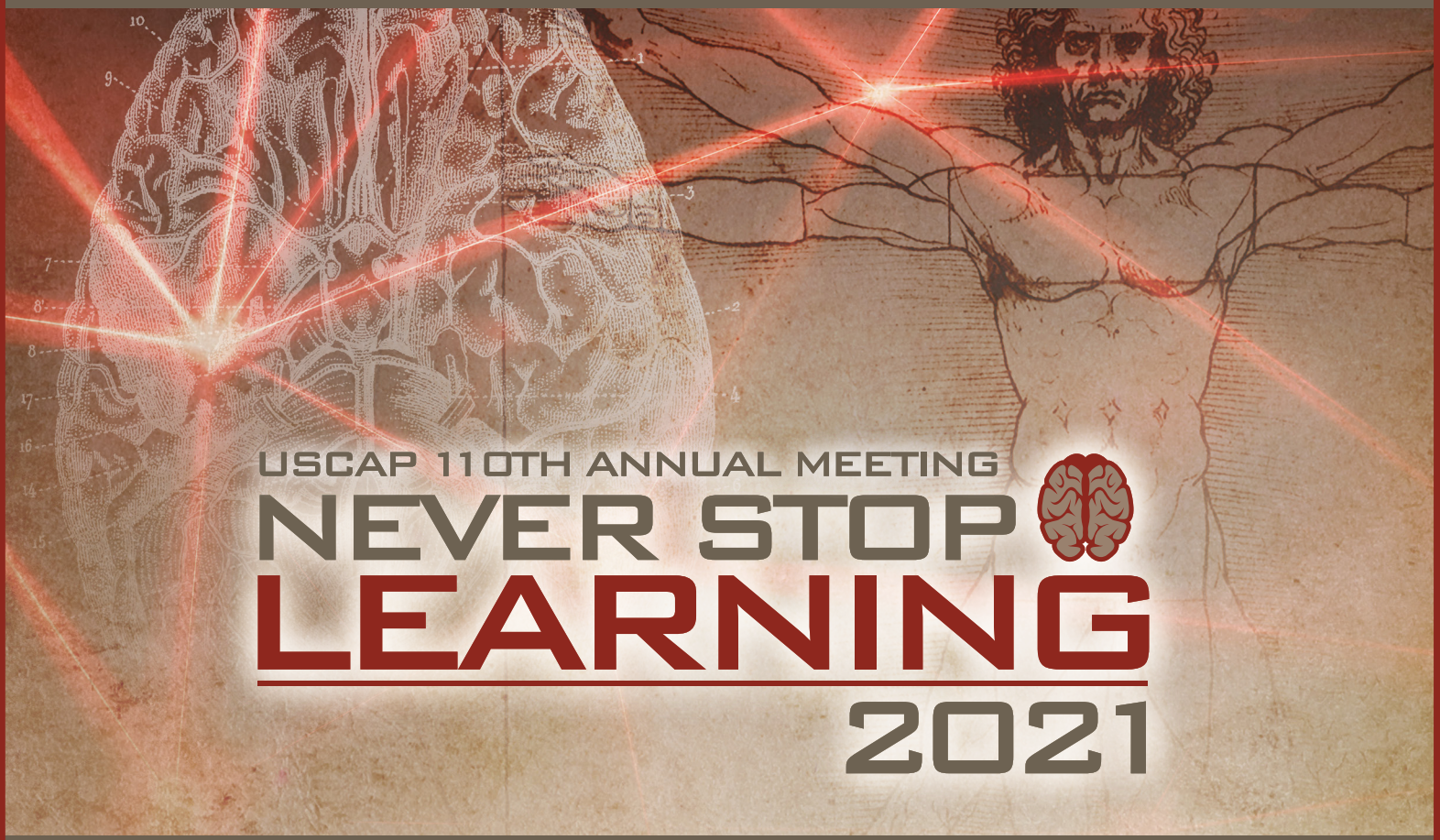

MARCH 13-18, 2021 | VIRTUAL AND INTERACTIVE

Published by
SPRINGER NATURE
www.ModernPathology.org

USCAP
Creating a Better Pathologist
AN OFFICIAL JOURNAL OF THE UNITED STATES AND CANADIAN ACADEMY OF PATHOLOGY

EDUCATION COMMITTEE

Jason L. Hornick
Chair

Rhonda K. Yantiss, Chair
Abstract Review Board and Assignment Committee

Kristin C. Jensen
Chair, CME Subcommittee

Laura C. Collins
Interactive Microscopy Subcommittee

Raja R. Seethala
Short Course Coordinator

Ilan Weinreb
Subcommittee for Unique Live Course Offerings

David B. Kaminsky
(Ex-Officio)
Zubair W. Baloch
Daniel J. Brat
Sarah M. Dry
William C. Faquin
Yuri Fedoriw
Karen Fritchie
Jennifer B. Gordetsky
Melinda Lerwill
Anna Marie Mulligan
Liron Pantanowitz
David Papke,
Pathologist-in-Training
Carlos Parra-Herran
Rajiv M. Patel
Deepa T. Patil
Charles Matthew Quick
Lynette M. Sholl
Olga K. Weinberg
Maria Westerhoff
Nicholas A. Zoumberos,
Pathologist-in-Training

ABSTRACT REVIEW BOARD

Benjamin Adam
Rouba Ali-Fehmi
Daniela Allende
Ghassan Allo
Isabel Alvarado-Cabrero
Catalina Amador
Tatjana Antic
Roberto Barrios
Rohit Bhargava
Luiz Blanco
Jennifer Boland
Alain Borczuk
Elena Brachtel
Marilyn Bui
Eric Burks
Shelley Caltharp
Wenqing (Wendy) Cao
Barbara Centeno
Joanna Chan
Jennifer Chapman
Yunn-Yi Chen
Hui Chen
Wei Chen
Sarah Chiang
Nicole Cipriani
Beth Clark
Alejandro Contreras
Claudiu Cotta
Jennifer Cotter
Sonika Dahiya
Farbod Darvishian
Jessica Davis
Heather Dawson
Elizabeth Demicco
Katie Dennis
Anand Dighe
Suzanne Dintzis
Michelle Downes
Charles Eberhart
Andrew Evans
Julie Fanburg-Smith
Michael Feely
Dennis Firchau
Gregory Fishbein
Andrew Folpe
Larissa Furtado
Billie Fyfe-Kirschner
Giovanna Giannico
Christopher Giffith
Anthony Gill
Paula Ginter
Tamar Giorgadze
Purva Gopal
Abha Goyal
Rondell Graham
Alejandro Gru
Nilesh Gupta
Mamta Gupta
Gillian Hale
Suntrea Hammer
Malini Harigopal
Douglas Hartman
Kammi Henriksen
John Higgins
Mai Hoang
Aaron Huber
Doina Ivan
Wei Jiang
Vickie Jo
Dan Jones
Kirk Jones
Neerja Kambham
Dipti Karamchandani
Nora Katabi
Darcy Kerr
Francesca Khani
Joseph Khoury
Rebecca King
Veronica Klepeis
Christian Kunder
Steven Lagana
Keith Lai
Michael Lee
Cheng-Han Lee
Madelyn Lew
Faqian Li
Ying Li
Haiyan Liu
Xiuli Liu
Lesley Lomo
Tamara Lotan
Sebastian Lucas
Anthony Magliocco
Kruti Maniar
Brock Martin
Emily Mason
David McClintock
Anne Mills
Richard Mitchell
Neda Moatamed
Sara Monaco
Atis Muehlenbachs
Bita Naini
Dianna Ng
Tony Ng
Michiya Nishino
Scott Owens
Jacqueline Parai
Avani Pendse
Peter Pytel
Stephen Raab
Stanley Radio
Emad Rakha
Robyn Reed
Michelle Reid
Natasha Rekhtman
Jordan Reynolds
Andres Roma
Lisa Rooper
Avi Rosenberg
Esther (Diana) Rossi
Souzan Sanati
Gabriel Sica
Alexa Siddon
Deepika Sirohi
Kalliopi Siziopikou
Maxwell Smith
Adrian Suarez
Sara Szabo
Julie Teruya-Feldstein
Khin Thway
Rashmi Tondon
Jose Torrealba
Gary Tozbikian
Andrew Turk
Evi Vakiani
Christopher VandenBussche
Paul VanderLaan
Hannah Wen
Sara Wobker
Kristy Wolniak
Shaofeng Yan
Huihui Ye
Yunshin Yeh
Anjana Yeldandi
Gloria Young
Lei Zhao
Minghao Zhong
Yaolin Zhou
Hongfa Zhu

To cite abstracts in this publication, please use the following format: **Author A, Author B, Author C, et al. Abstract title (abs#). In "File Title."** ***Laboratory Investigation*** **2021; 101 (suppl 1): page#**

532 Correlation of p53 Immunohistochemical Expression with TP53 Mutation in Extrauterine High-Grade Serous Carcinoma

Lina Abdul Karim[1], Richard Yang[1], Preetha Ramalingam[1], Barrett Lawson[1], Anais Malpica[1]
[1]*The University of Texas MD Anderson Cancer Center, Houston, TX*

Disclosures: Lina Abdul Karim: None; Richard Yang: None; Preetha Ramalingam: None; Barrett Lawson: None; Anais Malpica: None

Background: Extrauterine High-Grade Serous Carcinoma (EU-HGSC) is reportedly associated with *TP53* mutation in 96% of cases. The reported sensitivity of p53 immunohistochemical stain (IHC) in detecting *TP53* mutation ranges from 88-96% and its specificity from 38-100%. Factors including lack of uniformity in p53 scoring and reporting, lack of consistency in antibodies used and differences in sequenced exons of *TP53* gene may contribute to variable sensitivity and specificity. In this study we present the correlation of *TP53* mutation type with p53 immunohistochemical staining pattern, BRCA status and survival data.

Design: 101 EU-HGSC cases with *TP53* mutation by next generation sequencing (NGS), targeting the entire coding region of the *TP53* gene (exons 2-11), were retrieved from our files. Clinical information was recorded. The p53 IHC stains were scored as diffuse (75-100% nuclear staining), null-phenotype (no nuclear or cytoplasmic staining) wild-type (weak, variable nuclear staining), and cytoplasmic. Contingency (Fisher's exact test) and survival (log-rank) analysis was performed using GraphPad Prism v8.4.3.

Results: Table 1 summarizes the results of this study. The overall sensitivity of p53 IHC in detecting *TP53* mutations was 98%. The null phenotype was correlated with deleterious *TP53* mutations (frame-shift, nonsense and splice-site) using Fisher Exact test with a p-value <0.0001 (Fig. 1). Only one case with cytoplasmic p53 expression was identified and it was associated with the (c.750del p.I251fs) *TP53* frame-shift mutation and germline *BRCA2* mutation. Of note, we encountered a recent case of EU-HGSC with cytoplasmic p53 staining in a patient with germline *BRCA2* mutation, however, molecular analysis for that case is still pending. Two cases showed wild-type staining, both had nonsense *TP53* mutation and were associated with *BRCA1* mutation. Overall survival analysis did not show significant difference between deleterious versus non-deleterious TP53 mutation types (p-value = 0.6561) or p53 null versus diffuse staining phenotypes (p-value = 0.6450).

Table 1. Correlation of *TP53* Mutation with p53 Immunohistochemistry, and Clinical Features

		Overall	Diffuse	Null	Cytoplasmic	WT
	Number	101	82	16	1	2
Survival	**Alive w/o disease (follow up months)**	3 (72-134)	3 (72-134)	0	0	0
	Alive w/ Disease (follow up months)	48 (13-188)	43 (17-188)	5 (13-165)	0	0
	Dead of disease (follow up months)	48 (20-160)	34 (14-141)	11 (28-160)	1 (72)	2 (38-93)
	Unknown	2	2	0	0	0
BRCA	**BRCA1**	10	7	1	0	2
	BRCA2	7	3	3	1	0
	Metastasis	73	60	11	1	1
	Recurrence	84	67	14	1	2
***TP53* mutation**	**Missense**	69	69	0	0	0
	Frame-shift	7	1	5	1	0
	Nonsense	11	3	6	0	2
	Splice-site	9	4	5	0	0
	Inframe deletion	5	5	0	0	0
STAGE	**I**	2	1	1	0	0
	II	3	2	1	0	0
	III	60	48	9	1	2
	IV	32	28	4	0	0
	N/A	4	3	1	0	0
	Chemo*	73	60	10	1	2
	Age range	32-81	32-81	50-74	59	40-65

*This subset of cases had chemotherapy prior to IHC testing and mutation analysis

Figure 1 - 532

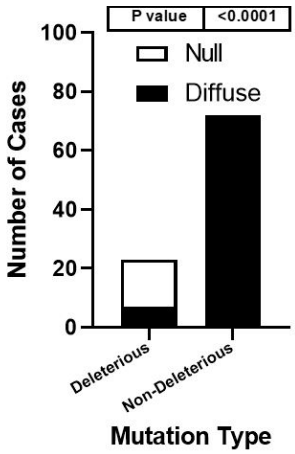

Figure 1. p53 IHC staining pattern and type of *TP53* mutation

Conclusions: In this study the null p53 phenotype cases only had deleterious type (frame-shift, nonsense and splice-site) *TP53* mutations, unlike the cases of diffuse nuclear staining that showed both deleterious and non-deleterious mutations; and this was statistically significantly. An association between cytoplasmic p53 staining and *BRCA2* mutation was observed in two cases and needs to be further investigated. The overall survival was not affected by the type of *TP53* mutation or p53 staining pattern.

533 The Significance of Uterine Cornu Involvement in Endometrial Cancer. A Retrospective Analysis of 523 Endometrioid Carcinomas

Hussain Abubakr[1], Vinita Parkash[2], Lina Irshaid[3], Oluwole Fadare[4]
[1]King Abdulaziz University, Jeddah, Saudi Arabia, [2]Yale School of Medicine, Yale School of Public Health, New Haven, CT, [3]Yale New Haven Hospital, Yale School of Medicine, New Haven, CT, [4]UC San Diego School of Medicine, La Jolla, CA

Disclosures: Hussain Abubakr: None; Vinita Parkash: None; Lina Irshaid: None; Oluwole Fadare: None

Background: The myometrial wall is significantly thinner in the region of the uterine cornu, wherein the uterus transitions to the fallopian tube. However, whether the thinness of the uterine wall at the cornu has any true biologic implications is unclear. This study evaluates whether there is any significance to 1) a tumor that is grossly centered in the region of the uterine cornu, and 2) the maximal depth of myometrial invasion being centered in the region of the uterine cornu.

Design: The initial dataset was comprised of 523 consecutive endometrioid carcinomas that were diagnosed in a hysterectomy specimen, including 264, 162, 44, 52, and 1 pT1a, pT1b, pT2, pT3 and pT4 cases respectively. Predominant tumoral locations within the uterine cavity were obtained from reported gross descriptions (157 fundus; 74 cornu; 105 diffuse; 23 LUS; 164 without a mass or site unclear). All available slides were reviewed for the 324 cases reported to have myometrial invasion, 306 of which were confirmed after review. Cases whose foci of maximal myometrial invasion was located in the region of the cornu (n=21; study group), were compared with a control group (n=63) regarding a variety of clinicopathologic parameters. For each case, the absolute depth of myometrial invasion (DOMI) was measured from the endomyometrial junction to the deepest myoinvasive focus. An age-matched control group was selected from a dataset of consecutive, myoinvasive, fundus-based and diffuse cancers using a 1:3 process, with each study group patient age matched with three control group patients that were within 5 years of age.

Results: In only 6.9% (21/306) of myoinvasive endometrioid carcinomas was the focus of maximal DOMI located in the cornual region, and in only 6 (29%) of those 21 cases was the mass described as being cornu-centered grossly. The 21 study group cases were significantly different than the 63 control group cases with a higher mean DOMI (p=0.03) and expectedly, lower mean myometrial thickness at point of maximal invasion (p=0.021). The two groups were otherwise similar regarding other clinicopathologic parameters, including frequency of adnexal involvement and recurrence rate (see table 1). Tumors that were grossly centered in the cornu region (n=74) were separately compared to their counterparts that were diffuse (n=105), fundus-centered (n=157), and in the rest of the combined dataset (n=449). For each comparison, there were no statistically significant differences between the cornu-centered tumors and the other groups regarding patient age, tumor grade, or frequency of adnexal involvement, lymph node involvement, serosal extension, lymphovascular invasion, and extrauterine extension.

Table I: A comparison between endometrial endometrioid carcinomas in which the maximal absolute depth of myometrial invasion is the region of the uterine cornu, and a control group

	Study group (maximal DOMI in cornual region)	Control group	P value
Number of cases	21	63	N/A
Mean DOMI in mm (range)	6.4 (3-23)	14 (6-43)	0.03
Mean myometrial thickness at site of maximal DOMI (mm)	9.8 (6-23)	24 (10-44)	0.021
Uterine serosal involvement	1/21 (4.8%)	0/63 (0%)	0.25
Mean tumor free distance to serosa in mm (range)	3.1 (0-23)	6 (1-21)	0.33
MI <50%	11/21 (52%)	37/63 (59%)	0.799
Adnexal involvement	0/21 (0%)	0/63 (0%)	1
Lymph node involvement	0/11 (0%)	0/41 (0%)	1
Lymphovascular invasion present	2/21 (9.5%)	9/63 (14.2%)	0.72
FIGO Grade I or II	18/21 (86%)	60/63 (95%)	0.33
Extrauterine extension present	1/21 (5%)	6/63 (9.5%)	0.67
Recurrences	0/21 (0%)	0/63 (0%)	1

Conclusions: Regarding patient outcomes, we could identify no significance to a tumor being grossly centered in the cornu or showing maximal myometrial invasion at that site. Notably, these tumors do not show a higher rate of adnexal or lymph node involvement.

534 HER2/neu Amplification in Endometrial Grade 3 Endometrioid Carcinoma and Correlation with p53 Status and Mismatch Repair Protein Expression/Microsatellite Instability

Adesola Akinyemi[1], Megan Sullivan[2], William Watkin[3], Ajit Paintal[4]
[1]University of Chicago Medical Center/NorthShore University HealthSystem, Evanston, IL, [2]North Shore University, Evanston Hospital, Evanston, IL, [3]NorthShore University HealthSystem, Evanston, IL, [4]NorthShore University HealthSystem, Glenview, IL

Disclosures: Adesola Akinyemi: None; Megan Sullivan: None; William Watkin: None; Ajit Paintal: None

Background: HER2/neu (HER2) is overexpressed in about 30% of endometrial serous carcinomas (SC) and patients with these tumors may benefit from trastuzumab. SC are also associated with p53 mutations. Recent studies show that a subset of endometrial endometrioid carcinomas (EC), particularly p53 mutant grade 3 EC, are similar to SC genetically and in prognosis. Prior literature, mostly utilizing older histotyping techniques and non-standard scoring systems have reported HER2 amplification in 0-60% of cases of EC.

This study examines the expression of HER2 in grade 3 EC and correlates these findings with the status of p53 expression by IHC, as well as mismatch repair protein (MMR) expression and microsatellite instability (MSI) in these tumors.

Design: Our electronic pathology records were reviewed for cases of endometrial carcinoma between 2014 and 2020. Slides from resected SC and grade 3 EC were reviewed by an expert gynecological pathologist to confirm the histologic diagnoses. IHC for p53 and MMR/MSI testing results were reviewed for all cases. IHC for HER2 was performed on whole sections from all EC cases and scored using the modified 2007 CAP/ASCO recommendations for the scoring of HER2, used in SC. HER2 ISH was performed in equivocal cases.

Results: 31 cases of grade 3 EC and 38 cases of SC were identified. 21/31 (68%), 5/31 (16%) and 5/31 (16%) EC cases had HER2 (IHC) scores of 0, 1+, and 2+, respectively. No case was scored 3+ (table). HER2 ISH results were available on 4 of 5 equivocal cases and all were negative.

3 of 19 (16%) cases of EC with p53 IHC available for review were p53 mutant, while MMR/ MSI testing was performed on 29 EC cases and 18/29 (62%) showed either MSI or MMR loss by IHC. None of our cases demonstrated MMR loss or MSI, together with a mutant pattern of p53 expression. Of the p53 mutant EC, 1/3 (33%) had a HER2 score of 2+, 4 (22%) of the 18 tumors with MMR loss or MSI had a HER2 score of 2+, while no tumor with wild-type patterns of MMR/MSI and p53 had a HER2 score of 2+.

HER2 testing was performed on 20 of our 38 cases of SC and 5 of 20 (25%) showed amplification. None of the 36 SC cases tested for MMR loss or MSI showed MMR loss or MSI.

HER2/neu in Endometrial Grade 3 Endometrioid Carcinoma (EC) and Endometrial Serous Carcinoma (SC)

	EC, p53 mutant	EC, MMR loss/MSI	EC, wild type p53 and intact MMR/MSS	EC, all	SC
HER2 positive	0/3 (0%)	0/18 (0%)	0/9 (0%)	0/31 (0%)	5/20 (25 %)
HER2 negative	3/3 (100%)	18/18 (100%)	9/9 (100%)	31/31 (100%)	15/20 (75%)
HER2 positive: 3+ score by IHC and/or positive by ISH HER2 negative: 0 or 1+ by IHC or 2+ by IHC and negative by ISH					

Conclusions: In our study set, no grade 3 EC was HER2 amplified regardless of p53 or MMR status, while similar to prior studies, 25% of SC were HER2 amplified. Also, equivocal expression of HER2 by IHC did not appear to correlate with p53 or MMR protein/MSI status. While 86% of EC showed MMR loss/MSI, no SC case showed this.

535 PD-L1 Expression and Clinico-Pathological Analysis of MELF Invasion Pattern in 335 Cases of Endometrial Carcinoma

Carmen Alborch[1], Armando Reques[1], Eva Coll-de la Rubia[2], Carlos López Gil[2], Teresa Moline[2], Eva Fuentes Camps[1], Xavier Ara Mancebo[1], Javier de la Torre[1], Antonio Gil-Moreno[1], Ángel García[1], Eva Colás[2], Santiago Ramon Y Cajal[1]

[1]Vall d'Hebron University Hospital, Barcelona, Spain, [2]Vall d'Hebron Research Institute (VHIR), Barcelona, Spain

Disclosures: Carmen Alborch: None; Armando Reques: None; Eva Coll-de la Rubia: None; Carlos López Gil: None; Teresa Moline: None; Eva Fuentes Camps: None; Xavier Ara Mancebo: None; Javier de la Torre: None; Antonio Gil-Moreno: None; Ángel García: None; Eva Colás: None; Santiago Ramon Y Cajal: None

Background: Endometrioid carcinoma (EC) is one of the most frequent neoplasms in the female genital tract. Despite being considered a tumor with a relatively good prognosis, 20% of the patients still present recurrence. In relation to this, MELF invasion pattern, characterized by microcystic, elongated and fragmented neoplastic glands, is present even in the early stages of the disease and has been associated with an epithelial-mesenchymal transition (EMT).

PD-L1 is a ligand of programmed death receptor 1 (PD-1), and its expression has been related with the EMT. The expression of PD-L1 could be a relevant finding because it opens the door to new targeted therapies. There are few

studies on PD-L1 in EC and the relationship between MELF pattern and PD-L1 expression has started to be studied recently.

Design: We included 335 consecutive patients diagnosed with EC between 2010 and 2017. We analyzed the presence of MELF pattern, lymphovascular space invasion (LVSI), lymph node metastasis (LNM) and the percentage of myometrial invasion. The expression of PDL1 (SP263, Ventana) was studied by immunohistochemistry in a selected cohort of 27 MELF cases and 39 non-MELF cases with similar clinico-pathological characteristics.

Results: From the total of 335 patients, 27 MELF cases (8.1%) were found in which we found a higher frequency of LNM (MELF: 45.8%, non-MELF: 6%, p<0.01), of LVSI (MELF: 48.1%, non-MELF: 16.2%, p<0.01), myometrial invasion >50% (MELF: 88.9%, non-MELF: 35.1%, p<0.01) and extrauterine invasion (MELF: 51.9%; non-MELF: 27.9%, p<0.01).

Regarding the immunohistochemical study, we found expression of PD-L1 in 22 cases (81,5%) of the neoplastic cells of the MELF areas. This expression contrasts with that found in the surface component [non-MELF: 4 (10.3%), MELF: 6 (22.2%)] and the invasion front [non-MELF: 4 (10.3%), MELF: 10 (37%)]. We observed significant differences (p<0.01) in the expression of PD-L1 in the epithelial cells of MELF areas with the expression in the invasion front.

		PDL1 expression	PDL1 non-expression
Non-MELF (n = 39)	Surface	4 (10.3%)	35 (89.7%)
	Invasive front	4 (10.3%)	35 (89.7%)
MELF (n = 27)	Surface	6 (22.2%)	21 (77.8%)
	Invasive front	10 (37%)	17 (63%)
	MELF areas	22 (81.5%)	5 (18.5%)

Figure 2 - 535

Figure 1 - 535

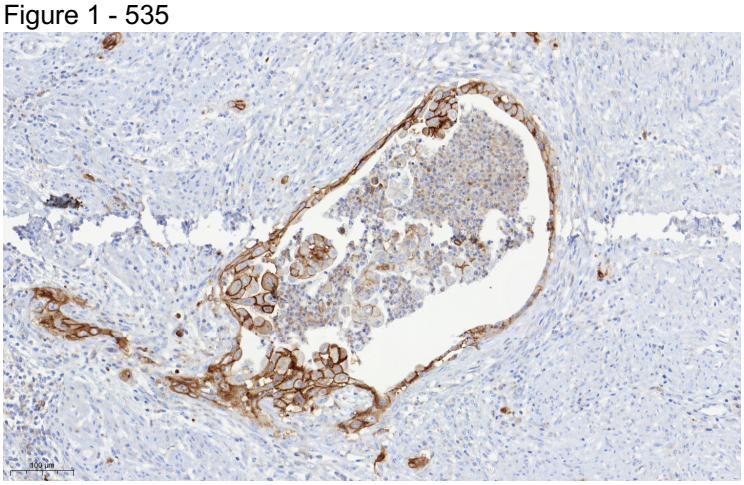

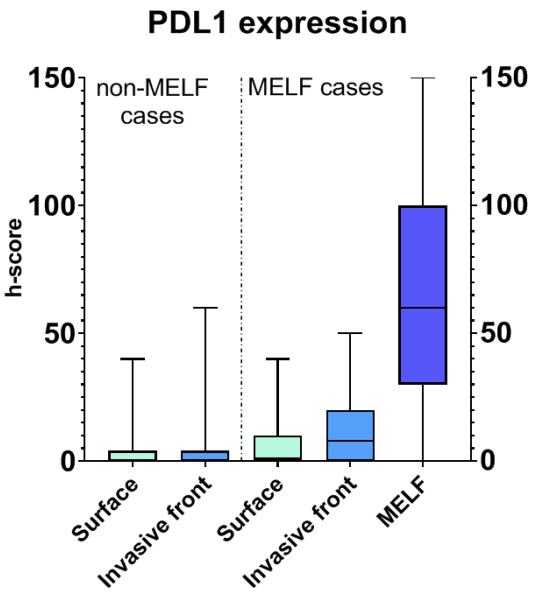

Conclusions: The presence of the MELF pattern is associated with a greater aggressiveness of the tumor, defined by a greater frequency of LNM, LVSI, extrauterine invasion and deeper myometrial invasion. We have found a high PD-L1 expression in the epithelial cells of MELF areas, corroborating the relationship between MELF pattern and PD-L1. These results point to the possible use of MELF pattern as a prognostic factor and a possible use of anti-PD-L1 as a therapeutic target in these patients.

536 Cancerous Involvement of The Fallopian Tubes of Hereditary Breast Ovarian Cancer Syndrome and Lynch Syndrome Mutation Carriers: A Report From The Creighton Hereditary Cancer Registry

Aaih Ali[1], Catherine Stoos[2], Poonam Sharma[2], Murray Casey[2], Carrie Snyder[3], Mark Stacey[3]
[1]Creighton University Medical Center, Omaha, NE, [2]CHI Health - Creighton University Medical Center - Bergan Mercy, Omaha, NE, [3]Creighton University, Omaha, NE

Disclosures: Aaih Ali: None; Catherine Stoos: None; Poonam Sharma: None; Murray Casey: None; Mark Stacey: None

Background: Hereditary breast ovarian cancer (HBOC) syndrome linked to cancer-associated mutations in *BRCA1* and *BRCA2* and the Lynch syndrome linked to mutations in mismatch repair (MMR) genes, predominantly *MLH1*, *MSH2*, and *MSH6* are characterized by increased life-time risks for gynecologic cancers as well as other cancers. Using WHO 2014 criteria, we demonstrated that most cancers involving fallopian tubes of HBOC syndrome mutation carriers were morphologically high grade serous carcinomas, and often associated with intraperitoneal serous carcinomas, while most cancers involving fallopian tubes of Lynch syndrome mutation carriers were endometrioid, clear cell, or mixed endometrioid with clear cell and serous components. Diagnostic morphologic features is important for cancer prevention and management to make these distinctions, as *TP53* mutations are common in high-grade serous gynecologic carcinomas (HGSC).

Design: Between 1/1/59 and 12/31/19, our Creighton Hereditary Cancer Registry accrued gynecologic and peritoneal cancers (n=264) in *BRCA1* (n=122), *BRCA2* (n=20), *MLH1* (n=43), *MSH2* (n=53), and *MSH6* (n=5) mutation carriers. Surgical pathology reports were available (n=104). We identified HBOC syndrome (n=55) and Lynch syndrome (n=49) mutation carriers with cancerous involvement of their fallopian tubes. Morphologic classification performed on tissue slides from HBOC syndrome (*BRCA1* =12, *BRCA2* =1) and cancers from Lynch syndrome mutation carriers (*MLH1* =3; *MSH2* =2). *P53* IHC tests performed on tissue slides from cancers linked to *BRCA1* mutation carries (n=9) and from all cancers linked to MMR gene mutation carriers (n=5).

Results: Only (n=5/12) tumors in *BRCA1* mutation carriers had classical papillary HGSC; others had solid (n=1), endometrioid (n=2) or transitional cell (n=2) features (SET pattern) and two had both solid and transitional cell features. The tumor in a *BRCA2* mutation carrier was a classical papillary HGSC. All tumors from *BRCA1* mutation carriers (n=9) showed *p53* IHC staining consistent with missense (n=7) or non-missense (n=2) mutations in *TP53*. Two high-grade solid endometrioid carcinomas ($\geq$50% solid components) in *MLH1* mutation carriers, a grade two endometrioid in *MLH2* and a clear cell carcinoma in another *MLH2*, all showed wild-type *p53* IHC staining.

Conclusions: This study demonstrates consistency in the identification of p53 IHC staining indicating the presence of TP53 mutations in carcinomas involving the fallopian tubes of hereditary BRCA1 mutation carriers and wild-type p53 staining consistent with the absence of TP53 mutations in cancers involving the fallopian tubes of hereditary MMR gene mutation carriers in spite of uncharacteristic or ambiguous morphologies in a large number of these tumors. These findings have important management and research implications not only for members of hereditary cancer families but possibly also from the general population.

537 Ovarian Mucinous Adenocarcinomas: Clinicopathologic Characterization and Invasive Growth Pattern Evaluation During the Intraoperative Consultation

Emad Alqassim[1], Mahyar Khazaeli[2], Al Amin[2], Devi Jeyachandran[3], Mohamed Desouki[3]
[1]University at Buffalo, Buffalo, NY, [2]University at Buffalo, SUNY, Buffalo, NY, [3]Roswell Park Comprehensive Cancer Center, Buffalo, NY

Disclosures: Emad Alqassim: None; Mahyar Khazaeli: None; Al Amin: None; Devi Jeyachandran: None; Mohamed Desouki: None

Background: Invasive ovarian mucinous carcinomas (MC) constitute ~ 5% of the malignant ovarian neoplasms. Most surgeons request intraoperative consultation to assess for tumor histotype, aggressiveness (benign, borderline and invasive) and the pattern of invasion (infiltrative vs expansile) to manage the patient accordingly. Lymphadenectomy is usually omitted with expansile while performed with infiltrative pattern. Most intraoperative

consultation (IOC) reports do not evaluate for the pattern of invasion partly due to limited material submitted beside other factors.

Design: Our goals were to 1) Evaluate the clinicopathologic features of ovarian MC, 2) study the impact of the invasive growth pattern on the surgical procedure mainly performing vs omitting lymphadenectomy, omentectomy/peritoneal biopsies and pelvic wash in patients diagnosed at our cancer institution over a period of 17 years. All ovarian MCs for the period 2003-2020 with IOC request were retrieved. H&E slides submitted during the IOC and representative sections from the permanent sections were reviewed if available. Clinical and pathologic characteristics including follow up data were recorded and analyzed.

Results: 41 cases were identified fulfilling the study inclusion criteria. No evaluation of the infiltrative growth pattern was performed during the IOC in any case. Re-evaluation of the sections submitted during the IOC has been performed for the tumor histotype and invasive pattern of growth. 18 cases exhibit infiltrative or mixed pattern while 16 cases exhibit expansile pattern only. The pattern can't be determined in 7 cases due to sampling issue or absent slides. Lymphadenectomy, appendectomy, pelvic wash, peritoneal biopsies/omentectomy and hysterectomy were surgically omitted in 39 vs 63%, 50 vs 19%, 44 vs 31%, 6 vs 13%, and 11 vs 13% on cases with infiltrative vs expansile pattern, respectively [Table 1].

Table 1: Clinicopathologic features of ovarian mucinous carcinomas and comparison between infiltrative and expansile growth pattern.

	All cases		Infiltrative pattern		Expansile pattern		
	number	percent	number	percent	number	percent	P value*
Age at onset							
Average (y)	59		55		62		
≤50 y	11	26.8	5	27.8	5	31.3	0.16
>50 y	30	73.2	13	72.2	11	68.8	
Total	41		18		16		
Survival							
Average follow up (m)	30.6		22		37		
Alive	23	57.5	10	58.8	9	56.3	
Dead	17	42.5	7	41.2	7	43.8	
Total	40		17		16		
Local recurrence/metastasis							
Yes	5	13.5	2	11.8	2	14.3	0.62
No	32	86.5	15	88.2	12	85.7	
Total	37		17		14		
Ovarian tumor							
Unilateral	26	70.3	14	77.8	11	68.8	0.42
Bilateral	11	29.7	4	22.2	5	31.3	
Total	37		18		16		
Borderline tumor component							
Absent	26	63.4	13	72.2	8	50.0	0.16
Present	15	36.6	5	27.8	8	50.0	
Total	41		18		16		
Tumor grade							
1	13	54.2	5	45.5	10	90.9	0.03*
2-3	11	45.8	6	54.5	1	9.1	
Total	24		11		11		
Tumor size (cm) (range 2.5-36)							
Average	18		18		18		
≤15	7	43.8	4	50.0	4	50.0	0.69
> 15	9	56.3	4	50.0	4	50.0	
Total	16		8		8		
Tubal involvement							
Absent	25	62.5	12	66.7	9	56.3	0.39
Present	15	37.5	6	33.3	7	43.8	
Total	40		18		16		
Omental/peritoneal involvement							
Absent	27	65.9	12	66.7	11	68.8	0.47
present	10	24.4	5	27.8	3	18.8	

not performed	4	9.8	1	5.6	2	12.5	
Total	41		18		16		
Peritoneal cytology							
Negative/atypical	18	43.9	6	33.3	7	43.8	0.33
positive/suspicious	10	24.4	4	22.2	4	25.0	
Not performed	13	31.7	8	44.4	5	31.3	
Total	41		18		16		
Tumor stage (pT)							
1a	18	64.3	7	53.8	9	81.8	0.63
1b-1c	5	17.9	2	15.4	2	18.2	
2 & 3	5	17.9	4	30.8	0	0.0	
Total	28		13		11		
Lymph node metastasis							
Absent (pN0)	20	48.8	10	55.6	6	37.5	0.15
present (pN1)	1	2.4	1	5.6	0	0.0	
Not performed (pNx)	20	48.8	7	38.9	10	62.5	
Total	41		18		16		
Appendix tumor							
absent	23	56.1	9	50.0	11	68.8	0.06
Present	2	4.9	0	0.0	2	12.5	
Not removed	16	39.0	9	50.0	3	18.8	
Total	41		18		16		
Tumor necrosis							
Absent	27	67.5	13	72.2	11	68.8	0.56
Present	13	32.5	5	27.8	5	31.3	
Total	40		18		16		
Hysterectomy							
Performed	35	85.4	16	88.9	14	87.5	0.65
omitted	6	14.6	2	11.1	2	12.5	
Total	41		18		16		

* Fisher exact probability test (* significant value)

Conclusions: In our cohort, ovarian mucinous adenocarcinomas were usually unilateral tumors (70%), presented at an early stage with indolent clinical course. Tumors with infiltrative growth pattern are significantly of high tumor grade. Evaluation of the pattern of invasion is crucial to guide the clinician in the surgical management of the patient.

538 Utility of p63 Staining and Morphologic Features in Distinguishing Between Cervical Microglandular Hyperplasia and Endometrial Carcinoma with Mucinous Features

Batoul Aoun[1], Stephanie Skala[2]
[1]Michigan Medicine, University of Michigan, Ann Arbor, MI, [2]University of Michigan, Ann Arbor, MI

Disclosures: Batoul Aoun: None; Stephanie Skala: None

Background: The distinction between well-differentiated endometrial carcinoma (EMCA) with microglandular and mucinous features and benign cervical microglandular hyperplasia (MGH) constitutes a diagnostic challenge, especially in limited endocervical or endometrial biopsy/curettage specimens. MGH is a benign lesion characterized by small tightly packed glands lined by bland cuboidal or columnar epithelium accompanied by a variable degree of stromal inflammation, luminal secretions, squamous metaplasia and reserve cell hyperplasia. Historically, microglandular lesions with nuclear atypia and increased mitotic activity were favored to be EMCA. However, EMCA can show microglandular architecture, bland cytology and low mitotic rate, sometimes resulting in misdiagnosis as MGH. The typical immunostains used to distinguish endocervical and endometrial carcinoma are less useful when the differential diagnosis is MGH. Here, we investigate the utility of p63 for aiding in diagnosis by highlighting cervical reserve cells.

Design: Twenty-two cases of EMCA with mucinous and microglandular features were identified from the pathology archive of a large academic institution. For comparison, 22 MGH cases and 6 atypical microglandular proliferation

cases were examined. Cases were assessed for glandular architecture, presence of mucinous and/or eosinophilic luminal secretions, inflammation, squamous metaplasia, cytologic atypia and mitotic activity. Immunohistochemistry for p63 was performed, and the presence as well as the pattern of staining were recorded.

Results: MGH and EMCA cases demonstrated a variable degree of inflammation and mucinous luminal secretions. Cytologic atypia, mitotic activity, and large, complex glands were seen in the majority of EMCA cases. Small to medium tightly packed glands, mucin-containing epithelial cells and squamous metaplasia were more commonly seen in MGH cases. All MGH cases displayed p63-positive subcolumnar reserve cells. Five EMCA cases showed non-specific focal p63 staining primarily at the surface of the tumor and in areas of squamous differentiation. The 6 cases of atypical microglandular proliferation had mild cytologic atypia, rare mitotic figures and complex glandular architecture suspicious for EMCA. Of the 6 cases, 3 were later confirmed to be EMCA FIGO grade 1.

Figure 1 - 538

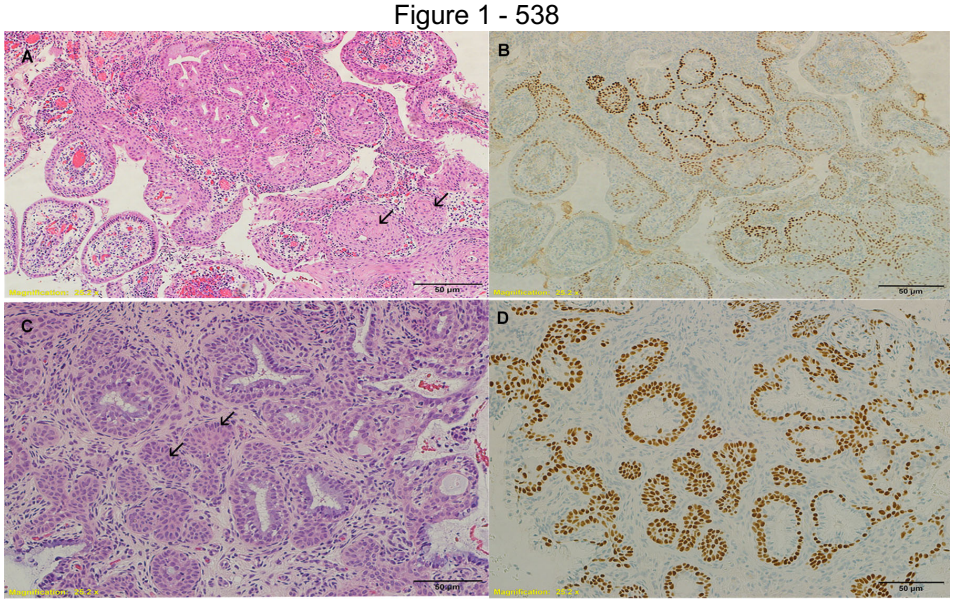

Figure 1. Morphologic features and p63 expression in microglandular hyperplasia. (A) Cervical biopsy showing small tightly packed glands with moderate stromal inflammation and foci of squamous metaplasia (*arrows*). (B Linear nuclear immunoreactivity for p63 in subcolumnar reserve cells and squamous metaplasia. (C) Endocervical curettage showing MGH and immature squamous metaplasia (*arrows*). (D) Linear nuclear immunoreactivity for p63 in subcolumnar reserve cells and squamous metaplasia.

Figure 2 - 538

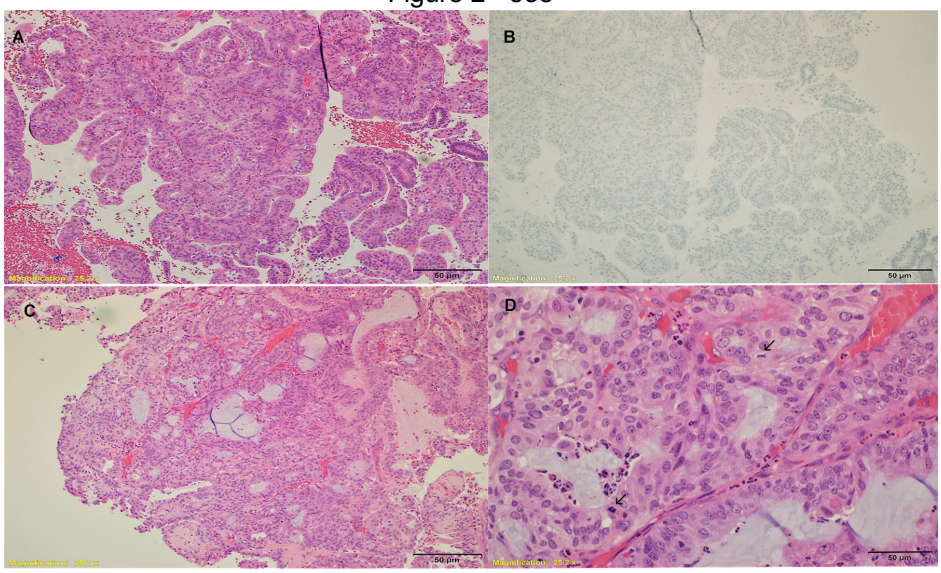

Figure 2. Morphologic features and p63 expression in endometrial carcinoma. (A) Endometrial biopsy showing EMCA, FIGO grade 1. The tumor is composed of large back-to-back glands with minimal cytologic atypia. (B) Lack of expression of p63 in tumor cells. (C) EMCA, FIGO grade 1 with squamous and mucinous differentiation. (D) Higher magnification image showing prominent nucleoli, intraluminal mucin, mild inflammation and mitotic figures (*arrows*).

Conclusions: Based on the analysis of 50 cases, microglandular proliferations with cytologic atypia, mitotic activity, and complex glandular architecture were more commonly EMCA, while small glands, bland nuclei, and squamous metaplasia were enriched in MGH. Nonetheless, there is frequent morphologic overlap between these entities. The pattern and extent of p63 staining can aid in the accurate classification of these processes, as consistent p63-positive subcolumnar reserve cells were seen only in MGH.

539 Evaluation of P53 Mutation in Uterine Serous Carcinoma

Sudeshna Bandyopadhyay[1], Mohamed Elshaikh[2], Evi Abada[1], Juliana Fucinari[3], Omar Fehmi[4], Julie Ruterbusch[5], Greg Dyson[6], Daniel Schultz[7], Michele Cote[1], Rouba Ali-Fehmi[1]
[1]Wayne State University, Detroit, MI, [2]Henry Ford Hospital, Detroit, MI, [3]Karmanos Cancer Institute, Detroit, MI, [4]University of Michigan, Ann Arbor, MI, [5]Wayne State University School of Medicine, Detroit, MI, [6]Detroit Medical Center/Wayne State University, Detroit, MI, [7]Henry Ford Health System, Detroit, MI

Disclosures: Sudeshna Bandyopadhyay: None; Mohamed Elshaikh: None; Evi Abada: None; Juliana Fucinari: None; Omar Fehmi: None; Julie Ruterbusch: None; Greg Dyson: None; Daniel Schultz: None; Michele Cote: None; Rouba Ali-Fehmi: None

Background: Serous carcinoma is a highly aggressive variant of endometrial carcinoma responsible for a large proportion of related deaths. Targeted therapy has become increasingly important to combat this disease. This has resulted in an increase in molecular and genomic studies in this field. The aim of this study was to evaluate the relevance of p53 mutations present in a cohort of uterine serous carcinoma cases from 2 academic institutions.

Design: 105 cases of endometrial serous carcinoma were included from 2 academic centers in the Detroit metropolitan area, diagnosed between 1997 and 2016. All cases had formalin fixed paraffin embedded (FFPE) blocks available for further analysis. After classification by a gynecologic pathologist (RAF), DNA isolation was performed using the QiAamp DNA Micro Kit (Qiagen Sciences LLC, Germantown, MD) according to the manufacturer's protocol. A total amount of 1.0 µg genomic DNA per sample was used as input material for the DNA library preparation. Sequencing libraries were generated using Agilent SureSelect Human All Exon kit (Agilent Technologies, CA, USA). Captured libraries were enriched by PCR to add index tags in preparation for hybridization. Products were purified using AMPure XP system (Beckman Coulter, Beverly, USA) and quantified using the Agilent high sensitivity DNA assay on the Agilent Bioanalyzer 2100 system. Next generation sequencing was conducted with the NovaSeq 6000 platform (Illumina).

Results: Some statistically significant differences in characteristics were seen by *TP53* functional mutation status (see table). Overall distribution of molecular classification significantly differed by *TP53* mutation status (global p <0.01), and average age (in years) at diagnosis was significantly lower among patients without *TP53* mutation (63.2 vs 65.8; p=0.04). None of these serous carcinoma samples were the POLE Ultramutated molecular subtype. Tumors classified as Copy-Number High were more likely to have a *TP53* mutation than Copy-Number Low tumors (corrected p=0.007), and were more likely to have *TP53* mutation than those classified as MSI Hypermutated (corrected p=0.001).

Serous only – 111 cases that have TCGA molecular classification

Table 1. Descriptive statistics for high grade serous subtype endometrial cancer cases at Henry Ford Hospital and Karmanos Cancer Institute (diagnosed 1997-2016) by *TP53* Functional Mutation Status

		P53 Mutation Status		
Characteristic	All (N=105)	Unmutated (n=20)	Mutated (n=83)	P value*
Demographics				
Patient Race				
NHW	31 (29.5)	7 (33.3)	24 (28.6)	0.67
NHB	74 (70.5)	14 (66.7)	60 (71.4)	
Age at Diagnosis				
Mean (Std)	65.3 (7.5)	63.2 (7.5)	65.8 (7.4)	0.04
Median (Range)	66.0 (33.0)	62.0 (29.0)	66.0 (33.0)	
Census Tract % in Poverty				
0-5%	13 (12.4)	2 (9.5)	11 (13.1)	0.79

5-10%	14 (13.3)	4 (19.1)	10 (11.9)	
10-20%	19 (18.1)	3 (14.3)	16 (19.1)	
20-100%	59 (56.2)	12 (57.1)	47 (56.0)	
Diagnosis				
Stage at Diagnosis				
I/II	62 (59.0)	12 (57.1)	50 (59.5)	0.84
III	43 (41.0)	9 (42.9)	34 (40.5)	
TCGA Molecular Subtype				
POLE Ultramutated	0 (0.0)	0 (0.0)	0 (0.0)	<0.01
MSI Hypermutated	3 (2.9)	2 (9.5)	1 (1.2)	
Copy-Number Low	62 (59.1)	18 (85.7)	44 (52.4)	
Copy-Number High	40 (38.1)	1 (4.8)	39 (46.4)	
Medical History				
Body Mass Index				
<25.0	10 (10.8)	2 (10.5)	8 (10.8)	0.97
>25.0	83 (89.3)	17 (89.5)	66 (89.2)	
Comorbidity Count				
None	49 (47.6)	9 (45.0)	40 (48.2)	0.41
1	24 (23.3)	3 (15.0)	21 (25.3)	
2 or more	30 (29.1)	8 (40.0)	22 (26.5)	
Hypertension				
Yes	85 (82.5)	18 (90.0)	67 (80.7)	0.33
No	18 (17.5)	2 (10.0)	16 (19.3)	
NCCN Guideline Compliant Treatment				
Yes	94 (89.5)	19 (90.5)	75 (89.3)	0.87
No	11 (10.5)	2 (9.5)	9 (10.7)	
Vital Status				
Living	39 (37.1)	6 (28.6)	33 (39.3)	0.36
Dead	66 (62.9)	15 (71.4)	51 (60.7)	
Overall Survival Time				
< 5 years	55 (52.4)	12 (57.1)	43 (51.2)	0.63
5 years or more	50 (47.6)	9 (42.9)	41 (48.8)	
Overall Survival Time (years)				
Median	4.7	4.7	4.8	0.85
Endometrial Cancer Survival				
Alive	39 (37.1)	6 (28.6)	33 (39.3)	0.65
Death by endometrial cancer	47 (44.8)	11 (52.4)	36 (42.9)	
Death by other cause	19 (18.1)	4 (19.1)	15 (17.9)	
Recurrence Status				
No recurrence	53 (51.5)	10 (50.0)	43 (51.8)	0.66
Recurrence	40 (38.8)	9 (45.0)	31 (37.4)	
Never Disease-free	10 (9.7)	1 (5.0)	9 (10.8)	
*calculated with Wilcoxon test for continuous variables, Cochran Armitage test for ordinal variables, Chi squared tests for categorical variables, and median one-way analysis for survival time variables				

Conclusions: Approximately 19% of the included cases did not demonstrate p53 mutations and this may reflect alternative pathways of carcinogenesis or undetected/novel mutations. Also p53 mutations were significantly associated with increased copy number abnormalities. Continued research in this field is necessary to identify effective targeted therapies.

540 WT1 Expression in Uterine Serous Carcinoma is Associated with Increased Chemosensitivity and Improved Progression-Free Survival in Afro-Caribbean Women

Agha Wajdan Baqir[1], Jennifer McEachron[1], Absia Jabbar[1], Kyra Gassmann[2], Raavi Gupta[1], Yi-Chun Lee[3], Daniel Levitan[1]

[1]SUNY Downstate Medical Center, Brooklyn, NY, [2]SUNY Downstate Health Sciences University, Brooklyn, NY, [3]SUNY Downstate Medical Center, New York, NY

Disclosures: Agha Wajdan Baqir: None; Jennifer McEachron: None; Absia Jabbar: None; Kyra Gassmann: None; Raavi Gupta: None; Yi-Chun Lee: None; Daniel Levitan: None

Background: Studies have shown that non-Hispanic black women have a higher incidence of aggressive histologic subtypes of endometrial carcinoma and a relatively poor disease-specific survival. Wilms tumor 1 (WT1) gene expression, historically used to differentiate ovarian serous carcinoma (OSC) from its uterine counterpart, has been

shown to be present in a considerable percentage of uterine serous carcinomas (USCs). Recent studies suggest that WT1 expression in USC may portend a shorter disease-free survival. We sought to examine the frequency and clinical implication of WT1 expression in USCs in our predominantly Afro-Caribbean patient population.

Design: We conducted a multicenter retrospective analysis of WT1 expression in USC diagnosed between 2000 to 2019. Immunohistochemical staining for WT1 was performed on one formalin-fixed paraffin-embedded tissue block for each case. Staining was considered positive if at least 1% of tumor cells showed WT1 immunoexpression. Pearson's chi-square test was used to identify differences in tumor stage, chemosensitivity, and site of disease recurrence between WT1-positive and WT1-negative cases. Analysis of progression-free survival (PFS) and overall survival (OS) was performed using Kaplan-Meier estimates. Multivariate analysis (MVA) was performed using Cox proportional hazards model.

Results: WT1 immunoexpression was evaluated in 56 cases of USC with adequate follow-up information. Positive staining was present in 13 (21.3%) cases. Chemosensitivity was significantly improved in WT1-positive (92.3%) vs. WT1-negative USCs (55.8%) (p = 0.016). Median PFS and OS did not differ significantly based on WT1 status (p = 0.544 and p = 0.759, respectively). However, a trend towards longer PFS was observed among patients with WT1-positive tumors (21 vs. 16 months, respectively). On MVA, stage (p < 0.001), WT1 status (p = 0.025), and chemosensitivity (p < 0.001) were independent predictors of PFS. However, only stage (p < 0.001) and chemosensitivity (p < 0.001) were independent predictors of OS.

	All Patients (N = 56)	**WT1 Positive (n = 13)**	**WT1 Negative (n = 43)**	**p-value***
Age at surgery Mean (range)	67 (57-81)	69 (59-75)	67 (57-81)	0.311
	n (%)	n (%)	n (%)	
Race				
Afro-Caribbean	54 (96)	13 (100)	41 (95)	0.227
Caucasian	1 (2)	0 (0)	1 (2.5)	
Other	1 (2)	0 (0)	1 (2.5)	
Stage				
I	18 (32)	5 (39)	13 (30)	0.158
II	3 (5)	0 (0)	3 (7)	
III	14 (25)	6 (46)	8 (19)	
IV	21 (38)	2 (15)	19 (44)	
Recurrence site†				
Abdomen	26 (57)	7 (58)	19 (56)	0.581
Pelvis	14 (30)	3 (25)	11 (32)	
Distant	6 (13)	2 (17)	4 (12)	
Chemosensitive‡	36 (64)	12 (92)	24 (56)	0.016
Chemoresistant	20 (36)	1 (8)	19 (44)	

Table. Clinical and pathologic characteristics based on WT1 status

** Statistical significance was defined as p < 0.05.*

† The majority of patients experienced recurrence in multiple locations simultaneously, percentages based on total number of recurrence sites

‡ Chemosensitive defined as recurrence >6 months from last platinum-based chemotherapy

Conclusions: WT1 positivity is observed in over 20% of USCs in Afro-Caribbean women, limiting its utility as a marker for differentiating between USC and OSC in this patient population. WT1 expression in USC is associated with improved chemosensitivity and longer PFS in this demographic. Our study suggests that WT1 may be a predictive marker for USCs in certain patient populations.

541 HER2 Overexpression in Uterine Serous and Clear Cell Endometrial Carcinomas is Associated with Chemoresistance and Worse Survival

Agha Wajdan Baqir[1], Jennifer McEachron[1], Absia Jabbar[1], Kyra Gassmann[2], Zaheer Bukhari[3], Yi-Chun Lee[3], Raavi Gupta[1]
[1]SUNY Downstate Medical Center, Brooklyn, NY, [2]SUNY Downstate Health Sciences University, Brooklyn, NY, [3]SUNY Downstate Medical Center, New York, NY

Disclosures: Agha Wajdan Baqir: None; Jennifer McEachron: None; Absia Jabbar: None; Kyra Gassmann: None; Zaheer Bukhari: None; Yi-Chun Lee: None; Raavi Gupta: None

Background: Serous (USC) and clear cell (CC) variants of endometrial carcinoma (EC) of uterus account for a markedly high proportion of EC related deaths, despite comprising only 20% of all cases of EC. Human epidermal growth factor receptor 2/neu (HER2) protein plays a major role in singling for growth, survival and proliferation of malignant cells. Latest data reveals a survival benefit for HER2 expressing USC with the use of trastuzumab, a monoclonal antibody against HER2, in combination with chemotherapy. However, the clinical implications of HER2 status on prognosis of USC remain unclear.

Design: A retrospective analysis of patients with USC and CC was conducted to include patients who had undergone comprehensive surgical staging/tumor debulking from 2000 – 2019. Clinical data and archival tissue were retrieved. HER2 (Cell Marque, Rocklin CA, EP3) immunohistochemistry (Ventana BenchMark Ultra) was performed on representative tumor block for each case. Immunostaining was considered positive with > 10% of cancer cells showing strong, circumferential and membranous staining. Equivocal cases were excluded for the purpose of this study. Chemosensitivity was defined as disease recurring >6 months from last platinum-based therapy. Pearson's chi-square test was used to identify the differences in the frequencies of race, stage, chemosensitivity and sites of disease recurrence. Progression free survival (PFS) and overall survival (OS) analysis was evaluated using Kaplan-Meier estimator. Multivariate analysis (MVA) was performed using Cox proportional hazards model. $p<0.05$ was considered significant.

Results: We identified 50 patients where complete clinical data and archival tissue was available. 39 (78%) patients were USC, 8 (16%) CC and 3 (6%) were mixed serous-clear cell type. Tumor was HER2 positive in 10/50 (20%) patients [Caucasians, 40% (2/5), African Americans, 18% (8/44)]. Chemosensitivity was significantly higher in HER2 negative (65%) vs. HER2 positive tumors (30%) ($p=0.044$). The median PFS was 21 months and the median OS was 29 months for all patients. The median PFS and OS did not differ significantly based on HER2 status ($p=0.229$ and $p=0.255$, respectively), however, a clinically relevant trend towards improved PFS (26 vs. 7 months) and OS (35 vs. 14 months) was observed in HER2 negative vs. positive tumors. On MVA, chemosensitivity ($p<0.001$) and HER2 ($p=0.027$) status were independent predictors of survival.

Characteristics	All Patients (N=50)	HER2 Positive (N=10)	HER2 Negative (N=40)	p-value
Age at surgery yrs. Mean (range)	67(57-81)	67(59-74)	68(57-81)	0.811
Race n(%)				
African American	44(88)	8(80)	36(90)	0.323
Caucasian	5(10)	2(20)	3(7.5)	
Other	1(2)	0(0)	1(2.5)	
Stage n(%)				
I	19(38)	2(20)	17(43)	0.471
II	4(8)	0(0)	4(10)	
III	9(18)	3(30)	6(15)	
IV	18(36)	5(50)	13(32)	
Chemo-sensitive	29(58)	3(30)	26(65)	0.044
Chemo-resistant	21(42)	7(70)	14(35)	

Table: Clinical characteristics of uterine serous and clear cell carcinoma based on HER2 immunohistochemistry status

Figure 1 - 541

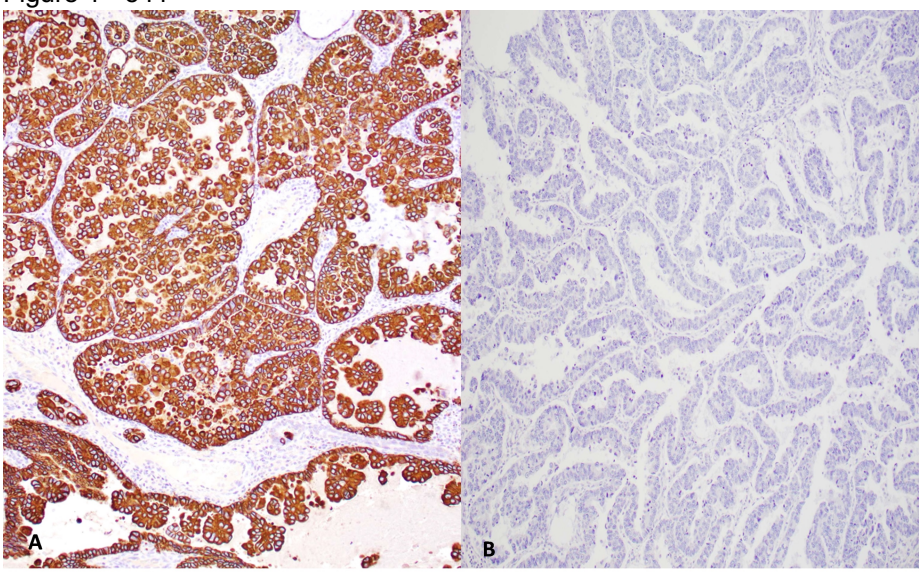

A: HER2 positive case with diffuse, membranous staining of tumor cells (HER2, 100x); B: HER2 negative case with absence of staining (HER2, 100x)

Conclusions: HER2 overexpression in USC and CC is associated with a more aggressive carcinoma with significant chemoresistance, and worse survival compared to HER2 negative carcinomas. Caucasians have a higher percentage of HER2 positive UCS and CC as compared to African American women. Patients with USC and CC should be routinely investigated for HER2 status for early treatment with monoclonal antibody, considering higher resistance of these tumors for chemotherapy.

542 Uterine PEComas: Correlation Between Melanocytic Marker Expression and TSC Alterations/TFE3 Fusions

Jennifer Bennett[1], Zehra Ordulu[2], Pankhuri Wanjari[3], Andre Pinto[4], Cristina Antonescu[5], Lauren Ritterhouse[6], Esther Oliva[6]
[1]University of Chicago, Chicago, IL, [2]Massachusetts General Hospital, Boston, MA, [3]University of Chicago Medical Center, Chicago, IL, [4]University of Miami Health System, Miami Beach, FL, [5]Memorial Sloan Kettering Cancer Center, New York, NY, [6]Massachusetts General Hospital, Harvard Medical School, Boston, MA

Disclosures: Jennifer Bennett: None; Zehra Ordulu: None; Pankhuri Wanjari: None; Andre Pinto: None; Cristina Antonescu: None; Lauren Ritterhouse: None; Esther Oliva: None

Background: PEComas are a diagnostically challenging group of neoplasms due to their morphological and immunophenotypic overlap with smooth muscle tumors. However, correct diagnosis is crucial as patients with aggressive PEComas may benefit from targeted therapy with mTOR inhibitors.

Design: We performed immunohistochemistry for HMB-45, Melan-A, and MiTF on 19 PEComas followed by *TFE3* FISH and next-generation sequencing on a 1213 gene panel. Stains were scored as 0 (negative), 1+ (1-5%), 2+ (6-25%), 3+ (26-50%), and 4+ (> 50%).

Results: Patients ranged from 32 to 77 (median 48) years and 2 had tuberous sclerosis. Using the WHO 2020 criteria, 7 (37%) were classified as malignant (m) and 13 (63%) as uncertain malignant potential (ump). All patients with m-PEComas were alive with disease/dead of disease at last follow-up. Although two patients in the latter category recurred, all with ump-PEComas are currently alive and well.

TSC1, TSC2, and *TFE3* alterations were mutually exclusive, being detected in 9 (47%), 8 (42%), and 1 (5%) PEComas, respectively. One tumor lacked any known PEComa-associated alterations. Most tumors (17; 89%) showed 3+/4+ HMB-45 expression, all of which harbored a *TSC1, TSC2,* or *TFE3* alteration. The remaining two were 2+ for HMB-45; one had a *TSC1* mutation while the other was wildtype for all genes tested. The former showed 2+ Melan-A and 1+ MiTF expression, while the latter was 1+ and 4+, respectively.

Other recurring alterations included *TP53* (4; 21%) and *ATRX* (3; 16%). Interestingly, these alterations were only noted in mPEComas. Two (11%) mPEComas were also microsatellite unstable, while the remaining tumors were either stable or indeterminate.

One tumor had two distinct morphologies resembling either a PEComa or leiomyosarcoma. These foci were also immunophenotypically different, with PEComa-like areas being positive for melanocytic markers, and LMS-like foci negative. Each area was independently sequenced and revealed an identical *ATRX* mutation. However, the PEComa-like area (case 10) had a *TSC1* mutation whereas the LMS-like foci (case 9) showed deletions in both *TSC2* and *TP53.*

Clinicopathological and molecular features are highlighted in Figure 1.

Figure 1 - 542

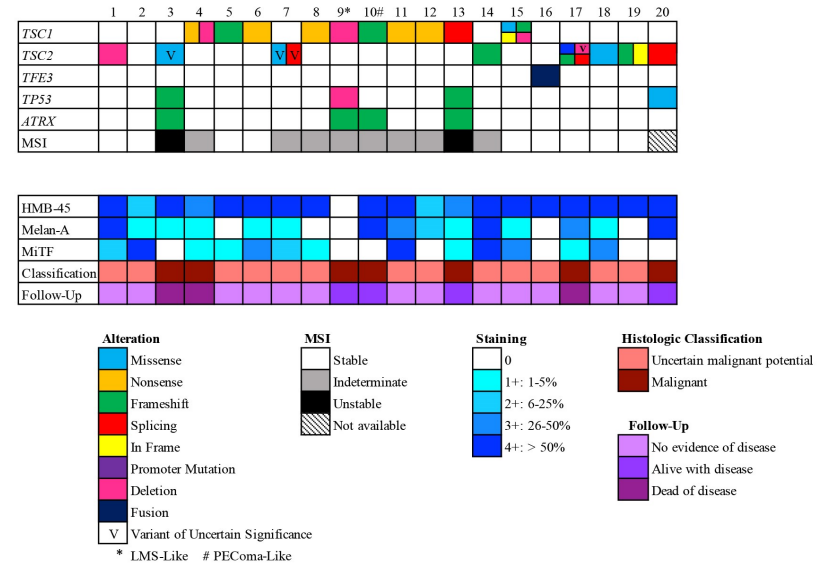

Conclusions: Tumors that are morphologically consistent with PEComas and express HMB-45 in > 25% of cells, consistently harbor PEComa-associated alterations. As < 25% expression was only noted in two of our tumors, one of which had a *TSC1* mutation, additional studies are warranted to correlate immunohistochemical and molecular findings in this subset. *TP53* and *ATRX* alterations, as well as microsatellite instability were only detected in mPEComas, and might be a helpful adjunct to morphological-based prediction models. Furthermore, immune checkpoint inhibitors may serve as a therapeutic option in patients with microsatellite unstable PEComas.

543 Uterine Tumor Resembling Ovarian Sex Cord Tumor-a Clinicopathologic and Molecular Analysis of 12 Cases Indicating Genetic Heterogeneity and Variable Behavior

Rui Bi[1], Yao Qianlan[1], Anqi Li[2], Gang Ji[1], Qianming Bai[2], Heng Chang[1], Xiaoyu Tu[2], Lin Yu[3], Huijuan Ge[4], Shaoxian Tang[5], Yufan Cheng[2], Bin Chang[1], Xu Cai[2], Wenhua Jiang[1], Zebing Liu[6], Xiaoyan Zhou[1], Wentao Yang[2]

[1]Fudan University Shanghai Cancer Center, Shanghai Medical College, Fudan University, Shanghai, China, [2]Fudan University Shanghai Cancer Center, Shanghai, China, [3]Fudan University Shanghai Cancer Center, Fudan University, Shanghai, China, [4]Fudan University, Shanghai, China, [5]Shanghai, China, [6]Rui Jin Hospital Shanghai Jiao Tong University School of Medicine, China

Disclosures: Rui Bi: None; Yao Qianlan: None; Anqi Li: None; Gang Ji: None; Qianming Bai: None; Heng Chang: None; Xiaoyu Tu: None; Lin Yu: None; Huijuan Ge: None; Shaoxian Tang: None; Yufan Cheng: None; Bin Chang: None; Xu Cai: None; Wenhua Jiang: None; Zebing Liu: None; Xiaoyan Zhou: None; Wentao Yang: None

Background: *Uterine tumor resembling ovarian sex cord tumors (UTROSCTs) are rare mesenchymal neoplasms. According to recent reports, these tumors mainly harbor NCOA1-3 rearrangements with partner genes, involving ESR1 and GREB1. Limited data indicate that patients carrying a GREB1-NCOA2 fusion experienced recurrence, while those with other genetic alterations did not relapse.*

Design: In this study, we explored the clinicopathologic, immunohistochemical, and molecular features in 12 UTROSCTs. Different fusion genes were detect by targeted RNA sequencing approach including 631 genes. Immunohistochemistry was performed for ER, PR, a-inhibin, calretinin, CD56, CD99, WT-1, CD10, Desmin, AE1/AE3, PAX8 and Ki-67. Gene fusions were further verified by reverse transcription polymerase chain reaction (RT-PCR) or fluorescence in situ hybridization (FISH).

Results: The average age of our cohort was 45y (33-56y). 5 of 12 patients recurred. Mitotic figures ranged 1-3/10HPF in primary tumors and increased to 4-9/10HPF in recurrent tumors. Twelve cases of UTROSCTs harbored 4 types of gene fusions, including *GREB1-NCOA2* (n=5), *GREB1-NCOA1* (n=2), *ESR1-NCOA2* (n=2) and *ESR1-*

NCOA3 (n=3). 3 of five (60%) *GREB1-NCOA2* cases recurred. Among them, a 33-year-old woman died of disease. The other two cases with lymphovascular invasion did not recur with relatively short follow-up. G*REB1-NCOA1* fusion was identified in 2 patients and neither of them recurred. One of two of *ESR1-NCOA2* fusion patients recurred twice after mass excision. *ESR1-NCOA3* fusion was identified in 3 patients, one of whom had a recurrent tumor. In our cohort, the age and the tumor size had no significant difference between *GREB1-NCOA1/2* and *ESR1-NCOA2/3* rearranged tumors (33-56y, average 49y vs. 34-50y, average 42y, *P* = 0.212; 8.6cm vs. 3.9cm, *P* = 0.080). All cases expressed at least one sex cord marker. All cases were negative for PAX8 and with patchy expression of Desmin, AE1/AE3 and CD10. Ki67 index was ~5-10% in most cases, and was about 20% in only one case. Interestingly, ER expression was weaker than PR in all 7 cases with *GREB1*-rearrangement, while the staining intensity of ER expression was similar as PR in all 5 patients with *ESR1*-rearrangement.

Figure 1 - 543

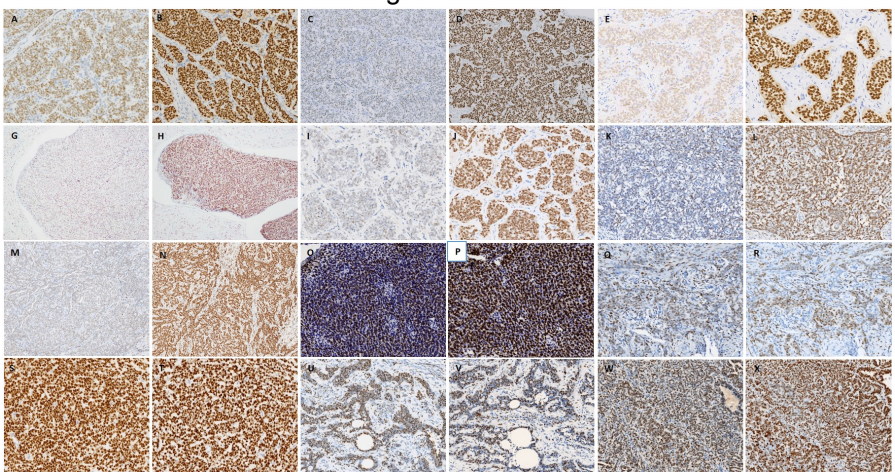

Figure 2 - 543

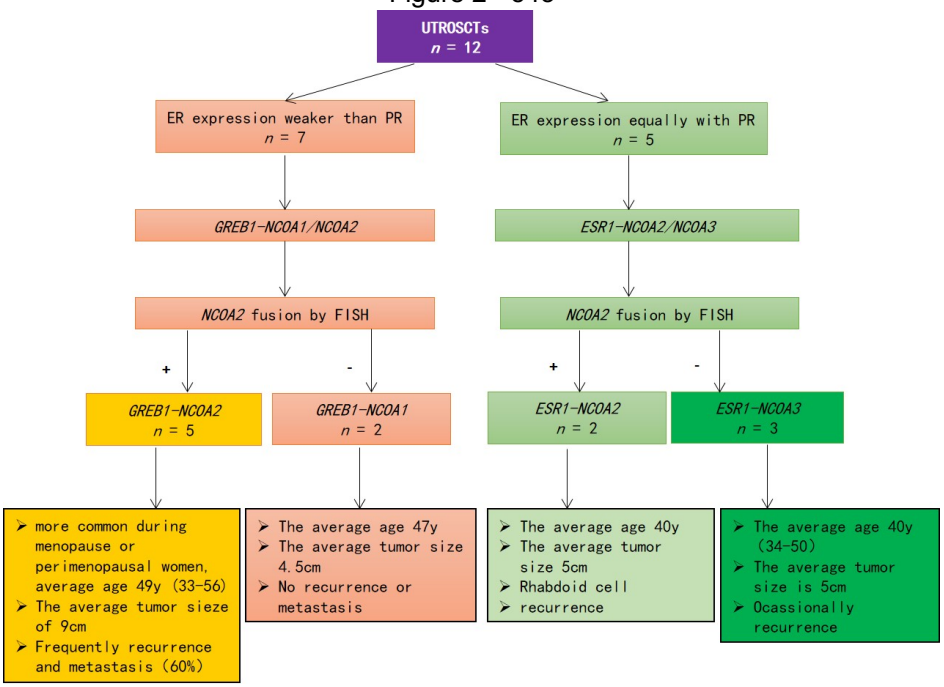

Conclusions: This study demonstrates that UTROSCTs are a group of tumors with heterogeneous genetic backgrounds and biological features. Tumors with *GREB1-NCOA2* fusion tend to behave more aggressively. The intensity of ER and PR expression might be used as screening markers to distinguish *GREB1-NCOA1/2* and *ESR1-NCOA2/3* fusions. However, more cases with molecular study and longer follow-up are needed to further clarify this.

544 Clinical Features of SARS-CoV-2 Infection During Pregnancy and Associated Placental Pathologies

Nivaz Brar[1], Emily Ryan[2], Virginia Winn[1], Ann Folkins[1], Brooke Howitt[1]
[1]Stanford Medicine/Stanford University, Stanford, CA, [2]Stanford University, Stanford, CA

Disclosures: Nivaz Brar: None; Emily Ryan: None; Virginia Winn: None; Ann Folkins: None; Brooke Howitt: None

Background: Severe acute respiratory syndrome coronavirus 2 (SARS-CoV-2) infection has variable presentations in pregnancy. The ACE2 receptor, expressed in placental syncytiotrophoblasts, is the entry point for SARS-CoV-2 and represents a potential mechanism of vertical transmission. We reviewed the clinicopathologic findings of SARS-CoV-2-exposed placentas at our institution including timing of infection and delivery, prevalence of placental pathologies, fetal infection rates and maternal/fetal outcomes.

Design: We identified patients with SARS-CoV-2 positive nasopharyngeal swabs during pregnancy (March-October 2020). Clinical data included weeks gestational age (WGA) at diagnosis and delivery, maternal symptoms, and maternal/fetal outcomes. H&E slides were reviewed for placental pathology (maternal vascular malperfusion, chronic villitis (CV), amniotic fluid infection (AFI), intervillous thrombi (IVT), fibrin deposition). Immunohistochemistry (IHC) for coronavirus spike protein and RNA in-situ hybridization (ISH) for SARS-CoV-2 was performed on a subset of blocks. A similar review of placentas evaluated from March-October 2019 was conducted as a comparison cohort.

Results: 52 patients with positive SARS-CoV-2 tests during pregnancy were identified (see Table 1). 48 (92%) were Hispanic. The mean time between positive test and date of delivery was 31 days. 29 (56%) patients were asymptomatic, 19 (37%) experienced minor symptoms and 4 (8%) had major symptoms (pneumonia requiring hospitalization or oxygen desaturation). 42 (81%) had uncomplicated deliveries/postpartum courses, while 10 (19%) had complicated deliveries/postpartum courses (preeclampsia with severe features, seizures, and/or retained placenta). Patients were diagnosed with SARS-CoV-2 infection throughout pregnancy with 79% in 3rd trimester and mostly term deliveries (83%). H&E examination revealed evidence of AFI in 29 (56%; vs 25% in 2019 cohort), lymphohistiocytic CV in 19 (37%; vs 9% in 2019 cohort), placental infarcts in 12 (23%; vs 7% in 2019 cohort), and IVT in 11 (21%; vs 21% in 2019 cohort). In the 7 cases with increased intervillous or subchorionic fibrin, all were negative by both IHC and ISH. Most neonates did well, though there was one case of intrauterine fetal demise (IUFD) at 30 WGA (placenta demonstrated avascular villi and CV), and one neonatal SARS-CoV-2 infection requiring neonatal intensive care but with no notable placental findings.

DEMOGRAPHICS	
Age	Number of cases (% of total cases)
18-19	4 (8%)
20-24	17 (33%)
25-29	13 (25%)
30-34	10 (19%)
35+	8 (15%)
Maternal ethnicity	
Hispanic	48 (92%)
Native Hawaiian or other Pacific Islander	1 (2%)
White	1 (2%)
Black	1 (2%)
Not designated	1 (2%)
CLINICAL FINDINGS	
Clinical presentation	
Asymptomatic	29 (56%)
Minor symptoms	19 (37%)
Major symptoms	4 (8%)
Gestational age at diagnosis	
First trimester	1 (2%)
Second trimester	9 (17%)
Early third trimester	15 (29%)
Early term	14 (27%)
Full term	12 (23%)
Late term	1 (2%)
Postterm	0 (0%)
Gestational age at delivery	
Second trimester	1 (2%)

Early third trimester	6 (12%)
Early term	17 (33%)
Full term	26 (50%)
Late term	2 (4%)
Postterm	0 (0%)
PATHOLOGIC FINDINGS	
Maternal vascular malperfusion	
Absent	37 (71%)
Present	15 (29%)
Chorioamnionitis	
Maternal	12 (23%)
Fetal	2 (4%)
Both	15 (29%)
None	23 (44%)
Chronic villitis	
Absent	33 (63%)
Present	19 (37%)
Infarcts	
Absent	40 (77%)
Present	12 (23%)
<1%	7 (58%)
1-5%	2 (17%)
6-10%	2 (17%)
>11%	1 (8%)
Intervillous thrombi	
Absent	41 (79%)
Present	11 (21%)
Increased fibrin deposition	
Absent	49 (94%)
Present	3 (6%)
Placental weight	
Percentile	
<3	3 (6%)
5-10th	1 (2%)
10th-25th	8 (15%)
25th-50th	15 (29%)
50th-75th	15 (29%)
75th-90th	8 (15%)
>90th	2 (4%)

Conclusions: The clinical implications for SARS-CoV-2 infection in pregnancy is unclear, though in our cohort there was one case of IUFD and one neonatal infection. SARS-CoV-2 infection during pregnancy disproportionately affects Hispanic women. Our data suggests SARS-CoV-2 exposed placentas have increased pathologic abnormalities including AFI and CV. Though our 7 tested blocks did not show IHC or ISH positivity, an expanded evaluation of the full cohort is in process.

545 Stromal p16 Expression Does Not Distinguish Atypical Polypoid Adenomyoma (APA) from its Benign Mimickers

Chau Bui[1], Fabiola Medeiros[1]
[1]*Cedars-Sinai Medical Center, Los Angeles, CA*

Disclosures: Chau Bui: None; Fabiola Medeiros: None

Background: Atypical polypoid adenomyoma (APA) is a polypoid biphasic lesion of low malignant potential that arises in the lower uterine segment and uterine corpus. The diagnosis of APA is often challenging on biopsy material, and both benign and malignant processes need to be considered in the differential. Stromal expression of p16 has recently been shown to distinguish APA from myoinvasive endometrioid carcinoma. We hypothesize that p16 immunohistochemistry could also aid in the distinction of APA from benign adenomyomatous polyp (AP) and endometrioid adenomyoma (EA).

Design: This was a retrospective analysis done on biopsy samples obtained from a tertiary medical center. H&E and immunohistochemistry for SMA, desmin, caldesmon, CD10, and p16 was performed and evaluated in all

cases. The immunoexpression of p16 was evaluated in the myofibromatous stroma in APA and both endometrial stroma and smooth muscle surrounding the glands in APs and EAs.

Results: The study comprised 12 APAs, 9 APs, and 12 EAs from patients aged 21 to 72 years. Three APAs had concurrent endometrioid carcinoma, one of which also showed atypical hyperplasia. The superficial myometrial invasion was present in one endometrioid carcinoma arising in APA. Immunohistochemistry for SMA, desmin, caldesmon, and CD10 revealed the previously published and expected pattern according to the diagnoses of APA, AP, and EA, respectively. 10 of 12 APAs (83%) showed diffuse stromal expression for p16 while 2 (17%) had only rare p16-positive stromal cells. 4 of 9 APs (44%) had a diffuse stromal expression for p16 while 5 (56%) were negative for p16 or only showed few scattered positive cells. 8 of 12 EMs (67%) showed diffuse stromal p16 positivity, while 4 (33%) were negative or only positive in a few scattered stromal cells.

Conclusions: Our findings demonstrate that the majority of APAs show diffuse p16 stromal expression. However, about half of APs and most EMs also have diffuse p16 stromal expression, limiting the use of this marker in the differential diagnosis of APA from its main benign mimickers. Alternative biomarkers need to be identified in order to more definitively differentiate among these entities.

546 Histologic Features of Vaginectomy Specimens From Female-Male Transgender Individuals

Jaswinder Chalia[1], Mahmoud Khalifa[2]
[1]University of Minnesota Medical Center, Minneapolis, MN, [2]University of Minnesota, Minneapolis, MN

Disclosures: Jaswinder Chalia: None; Mahmoud Khalifa: None

Background: Histologic changes associated with long-term androgen administration have been described in hysterectomy specimens from female-male transgender individuals. These included endometrial glandular paucity/atrophy, endometrial stromal decidua-like change, cystic ovarian follicles, higher follicular density than that expected for the age, and transitional cell metaplasia of the ectocervix. A rare case has also been described with paratubal virilization of the mesonephric duct remnants and two cases were reported with prostate-like glands within the cervix. Our aim through this study is to investigate the presence of similar findings in vaginectomy specimens.

Design: In our database, we identified six vaginectomy specimens from transgender males (2002-2020) ranging from 25 to 74 years old, all of whom had surgical affirmation for gender dysphoria. All six individuals had prior medical affirmation through long-term androgen administration for at least 2 years; and up to 5 years. Sections from the vaginectomy specimens were selected and were stained for P510S, PSA, and NKX3.1 immunohistochemistry to assess for the presence of prostate-like glands.

Results: On routine H&E, transitional cell metaplasia was seen in 3 specimens and epithelial atrophy in 2. Prostate-like glands located at the base of squamous epithelium were seen in 4 specimens. The remaining two cases showed poorly formed gland-like spaces that were not readily recognizable as "prostate-like". All 6 cases showed positive immunostaining for P501S and NKX3.1 in the subepithelial glandular structures. In five cases, these glands were also PSA-positive but the staining was negative in one case (61-year-old). To our knowledge, there results are the first documentation of the presence of prostate-like glands at the base of vaginal epithelium similar to those seen in the cervical epithelium.

Figure 1 - 546

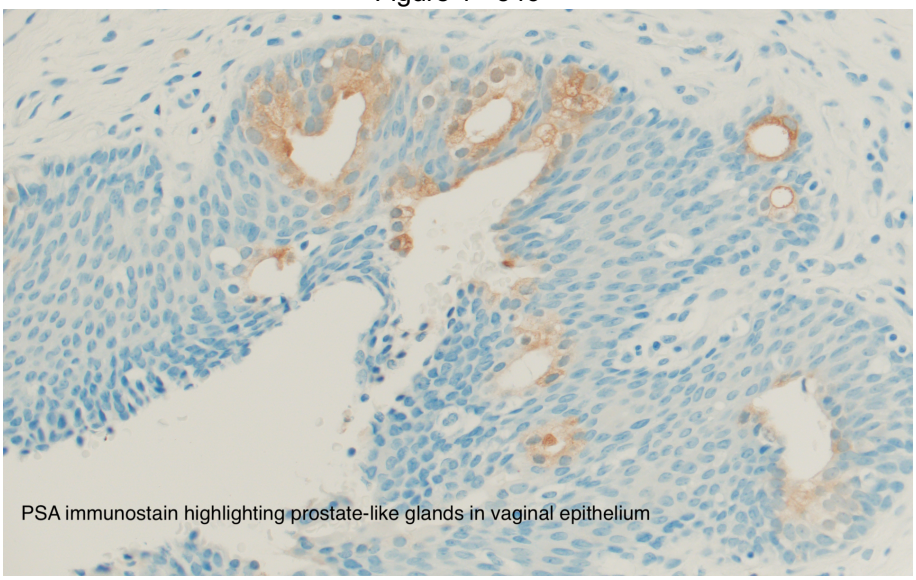

PSA immunostain highlighting prostate-like glands in vaginal epithelium

Figure 2 - 546

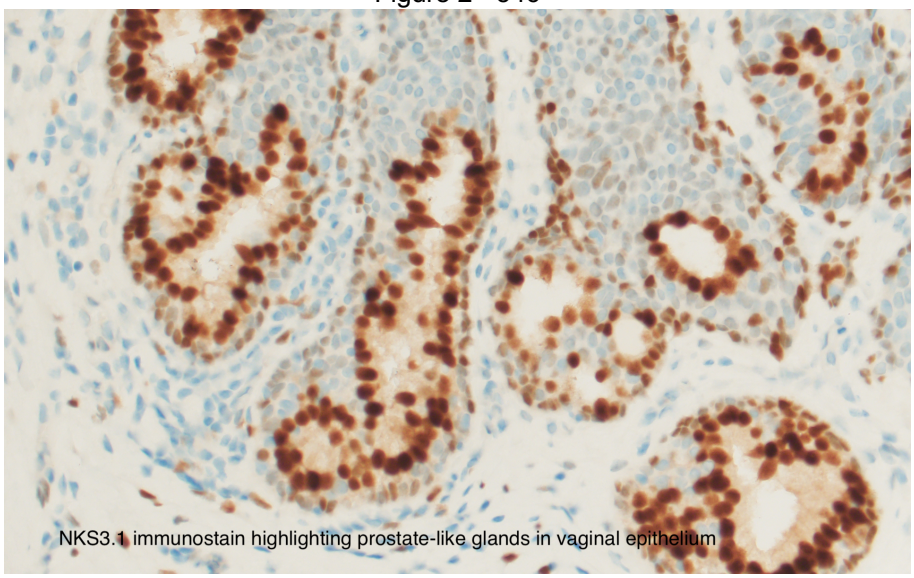

NKS3.1 immunostain highlighting prostate-like glands in vaginal epithelium

Conclusions: This small study described the histologic changes in vaginectomy specimens of male transgender individuals and hoped to assist practicing pathologists in their histologic evaluation. While it is believed that long-term androgen administration produces epithelial atrophy and interstitial cell metaplasia in some individuals, the presence of prostate-like glands at the base of vaginal epithelium is a common finding in these specimens. Demonstration of this finding is augmented by immunostaining for P501S, PSA, and NKX3.1.

547 Folate Receptor Alpha Signatures in the Fallopian Tube: Further Evidence Supporting Tubal Origin of "Ovarian" Endometriosis

Ruby Chang[1], Yan Wang[1], Wanrun Lin[1], Ruijiao Zhao[2], Yiying Wang[2], Yue Wang[3], Wenxin Zheng[1]
[1]UTSouthwestern Medical Center, Dallas, TX, [2]Henan Provincial People's Hospital, Zhengzhou, China, [3]Henan Provincial People's Hospital, People's Hospital of Zhengzhou University, School of Clinical Medicine, Henan University, Zhengzhou, China

Disclosures: Ruby Chang: None; Yan Wang: None; Wanrun Lin: None; Ruijiao Zhao: None; Yiying Wang: None; Yue Wang: None; Wenxin Zheng: None

Background: Endometriosis is a puzzling and debilitating disease that affects millions of women around the world. Ovary is the most common site involved by endometriosis. We recently hypothesized that fallopian tube contributes to the histogenesis of ovarian endometriosis. To examine if the hypothesis has scientific supporting evidence, we examined differentially expressed genes in tissue samples of fallopian tube, endometrium, and ovarian endometriosis.

Design: Gene expression array studies were performed in 3 paired fallopian tube and endometrium samples. Multiple differentially expressed genes were identified between the fallopian tube and the endometrium. The folate receptor alpha *FOLR1* represented one of the highly differentially expressed genes. The *FOLR1* gene and its corresponding FRA protein expression levels were studied in a total of 114 tissue samples of the fallopian tube, benign endometrium, and ovarian endometriosis. 32-paired tubal-endometrial-ovarian endometriosis samples were included to reduce individual case-related confounding factors in the study. Multiple comparisons among groups of ovarian endometriosis, fallopian tube and benign endometrium were performed.

Results: *FOLR1* represented one of the most differentially expressed genes between the tubal and eutopic endometrial epithelia. In this study, *FOLR1* was highly expressed both tubal epithelia and ovarian endometriosis, with paired endometrial samples showing a significantly lower level of expression. Similar differential studies for FRA protein were obtained using Western blot and immunohistochemistry. The expression of folate receptor alpha at both mRNA and protein levels in the tissues (tubal or ovarian endometriosis versus the endometrium) were significantly different ($p < 0.001$).

Conclusions: Viewed in the context of previously reported findings, the results further support the theory that fallopian tube contributes to the formation of ovarian endometriosis. Understanding the tubal contribution to ovarian endometriosis should ultimately contribute to ongoing investigative efforts aimed at identifying alternative ways to prevent and treat endometriosis.

548 Usual Type Endocervical Adenocarcinoma: Nuclear Grade 1 from Cervical Biopsy Bears Negligible Risk of Nodal Metastasis

Ruby Chang[1], Rongzhen Luo[2], M. Ruhul Quddus[3], Qingping Jiang[4], Wanrun Lin[1], Xiujie Sheng[4], Lili Liu[5], Yan-Lin Wen[6], Natalie Banet[3], C. James Sung[3], Ji-hong Liu[6], Wenxin Zheng[1]
[1]UTSouthwestern Medical Center, Dallas, TX, [2]Sun Yat-sen University Cancer Center, Dallas, TX, [3]Women & Infants Hospital/Alpert Medical School of Brown University, Providence, RI, [4]Third Affiliated Hospital, Guangzhou Medical University, Guangzhou, China, [5]Koo Foundation Sun Yat-Sen Cancer Center, Guangzhou, China, [6]Sun Yat-sen University Cancer Center, Guangzhou, China

Disclosures: Ruby Chang: None; Rongzhen Luo: None; M. Ruhul Quddus: None; Qingping Jiang: None; Wanrun Lin: None; Xiujie Sheng: None; Lili Liu: None; Yan-Lin Wen: None; Natalie Banet: None; C. James Sung: None; Ji-hong Liu: None; Wenxin Zheng: None

Background: Recurrence risk categories for early-stage endocervical adenocarcinoma (EAC), based mainly on cervical exam, radiology studies, and biopsies are used to risk-stratify and treat patients. However, findings from the above mentioned studies are poor in predicting risks for nodal metastasis (NM) and tumor recurrence (TR). Although Silva patterns of invasion can accurately predict the status of NM, pattern evaluation is mainly applied to resection specimens when the staging surgeries have been completed. In our recent study of 71 EAC with paired biopsy-resection specimens, we showed a possible association between grade 3 nuclei and a higher clinical stage. The goal of the current study is to further evaluate the utility of EAC nuclear grade by focusing on tumors with low nuclear grade on biopsies in predicting NM and TR risk in a multi-institutional study.

Design: This study included 397-paired cervical biopsy and resection of usual type EACs. In addition to tumor nuclear grade (TNG), pathological features from both biopsies and resections including tumor size, depth of invasion, lymphovascular invasion, resection margin, and NM as well as TR were evaluated. Standard statistical analyses were performed to address the relationship between TNG and the risks of NM and TR.

Results: Of the tumors from biopsies with grade 1 (G1) nuclei (n=86), 3 (3.5%) have NM and 2 (2.3%) have TR. In contrast, G2 (n=223) and G3 (n=88) tumors showed 26 (11.7%) and 33 (37.5%) with NM and 18 (8%) and 22 (25%) with TR, respectively. Detailed results including other pathological parameters are listed in Table 1. Notably,

51 (59%) of the 86 G1 tumors on biopsy showed concordant grade on resections and all these cases showed no NM. Of the 3 G1 biopsy cases showing NM, all had G2 tumors and Silva pattern C on resections. The grading discrepancy was likely due to the small tumor size from biopsies (mean biopsy size 0.6 cm vs. 2.6 cm for resection). Interestingly, 2 G1 biopsy cases with recurrence showed Silva invasive patterns B and C, respectively on resections.

LVI indicates lymphovascular invasion; RM, resection margin. Nuclear grade was calculated from cervical biopsy samples. Measurements of tumor size, depth of invasion, LVI, and RM were from resection specimens. * Nuclear grade was from biopsied tumor samples; ** Cochran-Armitage Trend Test; *** Fisher's Exact Test

TABLE 1. The relationship between tumor nuclear grade and other clinicopathologic features of patients with usual type cervical adenocarcinoma

	Nuclear Grade*			Tumor Size		Depth of Invasion			LVI		RM	
	1	2	3	<2cm	>2cm	<1/3	1/3-2/3	>2/3	-	+	-	+
Total Cases	86	223	88	171	226	144	124	129	366	31	379	18
Nodal Status												
Positive	3	26	33	6	56	5	18	39	47	15	57	5
Negative	83	197	55	165	170	139	106	90	319	16	322	13
p-value	<0.0001**			<0.0001***		<0.0001**			<0.0001***		<0.1761***	
Recurrence												
Yes	2	18	22	8	34	4	14	23	34	8	35	7
No	85	205	66	163	192	140	110	105	332	23	344	11
p-value	<0.0001**			0.0008***		0.0001**			0.0099***		0.0012***	

Conclusions: Usual type EACs with G1 nuclei have an extremely high negative predictive value for NM when nuclear grading is concordant in both biopsy and resection specimens. Cases with G1 nuclei also have no recurrences when Silva patterns of B or C is not identified on resection. Such findings may have a significant impact in clinical management, particularly for triaging patients who desires fertility.

549 Combination of Necrotic Tumor Debris and Tumor Nuclear Grade on Biopsy Predicts Clinical Behavior for Usual Type Endocervical Adenocarcinoma

Ruby Chang[1], Yu Jing[2], Xiaofei Zhang[3], Ruijiao Zhao[4], Huiting Zhu[2], Feng Zhou[5], Yiying Wang[4], Yue Wang[6], Wanrun Lin[1], Yan Wang[1], Glorimar Rivera Colon[1], Wenxin Zheng[1]

[1]UTSouthwestern Medical Center, Dallas, TX, [2]Shanghai First Maternity and Infant Hospital, Shanghai, China, [3]Women's Hospital, School of Medicine, Zhejiang University, [4]Henan Provincial People's Hospital, Zhengzhou, China, [5]Women's Hospital, School of Medicine, Zhejiang University, Hangzhou, China, [6]Henan Provincial People's Hospital, People's Hospital of Zhengzhou University, School of Clinical Medicine, Henan University, Zhengzhou, China

Disclosures: Ruby Chang: None; Yu Jing: None; Xiaofei Zhang: None; Ruijiao Zhao: None; Huiting Zhu: None; Feng Zhou: None; Yiying Wang: None; Yue Wang: None; Wanrun Lin: None; Yan Wang: None; Glorimar Rivera Colon: None; Wenxin Zheng: None

Background: The standard treatment for usual type endocervical adenocarcinoma (uEAC), stage IA2 and above, is radical hysterectomy with pelvic lymphadenectomy. However, vast majority of early-stage EAC have no nodal metastasis (NM) and may potentially benefit from conservative or non-radical therapy. Therefore, identifying EAC at low-risk for NM and tumor recurrence (TR) prior to the resection procedure is critical, especially in patients desiring fertility preservation. Currently, major prognosis related pathologic parameters for EAC include tumor size, depth of invasion (DOI), Silva invasive pattern, and lymphovascular invasion (LVI). However, these parameters are only accurately assessable on resection specimens. The limited information obtainable from biopsies makes pre-surgical decision of those needing conservative vs. aggressive surgical management impossible. Previously, a study at UTSW of 71 EAC cervical biopsies found that necrotic tumor debris (NTD) and tumor nuclear grade (NG) are correlated with NM. We further investigated the predictive value of the combination of NTD and NG for NM and TR in a large multi-institutional study.

Design: This study included 400 paired biopsy-resection of uEACs. In every pair of cases, status of NTD, NG and other parameters (tumor size, DOI, LVI, and resection margins) were examined and correlated with the status of NM and TR. Standard statistical analyses were performed to address the relationship between pathologic parameters by focusing on NTD and the risks of NM and TR. Examples of NTD and NG 1-3 are in Figure 1.

Results: Among 400 biopsies, 397 showed the status of NTD, which was present in 176 (44%) and absent in 221 (56%) specimens. 5% and 61% of NM, 5% and 17% of TR were identified correlating to absent and present NTD, respectively. Comparison of biopsies without to those with NTD revealed that absence of NTD significantly reduced risk for both NM (from 29% to 5%) and TR (from 18% to 5%). Furthermore, when combining cases of NG1 and absent NTD (n=73), no NM but 1 with TR was found. Detailed data are summarized in Table 1.

*NTD indicates necrotic tumor debris; TNG, tumor nuclear grade. **Samples analyzed NTD and TNG were from cervical biopsies. ***Nodal status and TR (tumor recurrence) were based on resection specimen. **** Cochran-Armitage Trend Test

TABLE 1. The relationship between necrotic tumor debris, tumor nuclear grade and nodal status as well as tumor recurrence of patients with usual type cervical adenocarcinoma

	NTD*		**NTD**	**Absence**			**Presence**		
	Absent	**Present**	**TNG***	**1**	**2**	**3**	**1**	**2**	**3**
All Samples**	221	176		73	126	22	13	97	66
Node Status***									
Positive	11	51		0	7	4	3	19	29
Negative	210	125		73	119	18	10	78	37
p-value	<0.0001**			<0.0001**					
TR***									
Yes	11	31		1	6	4	1	12	18
No	210	145		72	120	18	12	85	48
p-value	0.0002****			<0.0001****					

Figure 1 - 549

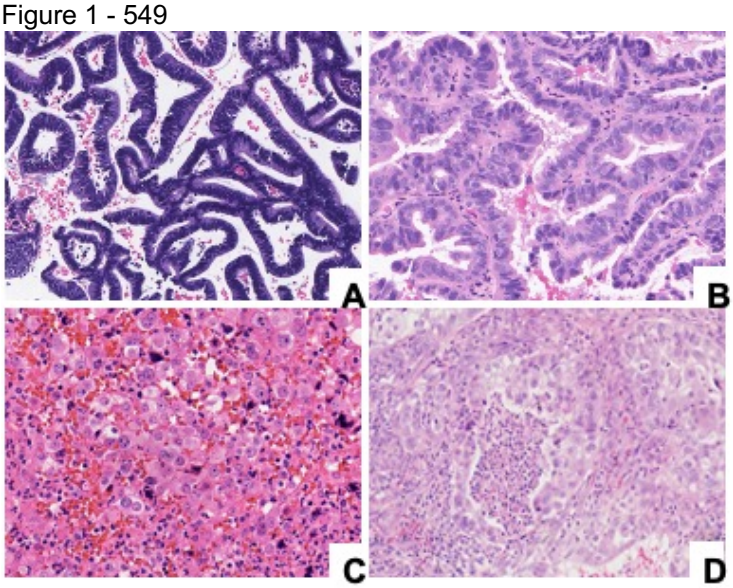

Figure 1. Representative pictures of tumor nuclear grade and necrotic tumor debris. Top panels show nuclear grade 1 (A, upper left) and grade 2 (B, upper right) without necrotic tumor debris; Lower panels show a case with nuclear grade 3 (C, lower left) without necrotic tumor debris, while a typical example of a case with nuclear grade 3 with necrotic tumor debris is present in panel D (low right).

Conclusions: The combination of NTD and NG on EAC biopsy has an excellent predictive value on NM and TR. Biopsy samples showing tumor NG1 and negative NTD delineate a low-risk patient group in which the risk of NM and TR is extremely low and thus conservative therapy, particularly fertility sparing procedures may be considered.

550 Atypical Uterine Polyps Are Molecularly Heterogeneous and Share Genomic Features with Uterine Adenosarcoma and Banal Endometrial Polyps

David Chapel[1], Annacarolina Da Silva[1], Lynette Sholl[1], Brooke Howitt[2], Paola Dal Cin[1], Marisa Nucci[3]
[1]Brigham and Women's Hospital, Boston, MA, [2]Stanford Medicine/Stanford University, Stanford, CA, [3]Brigham and Women's Hospital, Harvard Medical School, Boston, MA

Disclosures: David Chapel: None; Annacarolina Da Silva: None; Lynette Sholl: *Grant or Research Support*, Genentech; Brooke Howitt: None; Paola Dal Cin: None; Marisa Nucci: None

Background: A subset of uterine polyps has morphologic features that overlap with but are not diagnostic of uterine adenosarcoma. Approximately 10% of these "atypical uterine polyps" recur, although progression to uterine adenosarcoma has not been reported to our knowledge. While lesions classified as atypical uterine polyps have a benign clinical outcome, their pathogenetic relationship to banal uterine polyps and uterine adenosarcoma is unclear.

Design: We studied 19 atypical uterine polyps from 18 women. Fourteen were analyzed by a 447-gene targeted next-generation sequencing panel, 2 by *HMGA2* fluorescence in situ hybridization, and 3 by both assays. HMGA2 immunohistochemistry (IHC) was performed on each polyp. Morphologic parameters characteristic of adenosarcoma were evaluated. Clinical history and outcome were extracted from the medical record.

Results: Clinicopathologic features are in the table. Molecular and immunophenotypic findings are in the figure. HMGA IHC was positive in 6 of 19 (32%) polyps. Gene amplifications occurred in 12 polyps (63%), with recurrent amplifications of chr 6q25.1 (*ESR1*; 37%), chr 9q22.32 (*PTCH1*; 16%), and chr 12q13.2-12q15 (including *CDK4*, *HMGA2*, and *MDM2*; 32%). One case each contained amplification of chr 12q24.12-q24.13 and chr 1q (whole-arm). Amplifications of chr 9q22.32 and chr 12q13-q15 occurred only in endometrial polyps, whereas 6q25.1 amplification was seen in endometrial and endocervical polyps. Four polyps had no detectable copy number alterations, and three polyps had no detectable molecular alterations. Of 12 patients with follow-up pathology (endometrial sampling or hysterectomy), 6 (50%) had no lesion on repeat sampling (median follow-up, 5 months); 4 (33%) had a banal polyp (median follow-up, 5 months); and 2 (17%) recurred as atypical polyps at 8 and 11 months. For one patient (#5), primary and recurrent atypical polyps had the same molecular profile. A correlation between outcome and morphologic features or molecular alterations was not identified.

Location	
Endometrium	14
Endocervix	5
Age	
Range (years)	32-71
Median	52
Size	
Range (cm)	1-3.3
Median	1.6
Morphologic features	
Hypercellular stroma	7
Glandular stromal cuffing	15
Stromal atypia	3
Mitoses >2 per 10 hpf	8
Phyllodiform architecture	9
Rigid cystic architecture	13
Number of atypical features	
1	3
2	6
3	4
4	3
5	3
Outcomes	
No lesion	6
Banal polyp	4

Atypical polyp	2
Not available	7

Figure 1 - 550

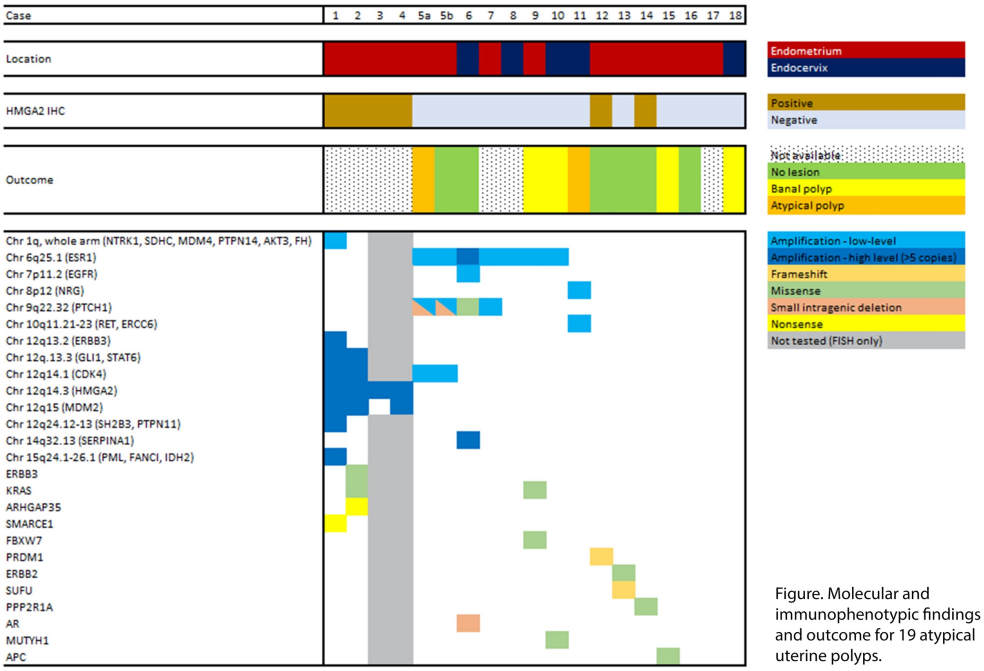

Figure. Molecular and immunophenotypic findings and outcome for 19 atypical uterine polyps.

Conclusions: Shared amplifications of chr 1q, chr 12q13-q15, and chr 12q24.12-q24.13 suggest that some atypical uterine polyps may be pathogenetically related to uterine adenosarcoma. Chr 12q13-q15 amplification may also suggest a pathogenetic link to the subset of banal endometrial polyps harboring this alteration. Although *ESR1* fusions occur in a subset of uterine adenosarcomas, *ESR1* and *PTCH1* amplifications are not described in adenosarcoma or banal endometrial polyps and may represent unique alterations in atypical uterine polyps, although these novel findings require orthogonal validation.

551 Clinicopathologic and Molecular Prognostic Factors in FIGO Stage I Uterine Leiomyosarcoma: Interim Analysis of a Large Population-Based Cohort

David Chapel[1], Annacarolina Da Silva[1], Bradley Quade[1], Marisa Nucci[2]
[1]Brigham and Women's Hospital, Boston, MA, [2]Brigham and Women's Hospital, Harvard Medical School, Boston, MA

Disclosures: David Chapel: None; Annacarolina Da Silva: None; Bradley Quade: None; Marisa Nucci: None

Background: Previous work has implicated patient age, tumor size, circumscription, histotype (spindled, epithelioid, myxoid), cytologic atypia, mitotic count, lymphovascular invasion, hormone receptor status, and recurrent copy number alterations as prognostic factors in FIGO stage I uterine leiomyosarcoma (uLMS). However, these factors have not been validated by multivariate modeling of a large cohort.

Design: We analyzed 15 clinical, morphologic, and immunophenotypic parameters in 149 stage I uLMS diagnosed between 2005-2020. Thirteen tumors were evaluated by a 447-gene targeted next-generation sequencing panel. Each clinicopathologic parameter and recurrent molecular alteration was evaluated by the log-rank test for overall (OS) and disease-free survival (DFS). Parameters significant on univariate analysis were included in a multivariate Cox proportional hazards regression model.

Results: Median OS was 85 months, with 61 (41%) patients dying over a follow-up ranging from 6-234 (median, 46) months. Median DFS was 30 months, with subsequent recurrence in 77 (57%) of 135 patients achieving clinical

disease-free status. On univariate analysis, shorter OS and shorter DFS were significantly associated with coagulative necrosis, higher mitotic count, and positive margins (Figure 1). Homozygous RB1 deletion was associated with shorter OS (P=0.01), whereas larger tumor size and ATRX mutation were associated with shorter DFS (P=0.0004 & 0.04, respectively). Age, stage IA vs IB, histotype, cytologic atypia, lymphovascular invasion, infiltrative growth, and hormone receptor status were not associated with OS or DFS. On multivariate analysis, positive margins, higher mitotic count, and necrosis were independently associated with shorter OS and DFS, and larger tumor size was independently associated with shorter DFS. (Molecular parameters were excluded from multivariate modeling due to low numbers.)

Figure 1 - 551

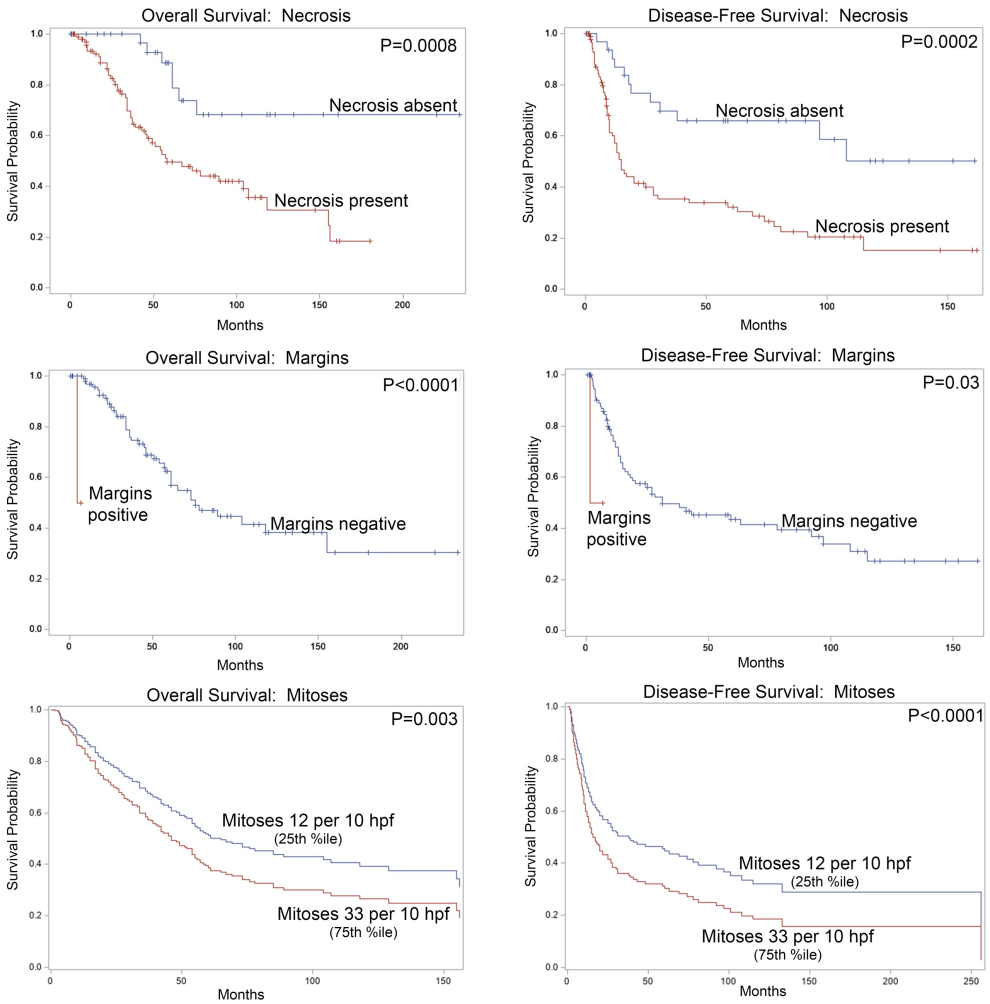

Conclusions: Multiple commonly evaluated morphologic parameters are independently associated with OS and DFS in stage I uLMS, including margin status, mitotic count, and coagulative necrosis. Tumor size is also independently associated with DFS. These parameters are clinically significant and should be routinely evaluated and reported for stage I uLMS. Certain molecular alterations, including RB1 deletion and ATRX mutation, are associated with shorter survival, but require further accrual for validation in multivariate models.

552 Genome-Wide 5-Hydroxymethylcytosine Profiling Is Prognostically Relevant in Stage IA Ovarian Clear Cell Carcinoma

David Chapel[1], Jason Karpus[2], Xiaolong Cui[2], Nida Safdar[3], Melanie Weigert[2], Ricardo Lastra[2], David Kolin[1], Thomas Krausz[4], Ernst Lengyel[2], Esther Oliva[5], Chuan He[2], Jennifer Bennett[2]
[1]Brigham and Women's Hospital, Boston, MA, [2]University of Chicago, Chicago, IL, [3]Massachusetts General Hospital, Boston, MA, [4]University of Chicago Medicine, Chicago, IL, [5]Massachusetts General Hospital, Harvard Medical School, Boston, MA

Disclosures: David Chapel: None; Jason Karpus: None; Xiaolong Cui: None; Nida Safdar: None; Melanie Weigert: None; Ricardo Lastra: None; David Kolin: None; Thomas Krausz: None; Ernst Lengyel: None; Esther Oliva: None; Chuan He: *Stock Ownership*, Epican Genetech; *Advisory Board Member*, Accent Therapeutics; *Advisory Board Member*, AccuraDX; Jennifer Bennett: None

Background: Ovarian clear cell carcinoma (OCCC) is a chemoresistant tumor where high stage disease is associated with a grim prognosis. However, reliable prognostic parameters to predict outcome in stage I tumors are lacking. Preliminary data indicate that genome-wide 5-hydroxymethylcytosine (5-hmC) burden and distribution may identify stage I OCCCs with a poor prognosis.

Design: Clinicopathologic data were collected for 121 OCCCs from three institutions. Each tumor was stained with 5-hmC immunohistochemistry (IHC) and analyzed by the genome-wide 5-hmC-Seal assay. Total 5-hmC marks were quantitated, and genomic distribution of 5-hmC marks was determined. Tumors were sorted by differentially hydroxymethylated genes using unsupervised clustering, and the clinicopathologic characteristics of distinct clusters were compared. Hydroxymethylation profiles in patients with adverse outcomes (alive with disease, dead of disease) were analyzed to identify significantly up- and down-regulated genes.

Results: Clinicopathologic data are summarized in the table. Seventy-two (60%) tumors were stage I (28 stage IA), 14 stage II, 26 stage III, and 9 stage IV. Total genome-wide 5-hmC peaks increased proportionately with increasing stage, and with increased extent and intensity of 5-hmC IHC. Over a median follow-up of 51 (range, 2-264) months, 46 patients had died of disease, 3 were alive with disease, 12 had died of other causes, and 60 were alive and well. Unsupervised clustering revealed two distinct 5-hmC profiles, which significantly predicted outcome for patients of all stages (P<0.0001; area under the curve, 0.84; Figure 1), as well as for patients with stage I disease (P=0.0007) and stage IA tumors (P<0.0001; Figure 2). Endometriosis- and adenofibroma-associated OCCC showed significantly different 5-hmC genomic distribution (P<0.0001). Hydroxymethylation profiles indicated significant (P<0.0001) downregulation of genes involved in cell-cell recognition and stress response in patients who died from disease.

Age		
	Range (years)	31-82
	Median	55
Size		
	Range (cm)	2-47
	Median	13
Stage		
	I	72
	II	14
	III	26
	IV	9
Associated precursor		
	Adenofibroma	34
	Endometriosis	81
	Both	21
	Neither	28
Outcome		
	No evidence of disease	60
	Alive with disease	3
	Dead of other causes	12
	Dead of disease	36

Figure 1 - 552

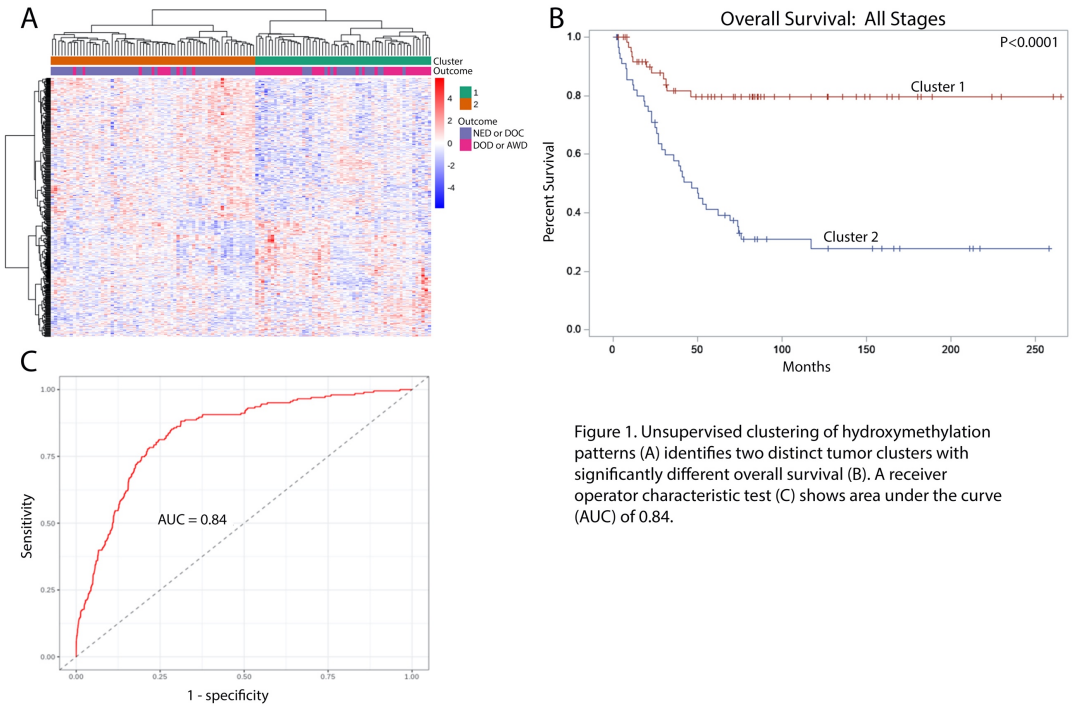

Figure 1. Unsupervised clustering of hydroxymethylation patterns (A) identifies two distinct tumor clusters with significantly different overall survival (B). A receiver operator characteristic test (C) shows area under the curve (AUC) of 0.84.

Figure 2 - 552

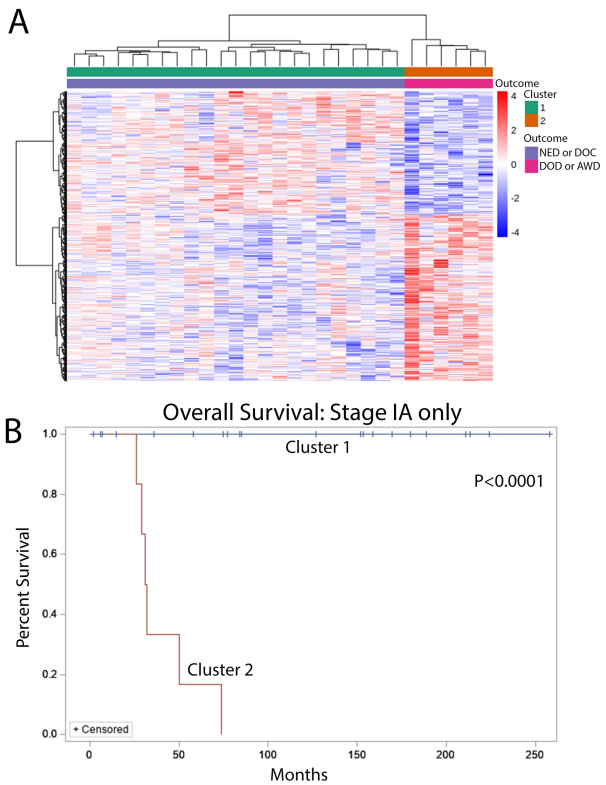

Figure 2. Unsupervised clustering of hydroxymethylation patterns (A) in stage IA tumors identifies two distinct clusters with significantly different overall survival (B).

Conclusions: 5-hmC profiling reveals biologically and clinically relevant differences between OCCCs. 5-hmC profiling on the primary surgical specimen accurately distinguishes patients with favorable outcomes from those

with unfavorable outcome, including in stage I and stage IA disease. Differences in 5-hmC profile between patients with endometriosis- and adenofibroma-associated OCCC suggests a biological difference between these classes. Differential hydroxymethylation may drive up- and downregulation of key genes, which may lend insights into pathogenesis and clinical management.

553 Uterine PEComas: A Clinicopathologic Study of 46 Cases

Katrina Collins[1], Preetha Ramalingam[2], Elizabeth Euscher[2], Julieta Barroeta[3], Isabel Alvarado-Cabrero[4], Mario Marques-Piubelli[2], Barrett Lawson[2], Anais Malpica[2]
[1]Indiana University, Indianapolis, IN, [2]The University of Texas MD Anderson Cancer Center, Houston, TX, [3]Cooper University Hospital, Camden, NJ, [4]Mexican Oncology Hospital SXXI, IMSS, Mexico City, Mexico

Disclosures: Katrina Collins: None; Preetha Ramalingam: None; Elizabeth Euscher: None; Julieta Barroeta: None; Isabel Alvarado-Cabrero: None; Mario Marques-Piubelli: None; Barrett Lawson: None; Anais Malpica: None

Background: Uterine PEComas are rare mesenchymal neoplasms which are diagnosed based on histological features and the expression of melanocytic and smooth muscle markers. Although its distinction from smooth muscle tumors can be challenging, its proper identification is required to ensure the potential use of targeted therapy in malignant cases. In this study we present the clinicopathologic features of 46 of such cases.

Design: 46 cases were identified from the files of the authors (1985 to 2020). Clinicopathologic parameters were recorded in all patients as well as ancillary studies, if available.

Results: The median pt age was 51 (range, 26-84) yrs. Clinical presentation was available in 33 pts: abnormal uterine bleeding (13), abdominal/pelvic pain (10), abdominal/pelvic mass (6), sacral pain (1). In 3 pts the tumor was an incidental finding in hysterectomy specimens. 6 pts had synchronous tumors including high-grade ovarian carcinoma, NOS (1); endometrial endometrioid adenocarcinoma (EAC), FIGO grade I (1), EAC, FIGO grade II (1); adult granulosa cell tumor of ovary (1), clear cell carcinoma of ovary (1), and lung adenocarcinoma (1). One pt had tuberous sclerosis (TS) and a history of subependymal astrocytoma; and 1 had confirmed *TSC2* gene alteration. The tumor size ranged from 0.3 to 44 (mean, 8.5) cm. The pathologic features and immunohistochemistry are summarized in Tables 1A and 1B, respectively. Initial discrepant diagnoses (n=27) were: leiomyosarcoma (14), poorly differentiated malignant neoplasm (8), high-grade endometrial stromal sarcoma (2), smooth muscle tumor of uncertain malignant potential (1), epithelioid intravenous leiomyomatosis (1) and cellular leiomyoma (1). FIGO stage was as follows: stage I (31), stage II (7), stage III (6), and stage IV (2). Clinical follow-up was available for 40 pts (3-94 months); 7 (18%) pts died of disease, 15 (38%) were alive with disease, and 18 (45%) were alive with no evidence of disease. 45/46 pts had surgery; 1 had only radiotherapy (XRT); 12 had adjuvant chemotherapy; 1 had adjuvant chemotherapy and immunotherapy, 4 had adjuvant chemotherapy and XRT, 1 had chemotherapy and whole body XRT, and 2 had adjuvant XRT.

Table 1A. Pathologic Features of Uterine PEComas		
Tumor size	< 5 cm	7/45 (16%)
	≥ 5 cm	38/45 (84%)
Border	Well-circumscribed	7/40 (18%)
	Infiltrative/permeative	33/40 (83%)
Architectural pattern	Diffuse sheets	13/46 (28%)
	Fascicular	2/46 (4%)
	Nested	13/46 (28%)
	Mixed	18/46 (39%)
Cell shape	Epithelioid	19/46 (41%)
	Spindled	1/46 (2%)
	Mixed	26/46 (57%)
Nuclear atypia	Mild	3/46 (7%)
	Moderate	15/46 (33%)
	Severe	28/46 (61%)
Cytoplasm	Eosinophilic	4/46 (9%)
	Clear	8/46 (17%)

	Mixed	34/46 (74%)
Stromal hyalinization	Present	24/46 (52%)
	Absent	22/46 (4%)
Vessel type	Thin and delicate	45/46 (98%)
	Thick walled	12/46 (26%)
	Staghorn	24/46 (52%)
Mitotic activity	<1	9/44 (20%)
	1-10	6/42 (14%)
(/50 HPF)	>10	25/42 (60%)
Necrosis	Present	25/46 (54%)
	Absent	21/46 (46%)
Lymphovascular invasion	Present	28/46 (61%)
	Absent	18/46 (39%)

Table 1B. Summary of Immunohistochemical Results in Uterine PEComas

Marker	**Number of Positive Cases Tested**
HMB-45*	40/46 (87%)
Melan-A	14/31 (45%)
MiTF	16/27 (59%)
Cathepsin K	16/22 (73%)
TFE3	15/22 (68%)
Tyrosinase	4/12 (33%)
Desmin	30/41 (73%)
h-Caldesmon	30/41 (73%)
SMA	25/32 (78%)
ER	21/27 (78%), Range 10-90%
PR	16/24 (64%), Range 10-100%

* In 4 cases HMB45 was positive only on repeat staining on different blocks.

Conclusions: PEComas are rare tumors that may present with advanced stage disease. In our study, the association with TS was uncommon. More than half of the cases had initial diagnosis of either benign or malignant uterine mesenchymal tumors, reiterating the challenge with making this diagnosis. HMB45 was the most commonly expressed melanocytic marker; however, intratumoral heterogeneity may contribute to variation in immunoreactivity patterns, requiring repeat staining on sections of different blocks. In the HMB45 negative cases, the diagnosis was made based on characteristic morphology and expression of TFE3 or other melanocytic markers.

554 Uterine Inflammatory Myofibroblastic Tumor with Aggressive Behavior-A Clinicopathologic Study of 8 Cases

Katrina Collins[1], Preetha Ramalingam[2], Elizabeth Euscher[2], Anais Malpica[2]
[1]Indiana University, Indianapolis, IN, [2]The University of Texas MD Anderson Cancer Center, Houston, TX

Disclosures: Katrina Collins: None; Preetha Ramalingam: None; Elizabeth Euscher: None; Anais Malpica: None

Background: Inflammatory myofibroblastic tumor (IMT) of the uterus is an uncommon neoplasm with a predominant indolent behavior. However, a subset of cases has an unfavorable outcome and the experience with these cases is limited. Furthermore, an accurate recognition of IMTs is critical as it has therapeutic implications. In this study, we present the clinicopathologic features of 8 such cases.

Design: 8 uterine IMTs were retrieved from our files (1985 to 2020). The following parameters were recorded: patients' (pts) age, clinical presentation, treatment, outcome, initial diagnosis, pathologic features, ALK testing by immunohistochemistry (IHC), fluorescence in situ hybridization (FISH) and molecular testing.

Results: Median pt age was 48 years (range 32 to 64 years). Clinical presentation: uterine bleeding (3), "fibroids" (2), pelvic pain (1), arthralgia and fever (1), incidental finding during C-section (1). Median tumor size was 9.4cm (range 4 -15 cm) with infiltrative borders (7) and well-circumscribed (1). Tumors were myxoid predominant (2), myxoid only (2), fascicular predominant (4). 7 tumors were spindled and 1 was epithelioid. The degree of nuclear

atypia was variable (5 tumors with grade 1-2 atypia and 3 with grade 3). Most had a lymphoplasmacytic infiltrate (7/8) and 1 had areas of hyalinization. 50% of cases had necrosis. Lymphovascular invasion was seen in 1 case. The mitotic index ranged from 1 to 8 (median, 2.5) mitoses per 10 HPFs. 7 of 8 (87.5%) referral cases were initially diagnosed as: leiomyosarcoma (3), leiomyoma (2), smooth muscle tumor of uncertain malignant potential (1), and high grade endometrial stromal sarcoma (1). Extrauterine disease at presentation was noted in 5/8 (62.5%) pts, involving the abdominal wall (1), pleura (1), pelvis (1), peritoneum, omentum and mesosalpinx (1), and ovary (1). 7/8 cases were positive for ALK by IHC. The ALK IHC negative case was positive for ALK fusion by FISH and had *FN1-ALK* fusion by next generation sequencing (NGS). Two other cases with NGS testing showed a *TNS1-ALK* fusion (1), and *RANBP2-ALK* fusion (1). Treatment information was available for 7 pts; all had surgery; (5 with adjuvant chemotherapy (CT) and 1 with adjuvant chemoradiation and 1 with neoadjuvant CT). Time to recurrence ranged from 2-38 months (mos) with most pts (87.5%) recurring within 12 mos. 5 pts are alive with disease with a follow-up range of 6-101 mos (median 22 mos), while 2 pts died of disease at 12 and 32 mos; 1 pt was lost to follow-up.

Conclusions: Majority of aggressive IMTs in our study presented with extrauterine disease or recurred within 12 mos of diagnosis. The tumors were usually large, with infiltrative borders, necrosis, and almost equal distribution of fascicular and myxoid patterns; however, most cases had 5 or less mitotic figures/10HPFs. Lack of recognition of these tumors is frequent resulting in under-utilization of targeted therapy.

555 Inflammatory Myofibroblastic Tumor of the Female Genital Tract: A Clinicopathologic Review with Ancillary Testing

Katrina Collins[1], Preetha Ramalingam[2], Elizabeth Euscher[2], Russell S. Vang[3], Maryam Shahi[4], Andres Chiesa-Vottero[5], Ángel García[6], Armando Reques[6], Glorimar Rivera Colon[7], Anais Malpica[2]
[1]Indiana University, Indianapolis, IN, [2]The University of Texas MD Anderson Cancer Center, Houston, TX, [3]Johns Hopkins University School of Medicine, Baltimore, MD, [4]Mayo Clinic, Rochester, MN, [5]Cleveland Clinic, Cleveland, OH, [6]Vall d'Hebron University Hospital, Barcelona, Spain, [7]UTSouthwestern Medical Center, Dallas, TX

Disclosures: Katrina Collins: None; Preetha Ramalingam: None; Elizabeth Euscher: None; Russell S. Vang: None; Maryam Shahi: None; Andres Chiesa-Vottero: None; Ángel García: None; Armando Reques: None; Glorimar Rivera Colon: None; Anais Malpica: None

Background: Inflammatory myofibroblastic tumor (IMT) is an uncommon neoplasm in the female genital tract. IMTs can have morphologic and immunohistochemical (IHC) overlap with smooth muscle and endometrial stromal cell neoplasms. Most IMTs are benign but some can be aggressive. Recognition of this tumor is important as tyrosine kinase inhibitors may be used in the recurrent/metastatic setting. This study presents the clinicopathologic features of 62 such cases.

Design: 62 gynecologic IMTs were retrieved from the files of the authors (1985 to 2020). Pathologic parameters and ancillary studies, including ALK testing by IHC, and/or fluorescence in situ hybridization (FISH) were recorded for all cases. Clinical information and molecular testing were recorded when available. Cases with suspicious morphology, but no IHC/FISH or next generation sequencing (NGS) testing to confirm the presence of *ALK* or other IMT related rearrangements were excluded.

Results: Median age was 38 (range 23 to 85) years. Clinical presentation: “fibroids” (21), uterine bleeding (13), incidental finding at time of delivery (7), uterine mass (4), incidental finding at time of hysterectomy for unrelated causes (4), pelvic/abdominal pain (3), cervical polyp (2), arthralgia and fever (1). Primary sites included uterus (54), placenta (8), vulva (1), and ovary (1). The pathologic features and IHC are summarized in Tables 1A and 1B, respectively. 61/62 (98%) cases were positive for ALK by IHC. ALK staining was characterized in 44 cases: cytoplasmic and granular (35), cytoplasmic/granular and membranous (5), cytoplasmic and smooth (2), cytoplasmic, smooth and membranous (1), and membranous only (1). 21 cases were ALK-FISH positive. One case negative for ALK IHC was positive for *ALK* fusion by FISH and had *FN1-ALK* fusion by next generation sequencing (NGS). Two other cases with NGS testing showed a *TNS1-ALK* fusion (1), and *RANBP2-ALK* fusion (1). 46 of 64 (72%) referral cases were initially diagnosed as: leiomyosarcoma (11), atypical smooth muscle tumor (SMT) (8), spindle cell proliferation (5), SMT of uncertain malignant potential (7), atypical leiomyoma (3), myxoid SMT (3), leiomyoma with degenerative changes (1), leiomyoma (1), endometrial stromal tumor (3), endometrial stromal

sarcoma (2), high grade malignant neoplasm (1), and high grade sarcoma (1). 16 pts had follow-up (F/U) information: 5 are alive with disease [median F/U) 51 months (mos)], 4 pts died of disease at 10, 12, 32 and 68 mos; 7 pts alive without evidence of disease (median F/U 29 mos).

Table 1A. Pathologic Features of Gynecologic IMTs		
Tumor size	< 5 cm	23/51(45%)
	≥ 5 cm	28/51 (55%)
Gross appearance	Single	41/49 (84%)
	Multiple	8/49 (16%)
Border	Well-circumscribed	16/45 (36%)
	Infiltrative	19/45 (42%)
	Irregular	10/45 (22%)
Architectural pattern	Myxoid predominant	9/61 (15%)
	Fascicular predominant	15/61 (25%)
	Myxoid only	22/61 (36%)
	Fascicular only	15/61 (25%)
Cell shape	Epithelioid	2/61 (3%)
	Spindled	46/61 (75%)
	Mixed	13/61 (21%)
Nuclear atypia	Mild to moderate	42/61(69%)
	Severe	19/61 (31%)
Endometrial stromal sarcoma-like component	Present	3/61 (5%)
	Absent	58/61(95%)
Stromal hyalinization	Present	8/61 (13%)
	Absent	53/61 (87%)
Inflammatory infiltrate	L	22/60 (37%)
	L, P	18/60 (30%)
	L, P, E	11/60 (18%)
	L, E	3/60 (5%)
	L, E, N	2/60 (2%)
	L, N, P	1/60 (2%)
	P	1/60 (2%)
	P, E	1/60 (2%)
	None	1/60 (2%)
Mitotic activity	<1	10/60 (17%)
	1-10	47/60 (78%)
(/10 HPF)	>10	2/60 (3%)
Necrosis	Present	20/60 (33%)
	Absent	40/60 (67%)
Lymphovascular invasion	Present	2/60 (3%)
	Absent	58/60 (97%)

Table 1B. Summary of Immunohistochemical Results in Gynecologic IMTs	
Marker	**Number of Positive Cases Tested**
ALK	61/62 (99%)
SMA	25/33 (76%)
Desmin	40/55 (73%)
h-Caldesmon	8/16 (50%)
SMM	0/6 (0%)
MSA	3/9 (33%)
ER	20/31 (65%), Range 20-90%
PR	21/25 (84%),Range 30-90%

E, eosinophils; L, lymphocytes; N, neutrophils; P, plasma cells

Conclusions: The distinction of IMT from other SMTs continues to be a challenge, as in addition to the morphologic overlap, at least 50% of IMTs express SM markers. A high index of suspicion in myxoid mesenchymal tumors and a low threshold for performing ALK IHC will facilitate the correct diagnosis. Although most cases are positive for ALK IHC, some may be negative, and FISH should be pursued.

556 Response of Endometrial Endometrioid Adenocarcinoma With and Without Mismatch Repair Deficiency to Exogenous Progestin Therapy

Eleanor Cook[1], Sindhu Shetty[2], Surabhi Tewari[2], Amy Joehlin-Price[2]
[1]Cleveland Clinic Foundation, Cleveland, OH, [2]Cleveland Clinic, Cleveland, OH

Disclosures: Eleanor Cook: None; Sindhu Shetty: None; Surabhi Tewari: None; Amy Joehlin-Price: None

Background: Incidence of endometrial cancer (EC) is on the rise. Standard treatment is surgical with or without adjuvant chemoradiation. Alternatively, some with low grade EC choose high dose progestin therapy (PT) to maintain fertility or avoid surgery. The efficacy of PT in mismatch repair deficient (MMRd) tumors is not well studied. We aim to catalog our institutional progestin-treated EC with attention to MMRd.

Design: The institutional databases were searched for EC or "atypical hyperplasia bordering on EC" in patients with concurrent PT >6 months. Additional clinical information such as age, BMI, reason for PT, MMR status, MLH1 promoter hypermethylation, genetic test results, and clinical outcomes and recurrences were recorded.

Results: Sixty EC patients with median age of 51.5 years (range 23-89) met criteria and were on PT for reasons including fertility preservation (n=21, 35%), multiple medical comorbidities (n=26, 43%), or had unclear reasons for PT (n=13, 22%). Median BMI was 41.4 kg/m^2 (range 21.2-68.7 kg/m^2). Four-protein MMR IHC was available in 40 patients, and 4 had PMS2/MSH6 results in isolation. Eight patients (20%) were MMRd, including 6 with MLH1/PMS2 loss, one with PMS2 loss alone, and one with MSH2/MSH6 loss. All 6 MLH1/PMS2 patients underwent MLH1 promoter hypermethylation (PH) testing and 5 were positive. The remaining case demonstrated double somatic MLH1 mutations in tumor tissue without germline alterations. The patient with isolated PMS2 loss underwent MLH1 PH testing for unclear reasons and showed MLH1 PH. Germline testing was not available in the MSH2/MSH6 loss case.

Eight patients demonstrated pathologic resolution after a median of 16 months (range 4-36 months), 5 achieved resolution with subsequent recurrence, and 1 demonstrated resolution, then recurrence, then repeat resolution. Resolution was not achieved in the remaining 47 patients after a median of 12.5 months PT (range 6-128 months). Hysterectomy was performed in 36 (60%). Only one patient successfully conceived: the double somatic MLH1 mutation woman via in vitro fertilization. No MMRd patients resolved their EC with PT. Two MMRd patients recurred with distant metastases.

Conclusions: PT successfully treated EC in 15% of patients, none of which demonstrated MMR deficiency, suggesting that this patient demographic may not derive benefit from PT. Larger studies investigating this relationship are necessary.

557 NTRK-Fusion Uterine Sarcomas: Clinicopathologic, Immunohistochemical, and Molecular Features Of 12 Cases

Danielle Costigan[1], Marisa Nucci[1], Martin Chang[2], Brendan Dickson[3], Christopher Fletcher[4], David Kolin[4]
[1]Brigham and Women's Hospital, Harvard Medical School, Boston, MA, [2]University of Vermont Medical Center, Burlington, VT, [3]Mount Sinai Health System, Toronto, Canada, [4]Brigham and Women's Hospital, Boston, MA

Disclosures: Danielle Costigan: None; Marisa Nucci: None; Martin Chang: None; Brendan Dickson: *Grant or Research Support*, Illumina; Christopher Fletcher: None; David Kolin: None

Background: *NTRK*-rearranged uterine sarcomas are a recently described subset of rare uterine sarcomas that have fibrosarcoma-like morphology, occur predominantly in the uterine cervix and typically express Pan-Trk and S100 by immunohistochemistry. Distinguishing these tumors from morphologic mimics has potential clinical significance as Trk inhibitors may benefit patients with recurrent or metastatic disease.

Design: Uterine sarcomas classified as *NTRK*-fusion uterine sarcomas or with characteristic morphologic and immunohistochemical findings suggestive of *NTRK*-fusion uterine sarcomas were retrospectively identified from the consultation files of two institutions. Immunohistochemistry for Pan-Trk, S100, and CD34 and targeted RNA-

sequencing was performed on all cases with available tissue. Results were correlated with clinicopathologic features and patient outcome.

Results: Uterine sarcomas with morphologic, immunohistochemical and/or molecular findings consistent with a diagnosis of *NTRK*-rearranged uterine sarcoma were evaluated (n=12). The median age was 34 (range 16-61) years. Eleven tumors were in the uterine cervix with a single tumor arising in the uterine corpus. The average tumor size was 5.5 (range 4.0-7.8) cm. Five cases exhibited moderate to severe cytologic atypia. The average mitotic count was 11 per 10 HPF (range 1-19). RNA-sequencing identified the following fusions: *TPR-NTRK1* (2 cases), *TPM3-NTRK1* (3 cases), *C16orf72-NTRK1* (1 case), and is currently pending on 5 cases. Pan-Trk immunohistochemistry was positive in all cases (9/9). S100 was positive in 80% (8/10 cases). CD34 was also commonly, at least focally, expressed (7/7 cases). Most cases were negative (or had rare positive cells) for desmin, ER, PR and SOX10. Half of cases (5/10) expressed some SMA. One patient developed a pulmonary metastasis 6 years after diagnosis.

Conclusions: *NTRK*-rearranged uterine sarcomas are a rare subset of uterine sarcomas that exhibit a characteristic morphology and immunophenotype allowing for distinction from morphologic mimics. Our series is the largest to date and contributes significantly to the existing body of knowledge on this tumor type, including reporting the youngest and oldest patients, confirming corpus as a primary location of disease, and by identifying a novel fusion partner (*C16orf72)*.

558 The Utility of IGF-2 Immunohistochemistry in Distinguishing Between Adrenal Cortical Carcinoma and Steroid-Cell Tumors of the Ovary

Danielle Costigan[1], Justine Barletta[1], Marisa Nucci[1]
[1]Brigham and Women's Hospital, Harvard Medical School, Boston, MA

Disclosures: Danielle Costigan: None; Justine Barletta: None; Marisa Nucci: None

Background: Steroid cell tumors of the ovary are primary ovarian neoplasms composed of cells that can resemble hormone-secreting cells of adrenal cortex. These tumors, particularly when advanced stage, cannot be reliably distinguished from metastatic adrenocortical carcinoma (ACC) on microscopic examination alone. IGF2 (insulin-like growth factor 2) is a well-established marker of ACC; peri-nuclear dot-like staining is seen in approximately 80% of ACCs. To our knowledge, the expression of IGF-2 in steroid-cell tumors of the ovary has not been studied to date.

Design: Eighteen steroid cell tumors (15 steroid cell tumor NOS, 1 leydig cell tumor, 1 hilus cell tumor, 1 pregnancy luteoma), one steroid cell-like proliferation (hilus cell heterotopia of fallopian tube) , fourteen adrenal cortical carcinomas (11 primary, 3 metastatic) were identified retrospectively from the files of a single institution. Immunohistochemistry for IGF2 was performed in all cases.

Results: Nearly all tumors primary to the gynecologic tract demonstrated absent expression of IGF2 (n=17; 89.4%) whilst all but one adrenal cortical carcinoma (n=13; 92.8%) exhibited peri-nuclear dot-like staining for IGF2 resulting in high sensitivity (92.86%; 95% CI 66.1-99.8) and specificity of IGF2 for ACCs in this setting. Of note, both gynecologic tumors with IGF2 expression were steroid cell tumors, NOS.

Conclusions: IGF-2 expression is a sensitive and specific marker for distinguishing between ACCs and steroid cell tumors of the gynecologic tract and thus offers potential clinical utility when pathologists encounter this differential diagnosis.

559 H3K27me3 Expression Correlates With Patient Outcome In Cervical Cancer

Sara da Mata[1], Joana Ferreira[2], Fernanda Silva[3], Ana Felix[4]
[1]Instituto Português de Oncologia de Lisboa Francisco Gentil, Portugal, [2]Instituto Português de Oncologia de Lisboa Francisco Gentil, Lisbon, Portugal, [3]NOVA Medical School, Queijas, Portugal, [4]Instituto Portugues de Oncologia de Lisboa, Lisbon, Portugal

Disclosures: Sara da Mata: None; Joana Ferreira: None; Fernanda Silva: None; Ana Felix: None

Background: Recent studies demonstrated the prognostic utility of histone modifications in cancer with potential therapeutic implications. H3K27me3 is a histone modification marker involved in transcriptional repression of several genes including *CDKN2A.* EZH2 tri-methylates H3K27 into H3K27me3 while KDM6A is responsible for its demethylation. HPV-related carcinomas over-express EZH2, KDM6A and p16. EZH2 inhibitors were studied in oropharyngeal HPV+ carcinomas. We aim to determine the prognostic role of H3K27me3 expression in invasive cervical cancer and its relation to p16 and HPV.

Design: Retrospective clinicopathologic analysis of 237 patients with cervical cancer diagnosed from 1978 to 2008. H3K27me3 immunohistochemical expression (clone C36B11, Cell Signaling 9733S) was evaluated in tissue microarrays. Expression was deemed negative if there was no or rare nuclear staining in neoplastic cells and positive if otherwise. HPV was determined by SPF-10 PCR-DEIA-LIPA v2 system. Statistical analysis was performed with Fischer's exact test for parametric variables and with log-rank test and Cox proportional hazards regression model for overall survival.

Results: Patient mean age at diagnosis was 53 years (range 27-94), 75 (32.6%) had localized disease (FIGO stage I) and the median follow-up was 87.32 months (range 0.23-444.87). H3K27me3 was positive in 163 cases (68.8%), mainly strong and diffusely, and negative in 74 (31.2%). 147 (62.03%) cases shared H3K27me3 expression and HPV presence and 124 (56.11%) cases shared H3K27me3 expression, HPV presence and p16 expression. H3K27me3 expression positively correlated with advanced FIGO stage (75.0% vs 51.4%; p=0.0005), disease persistence (24.2% vs 8.1%; p=0.0036) and worse mean overall survival (78 months vs 106 months; p=0.0011) on univariate analysis. There was no correlation between H3K27me3 and histological type, p16 expression or HPV status or genotype. When considering FIGO stage, p16 and HPV status, H3K27me3 expression did not independently influenced the overall survival (p=0.066).

Clinicopathological variables	H3K27me3		
	Positive	Negative	*P**
Histological type			
Adenocarcinoma	40	26	0.1189
Squamous cell carcinoma	121	48	
HPV status			
Positive	147	66	0.7985
Negative	14	5	
HPV genotype			
A7	24	12	0.8423
A9	105	47	
p16 expression			
Positive	134	51	1
Negative	13	4	
FIGO stage			
I (localized)	39	36	**0.0005**
≥II (advanced)	117	38	
Disease persistence			
Yes	37	6	**0.0036**
No	116	68	

Fisher Exact Test. *p< .01.

Conclusions: To our knowledge, this is the first study reporting the expression of H3K27me3 in invasive cervical cancer patients and suggesting a potential prognostic value. More than half of HPV positive invasive cervical cancers co-express H3K27me3 and p16, an intriguing result as H3K27me3 represses *CDKN2A* gene. Frequent over-expression of H3K27me3 in cervical cancer and its detrimental impact on prognosis is in keeping with EZH2 literature results.

560 Solitary Fibrous Tumors of the Female Genital Tract: A Detailed Morphologic Study of 27 Cases

Kyle Devins[1], Sabrina Croce[2], Eike-Christian Burandt[3], Jennifer Bennett[4], Anna Pesci[5], Gian Franco Zannoni[6], G. Pétur Nielsen[7], Robert Young[8], Esther Oliva[7]
[1]Massachusetts General Hospital, Boston, MA, [2]Institut Bergonié, Bronx, France, [3]University Medical Center Hamburg-Eppendorf, Hamburg, Germany, [4]University of Chicago, Chicago, IL, [5]IRCCS Ospedale Sacro Cuore Don Calabria, Negrar, Verona, Italy, [6]Catholic University of Sacred Heart, Rome, Italy, [7]Massachusetts General Hospital, Harvard Medical School, Boston, MA, [8]Harvard Medical School, Boston, MA

Disclosures: Kyle Devins: None; Sabrina Croce: None; Eike-Christian Burandt: None; Jennifer Bennett: None; Anna Pesci: None; Gian Franco Zannoni: None; G. Pétur Nielsen: None; Robert Young: None; Esther Oliva: None

Background: Solitary fibrous tumors (SFT) are uncommon mesenchymal tumors and most examples in the female genital tract described to date have been in the vulva. They may be mistaken for a variety of tumors depending upon their location. Herein we report the largest series of gynecologic (GYN) SFT to date focusing on variant morphology and drawing attention to non-vulvar locations.

Design: Cases were identified from the departmental pathology files of participating institutions as well as our consultation files. All available H&E and immunohistochemical slides were reviewed.

Results: 27 primary GYN tract SFT were identified, involving the vulva (n=7), vagina (n=2), cervix (n=2), corpus (n=6), fallopian tube/peritubal soft tissue (n=5), and ovary (n=5). An average of 10 H&E slides were reviewed (range 2 – 51). Size of tumors ranged from 1.5 – 30 (mean = 9.8) cm. Upper GYN-SFT tended to be larger (mean 12.4 vs. 5.4 cm, p = 0.05) than lower GYN-SFT. Based on soft tissue classification of these tumors, 21 were classic; 5 were malignant based on the presence of ≥4 mitoses/10 hpf +/- infiltrative borders; and one showed de-differentiation with pleomorphic and undifferentiated spindle cell components. Upper GYN-SFT were typically more cellular than lower GYN-SFT. Tumors often demonstrated variant morphologies comprising 5 to >50% of tumor including microcysts (n=9), myxoid background (n=7), cords (n=6), fascicular growth (n=5), multinucleated cells (n= 5), adipocytic differentiation (n=2), nuclear palisading (n=2), and dilated anastomosing vascular channels (n=2). More than one of these features was often seen within the same tumor. Additional features not previously reported included entrapped thick-walled vessels (n=7), “alveolar” edema (n=7), and epithelioid cells with pseudotubular formation (n=1), although these findings were present only focally. STAT6 was positive in 25/25 tumors tested. Two older cases with classic histologic features (vagina and vulva) had no blocks available for staining. Follow-up was available in two patients with malignant SFT; both were alive with recurrent intra-abdominal disease after 12 and 47 months. Time to recurrence was 12 and 17 months respectively.

Conclusions: SFT in the GYN tract demonstrate a wide range of variant morphologies and occur in diverse sites in addition to the vulva. Awareness of these features may improve recognition of these rare tumors which have likely been overlooked when arising at unusual sites such as the ovary.

561 BAP1 and Claudin-4 Reliably Distinguish Borderline and Low-Grade Serous Ovarian Tumors from Peritoneal Malignant Mesothelioma

Kyle Devins[1], Lawrence Zukerberg[1], Jaclyn Watkins[2], Yin Hung[1], Esther Oliva[2]
[1]Massachusetts General Hospital, Boston, MA, [2]Massachusetts General Hospital, Harvard Medical School, Boston, MA

Disclosures: Kyle Devins: None; Lawrence Zukerberg: None; Jaclyn Watkins: None; Yin Hung: None; Esther Oliva: None

Background: Peritoneal malignant mesothelioma (MM) and ovarian serous neoplasms can be difficult to differentiate, particularly in small biopsies, due to overlapping clinical, morphologic, and immunohistochemical features. BRCA1-associated protein 1 (BAP1) is expressed in most tissues, but over 50% of peritoneal MM demonstrate complete loss of nuclear staining by immunohistochemistry (IHC). Claudin-4 is a tight junction protein expressed in most epithelial tumors but absent in mesothelial cells. These markers have proven useful in differentiating MM from morphologically similar tumors, particularly in the pleural cavity. In addition, BAP1 loss was

recently shown to occur only rarely in high grade serous ovarian carcinomas. However, to our knowledge, these markers have not been evaluated to distinguish MM from ovarian serous borderline tumors (SBT) and low-grade serous carcinoma (LGSC), often a difficult differential diagnosis. Thus, we sought to evaluate the utility of these markers in this context.

Design: A search of the institutional surgical pathology database was performed. Peritoneal MM (n=18), LGSC (n=24), and SBT (n=25) since the year 2000 were identified. All slides were reviewed to confirm the original diagnoses. Representative FFPE blocks were stained for BAP1 and Claudin-4.

Results: The MM cohort included 16 tumors of epithelioid type, along with one biphasic and one sarcomatoid type. Loss of BAP1 nuclear expression was observed in 12 (67%) MM, including 11 epithelioid MM and the biphasic MM. Nuclear BAP1 expression was retained in all SBT and LGSC. Claudin-4 showed strong and diffuse membranous positivity in all serous tumors, and was negative in all MM. No difference in claudin-4 expression was noted between SBT and LGSC.

Conclusions: Immunohistochemical expression of BAP1 is retained in SBT and LGSC. Complete loss of nuclear staining in this setting is specific for MM, although not particularly sensitive as more than 30% of MM still express BAP1. Claudin-4 is a reliable marker to exclude MM, as it is consistently expressed in low grade serous tumors but negative in all MM.

562 ARHGAP35 Loss in Endometrial Cancer: A Potential Candidate Driver of MELF-Pattern Myoinvasion and Lymphovascular Space Invasion

Chien-Kuang Ding[1], Lara Richer[1], Walter Devine[1], Joseph Rabban[1]
[1]University of California, San Francisco, San Francisco, CA

Disclosures: Chien-Kuang Ding: None; Lara Richer: None; Walter Devine: None; Joseph Rabban: None

Background: MELF-pattern myoinvasive endometrial cancer has been suggested to represent a form of epithelial to mesenchymal transformation (EMT) in carcinogenesis. We hypothesized that *ARHGAP35* (p190A), a small guanosine triphosphatase (GTPase) known for regulating cell-cell junctions, cell migration and invasion, might be associated with endometrial carcinoma with MELF-pattern myoinvasion. Large-scale sequencing studies mapping somatic mutations in tumors have identified *ARHGAP35* is mutated in 14% of endometrial tumors, however, the clinical and histological features of *ARHGAP35*-mutant (*ARHGAP35*-mut) endometrial carcinoma have not been studied.

Design: We queried our institutional database of tumor sequencing and identified 8 primary uterine endometrial carcinomas that had a loss-of-function mutation in *ARHGAP35.* Clinicopathologic features of these cases were reviewed. To supplement this dataset, we analyzed publicly available data from The Cancer Genome Atlas Program (TCGA) that included clinical and genomic information for 514 primary uterine endometrial carcinomas.

Results: 65 (13%) cases in TCGA datasets carry an *ARHGAP35* alteration, 99% are loss-of-function mutations . 60% of these cases also carry POLE mutations, thus determining whether the *ARHGAP35* mutation represents a driver versus passenger mutation is challenging. For the purposes of further analysis, we excluded these POLE-mut cases. The remaining POLE wild type (-wt) *ARHGAP35*-mut cases are enriched for MSI-high (71%, vs. 32% in *ARHGAP35*-wt cases, $p<0.05$) and FIGO Grade 1 tumor (47% vs. 24%, $p<0.05$). Notably, there is no significant difference in survival between *ARHGAP35*-mut vs. *ARHGAP35*-wt in POLE-wt cases.
Similarly, 4 out of 8 (50%) of our institutional cases are also POLE-mut cases, which are excluded from analysis. In the remaining POLE-wt cases, there are 2 MSI-high cases and 2 copy-number high cases. Histologically, 3 cases demonstrate focal to prominent MELF pattern of myoinvasion and 2 of them show features of LVSI, while 1 case shows no MELF or LVSI but later presents with lymph node metastasis.

Conclusions: Collectively, we demonstrate that *ARHGAP35*-mut-POLE-wt uterine endometrial carcinoma is associated with MSI-high status, FIGO Grade 1, and histological features of MELF and LVSI. Though it does not appear to affect survival, these findings may suggest a role of *ARHGAP35* in epithelial to mesenchymal transition in carcinogenesis that merits further investigation.

563 HER2 Protein Expression and Gene Amplification in Tubo-Ovarian High-Grade Serous Carcinomas: Single Institutional Study of 100 Cases

Esma Ersoy[1], Qing Cao[2], Christopher Otis[3]
[1]UMMS-Baystate Medical Center, Springfield, MA, [2]Baystate Health, Springfield, MA, [3]University of Massachusetts Medical School-Baystate, Springfield, MA

Disclosures: Esma Ersoy: None; Qing Cao: None; Christopher Otis: None

Background: Most tubo-ovarian high-grade serous carcinomas (TO-HGSC) are diagnosed in advanced stages. Although the majority of patients achieve initial remission with cytoreductive surgery and chemotherapy, death due to progressive/recurrent disease is common. Following encouraging results of trastuzumab as an adjunctive therapy in HER2-overexpressed uterine serous carcinomas; HER2 overexpression/amplification has become the center of interest in TO-HGSC. The goals of this study were to determine the percentage of HER2 overexpression/amplification in TO-HGSC and reveal the utility of ASCO/CAP HER2 testing in breast cancer for TO-HGSC.

Design: From 2011 to 2019, 100 patients who underwent cytoreductive surgery for TO-HGSC were identified. The cases were reviewed retrospectively to select the best representative blocks with sufficient cellularity and to avoid blocks with necrosis. For all the cases, HER2 expression was assessed by immunohistochemistry (IHC) with 4B5 antibody on a standardized FDA approved platform and scored from 0 to 3+. HER2 amplification was assessed by an FDA approved dual-probe florescence in-situ hybridization (FISH) assay for all the 2+ and 3+ cases as well as five of the 0/1+ cases (negative controls). 2018 ASCO/CAP HER2 testing guideline in breast cancer was used for interpretation. Follow up data was obtained through chart review. None of the patients received HER2-targeted therapy.

Results: Among 100 cases (13 neoadjuvant and 87 non-neoadjuvant), IHC scores were 0/1+ in 81 cases, 2+ in 18 cases and 3+ in 1 case. All five 0/1+ cases were HER2 non-amplified; one out of 18 2+ cases was HER2-amplified and the only 3+ case was also confirmed to be amplified. These two non-neoadjuvant cases with HER2 overexpression/amplification were at stage pT3b and pT3c; the patients are in remission with no recurrences on their 3-years and 6-years follow-up, respectively. Among the neoadjuvant cases, one case showed a subclone with HER2-overexpression/amplification comprising <10% of the entire tumor; this patient developed brain metastasis and is currently under hospice care. All other neoadjuvant cases were 0/1+.

Conclusions: HER2 was overexpressed/amplified in 2% of TO-HGSC. 2018 ASCO/CAP HER2 IHC and FISH testing guideline for breast cancer is appropriate to utilize in TO-HGSC. Future studies are needed to expand the patient population who may get benefit from HER2-targeted therapies such as patients with activating mutations in HER2 gene but with no overexpression/amplification.

564 Comparison of KRAS-Mutated Mesonephric-Like and Non Mesonephric-Like Carcinoma of the Endometrium

Elizabeth Euscher[1], Preetha Ramalingam[1], Mario Marques-Piubelli[1], Barrett Lawson[1], Asif Rashid[1], Anais Malpica[1]
[1]The University of Texas MD Anderson Cancer Center, Houston, TX

Disclosures: Elizabeth Euscher: None; Preetha Ramalingam: None; Mario Marques-Piubelli: None; Barrett Lawson: None; Asif Rashid: None; Anais Malpica: None

Background: *KRAS* mutation (mut) is found in up to 24% of endometrial carcinoma (CA) increasing to 50% in cases with proofreading gene defects (mismatch repair [MMR], POLE). It is associated with advanced-stage endometrioid (ECA) in some studies. Endometrial mesonephric-like CA (MCA) behaves more aggressively than ECA or serous CA (SCA) with *KRAS* mut in >80% of MCA. A subset have additional mut (*PIK, PTEN, CTNNB1*) but none thusfar have *TP53, POLE* or MMR mut. Despite mut overlap with ECA and lack of *TP53* mut, MCA behaves more aggressively than either ECA or SCA. This study compares MCA and nonMCA with *KRAS* mut.

Design: Pathology files were searched (2006 to present) for all MCA and nonMCA endometrial CA with *KRAS* mut. Clinical information, uterine risk factors, tumor stage and genomic test results were obtained from the electronic medical record and pathology report.

Results: 20 MCA and 34 nonMCA (ECA FIGO 2, 15; ECA FIGO 3, 2; ECA+Clear cell CA, 7; ECA+SCA, 4; ECA+neuroendocrine CA, 1; carcinosarcoma, 3; undifferentiated CA, 2) were identified with follow up (fu) ranging from 4-156 months (mean 43). Table 1 compares outcome-associated factors in MCA and nonMCA cases. At the time of last fu, 1/20 MCA and 8/34 nonMCA had no evidence of disease. All MCA had an exon 2 *KRAS* mut; 70% had additional mut. 7 tested MCA had intact MMR. 27 nonMCA had an exon 2 *KRAS* mut; 7 had exon 3, 4 or 5 mut. 91% of nonMCA had additional muts.11 (32%) nonMCA with *KRAS* mut had POLE mut (3) or a MMR defect (8). *TP53* mut were identified in MMMT (3), mixed ECA/SCA (4) and ECA FIGO2 (1). Other mut detected in MCA and nonMCA are summarized in Table 1.

Table 1 Factors and mutations associated with MCA and nonMCA

	MCA	nonMCA	p Value
>50% myoinvasion (MI)	17/18 (94%)	18/32 (56%)	0.05
Cervical stromal invasion	11/18 (61%)	11/33 (33%)	0.056
Lymphovascular invasion	14/18 (77%)	23/32 (72%)	0.65
FIGO stage III/IV	11/20 (55%)	19/34 (56%)	0.95
Recurrence	19/20 (95%)	29/34 (85%)	0.3
PTEN	4	18	0.21
PIK	8	17	0.36
CTNNB1	2	2	0.62
ARID1A	0	6	0.04
TP53	0	8	0.015

Conclusions: All MCA had*KRAS* mut restricted to exon 2 and all tested cases were microsatellite stable. In contrast, *KRAS* mut in nonMCA is more variable and associated with proofreading gene defects in nearly a third of cases. The proportion of advanced stage and recurrent cases was similar between MCA and nonMCA in this study suggesting that the *KRAS* mut alone may not be driving aggressive behavior in MCA.

565 Pattern A Endocervical Adenocarcinomas with Ovarian Metastases – Enrichment with Corpus Involvement, Mucinous Differentiation, and KRAS Mutations

Jacqueline Feinberg[1], Anjelica Hodgson[1], Kara Long Roche[1], Kay Park[1]
[1]Memorial Sloan Kettering Cancer Center, New York, NY

Disclosures: Jacqueline Feinberg: None; Anjelica Hodgson: None; Kara Long Roche: None; Kay Park: None

Background: Ovarian metastases from endocervical adenocarcinomas (EAs) are rare but well-described. Silva pattern A EAs (i.e. those that do not exhibit destructive stromal invasion, typically composed of groups of well-demarcated glands with rounded contours that may be difficult to distinguish from adenocarcinoma in situ) are considered to have no risk for lymph node metastases or recurrence. Ovarian metastases specifically in the context of the pattern-based classification system including pattern A tumors has not been studied. Here, we report the clinicopathologic features of 7 pattern A EAs which involved the ovary(ies), either in a synchronous or metachronous fashion.

Design: 7 human papillomavirus (HPV)-associated pattern A EAs with ovarian involvement were identified in our institutional files. All cases were surgically treated by hysterectomy with the entire tumor submitted for histologic evaluation. Each case was reviewed by a gynecologic pathologist and a gynecologic pathology fellow to confirm a pattern A designation and all showed strong block-like expression of p16 and/or positivity for high risk HPV in situ hybridization. Demographic, clinicopathologic, and molecular features were recorded (Table 1).

Results: Synchronous and metachronous ovarian involvement was seen in 4 and 3 cases, respectively. Patients ranged in age from 31-58 years (median 38 years). All synchronous cases were clinically suspected to be ovarian

primaries and in two with available follow up, both tumors were greater than 2 cm and recurred, one in the vagina twice, and one in the lung. The 3 cases with metachronous ovarian involvement were confined to the uterus at the time of initial diagnosis with ovarian metastasis occurring 5, 17 and 108 months after hysterectomy. Morphologically, all tumors were predominantly gland-forming and 5 of 7 displayed prominent mucinous (intestinal or NOS) differentiation. Corpus involvement was also noted in 5/7 (71%) tumors. All tumors had either no definite stromal invasion (exophytic or difficult to distinguish from adenocarcinoma in situ) or invaded to a depth of 5 mm or less (pattern A invasion). No lymph node metastases were seen in 3 cases with nodal assessment. In 3 of the 4 tested cases, *KRAS* mutations were detected via next generation sequencing. All patients with follow up (5/7) had at least one recurrence in the follow up period (31 to 127 months), although all patients were without evidence of disease at the time of last clinical assessment.

Case	Presenting symptoms/ findings	Initial surgical procedure	EA subtype	Primary cervical tumor size (mm)	Definite Pattern A stromal invasion?	Corpus involvement?	FIGO Stage 2009	Extra-uterine sites of disease at time of primary surgery	Size of ovarian metastases (cm)	Timing of ovarian metastases related to primary surgery (months)	Disease recurrence sites (time to recurrence in months)	Molecular alterations*
Synchronous ovarian involvement												
1	Ovarian mass	Total hysterectomy, BSO, appendectomy, omentectomy, peritoneal biopsies	Mucinous Intestinal	16	Yes (2 mm)	Endometrium, myometrium (focal)	IVA	Bilateral ovaries, sigmoid serosa, omentum	16.0, 3.5	SYN	Unknown	N/A
2	Endometrial "simple hyperplasia", ovarian mass, ascites	Total hysterectomy, BSO, appendectomy, omentectomy, peritoneal biopsies	Usual	At least 12	Yes (2 mm)	LUS	IB1	Right ovary, bilateral fallopian tubes	6.0, 4.0	SYN	Unknown	N/A
3	Post-menopausal bleeding, ovarian mass and abdominal masses, ascites	Total hysterectomy, BSO, right hemicolectomy, peritoneal biopsies	Mucinous Intestinal	At least 25	Yes (4 mm)	Endometrium	IB1	Bilateral ovaries, acellular mucin in peritoneal biopsies	13.5, 3.0	SYN	1st recurrence - vaginal apex (9); 2nd recurrence - vaginal apex (22)	*GNAS, KRAS, PAX7 (deletion), NKX3-1 (loss), DUSP4 (loss), PDGFRB, PREX2*
4	History of abnormal Pap, ovarian mass	Total hysterectomy, BSO, omentectomy, LND	Mucinous NOS	22	Yes (3.5 mm)	No	IB1	Left ovary	24.0	SYN	Lung (39)	*KRAS, MYC (amplification)*
Metachronous ovarian involvement												
5	Abnormal Pap	Radical hysterectomy, LND	Usual	Carcinoma in curettings only	No	Tumor in endometrial curettings	IB1	None	7.5	108	Left ovary, rectal serosa (108)	N/A
6	Abnormal Pap	Simple trachelectomy converted to hysterectomy, BS	Mucinous Intestinal	At least 15	Yes (4 mm)	No	1B1	None	25.0, 12.0	5	1st recurrence - bilateral ovaries (5); 2nd recurrence - vaginal apex (51); 3rd recurrence – lung (125)	*GNAS, KRAS, DNMT1, NKX2-1*
7	Abnormal Pap	Hysterectomy, BS, SLN biopsies	Mucinous NOS	9	Yes (5 mm)	Endometrium	1B1	None	5.2	17	Left ovary (17)	*ARID1A, ERBB2*

BSO, bilateral salpingo-oophorectomy; LND, lymph node dissection; BS, bilateral salpingectomy; SLN, sentinel lymph node; EA, endocervical adenocarcinoma; NOS, not otherwise specified; LUS, lower uterine segment; SYN, synchronous.

*Unless otherwise noted, the molecular alteration in each listed gene is a single nucleotide mutation.

Conclusions: Pattern A EAs that involve the ovaries seem to frequently involve the corpus, exhibit mucinous differentiation, and may harbor *KRAS* mutations. In the 2 synchronous cases with recurrence, tumor size was >2 cm. In an otherwise typical pattern A tumor, identification of the above findings may be associated with a possible risk for synchronous or metachronous ovarian involvement.

566 HMGA2 and p53 Axis in Evaluation of High Grade Endometrial Carcinoma

Jean Fischer[1], Yinuo Li[1], Jenna Purdy[2], Jian-Jun Wei[3]
[1]Feinberg School of Medicine/Northwestern University, Chicago, IL, [2]University of Cincinnati Medical Center, Cincinnati, OH, [3]Northwestern University, Chicago, IL

Disclosures: Jean Fischer: None; Yinuo Li: None; Jenna Purdy: None; Jian-Jun Wei: None

Background: FIGO grade 3 endometrioid (G3EC) and serous carcinomas (SEC) are both considered “high-grade endometrial carcinomas” (HGECs). Diagnosis of G3EC is not highly reproducible due to the question of serous like endometrioid carcinoma or p53 alteration. Genomic study of endometrial cancer permits molecular tumor classification which can separate prognostically favorable from unfavorable types of G3EC. A recommendation for combined genomic and FIGO grade was recently proposed (IJGyP 2019, 38:S64–S74). When unavailable for genomic analysis, p53 and MSI immunostains can discriminate some but not all G3EC. Investigation of additional immunomarkers are required for aggressive HGECs. HMGA2 is highly overexpressed in high grade ovarian serous carcinoma (AJSP 2010 Jan;34(1):18-26). HMGA2 expression in HGECs remains largely unknown. In this study, we explore the value of HMGA2 in HGECs.

Design: After IRB approval, candidate cases of HGECs from our institution were selected for slide review. Endometrial cancer cases with well characterized pathologic and clinical parameters were selected for this study including G3EC (n=21) and SEC (n=23). Twenty-one FIGO grade 1 endometrioid carcinomas (G1EC) were used as controls. All H&E and immunostained slides were reviewed by three pathologists for a consensus diagnosis. G3EC were those with squamous or mucinous differentiation or typical endometrioid histology and immunoprofile. Immunostains for HMGA2, HER2, MSI proteins, p16, p53, and WT-1 were evaluated. Significance and correlation analysis were performed.

Results: The mean age and tumor size for G1EC, G3EC, and SEC were 62.6, 62.4, and 66.3 yrs and 3.0, 4.2, and 3.1 cm, respectively. The nuclear grade, tumor infiltrating lymphocytes (TIL), presence of destructive invasion, depth of invasion >50% of myometrial thickness, cervical involvement, lymph-vascular invasion (LVI), lymph node (LN) metastasis, and extrauterine extension were well documented for all cases and significantly different among the three different tumor types ($p<0.001$-0.05, Table 1). A mutant p53 staining pattern (diffusely positive or null negative) was found in 0%, 33.3%, and 94.7% of G1EC, G3EC, and SEC ($p<0.001$). HMGA2 overexpression was found in 0%, 42.9%, and 73.7% of G1EC, G3EC, and SEC ($p<0.0001$). Importantly, 56% (5/9) of G3EC with HMGA2 positivity also had p53 alterations, and 19% (4/21) of G3EC were positive for HMGA2 alone (Figure 1). HMGA2 overexpression was associated with a higher rate of LVI and LN metastasis. WT-1 expression was found in SEC (31.6%) and less commonly in G3EC (4.8%) and G1EC (9.5%).

Table 1. Summary of clinicopathologic findings in FIGO 1 endometrioid carcinoma, FIGO 3 endometrioid carcinoma, and serous carcinoma

	FIGO 1 endometrioid carcinoma	FIGO 3 endometrioid carcinoma	Serous carcinoma
No. cases	21	21	23
Age (yrs)	62.6	62.4	66.3
Size (cm)	3.0	4.2	3.1
Nuclear grade	1.4	2.5	2.7
TIL (%)	10.5	52.4	65.2
Necrosis (%)	24.2	38.1	21.7
Destructive invasion (%)	14.3	38.1	8.7
>50% depth myometrial invasion (%)	1.4	47.6	30.4
Cervical involvement (%)	0.0	19.1	13.0
LVI (%)	4.8	52.4	34.8
LN metastasis (%)	0.0	9.5	26.1
Extra-uterine involvement (%)	0.0	9.5	17.4
HMGA2 + (%)	0.0	42.9	73.7
p53 mutant (%)	0.0	33.3	94.7
P16 + (%)	0.0	19.1	95.0
MSI loss (%)	9.5	23.8	5.0
HER2 Score 3+ (%)	0.0	4.8	10.0
WT-1 (%)	9.5	4.8	31.6

Figure 1 - 566

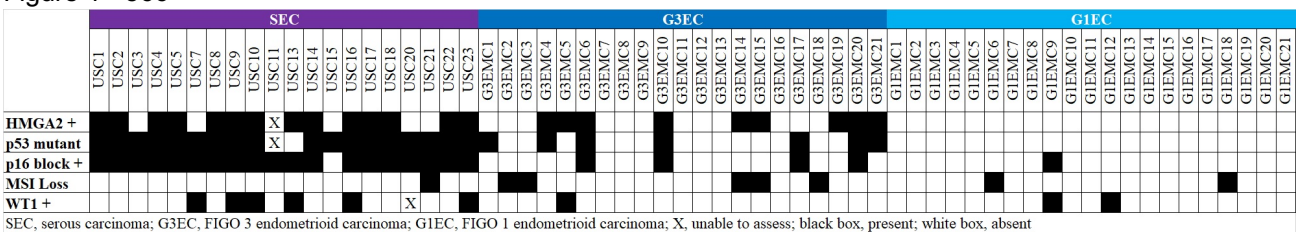

SEC, serous carcinoma; G3EC, FIGO 3 endometrioid carcinoma; G1EC, FIGO 1 endometrioid carcinoma; X, unable to assess; black box, present; white box, absent

Conclusions: HMGA2 overexpression can be detected in 74% of SEC and 43% of G3EC but not in G1EC. HMGA2 expression is associated with mutant p53 expression and aggressive histologic features. Findings suggest HMGA2 can be used to discriminate aggressive high grade G3EC in conjunction with p53.

567 The Prognostic Value of Pelvic Wash Cytology on Uterine Serous Carcinoma Outcomes

Juliana Fucinari[1], Feras Zaiem[2], Rania Daboul[3], Mohamed Elshaikh[4], Julie Ruterbusch[5], Michele Cote[1], Daniel Schultz[6], Greg Dyson[7], James Naaman[8], Sudeshna Bandyopadhyay[9], Rouba Ali-Fehmi[9]
[1]Karmanos Cancer Institute, Detroit, MI, [2]Barbara Ann Karmanos Center and Wayne State University School of Medicine, Detroit, MI, [3]Oakland University William Beaumont School of Medicine, Rochester Hills, MI, [4]Henry Ford Hospital, Detroit, MI, [5]Wayne State University School of Medicine, Detroit, MI, [6]Henry Ford Health System, Detroit, MI, [7]Detroit Medical Center/Wayne State University, Detroit, MI, [8]Michigan State University, East Lansing, MI, [9]Wayne State University, Detroit, MI

Disclosures: Juliana Fucinari: None; Feras Zaiem: None; Rania Daboul: None; Mohamed Elshaikh: None; Julie Ruterbusch: None; Michele Cote: None; Daniel Schultz: None; Greg Dyson: None; James Naaman: None; Sudeshna Bandyopadhyay: None; Rouba Ali-Fehmi: None

Background: Endometrial cancer is one of the few cancers where incidence is increasing, with ~ 60,000 annual new cases in the US. In particular, uterine serous carcinoma is an aggressive subtype that is rapidly increasing. The aim of this study is to evaluate the prognostic value of pelvic washing cytology among other clinical-pathological parameters in uterine serous carcinoma.

Design: A retrospective study of 175 patients diagnosed with uterine serous carcinoma from 1997-2016 at two academic medical centers in the Detroit metropolitan area was done. We assessed the prognostic impact of various clinicopathological parameters on overall survival (OS) and endometrial cancer-specific death (ECSD). Those parameters included race, body mass index, stage at diagnosis, tumor size, lymphovascular invasion, pelvic washing cytology, guideline-concordant treatment and comorbidity count using the Charlson Comorbidity Index (CCI). We used Cox proportional hazards models and 95% confidence intervals for statistical analysis.

Results: Positive pelvic washing cytology had a statistically significant effect on OS (HR: 2.04, 95% CI: [1.18, 3.53]) but not on ECSD. Lymphovascular invasion and comorbidity count using CCI had a statistically significant effect on both OS (HR: 2.67, 95% CI: [1.41, 5.07] and HR: 1.39, 95% CI: [1.13, 1.71], respectively) and ECSD (HR: 5.51, 95% CI: [2.73, 11.14] and HR: 1.41, 95% CI: [1.09, 1.82], respectively). Other factors including body mass index and tumor size > 1 cm did not show a statistically significant impact on OS or ECSD.

Cox model for clinical-pathological parameters effect on overall survival (OS)		
Covariate	**Hazard Ratio (95% CI)**	**P value**
Race		
White	Ref	
Black	1.70 (0.97, 2.99)	0.06
Stage at Diagnosis		
I/II	Ref	
III	1.84 (1.02, 3.33)	0.04

Tumor Size		
< 1.0 cm	Ref	
> 1.0 cm	0.84 (0.46, 1.54)	0.57
Comorbidity Count	1.39 (1.13, 1.71)	<0.01
Lymphovascular Invasion		
Absent	Ref	
Present	2.67 (1.41, 5.07)	<0.01
Pelvic Washing Cytology		
Negative	Ref	
Positive	2.04 (1.18, 3.53)	0.01
Cox model for clinical-pathological parameters effect on endometrial cacner spedicf death (ECSD)		
Covariate	**Hazard Ratio (95% CI)**	**P value**
Race		
White	Ref	
Black	1.60 (0.81, 3.15)	0.18
Tumor Size		
<1.0 cm	Ref	
> 1.0 cm	0.76 (0.37, 1.55)	0.45
Lymphovascular Invasion		
Present	Ref	
Absent	5.51 (2.73, 11.14)	<0.01
Pelvic Washing Cytology		
Negative	Ref	
Positive	1.66 (0.83, 3.31)	0.15
Guideline Concordant Treatment		
Yes	Ref	
No	1.68 (0.49, 5.73)	0.41
Comorbidity Count	1.41 (1.09, 1.82)	<0.01
Body Mass Index		
< 25.0	Ref	
> 25.0	1.64 (0.65, 4.16)	0.30

Conclusions: Pelvic washing is an important prognostic tool that may have a significant impact on overall survival in uterine serous carcinoma. Lymphovascular invasion and comorbidity count using CCI may also provide additional tools for prognosis.

568 Reconsideration of Under-Diagnosed and Under-Reported Early Stage Placental Mesenchymal Dysplasia

Masaharu Fukunaga, Shin-Yurigaoka General Hospital, Kawasaki, Japan

Disclosures: Masaharu Fukunaga: None

Background: Placental mesenchymal dysplasia (PMD) can be clinically and macroscopically mistaken for partial mole (PM) or complete mole (CM) with a twin. Early stage PMD is very rare but may be both under-diagnosed and under-reported. Androgenetic-biparental mosaicism has been the most consistent molecular alteration observed patients with PMD.

Design: In order to reconsider for microscopic features, complications, and differential diagnoses of early PMD, 825 cases of hydropic placental tissue, all of which were in the first trimester, were histopathologically reviewed and an immunohistochemical study of p57 (Kip2) (p57) and TSSC3, both of which are products of paternally imprinted, maternally expressed genes, was also conducted.

Results: Eight cases of pure PMD, 4 cases of twins with PMD and CM and 13 case of PMD with mosaic CM were identified. Their initial histopathologic diagnoses were hydropic abortion in 14 cases, PM in 9, twins with CM in 2 and PMD in 0. Early-stage pure PMD and PMD component in twins with CM were histologically characterized by moderate swelling of stem villi with cistern formation, dilated veins, mild vascular proliferation, mild stromal cell proliferation, myxoid changes, and the absence of trophoblastic hyperplasia. In cases of PMD with mosaic CM, many villi were characterized by mixed of PMD and CM morphologies, and fetal parts were observed in 4 cases. There was a discordant pattern of p57 expression, with positive staining in villous cytotrophoblasts and negative stromal cells, indicating a mixture of androgenetic and biparental cells, in all cases. TSSC3 was positive for cytotrophoblast and negative for stromal cells in PMD and PMD components. TSSC3 was negative for cytotrophoblast in CM and CM components. A patient with twins with PMD and CM developed persistent trophoblastic disease.

Conclusions: PMD can be clinically or pathologically misdiagnosed. This study showed that pure early PMD was relatively rare and PMD was often complicated by CM. PMD and CM components are easily under-diagnosed and more than half of fetuses with PMD lesions may be aborted in the first trimester. Immunohistochemical examinations of p57 and TSSC3 expressions are useful for differential diagnosis in PMD and mosaic cases. It is important to identify PMD or CM components at an early stage to reduce the risk of fetal morbidity, mortality or persistent trophoblastic disease. Patients with twins with PMD and CM, or PMD with mosaic CM should be followed-up with human chorionic gonadotropin monitoring.

569 BAP1 and Claudin 4 Expression in Ovarian Carcinomas

Zeina Ghorab[1], Dina Bassiouny[1], Ekaterina Olkhov-Mitsel[2], Sharon Nofech-Mozes[1]
[1]Sunnybrook Health Sciences Centre, University of Toronto, Toronto, Canada, [2]Sunnybrook Health Sciences Centre, Toronto, Canada

Disclosures: Zeina Ghorab: None; Dina Bassiouny: None; Ekaterina Olkhov-Mitsel: None; Sharon Nofech-Mozes: None

Background: Differentiating ovarian carcinoma from malignant mesothelial proliferation is a common challenging task for pathologists because a significant subset of ovarian carcinoma patients are diagnosed with advanced stage. Loss of BRCA1-associated protein 1 (BAP1), a tumor suppressor gene, has been recently described as a highly specific and sensitive marker for malignant mesothelioma. Unlike other carcinoma markers, Claudin 4 is a broad spectrum carcinoma marker that does not cross react with mesothelial cells. We study the expression of BAP1 and Claudin 4 in a large set of ovarian carcinomas.

Design: BAP1 (Sc-28383, Santa Cruz) and Claudin 4 (AC13121B, Biocare) immunohistochemistry was studied in tissue microarrays containing archival tissue from resection specimens of 692 ovarian carcinomas. Nuclear staining for BAP1 was scored as lost (complete absence of nuclear staining in tumor cells with retaining of variable immunostaining in non-neoplastic cells), positive/retained (>1%, any intensity) or equivocal (no nuclear staining in tumor but absent internal control). Equivocal or lost cases were further assessed on full sections. Membranous staining for Claudin 4 was scored as negative, low positive (1-10%) or positive (>10%).

Results: Our data set included 692 ovarian carcinomas with 687 available tumor tissue for BAP1 scoring and 681 cases for Claudin 4. After assessing 20 equivocal cases on full sections, BAP1 was retained in all the cases. Claudin 4 was positive/low positive in 371/416 (89.2%) of high grade (HG) serous, 25/34 (73.5%) low grade (LG) serous, 55/56 (98.2%) HG endometrioid, 32/37 (86.5%) LG endometrioid, 93/98 (94.9%) Clear cell and 39/40 (97.5%) mucinous carcinomas (Table 1).

Table 1: BAP1 and Claudin 4 immunohistochemistry by histologic subtype:

Histologic type	Number of cases	BAP1		Claudin 4			
		Retained	N/A	Negative	Low Positive(+)	Positive	N/A
HG Serous	426	422	4	45	45	326	10
LG Serous	35	35	0	9	10	15	1
HG Endometrioid	56	56	0	1	3	52	0
LG Endometrioid	37	36	1	5	3	29	0
Clear cell	98	98	0	5	2	91	0
Mucinous	40	40	0	1	0	39	0
Total (%)	692	687(99.3)	5	66 (9.7)	63 (9.3)	552 (79.8)	11(1.6)

N/A= not available

Conclusions: BAP1 and claudin 4 are positive in 100% and 89.1% of ovarian carcinomas, respectively. This observation further consolidates their role as adjunct diagnostic tool when ovarian carcinomas need to be distinguished from malignant mesotheliomas.

570 Low-Grade Endometrial Endometrioid Adenocarcinomas with MELF Pattern Invasion Harbor ARID1A Mutations

Evan Goyette[1], Laura Tafe[1], Donald Green[1], Sophie Deharvengt[1], Kimberly Winnick[1], Gregory Tsongalis[2], Kristen Muller[1], Jessica Dillon[1]
[1]Dartmouth-Hitchcock Medical Center, Lebanon, NH, [2]Dartmouth Geisel School of Medicine, Lebanon, NH

Disclosures: Evan Goyette: None; Laura Tafe: None; Donald Green: None; Sophie Deharvengt: None; Kimberly Winnick: None; Gregory Tsongalis: None; Kristen Muller: None; Jessica Dillon: None

Background: Endometrial endometrioid adenocarcinoma (EC) is the most common primary malignancy of the gynecologic tract. Historically, patients with low-grade tumors identified in early stage disease exhibit an excellent prognosis. However, studies have shown that low-grade EC with a microcystic, elongated and fragmented glands (MELF) pattern of myometrial invasion frequently present with nodal metastasis and are more likely to recur. Therefore, recognition of this subtle, and often focal, pattern of invasion is important for clinical management. Kir *et al* recently published an immunohistochemical study which demonstrated an association between ARID1A loss and MELF pattern invasion, but the molecular underpinnings of these tumors remain poorly understood. Herein, we report the genetic alterations found in a series of EC with MELF pattern invasion, including, but not limited to, *ARID1A* mutation status.

Design: Ten consecutive cases of EC with MELF pattern invasion were retrospectively selected from the Pathology archives. Patient demographics and pertinent clinicopathologic data were gathered for all cases and MELF pattern invasion was separately confirmed by two gynecologic pathologists. Invasive tumor nests were macrodissected from FFPE slides and next-generation sequencing was performed using the Illumina TruSight Tumor 170 gene panel. Data analysis was performed using the TST170 Local App v1.0.1 (Illumina). Ten consecutive cases of EC without MELF pattern invasion are currently being analyzed as a control group.

Results: Nine cases (9/10, 90%) showed *ARID1A* alterations, with 12 unique nonsense/frameshift variants identified. Eight of those cases (8/9, 89%) harbored *PTEN* variants that co-occurred with *PIK3CA* or *PIK3R1* alterations, indicating concurrent dysregulation of the PI3K pathway in these tumors. Additionally, *KRAS* and *CTNNB1* variants were identified in four of these tumors (*KRAS* 2/9, 22%; *CTNNB1* 2/9, 22%). One case (1/10, 10%) did not display *ARID1A* variants but did show PI3K pathway alterations, as well as *MSH3* (Table 1).

Table 1. Mutational status and clinicopathologic data of 10 EC with MELF pattern invasion (VAF - variant allele fraction).

Case	Age	Diagnosis	Tumor Size (cm)	FIGO Grade	FIGO Stage	Nodal Involvement	Isolated Tumor Cells	Mutations (VAF)
1	63	EC with squamous differentiation	2.8	1	IIIC1	1 of 9	Present (1 of 9)	TSC2 (26%)
								MSH3 (21%)
								ARID1A (11%)
								PIK3CA (11%)
								PTEN (10%)
								ATM (10%)
								KRAS (9%)
2	57	EC with squamous differentiation	4.5	1	IIIC1	1 of 8	Absent	PTEN (18%)
								ARID1A (9%)
								KRAS (9%)
								PIK3R1 (9%)
								PIK3CA (8%)
3	67	EC with squamous and mucinous differentiation	3.5	1	IIIC1	3 of 3	Absent	PTEN (12%)
								PIK3CA (10%)
								ARID1A (8%)
								HNF1α (8%)
								GNAS (7%)
								EP300 (6%)
4	59	EC	5.5	1	IIIC1	2 of 10	Absent	ARID1A (38%)
								PIK3CA (23%)
								PTEN (14%)
								CCND1 (12%)
								FBXW7 (12%)
5	61	EC with squamous and mucinous differentiation	7.5	1	IIIC1	1 of 7	Present (2 of 7)	ARID1A (10%)
								RB1 (5%)
6	53	EC with squamous and secretory differentiation	7.1	2	IIIC1	4 of 4	Absent	PIK3R1 (25%)
								MYC (20%)
								RPS6KB1 (13%)
								PTEN (11%)
								FBXW7 (11%)
								MSH3 (10%)
								ARID1A (9%)
								RB1 (9%)
								CTNNB1 (8%)
7	73	EC with squamous differentiation	4.5	1	IA	0 of 13	Absent	ARID1A (22%)
								PTEN (21%)
								PIK3R1 (10%)
								PIK3CA (10%)
								CTNNB1 (9%)
8	70	EC	3.4	1	IIIC1	1 of 4	Absent	PTEN (10%)

								ALK (7%)
								PIK3R1 (7%)
								KMT2A (6%)
								ARID1A (5%)
9	63	EC with mucinous differentiation	2.8	1	IB	0 of 2	Absent	PTEN (10%)
								PIK3R1 (9%)
								ARID1A (8%)
10	54	EC	5.5	1	IIIC1	1 of 1	Absent	PTEN (35%)
								MSH3 (23%)
								PIK3R1 (12%)
								KDR (11%)
								FGFR2 (9%)
								PIK3CA (7%)

Conclusions: In our cohort, truncating *ARID1A* variants were identified in 90% of EC with a MELF pattern of myometrial invasion. To our knowledge, this is the first study to characterize *ARID1A* at the molecular level in low-grade EC with MELF pattern invasion. These findings support molecular classification of EC as an emerging tool for better risk stratification and selection of molecularly informed therapies.

571 HMGA2 Overexpression is Common in a Hypercellular Sclerosing Variant of Leiomyoma

Brannan Griffin[1], Jean Fischer[2], Debabrata Chakravarti[2], Jian-Jun Wei[3]
[1]The University of Texas MD Anderson Cancer Center, Houston, TX, [2]Feinberg School of Medicine/Northwestern University, Chicago, IL, [3]Northwestern University, Chicago, IL

Disclosures: Brannan Griffin: None; Jean Fischer: None; Jian-Jun Wei: None

Background: HMGA2 overexpression is the 2nd most common molecular alteration in leiomyoma and has been identified in certain histologic variants, including hydropic leiomyoma and intravenous leiomyomatosis. Leiomyomas with HMGA2 overexpression are characteristically large and fast growing tumors with increased clinical burden. Pathology diagnosis is complicated by overlapping histologic features with other mesenchymal entities, such as endometrial stromal tumors and cellular leiomyoma. In this study, we describe and analyze a hypercellular sclerosing variant of leiomyoma highly related to HMGA2 overexpression.

Design: In our previous large study cohort of randomly selected leiomyomas, 10% demonstrated HMGA2 overexpression. Further analysis of these select leiomyomas showed distinct histology: increased vascularity, hydropic variant, and a hypercellular sclerosing variant. We collected 30 leiomyomas with hypercellular and sclerosing/hyaline features and analyzed their clinical parameters, histomorphology, and IHC profile. Material from 20 cases was available for *HMGA2* mutation analysis by FISH (12q14.3 break apart probe) and RT-PCR.

Results: Diagnosis of hypercellular sclerosing leiomyoma (HSLM) was based on diffuse presence of hypercellularity and sclerosis/hyalinization. Leiomyomas with HMGA2 overexpression that showed diagnostic criteria for hydropic leiomyoma were excluded. Clinical features of HSLM included: avg age 45.4 years (range 26-75); avg tumor size 11.9 cm (range 1-28); and anatomic locations cervix (2), uterine submucosal (7), uterine intramural (14), uterine serosal (6), intrapelvic/intra-abdominal (1). 20/30 patients, 66%, required definitive surgery (hysterectomy/resection). Histology demonstrated tumor cells with small, round-oval nuclei and pinpoint nucleoli; arranged in hypercellular sheets and cords with frequent streaming, disorganization and only vague fascicles. Background elements included well-formed dense pink collagen forming bands of sclerosis and nodules/balls separating tumor cell groups ("mosaic pattern"; Figure 1), and increased vascular density (avg 13.5 thick-walled vessels /10x-mpf (range 3-29)). Data of select IHC, FISH, and RT-PCR are summarized in Table 1, with usual-type leiomyomas as controls.

Table 1. Select immunohistochemistry and molecular analysis of hypercellular sclerosing leiomyoma (HSLM) and usual-type leiomyoma (ULM).

	Desmin IHC	HMGA2 IHC	*HMGA2* FISH	*HMGA2* RT-PCR
HSLM (n=30)	Positive: 30/30 (100%) Negative: 0/30 (0%)	Positive: 28/30 (93%) Negative: 2/30 (7%)	Positive: 5/20 (25%) Negative: 15/20 (75%)	*HMGA2* upregulation*, 5-80 fold: 15/17 (88%) *vs. matched myometrium
ULM (n=21)	Positive: 21/21 (100%) Negative: 0/30 (0%)	Positive: 2/21 (10%) Negative: 19/21(90%)	Positive: 0/6 (0%) Negative: 0/6 (100%)	N/A

Figure 1 - 571

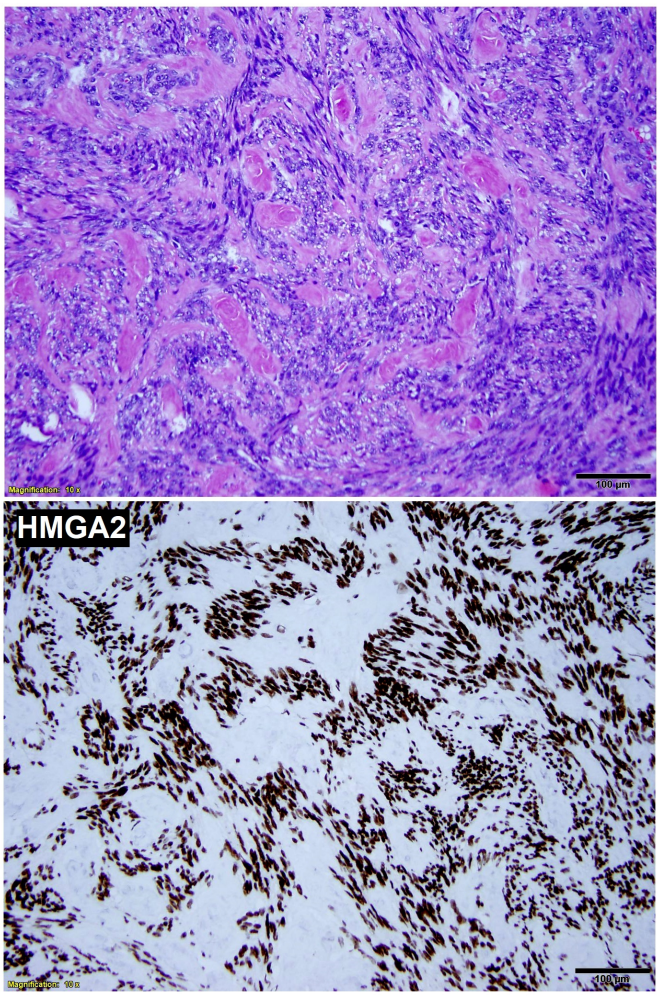

Conclusions: HSLM demonstrates specific histologic features and a strong relation to HMGA2 overexpression. Similar to other HMGA2-related leiomyomas, HSLMs are relatively large tumors with increased clinical burden often requiring definitive surgery. The differential diagnosis includes cellular leiomyoma, endometrial stromal tumors with sclerosis/hyalinization and, reasonably, smooth muscle tumor of uncertain malignant potential. Our findings aid the recognition of HSLM and add to the spectrum of leiomyomas with HMGA2 overexpression. Pathology identification of these leiomyomas may help optimize clinical management.

572 Evaluation of HER2 Expression in Gynecologic Cancers: An Oncologic Institutional Experience

Brannan Griffin[1], Anais Malpica[1], Barrett Lawson[1]
[1]*The University of Texas MD Anderson Cancer Center, Houston, TX*

Disclosures: Brannan Griffin: None; Anais Malpica: None; Barrett Lawson: None

Background: HER2 testing of gynecologic cancers (Gyn CA) is currently performed and interpreted according to the ASCO/CAP 2018 guidelines for breast carcinoma. Gyn CA demonstrate poor correlation between HER2 protein expression and gene amplification, as well as intratumoral heterogeneity, which confound pathology interpretation and results vital for clinical management. This study reviews and assesses HER2 testing results on Gyn CA at a major oncology treatment center.

Design: We retrospectively searched our pathology database from 2000 to 2020 for Gyn CA cases with HER2 testing, including immunohistochemistry (IHC) and/or in situ hybridization (ISH). 246 total cases were identified. Data recorded included: age, histotype, tumor primary and tested sites, reported IHC and FISH results (updated to the 2018 guidelines with hybridization groups), and anti-HER2 therapy status. For cases with materials available for review, IHC was evaluated for confirmatory score, cell membrane staining patterns and variability in intensity, and distribution of tissue staining. Intratumoral heterogeneity was determined by IHC score in two ways: tumor displaying on a single slide 1) a difference of 1 point and 2) a difference of 2 points.

Results: Clinical data is displayed in Table 1. Reported IHC for 238 cases showed scores: “negative” (52, 22%); 0 (73, 31%); 1+ (45, 19%); 2+ (43, 18%); 3+ (25, 10%). IHC was available for review on 29 cases on which FISH was performed and showed scores: 0 (7, 24%); 1+ (2, 7%); 2+ (17, 59%); 3+ (3, 10%). In 11/29 cases (38%), tumors displayed areas of higher IHC intensity in a percentage below threshold to upgrade the overall score. 3 cases scored 2+ had areas of 3+ intensity and basolateral staining pattern (Fig. 1); 2 of the 3 showed *HER2* amplification by FISH. IHC review for all cases is ongoing. For the 29 cases, average cell membrane staining was 50% (range 0-85%). IHC tumor staining distribution was: none (2), focal (5), patchy (9), diffuse (13). Amongst the 29 cases, 23 (79%) demonstrated intratumoral heterogeneity by 1 point difference and 13 by 2 point difference (45%) (Fig. 2). FISH results were available for 48 cases and were: negative (37, 77%); positive (10, 21%). The remaining case showed genetic heterogeneity with a non-amplified area (95% of tumor) and amplified area (5% discrete tumor population). In the 10 amplified cases, the average *HER2* signal, CEP17 signal, and *HER2*:CEP17 ratio were 7.7, 3.4, and 2.3, respectively. For 45/48 cases, information available to classify hybridization groups revealed: Group 1 (5); Group 2 (1); Group 3 (4); Group 4 (6); Group 5 (28); while the heterogeneous case was mixed Groups 1 and 2.

Characteristic	N(%)
Age, median yrs (range)	60 (27-83)
Primary site	
Uterus	103 (42%)
Ovary	128 (52%)
Fallopian tube	8 (3%)
Peritoneum	7 (3%)
Histotype	
Uterine Serous Carcinoma	46 (19%)
Extrauterine High Grade Serous Carcinoma	100 (41%)
Low Grade Serous	10 (4%)
Serous Borderline Tumor	2 (1%)
Uterine Mixed Carcinoma	28 (11%)
Ovarian Mixed Carcinoma	15 (6%)
Uterine Carcinosarcoma	15 (6%)
Ovarian Carcinosarcoma	2 (1%)
Ovarian Mucinous Carcinoma	1 (0.5%)
Endometrial Endometrioid Adenocarcinoma	2 (1%)
Ovarian Endometrioid Adenocarcinoma	1 (0.5%)
Ovarian Clear Cell Carcinoma	3 (1%)
Uterine Clear Cell Carcinoma	2 (1%)
Other	19 (8%)
Site tested for HER2 status	
Primary	68 (27%)
Metastasis	122 (50%)
Unknown	56 (23%)
Treated with anti-HER2 therapy	6 (2%)

Figure 1 - 572

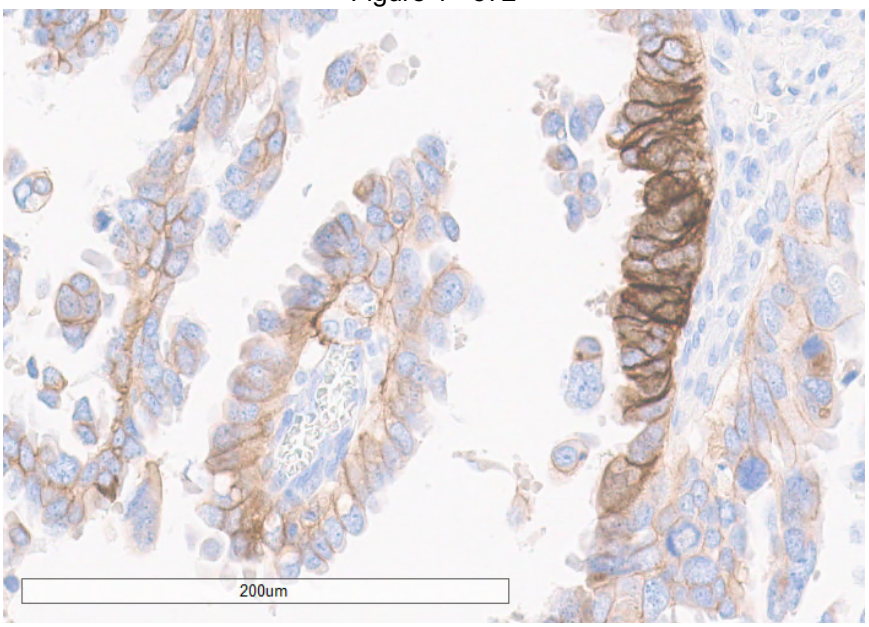

Figure 2 - 572

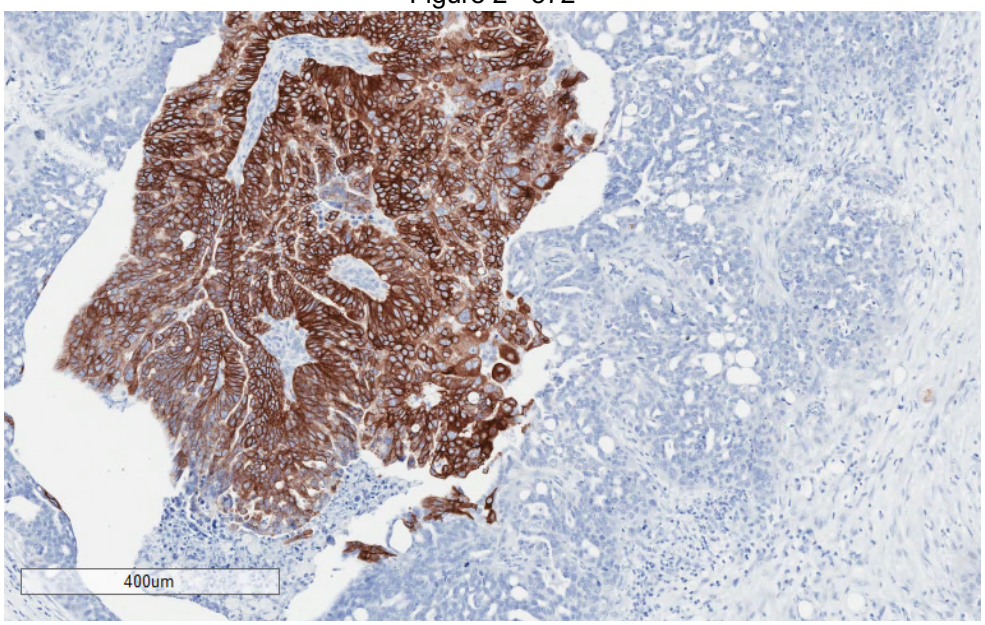

Conclusions: Our findings support HER2 expression heterogeneity in Gyn CA. Patients with *HER2* amplification may be candidates for targeted therapy. More studies are warranted to assess accurate HER2 testing interpretation and the utility of the 2018 guidelines in this specific population.

573 Prognostic Impact of Tumor Microenvironment in Carcinosarcoma of the Female Genital Tract: A Study of CD8+ Tumor Infiltrating Lymphocytes and Programmed Death-Ligand 1 (PD-L1) Expression

Jose Manuel Gutierrez Amezcua[1], Jeffrey Ordner[2], Pratibha Shukla[3]
[1]New York University Medical Center, New York, NY, [2]New York University Langone Health, New York, NY, [3]NYU School of Medicine, New York, NY

Disclosures: Jose Manuel Gutierrez Amezcua: None; Jeffrey Ordner: None; Pratibha Shukla: None

Background: Carcinosarcoma (CS) of the female genital tract is an uncommon and highly aggressive malignancy which lacks effective therapeutic strategies and has poor prognosis. Tumor immune microenvironment (TME) profiles of various cancers based on PD-L1 expression and tumor-infiltrating lymphocytes (TILs) have been shown to affect prognosis. We aimed to investigate the prognostic significance of PD-L1 expression and CD8 positive TILs in CS cases treated at our Institution.

Design: A total of 81 cases: 68 uterine (84%), 10 ovarian (12.3%), 1 fallopian tube (1.2%) and 2 primary peritoneal (2.5%) were identified from our Pathology Department database after IRB approval. Pathology slides from all cases were reviewed, original diagnosis was confirmed and areas with the highest TILs were identified. 3 mm tissue microarrays were constructed from formalin-fixed, paraffin embedded tissue from areas with highest TILs and immunostaining for PD-L1 and CD8 was performed. PD-L1 was scored using Tumor Proportion Score (TPS) and Combined Positive Score (CPS) with either TPS or CPS ≥1 considered positive. Cases were classified as CD8- (< 5 CD8+ TILs/hpf), CD8+ (≥5 CD8+ TILs/hpf) and $CD8^{HIGH}$ (>25 CD8+ TILs/hpf). We further subclassified the cases into four TME groups based on PD-L1 expression and CD8+ TILs: 1) PD-L1+/CD8+, 2) PD-L1+/CD8-, 3) PD-L1-/CD8+ and 4) PD-L1-/CD8- (Fig. 1). Clinical follow-up data was obtained from medical charts. Kaplan-Meier curves with log rank test were used to compare overall survival.

Results: Median overall survival was 37.4 months (range: 1-176 months). PD-L1 expression in tumor tissue (TPS) and microenvironment (CPS) was detected in 19.8% and 39.6% of cases, respectively. PD-L1 expression alone was not associated with difference in overall survival (p=0.28). In contrast, higher numbers of CD8+ TILs were associated with better survival (p=0.054 for ≥5 CD8+ TILs/hpf and p=0.019 for >25 CD8+ TILs/hpf, Fig. 2A,B). Among the TME groups, the PD-L1+/CD8+ group showed better survival compared to those with PD-L1-/CD8- (p=0.05, Fig. 2C,D).

Figure 1 - 573

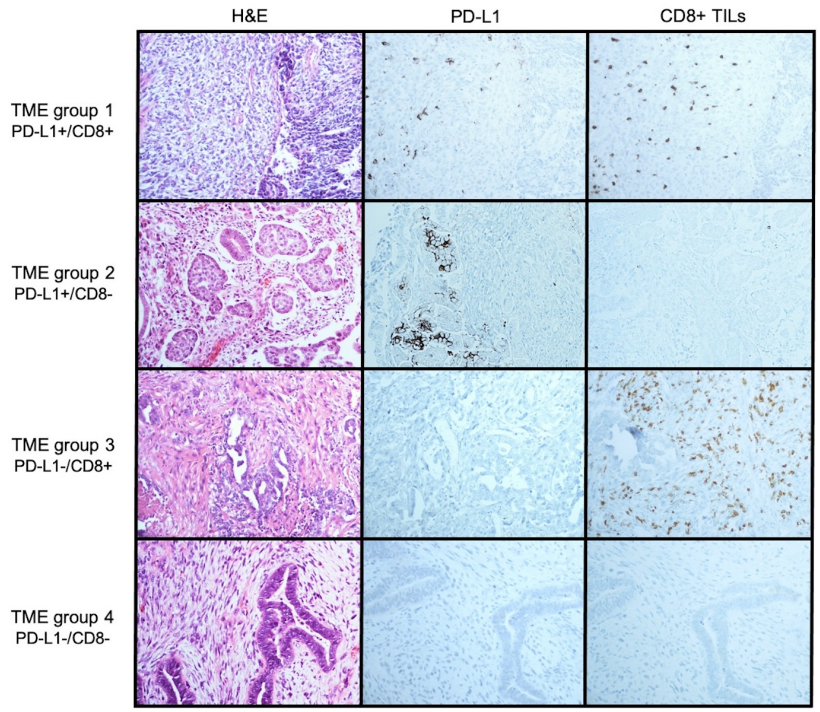

Figure 2 - 573

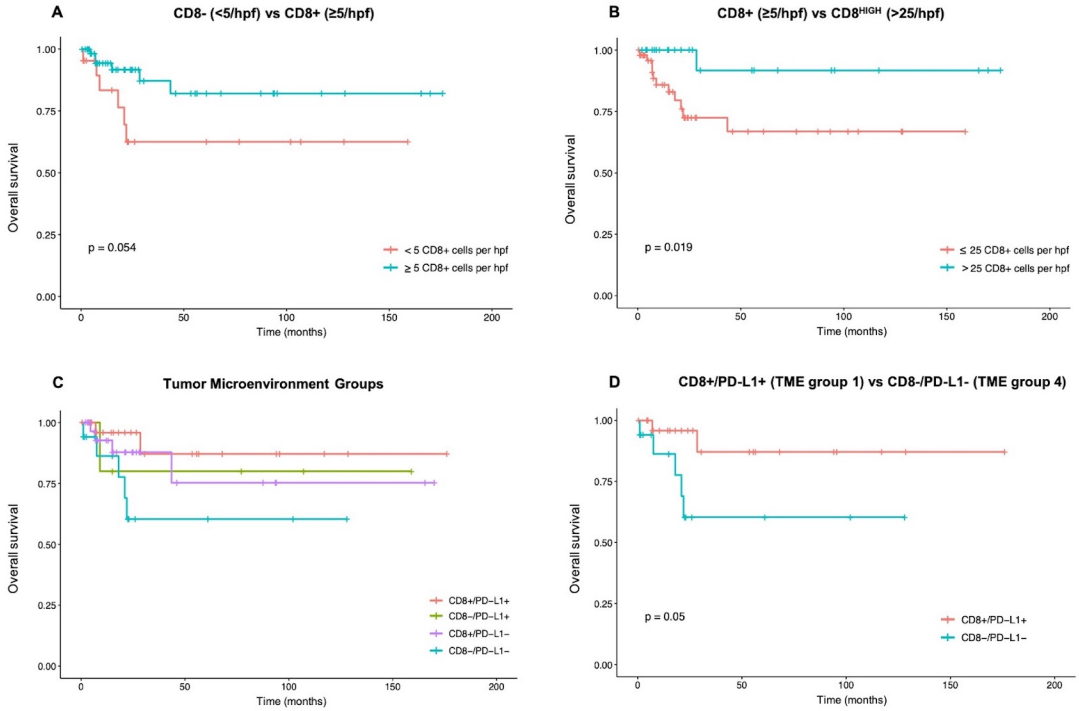

Conclusions: Our study found that higher numbers of CD8+ TILs are associated with significantly better survival in patients with CS. Although PD-L1 expression alone does not seem to impact survival, patients with expression of PD-L1 and high CD8+TILs have a survival advantage over those with negative PD-L1 and low CD8+TILs. These preliminary findings suggest TME has prognostic implications in patients with CS of the female genital tract.

574 Molecular Classification of Endometrial Carcinomas with Long-Term Follow-up

Phoebe Hammer[1], James Albro[2], Cheri Squires[3], Grace Peters-Schulze[4], Brittany Sharp[3], Vivek Charu[1], Melissa Cessna[5], Brooke Howitt[1]
[1]Stanford Medicine/Stanford University, Stanford, CA, [2]Intermountain Biorepository, Murray, UT, [3]Intermountain Biorepository, Salt Lake City, UT, [4]Stanford University, Stanford, CA, [5]Intermountain Medical Center, Murray, UT

Disclosures: Phoebe Hammer: None; Cheri Squires: None; Grace Peters-Schulze: None; Brittany Sharp: None; Vivek Charu: None; Melissa Cessna: None; Brooke Howitt: None

Background: Molecular classification of endometrial carcinoma using The Cancer Genome Atlas (TCGA) categories (POLE-mutated, microsatellite instability (MSI), copy number high/serous-like (p53 abnl), and no specific molecular profile (NSMP)) adds prognostic value in the pathologic evaluation. However, long-term survival data is limited. We report the clinical, histologic, immunophenotypic, and molecular features of a cohort of endometrial carcinomas with extended (minimum 10 years) follow-up.

Design: Endometrial endometrioid carcinomas (EEC) with a minimum follow-up period of 10 years were identified in the Intermountain Biorepository and included in this study (pilot cohort=176 cases). Patient age, BMI, histologic grade, stage, recurrence-free survival and overall survival were recorded. All cases underwent sequencing of 14 POLE exonuclease domain mutations. Immunohistochemistry (IHC) for MSH6, PMS2, MSH2, MLH1, and p53 were performed on tissue microarray sections while beta-catenin, estrogen receptor (ER), and progesterone receptor (PR) were performed on whole sections. Disease-specific survival (DSS) and recurrence-free survival (RFS) were analyzed using Kaplan-Meier curves and log rank test.

Results: We classified EECs into four molecular subgroups: POLE-mutated (10%, n=18), MSI (30%, n=52), p53 abnormal (3%, n=6), and NSMP (57%, n=100). Age at presentation and BMI varied depending on molecular classification, with POLE-mutated tumors generally presenting at younger age with lower BMI (Table 1). Disease-specific and recurrence-free survival plots are shown in Figures 1-2. In the POLE EECs (n=18), 3 tumors also had abnormal p53 expression (17%). Within the MSI group, 5 had abnormal p53 expression (10%); of these, 2 died of disease while 3 were alive with no evidence of disease. The MSI group was enriched for ER/PR negativity, with 3 EEC (2% overall) showing <10% positivity for ER, all within the MSI subgroup, and 9 EEC (5% overall) showing <10% positivity for PR (5 MSI, 3 NSMP, 1 p53 abnl). 78% of stage 3-4 NSMP EECs had abnormal (nuclear) beta-catenin expression in contrast to 53% of stage 1-2 NSMP EEC; however beta-catenin expression was not associated with significantly different RFS or DSS.

Total=176 endometrioid endometrial carcinomas				FIGO Stage				FIGO Grade		
	Number (%)	Mean age (range)	Median BMI (range)	1	2	3	4	1	2	3
POLE	18 (10%)	56.9 (32-72)	27.5 (23-47.7)	13 (72%)	3 (17%)	2 (11%)	0 (0%)	8 (44%)	6 (33%)	4 (22%)
MSI	52 (30%)	61.7 (43-90)	31.9 (21.5-60.1)	35 (67%)	9 (17%)	8 (15%)	0 (0%)	28 (54%)	19 (36%)	5 (10%)
P53 abnl	6 (3%)	63.3 (55-74)	33.7 (17-44.8)	3 (50%)	0 (0%)	1 (17%)	2 (33%)	1 (17%)	0 (0%)	5 (83%)
NSMP	100 (57%)	60.3 (32-90)	33.8 (18.7-65.2)	74 (74%)	12 (12%)	11 (11%)	3 (3%)	82 (82%)	13 (13%)	5 (5%)

Figure 1 - 574

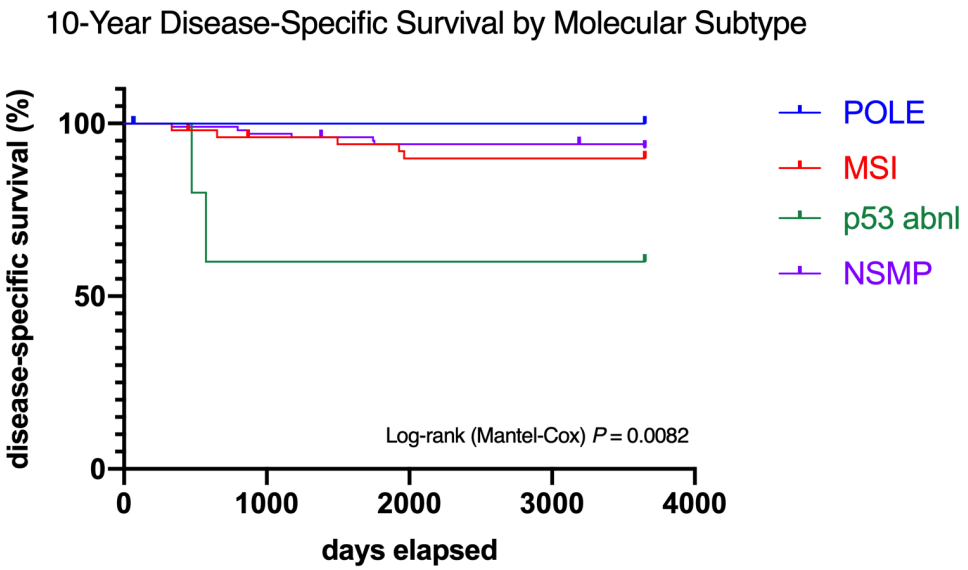

10-year DSS rates: *POLE*: 100%, MSI: 90%, p53 abnl: 60%, NSMP: 93%

Figure 2 - 574

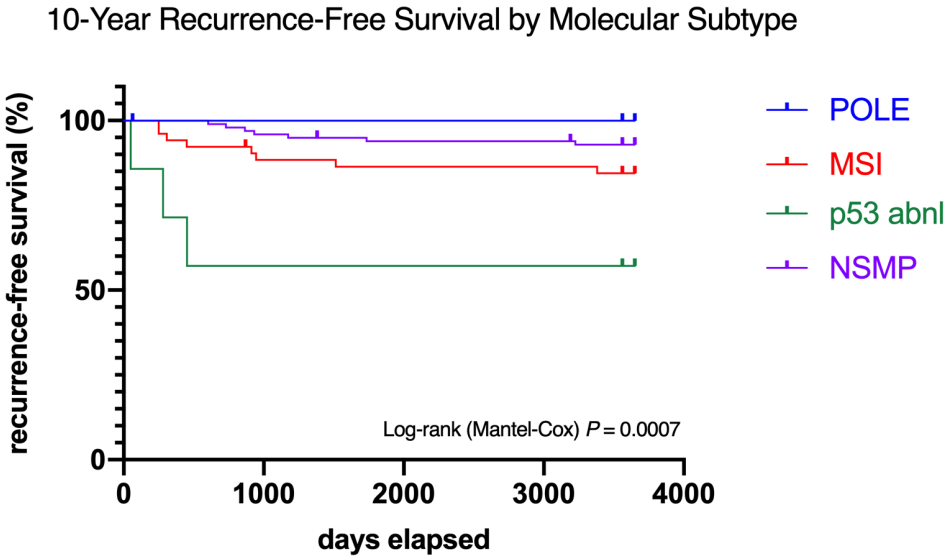

10-year RFS rates: *POLE*: 100%, MSI: 84%, p53 abnl: 53%, NSMP: 93%

Conclusions: This study highlights the clinicopathologic and long-term prognostic significance of molecular classification in EEC, particularly for the p53 abnormal subgroup. Expansion of this study is ongoing to determine long-term outcomes and prognostic significance within POLE, MSI, and NSMP groups.

575 DNA Mismatch Repair Deficient Non-Neoplastic Endometrial Glands are Common in Lynch Syndrome Patients and Present at a Higher Density Compared to Colorectal Mucosa

Shaymaa Hegazy[1], Beth Dudley[1], Eve Karloski[1], Randall Brand[1], Rohit Bhargava[2], Esther Elishaev[2], Reetesh Pai[3]
[1]University of Pittsburgh, UPMC, Pittsburgh, PA, [2]UPMC Magee-Womens Hospital, Pittsburgh, PA, [3]UPMC Presbyterian Hospital, Pittsburgh, PA

Disclosures: Shaymaa Hegazy: None; Beth Dudley: None; Eve Karloski: None; Randall Brand: None; Rohit Bhargava: *Advisory Board Member*, Eli Lilly & Company; Esther Elishaev: None; Reetesh Pai: None

Background: Lynch syndrome (LS) is the most common hereditary cancer syndrome. However, distinguishing between LS and sporadic DNA mismatch repair (MMR) deficiency can be challenging. In women with LS, the incidence of endometrial cancer equals or exceeds that of colorectal cancer, and up to 40-60% of women initially present with gynecologic tract cancer. Recently, MMR deficiency of non-neoplastic colonic crypts has been identified as a novel indicator of LS. The aim of this study was to determine if MMR deficient non-neoplastic endometrial glands can help to distinguish between patients with or without LS and to compare the density of MMR deficiency in non-neoplastic glands in the endometrium versus colon in LS patients.

Design: We evaluated the immunohistochemical expression of MMR proteins in normal endometrial mucosa from 64 patients including 34 confirmed LS (17 with endometrial cancer and 17 without cancer), and 30 patients with endometrial cancer without LS (10 with tumors with MLH1 promoter hypermethylation and 20 with MMR proficient tumors). We compared the pattern of MMR deficiency in LS in normal endometrial mucosa (N=34) and normal colonic mucosa (N=30).

Results: MMR deficient non-neoplastic endometrial glands were identified in 16 of 34 (47%) LS patients, compared to 0 of 30 (0%) patients without LS (including 0/10 sporadic MLH1 deficient endometrial cancer due to MLH1 promoter hypermethylation, and 0/20 with MMR proficient endometrial cancer) (p <0.001). MMR deficient non-neoplastic endometrial glands were more often identified in LS patients with endometrial cancer (65%) compared to LS patients who had a risk-reducing hysterectomy without endometrial cancer (29%) (p=0.04). We identified

significant differences in the patterns of MMR deficiency in glands within normal endometrial and colorectal mucosa in LS patients. Compared to normal colorectal mucosa, MMR deficient glands in normal endometrial mucosa were mostly seen as contiguous groups of glands, ranging in number from 3 to 101 (87% vs. 45%, p=0.02). In LS patients, MMR deficient glands were identified at a higher density in normal endometrium compared to colonic mucosa (median number of MMR deficient glands 22 vs. 2, p=0.02).

Table. Patients with DNA Mismatch Repair (MMR) Protein Deficient Non-Neoplastic Endometrial Glands

Case Number	Cancer History	Tumor MMR Protein Expression 5252Pattern by IHC	Germline MMR Gene with Variant	Age at Diagnosis (years)	Estimated Number of Non-Neoplastic Endometrial Glands Evaluated	MMR Protein Evaluated by IHC	Number of MMR Deficient Non-Neoplastic Endometrial Glands by IHC	Percent of Endometrium with MMR Deficient Non-Neoplastic Endometrial Glands (%)	Pattern of MMR Deficient Non-Neoplastic Endometrial Glands (Solitary vs. Grouped)
1	Endometrium	MSH2/MSH6 loss	MSH2	40	400	MSH2	30	8	Grouped
2	Endometrium	MSH6 loss	MSH6	58	105	MSH6	82	78	Grouped
3	Endometrium	MSH2/MSH6 loss	MSH2	40	160	MSH2	96	60	Grouped
4	Endometrium and Colon	MSH2/MSH6 loss	MSH2	51	154	MSH2	13	8	Grouped
5	Endometrium and Colon	PMS2 loss	MLH1	62	138	PMS2	5	4	Grouped
6	Endometrium and Colon	MSH6 loss	MLH6	63	72	MSH6	51	71	Grouped
7	Endometrium	PMS2 loss	MLH1	48	105	PMS2	57	54	Grouped
8	Endometrium	MSH6 loss	MSH6	55	90	MSH6	1	1	Solitary
9	Endometrium	MSH6 loss	MSH6	72	15	MSH6	4	27	Grouped
10	Endometrium	MSH6 loss	MSH6	63	165	MSH6	5	3	Grouped
11	Endometrium	MSH6 loss	MSH6	68	21	MSH6	2	10	Grouped
12	None	Not applicable	MSH2	54	203	MSH2	53	26	Grouped
13	None	Not applicable	PMS2	58	161	PMS2	35	22	Grouped
14	None	Not applicable	MSH2	43	288	MSH2	101	35	Grouped
15	None	Not applicable	MSH6	37	330	MSH6	1	3	Solitary
16	None	Not applicable	PMS2	52	370	PMS2	3	8	Grouped

MMR, mismatch repair; IHC, immunohistochemistry

Figure 1 - 575

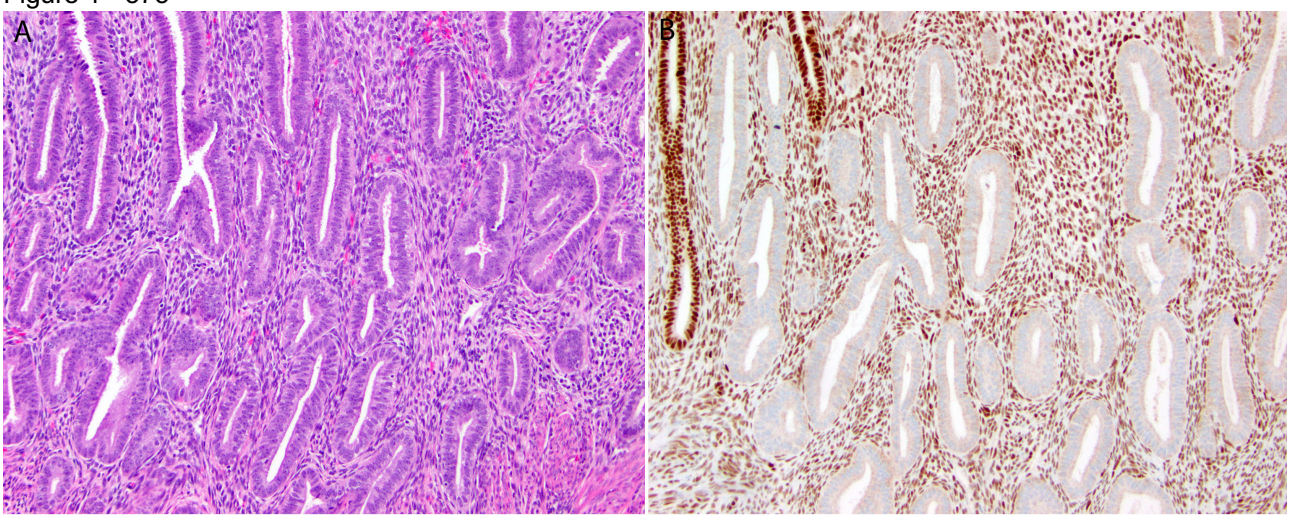

40 year old woman with a germline pathogenic variant in *MSH2* with hysterectomy performed for endometrial carcinoma. The non-neoplastic endometrium (A, 10x) demostrated a large focus of normal endometrial glands with loss of MSH2 expression by immunohistochemistry (B, MSH2 immunohistochemistry, 10x).

Conclusions: Our findings indicate that MMR deficient non-neoplastic endometrial glands are a reliable indicator of LS and can be a tool to distinguish LS from sporadic MMR deficiency. Compared to colorectal mucosa, MMR deficient glands in endometrial mucosa in LS patients are present at higher density and in a pattern of contiguous large groups of histologically normal glands.

576 Uterine Sarcomas With A Novel SS18-VEZF1 Fusion – Another Neoplasm in the Uterine Myxoid Neoplasm Differential Diagnosis

Anjelica Hodgson[1], Ryma Benayed[1], Marc Ladanyi[1], Matija Snuderl[2], Cathleen Matrai[3], Roger James[4], Alessandro Aldera[5], Kay Park[1], Cristina Antonescu[1], W. Glenn McCluggage[6], Sarah Chiang[1]
[1]Memorial Sloan Kettering Cancer Center, New York, NY, [2]New York University, New York, NY, [3]New York-Presbyterian/Weill Cornell Medical Center, New York, NY, [4]Cape Town, South Africa, [5]University of Cape Town, Cape Town, South Africa, [6]The Royal Hospitals/Queen's University of Belfast, Birmingham, United Kingdom

Disclosures: Anjelica Hodgson: None; Marc Ladanyi: None; Cathleen Matrai: None; Roger James: None; Alessandro Aldera: None; Kay Park: None; Cristina Antonescu: None; W. Glenn McCluggage: None; Sarah Chiang: None

Background: Myxoid uterine mesenchymal tumors often harbor gene fusions. Molecular testing may aid in the diagnostic evaluation of these neoplasms which often exhibit morphologic and immunohistochemical overlap. We describe the clinicopathologic features and fusion status of 2 myxoid uterine sarcomas with features of smooth muscle and endometrial stromal neoplasia harboring a novel *SS18-VEZF1* fusion.

Design: Two uterine sarcomas with myxoid matrix and hybrid features of smooth muscle and endometrial stromal neoplasia were studied. Available clinicopathologic data was recorded. RNA was extracted from microdissected formalin-fixed, paraffin-embedded tumor tissues and subjected to next generation RNA sequencing using the MSK-Fusion targeted assay. *SS18* and *VEZF1* break-apart fluorescence in situ hybridization (FISH) was performed.

Results: One patient was a 42 year old woman with symptomatic "fibroids" and infertility who underwent morcellated myomectomy. The tumor was rubbery and tan-white to yellow-pink. Histologically, spindled and ovoid cells with irregular hyperchromatic nuclei, prominent nucleoli (Fig. 1A) and foamy cytoplasm (Fig. 1B) were associated with a myxoid matrix, a mitotic index of 1/10 HPF, and lymphovascular invasion. The second patient was a 39 year old woman with symptomatic "fibroids" and abnormal uterine bleeding who underwent myomectomy and was initially diagnosed with a myxoid leiomyoma (Fig. 2A) at an outside hospital. She developed a recurrence in the abdominal scar 44 months later (Fig. 2B). The recurrent tumor had abundant myxoid stroma and was composed of infiltrative nodules and sex cord-like formations of uniform spindle cells with hyperchromatic oval to elongated nuclei and minimal cytoplasm (Fig. 2C). The mitotic index was 20/10 HPF. Hysterectomy was performed and the residual uterine tumor was morphologically similar to that seen previously. The immunohistochemical profile of both cases is shown in Table 1. Targeted RNA sequencing detected an *SS18-VEZF1* fusion (breakpoint: exon10-exon2) in each tumor; *SS18* and *VEZF1* rearrangements were confirmed by FISH.

	Case 1	Case 2
Desmin	Diffuse +	Diffuse +
h-caldesmon	-	-
CD10	Patchy +	-
Cyclin D1	Patchy +	Patchy +
Estrogen receptor	Patchy +	- (myomectomy/scar)/ Diffuse + (hysterectomy)
TLE1	Patchy +	Patchy +

Figure 1 - 576

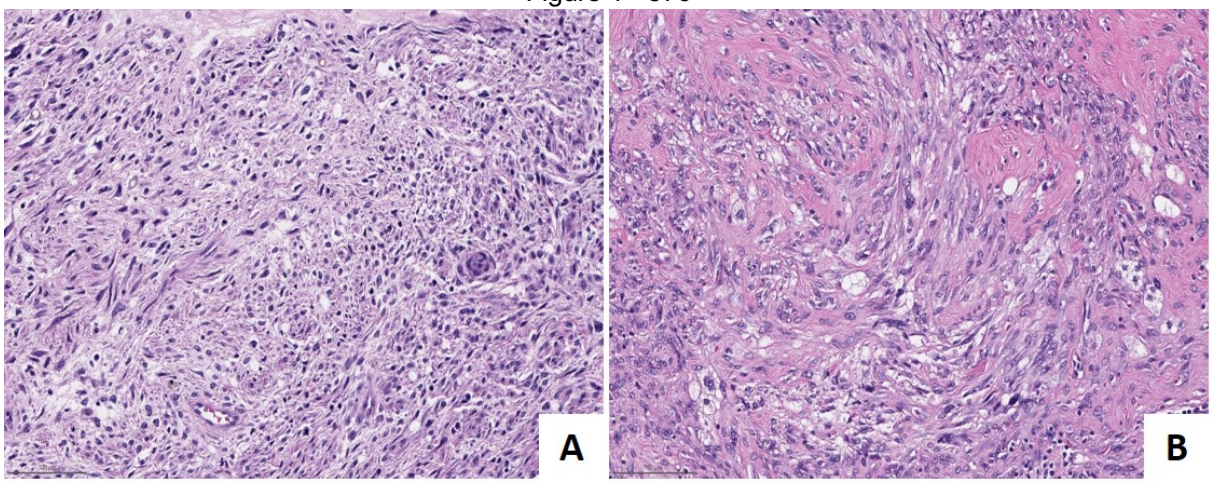

Figure 2 - 576

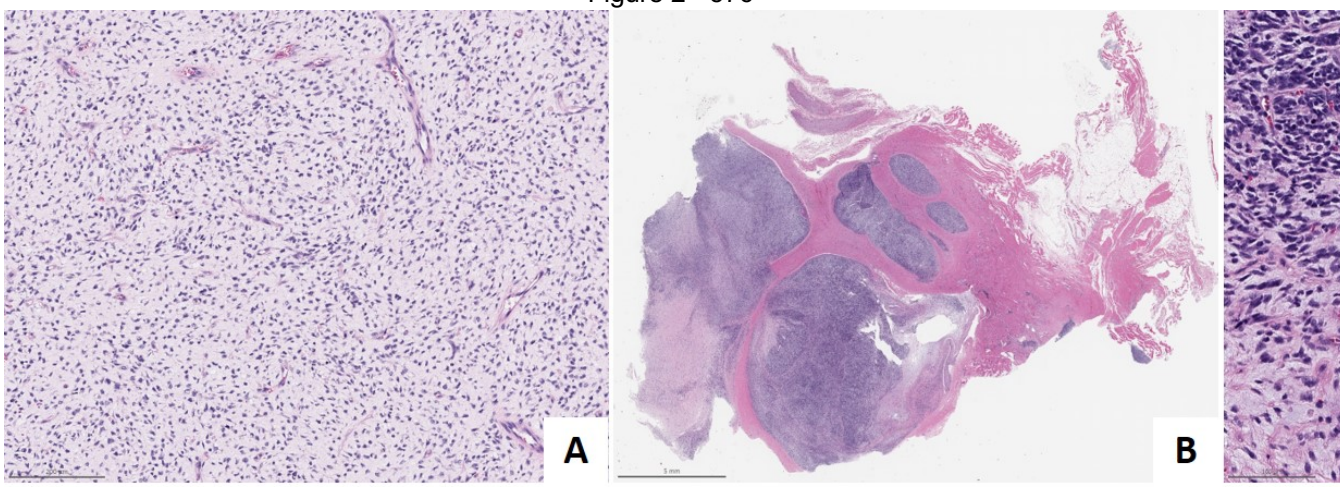

Conclusions: We report on a novel subset of uterine sarcomas with myxoid matrix and hybrid features of smooth muscle and endometrial stromal neoplasia that harbor novel *SS18-VEZF1* fusions. Further investigations are need to evaluate the pathogenetic relationship of these neoplasms to other myxoid uterine mesenchymal tumors.

577 Patterns of Major Histocompatibility Complex (MHC) Antigen Expressions in Non-HPV Related Vulvar Dysplasia and Carcinoma: A Long-Term Follow-up Study of over 20 Years

K M Islam[1], Renan Ribeiro e Ribeiro[2], C. James Sung[1], M. Ruhul Quddus[1]
[1]Women & Infants Hospital/Alpert Medical School of Brown University, Providence, RI, [2]Women and Infants Hospital, Providence, RI

Disclosures: K M Islam: None; Renan Ribeiro e Ribeiro: None; C. James Sung: None; M. Ruhul Quddus: None

Background: Major Histocompatibility Complex Antigen Class I (MHC I) is universally expressed on the surface of all nucleated cells. MHC class I molecules present peptides, including tumor-associated antigens, to cytotoxic CD8+T cells, and therefore play an important role in tumor immunity. Tumor cells often harbor a loss or down-regulation of the MHC I molecules and escape recognition. Deregulated MHC class I genes expression has been demonstrated in various tumor types. Preservation or loss of MHC expression may help predict success or failure of immune checkpoint inhibitor treatment.

In this study, we assessed the patterns of MHC expression in non-HPV related lesions of the vulva, including atypical squamous hyperplasia (ASH), differentiated vulvar intraepithelial neoplasia (dVIN) and invasive squamous cell carcinoma (SCC) in two patients with over 20-years of follow up.

Design: Sequential biopsies and excisions from two patients were collected for over 20 years, with diagnoses including ASH, dVIN and SCC. All samples were stained with anti-HLA class 1 ABC antibody [EMR8-5], cat# ab70328, Abcam, dilution 1:2000.

The expression pattern of MHC I (Fig 2, A-D) in the tumor cell membrane and/or cytoplasm was noted. The staining pattern was considered “preserved” when greater than 90% of tumor cells showed membranous and/or cytoplasmic expression of MHC class I, "focal loss" when staining ranged from 10-90% and "complete loss" when less than 10% of tumor cells showed consistent expression.

Results: A total of 44 samples from two patients were stained, including 13 sections of ASH (30%), 23 sections of dVIN (52%) and 8 sections of SCC (18%). MHC I expression pattern results are shown in Table 1.

		ASH (n=13)		dVIN (n=23)		SCC (n=8)	
		Membranous	Cytoplasmic	Membranous	Cytoplasmic	Membranous	Cytoplasmic
MHC expression	Preserved	09 (69%)	11 (85%)	15 (65%)	04 (17%)	00 (0%)	1 (13%)
	Focal loss	04 (31%)	02 (15%)	08 (35%)	19 (83%)	07 (87%)	07 (87%)
	Complete loss	00 (0%)	00 (0%)	00 (0%)	00 (0%)	01 (13%)	00 (0%)

Figure 1 - 577

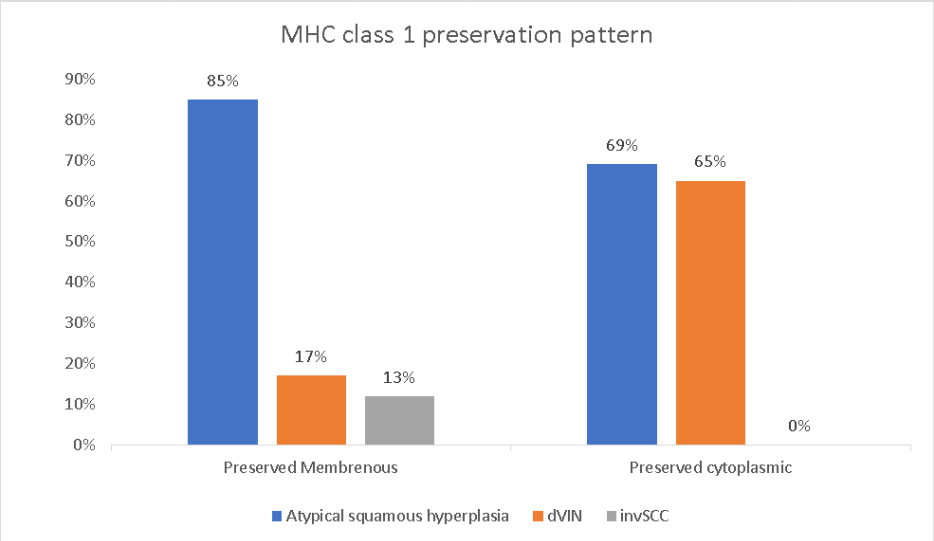

Figure 2 - 577

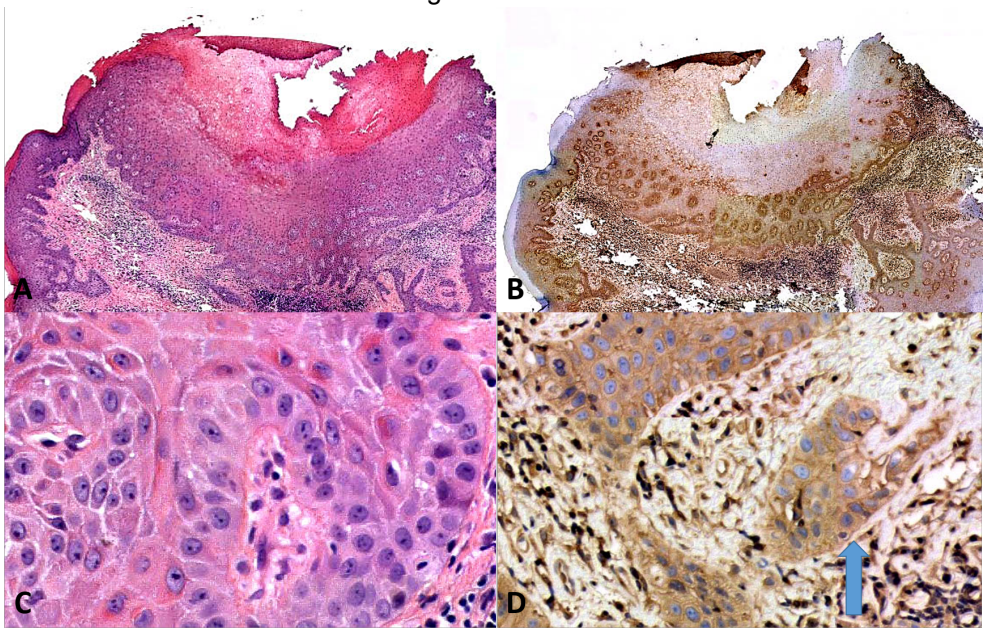

Conclusions: Membranous and cytoplasmic MHC class 1 expression progressively diminishes from atypical squamous hyperplasia to dVIN to invasive squamous cell carcinoma. MHC class 1 immunostain can be a useful marker for distinguishing in situ versus a minimally invasive squamous lesion. Immune checkpoint treatment may not be effective in cases where MHC class 1 expression is lost.

578 HER2 Overexpression and Amplification in Uterine Carcinosarcomas with Serous Morphology

Taylor Jenkins[1], Leigh Cantrell[1], Mark Stoler[1], Anne Mills[2]
[1]University of Virginia Health System, Charlottesville, VA, [2]University of Virginia, Charlottesville, VA

Disclosures: Taylor Jenkins: None; Leigh Cantrell: None; Mark Stoler: None; Anne Mills: None

Background: Uterine carcinosarcoma (UCS) is an aggressive malignancy with few adjuvant treatment options. Recent studies have shown an increase in progression-free survival in patients with HER2-positive endometrial serous carcinomas (ESC) treated with trastazumab. Few studies have evaluated HER2 expression/amplification in UCS. Similar to ESC, the majority of UCS have *TP53* mutations and a serous epithelial component, suggesting that UCS may show similar rates of HER2-positivity and therapeutic response. Therefore, we evaluated HER2 expression/amplification in a cohort of UCS.

Design: A tissue microarray was constructed using cases diagnosed as uterine carcinosarcoma over a 5-year period. Mismatch repair protein (MMR), p53, and PD-L1 expression status was obtained from prior whole section analyses, and H&E slides were reviewed for diagnostic confirmation. HER2 immunohistochemistry (IHC) and chromogenic in-situ hybridization (CISH) were performed on the TMA; HER2 was scored according to CAP guidelines.

Results: 48 of 55 cases were confirmed to be UCS. 5 cases were reclassified as dedifferentiated carcinoma (DC) and 2 as sarcoma NOS. 3 UCS (6%) had strong (3+) HER2 IHC expression and 1 case was equivocal (2+). Overexpression was seen in both epithelial and mesenchymal components in 1 case and limited to the epithelial component in 2 cases. 5 cases (10%) had HER2 amplification by CISH, including all 3 with overexpression by IHC. Amplification was seen in both tumor components in 3 cases and limited to the epithelial component in 2 cases. All HER2-positive cases had a serous morphology and aberrant p53 expression. Only minimal PD-L1 expression was seen in the HER2-positive cases, and none had MMR loss. No cases of DC or sarcoma NOS had HER2-positivity.

Conclusions: A subset of UCS with serous morphology have overexpression and/or amplification of HER2, which may predict response to HER2-targeted therapies. HER2-positive UCS may be less susceptible to immune checkpoint inhibition as they uncommonly show MMR deficiency and/or strong PD-L1 expression. Thus, HER2-targeted therapies could be of clinical utility in a subset of UCS without other adjuvant treatment options. Additional studies are needed to determine whether HER2 CISH is the superior screening method, given the improved sensitivity over IHC in our cohort.

579 Pathological Evaluation of Cervical Adenocarcinoma from Biopsies in Predicting Tumor Invasive Patterns and Status of Nodal Metastasis

Yu Jing[1], Yiyao Liu[1], Sun Wenwen[1], Zhao Jingjing[1], Li Shuxia[1], Wei Dong[1], Yu Zhang[1], Bin Du[1], Huiting Zhu[1]
[1]Shanghai First Maternity and Infant Hospital, Shanghai, China

Disclosures: Yu Jing: None; Yiyao Liu: None; Sun Wenwen: None; Zhao Jingjing: None; Li Shuxia: None; Wei Dong: None; Yu Zhang: None; Bin Du: None; Huiting Zhu: None

Background: Nodal metastasis represents a poor prognostic factor for cervical adenocarcinoma (CAC). In 2013, invasive pattern based system (Silva system or PBS) was found to be highly predictive for the status of nodal metastasis (SNM). However, application of PBS is mainly in the resection specimens when definitive surgeries are done. A recent study from Zheng group at UTSW showed necrotic tumor debris (NTD) and tumor nuclear grade (TNG) can reliably predict SNM from biopsy specimens. We independently evaluate pathologic features from cervical biopsies to predict SNM for patients with usual type CAC.

Design: The 32-paired biopsy-resection (fully staged) samples of CAC from 2013 to 2019 were selected from Shanghai first Maternal and Infant Health Care Hospital, Tongji University. Standard statistical analyses were performed among pathologic features including pattern of invasion (POI), NTD, TNG, mitotic count and the SNM.

Results: Because biopsied tumor samples were small, patterns of invasion were assessible in only 14 (43.8%) of 32 cases. In resections, POIs were all identified in 32 cases. There was no nodal metastasis found in patterns A and B, but 6 (31.5%) of 19 pattern C showed positive nodes ($p<0.05$). In contrast, TNG and NTD were all assessible in biopsies. We found that TNG1 and absence of NTD were associated with mostly pattern A and a few pattern B, but not pattern C, while TNG3 and present NTD were highly associated with pattern C. Detailed data is presented in Table 1.

TABLE 1. The relationship between tumor nuclear grade, necrotic tumor debris and POI as well as nodal status of patients with usual type cervical adenocarcinoma

	Nuclear Grade			Necrotic tumor debris	
	G1	**G2**	**G3**	**Yes**	**No**
All Samples	7	6	19	10	22
POI[a]					
A	4	3	0	0	7
B	0	5	1	1	5
C	0	8	11	9	10
p-value	<0.05[b]			<0.05[b]	
Nodal Status					
Positive	0	1	5	4	2
Negative	7	5	14	6	20
p-value	<0.05[b]			<0.05[c]	

Nuclear grade and necrotic tumor debris were from cervical biopsies. POI and nodal status were based on resection specimen.

a: POI, patterns of invasion.

b: Pearson's Chi-Squared Test

c: Fisher's Exact Test

Conclusions: Evaluation of NTD and TNG in biopsies for usual type CAC provides outstanding predictive value for the status of nodal metastasis. Although PBS was remarkable in resection specimens, it has limited value from cervical biopsy in predicting SNM. Additional studies including prospective clinical trials are necessary to confirm the findings before clinical application is considered.

580 Potential Influence of MHC Class I Expression in Uterine Carcinosarcomas on the Outcome of PD-L1 Immunotherapy

Terri Jones[1], Rohit Bhargava[2], Thing Rinda Soong[3], Esther Elishaev[2], Mirka Jones[3]
[1]University of Pittsburgh Medical Center, Pittsburgh, PA, [2]UPMC Magee-Womens Hospital, Pittsburgh, PA, [3]University of Pittsburgh, Pittsburgh, PA

Disclosures: Terri Jones: None; Rohit Bhargava: *Advisory Board Member*, Eli Lilly & Company; Thing Rinda Soong: None; Esther Elishaev: None; Mirka Jones: None

Background: The Major Histocompatibility Complex (MHC) class I is a cell surface protein expressed in all nucleated human cells which presents portions of intracellular proteins to cytotoxic T-cells. Tumor cells displaying their neoantigens on MHC class I are vulnerable to immune attack. Loss of MHC class I expression in cancer acts as an immune evasion mechanism upstream of the PD-L1 pathway and has not yet been evaluated in uterine carcinosarcomas (UCS).

Design: MHC class I expression was assessed by immunohistochemistry in 37 UCS, including 18 low clinical stage (stage I and II) and 19 high stage (III and IV). The results were compared with PD-L1 expression and mismatch repair protein (MMR) status. Membranous and cytoplasmic expression of MHC was scored as intact (<90% positive), subclonal loss (10-90% positive), and diffuse loss (<10% positive) in the epithelial component, stromal component, or both. PD-L1 positivity was scored as 5% or more of partial or complete membranous staining. Tumors were designated as MMR intact when they retained expression of MLH1, PMS2, MSH2, and MSH6.

Results: The majority of UCS (26 of 37, 70%) showed either subclonal (25) or complete (1) loss of MHC class I expression. Fifteen of 26 UCS with lost MHC class I expression (58%) were PD-L1 positive, including 6 MMR deficient and 9 MMR preserved tumors. The intact MHC class I expression was present in 11 tumors (30%), six of which were PD-L1 positive, including 2 MMR deficient and 4 MMR preserved (Table 1). Expression in the intact and subclonal loss groups was mostly seen in the epithelial component (68% of tumors). Furthermore, the group with subclonal loss showed heterogeneous staining patterns; 16 UCS exhibited patchy strong to moderate staining, surrounded by negative foci (>60%). The MHC class I staining pattern did not show any significant correlation with either low or high clinical stage tumors.

Comparison of MHC class I expression and PD-L1 status in 37 UCS

	MHC Intact	MHC Subclonal Loss	MHC Diffuse Loss
PD-L1 Positive (21/37)	6	14	1
PD-L1 Negative (16/37)	5	11	0

Conclusions: Clinical trials for anti-PD-L1 therapy in UCS are ongoing. MHC class I expression has not been yet investigated in UCS, but in advanced stage endometrial carcinoma, it is considered an important biomarker qualifying for immunotherapy in PD-L1 positive tumors, regardless of MMR status. Of our PD-L1 positive UCS, 58% showed either subclonal or diffuse loss of MHC expression, which may reveal a subset of patients who might not respond to anti-PD-L1 therapy.

581 Co-Expression of TIM-3, Gal-9, and PD-L1 in Uterine Carcinosarcomas and the Potential Therapeutic Implications

Terri Jones[1], Rohit Bhargava[2], Thing Rinda Soong[3], Esther Elishaev[2], Mirka Jones[3]
[1]University of Pittsburgh Medical Center, Pittsburgh, PA, [2]UPMC Magee-Womens Hospital, Pittsburgh, PA, [3]University of Pittsburgh, Pittsburgh, PA

Disclosures: Terri Jones: None; Rohit Bhargava: *Advisory Board Member*, Eli Lilly & Company; Thing Rinda Soong: None; Esther Elishaev: None; Mirka Jones: None

Background: Due to the failure of single-agent immunotherapy, a combination approach to checkpoint inhibition has been already considered in several tumors. We study the expression of TIM-3, Gal-9, and PD-L1 in uterine carcinosarcoma (UCS). Binding of T cell immunoglobulin and mucin-domain containing-3 (TIM-3) to its ligand, galectin-9 (Gal-9), dampens the immune response and prevents autoimmunity. The expression of both markers in PD-L1 positive tumors suggests a possible involvement of both pathways as mechanisms of immune evasion.

Design: Membranous TIM-3 and Gal-9 expression was assessed by immunohistochemistry in 37 UCS, including 18 low stage (stages I and II) and 19 high stage (III and IV) tumors. The percentage of positive staining in immune cells and epithelial and stromal components of UCS was determined. PD-L1 positivity was scored as 5% or more of partial or complete membranous staining and correlated with staining of TIM-3 and Gal-9 and with the clinical stage.

Results: Co-expression of TIM-3, Gal-9, and PD-L1 in both tumor and immune cells was found in 26/37 of UCS (70%). TIM-3 was expressed in tumor cells of 16 UCS (14 in the stromal component and 2 in both components). Gal-9 was expressed in tumor cells of 19 UCS (6 in epithelial component, 4 in stromal component, and 9 in both components). TIM-3 and Gal-9 were co-expressed in immune cells of all 37 tumors. Eight UCS showed tumor cell only positivity for PD-L1, TIM-3, and Gal-9, including 6 low stage (I and II) and 2 high stage (III and IV). Eight tumors were negative in tumor cells for all 3 markers, including 3 low and 5 high stage UCS. Positive tumoral Gal-9 expression was associated with a 5-fold increased odds of tumoral PD-L1 co-expression (OR 4.8; p=0.03).

Conclusions: Clinical trials for anti-TIM-3 therapy in various tumors are in progress, while anti-PD-L1 trials in UCS are ongoing. We found that 70% of PD-L1 positive UCS co-express TIM-3 and its ligand Gal-9. Significantly increased odds of the co-expression of Gal-9 and PD-L1 in tumor cells suggest the involvement of both the PD-1/PD-L1 and TIM-3/Gal-9 axes in UCS and potential interaction between them. In addition, although not statistically significant, positivity for all 3 markers appeared to be more common in low rather than high stage tumors, which could suggest a better response to immunotherapy in earlier disease. Should PD-L1 therapeutics be approved for UCS, the further investigation of anti-TIM-3 agents as a combination immunotherapeutic regimen could be warranted.

582 Mesonephric-Like Carcinoma of the Ovary is a Rare and Aggressive Histotype of Ovarian Carcinoma

Eun-Young Kang[1], Monica Rodriguez[2], Sandra Lee[3], Nicholas Wiebe[1], Ying Liu[4], Linda Cook[5], Cheng-Han Lee[6], Anthony Karnezis[4], Martin Kobel[1]
[1]University of Calgary, Calgary, Canada, [2]Cumming School of Medicine, University of Calgary, Calgary, Canada, [3]Alberta Precision Laboratories, Calgary, Canada, [4]UC Davis Medical Center, Sacramento, CA, [5]University of New Mexico Health Sciences Center, Albuquerque, NM, [6]BC Cancer, Vancouver, Canada

Disclosures: Eun-Young Kang: None; Monica Rodriguez: None; Sandra Lee: None; Nicholas Wiebe: None; Ying Liu: None; Linda Cook: None; Cheng-Han Lee: None; Anthony Karnezis: None; Martin Kobel: None

Background: The 2020 World Health Organisation (WHO) Classification of Tumours of the Female Genital Tract lists mesonephric-like adenocarcinoma as a separate histotype of ovarian carcinoma. Our aim was to determine the frequency of ovarian mesonephric-like adenocarcinomas in population-based cohorts.

Design: Following an index case (Fig. 1), we screened 1,512 ovarian epithelial neoplasms represented on tissue microarrays using GATA3, TTF1, and ER/PR immunohistochemistry (IHC). A mesonephric-like IHC profile was defined as per the WHO classification: GATA3 and/or TTF1 expression with absence of ER/PR staining. Cases with a mesonephric-like IHC profile underwent morphological review by 4 gynecological pathologists. Kaplan-Meier survival analyses comparing the survival of mesonephric-like to endometrioid carcinomas were performed.

Results: GATA3 expression was seen in 5.5% and TTF1 in 3.6% of cases, with the highest proportion observed in ovarian endometrioid carcinomas (GATA3, 9.4%; TTF1, 8.5%). A mesonephric-like IHC profile was found in 2.9% (44/1,512) of cases. Eleven cases were identified by at least one observer to show morphological features consistent with mesonephric-like carcinoma (7 with consensus among all pathologists; 3 indicated as mesonephric-like by majority; 1 with only 1 observer identifying the case as mesonephric-like) and had previously been classified as endometrioid, accounting for 2.9% (11/381) of endometrioid carcinomas. All cases expressed GATA3 (8 diffuse, 3 focal) and 7/10 TTF1 (6 diffuse, 1 focal) and were ER/PR negative, mismatch repair proficient, p53 normal, and WT1 negative. 2/11 showed absence of ARID1A expression. Seven cases with available data were positive for PAX8. The mean age of patients with mesonephric-like adenocarcinoma was 61.2 years (compared to 54.2 for endometrioid). Patients were diagnosed at stage I (6), II (3), and III (1) and the assigned grades were 1 (2), 2 (4), or 3 (2). Endometriosis was present in 6/8 patients and no synchronous endometrial primaries were present in 7 cases with available data. The overall survival rate for mesonephric-like adenocarcinomas was significantly lower than endometrioid carcinomas (Fig. 2; 5-year survival 60% vs. 85.8%; HR=5.25, 95%CI 2.33-10.27, p=0.0003 in univariable analysis; HR=6.14, 95%CI 2.67-12.37, p=0.0001 in multivariable analysis adjusting for age and stage).

Figure 1 - 582

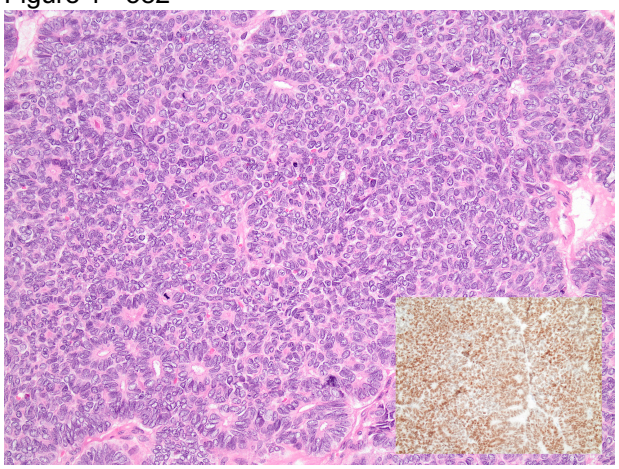

Figure 2 - 582

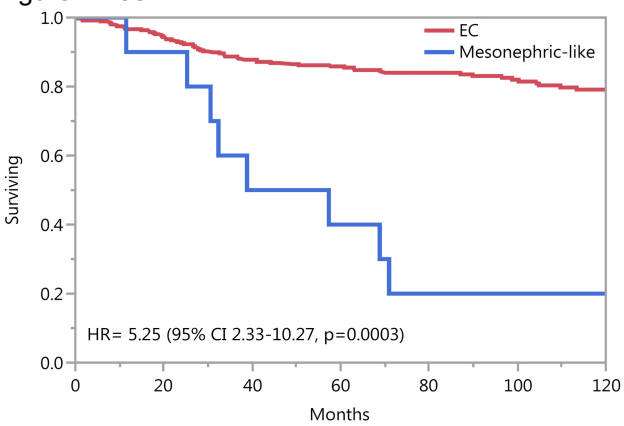

Conclusions: Mesonephric-like adenocarcinomas are a rare histotype of ovarian carcinoma with shorter survival compared to endometrioid carcinomas.

583 Frequent Neuroendocrine Marker Expression in SWI/SNF-Deficient Dedifferentiated/Undifferentiated Endometrial Carcinomas

Eun-Young Kang[1], Basile Tessier-Cloutier[2], Colin Stewart[3], Martin Kobel[1], Cheng-Han Lee[4]
[1]University of Calgary, Calgary, Canada, [2]The University of British Columbia, Vancouver, Canada, [3]King Edward Memorial Hospital, Subiaco, Australia, [4]BC Cancer, Vancouver, Canada

Disclosures: Eun-Young Kang: None; Basile Tessier-Cloutier: None; Colin Stewart: None; Martin Kobel: None; Cheng-Han Lee: None

Background: Dedifferentiated and undifferentiated endometrial carcinoma (DDEC/UEC) frequently harbors genomic activation of SWItch/Sucrose Non-Fermentable (SWI/SNF) complex proteins in the undifferentiated tumor that is associated with highly aggressive clinical behavior. The SWI/SNF-deficient undifferentiated carcinoma can possess scanty cytoplasm in some cases, imparting a small round blue cell tumor appearance that mimics a neuroendocrine carcinoma, particularly in small biopsy samples. The aim of this study was to evaluate for the presence and extent of neuroendocrine differentiation in SWI/SNF-deficient DDEC/UEC.

Design: We examined the expression of synaptophysin, chromogranin, and CD56 in a series of 30 SWI/SNF-deficient DDEC/UEC (15 ARID1A/1B-deficient, 9 SMARCA4-deficient, and 6 SMARCB1-deficient) by whole-section immunohistochemistry.

Results: 9 of 15 (60%) ARID1A/1B-deficient, 8 of 9 (89%) SMARCA4-deficient, and 4 of 6 (67%) of SMARCB1-deficient undifferentiated carcinomas displayed expression of at least one neuroendocrine marker. Overall, 16 (53%), 6 (20%), and 14 (47%) of 30 SWI/SNF-deficient tumors showed synaptophysin, chromogranin, and CD56 expression, respectively, with expression seen in > 1% of the tumor cells in 9 (30%), 4 (13%), and 6 (20%) of 30 cases, respectively. However, none of the cases showed greater than 33% tumor expression for the neuroendocrine markers examined. Among the 24 dedifferentiated carcinomas, chromogranin and CD56 expression was seen in the corresponding endometrioid-type carcinoma components in 7 cases and 8 cases, respectively, while none of the differentiated tumor components showed synaptophysin expression.

Conclusions: These findings indicate frequent neuroendocrine marker expression in SWI/SNF-deficient DDEC/UEC, but the extent of expression was consistently focal to patchy (<33%) and none of the undifferentiated tumors showed diffuse expression of any of the neuroendocrine markers.

584 Chorionic Vesicle in Early Trimester Products of Conception: A Rare Mimic of Early Complete Hydatidiform Mole

Neslihan Kayraklioglu[1], Soo-Jin Cho[1], Janice Lage[2], Joseph Rabban[1]
[1]University of California, San Francisco, San Francisco, CA, [2]The Ottawa Hospital, University of Ottawa, Ottawa, Canada

Disclosures: Neslihan Kayraklioglu: None; Soo-Jin Cho: None; Janice Lage: None; Joseph Rabban: None

Background: The chorionic vesicle is the very early first trimester shell of primary villi and proliferating trophoblast that radiate circumferentially from the surface of the chorionic plate surrounding the developing yolk sac, amnionic sac and embryo. Though it usually is fragmented in products of conception (POC) specimens, the intact form bears striking resemblance to an early complete hydatidiform mole (CHM), resulting in a potential diagnostic pitfall. We report 10 cases of intact chorionic vesicle, emphasizing morphological features that distinguish it from early CHM.

Design: The morphologic features of 10 cases of intact chorionic vesicle from early POC were evaluated and compared to morphologic diagnostic criteria for early CHM. p57 immunohistochemical staining was performed on all cases and nuclear expression was evaluated in the villous cytotrophoblast and mesenchyme.

Results: Four of 10 (40%) cases were originally suspected to be early CHM by the referring pathologist. Average maternal age was 36 years and average gestational age was 6-7 weeks. 9 were intrauterine pregnancies and 1 was a tubal ectopic pregnancy. The chorionic vesicle (5.5 mm avg diameter) was directly implanted on the endometrium in 4 cases but was free-floating in 6 (see Figure). Circumferential/nearly circumferential radiating primary villi were present in all cases. Villous trophoblast proliferation mimicking CHM was circumferential (2/10) or focal (5/10); the proliferation pattern was solid/stratified (4/10) or lace-like (3/10). None showed trophoblast atypia. Additional CHM-like features were cistern-like spaces (8/10), extra-embryonic mesoderm with blue-grey myxoid features (8/10) and apoptotic debris (8/10), however the mesoderm was not hypercellular. Unlike CHM, perivillous fibrin was notable in 5/10; non-viable/denuded villous trophoblast in 5/10, and decidual stromal breakdown in 8/10. p57 was intact in all cases.

Figure 1 - 584

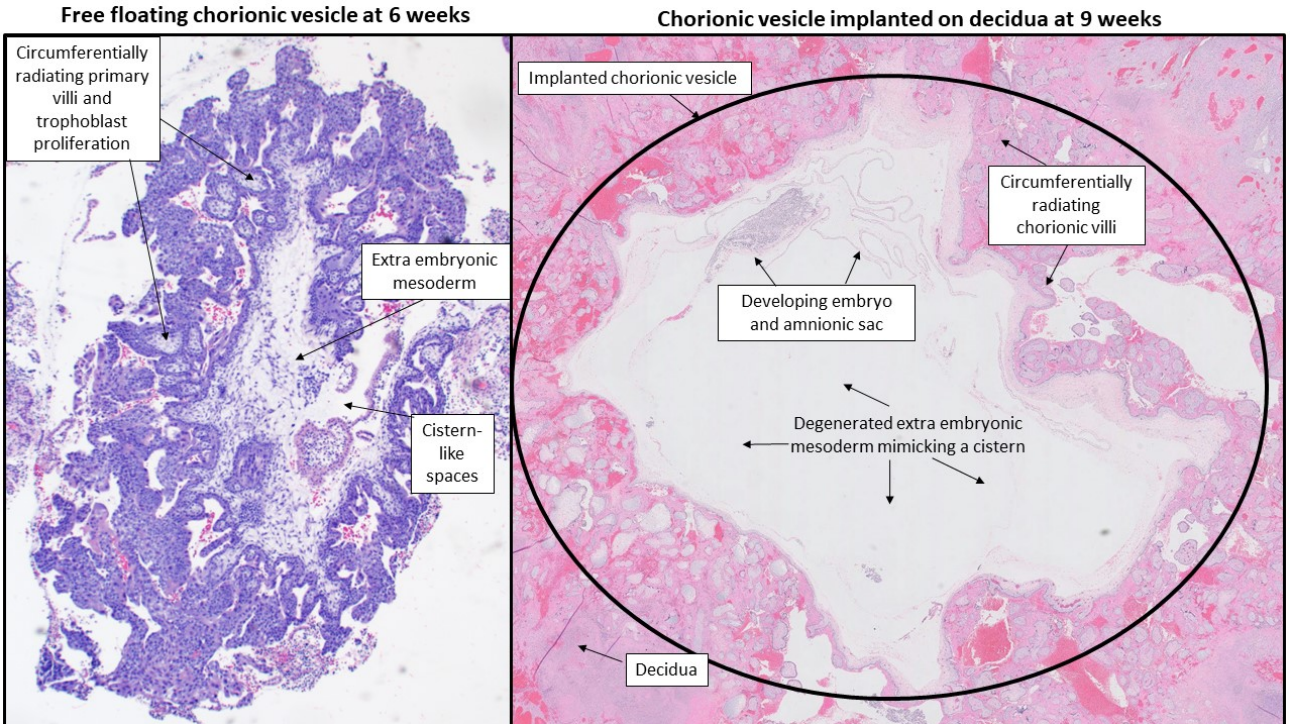

Conclusions: Intact chorionic vesicle is a rare mimic of early CHM. Attention to the presence of perivillous fibrin and decidual stromal breakdown, as well as the absence of villous stromal hypercellularity and trophoblast atypia distinguishes chorionic vesicle from CHM, which can be confirmed by intact p57 staining.

585 Nuclear Beta-Catenin Expression in the Context of Abnormal p53 Endometrial Carcinoma Indicates a Non-Serous Histotype

Kianoosh Keyhanian[1], Eric Yang[1], Brooke Howitt[1]
[1]Stanford Medicine/Stanford University, Stanford, CA

Disclosures: Kianoosh Keyhanian: None; Eric Yang: None; Brooke Howitt: None

Background: The Cancer Genome Atlas (TCGA) molecular classification in endometrial carcinoma (EC) carries significant prognostic significance. However, histologic subtyping continues to be clinically relevant within specific molecular groups. Although beta-catenin status is not a defining parameter in the current TCGA molecular classification, its prognostic significance has been proposed in specific pathologic (low-grade/low-stage tumors) and molecular (No Specific Molecular Profile (NSMP) subgroup) contexts. It has been shown that the interobserver reproducibility is low for histotyping within p53 abnormal ECs; thus biomarkers that can aid in reproducible classification are clinically useful. The diagnostic utility for beta-catenin expression patterns in determining the histotype of p53 abnormal ECs has not been well studied.

Design: Our pathology database was searched to identify ECs prospectively classified as “p53 abnormal.” The p53 abnormal classification was defined as tumors with 1) no evidence of *POLE* exonuclease domain hotspot mutations 2) intact mismatch repair protein expression, and 3) abnormal p53 expression (null or overexpression). Identified cases were reviewed for histotype and beta-catenin expression patterns. Beta-catenin immunohistochemistry (IHC) was reviewed for all cases and scored as abnormal (nuclear and cytoplasmic) or normal (membranous).

Results: 66 ECs were identified with a “p53 abnormal” molecular classification; 23 (35%) were uterine serous carcinomas and 43 (65%) were of non-serous histotype (14 endometrioid, 3 clear cell carcinoma, 18 carcinosarcoma and 8 high-grade EC with ambiguous morphology). All 23 serous carcinomas demonstrated normal

membranous staining for beta-catenin. Of the 43 non-serous ECs, 9 (21%) showed abnormal (nuclear) beta-catenin expression including 5 endometrioid carcinomas (4 FIGO grade 3, 1 FIGO grade 2), 2 carcinosarcomas (both with an ambiguous carcinomatous component) and 2 high grade ECs with ambiguous morphology. The specificity of abnormal beta-catenin expression for non-serous histotypes is high (100%) although the sensitivity is low (21%) with positive and negative predictive values of 100% and 40%, respectively.

Conclusions: Our data shows that abnormal beta-catenin expression in the context of p53 abnormal EC is highly specific, but not sensitive, for non-serous histotypes. Beta-catenin IHC may be of value as part of a panel in classifying high-grade endometrial carcinomas, specifically to exclude a serous histotype.

586 Clinicopathologic Features of Endometrial Carcinomas with and without Microsatellite Instability

Mahyar Khazaeli[1], Mehran Taherian[1], Farshid Kashef[2], Emad Alqassim[2], Al Amin[1], Devi Jeyachandran[3], Mohamed Desouki[3]
[1]University at Buffalo, SUNY, Buffalo, NY, [2]University at Buffalo, Buffalo, NY, [3]Roswell Park Comprehensive Cancer Center, Buffalo, NY

Disclosures: Mahyar Khazaeli: None; Mehran Taherian: None; Farshid Kashef: None; Emad Alqassim: None; Al Amin: None; Devi Jeyachandran: None; Mohamed Desouki: None

Background: Microsatellite Instability (MSI) has been shown as a major pathway in endometrial carcinogenesis, especially in the endometrioid phenotype. IHC for mismatch repair (MMR) protein expression is the most common primary screen used as a surrogate marker for MSI, identification of Lynch syndrome, genetic counseling, and management. Limited studies with conflicting results are available on pathological features of MSI-high endometrial cancers. We evaluated the clinicopathologic features of endometrial carcinomas with intact and loss of MMR proteins in a single academic cancer institute.

Design: Endometrial carcinomas that have been tested for the expression of MMR proteins (MLH1, MSH2, MSH6, and PMS2) as a part of clinical care for the period 2012-2020 were retrieved. Patients' age and pathologic characteristics of the tumors from the pathology reports were recorded and analyzed.

Results: Loss of at least one of the MMR proteins has been identified in 65/209 (31%) of the endometrial carcinomas tested. In our cohort, patients with MMR loss are older, have high grade and more deeply invasive tumors, and show positive pelvic wash cytology with statistically significant difference compared to patients with all MMR proteins intact. No significant difference has been identified with the tumor or nodal stage (pTpN), lymphovascular invasion, lower uterine segment, cervical or adnexal extension [Table 1].

Figure 1 - 586

Table 1: Age and pathologic characteristics of endometrial carcinomas with intact and loss mismatch repair proteins (n=209).

	Intact expression (n=144)			MSI-H (n=65)			Total	p-value**
	number	percent		number	percent			
MLH1 & PMS2				58	89.2		58	
MSH2 & MSH6				3	4.6		3	
MSH6				4	6.2		4	
Histology								
Endometrioid (n=189)	128	67.7		61	32.3		189	
mucinous features (n=26)			14 (53.8%)			12 (46.2%)		
squamous features (n=25)			16 (64%)			9 (36%)		
secretory features (n=16)			10 (62.5%)			6 (37.5%)		
Clear cell carcinoma (n=3)	1	33.3		2	66.7		3	
serous (n=13)	12	92.3		1	7.7		13	
carcinosarcoma (n=4)	3	75.0		1	25.0		4	
Total	144			65			209	
Age at onset	Average of 60.7 y			Average of 63.7 y				
≤50 y	28	19.4		6	9.2		34	**0.046***
> 50 y	116	80.6		59	90.8		175	
Total	144			65			209	
Tumor stage (pT)								
1	128	89.5		57	87.7		185	0.43
2-4	15	10.5		8	12.3		23	
Total	143			65			208	
Lymph node metastasis								
absent	76	96.2		36	87.8		112	0.09
present	3	3.8		5	12.2		8	
Total	79			41			120	
Tumor grade								
1	74	51.4		23	35.4		97	**0.02***
2-3	70	48.6		42	64.6		112	
Total	144			65			209	
Myometrial invasion								
≤50%	106	78.5		40	64.5		146	**0.03***
> 50%	29	21.5		22	35.5		51	
Total	135			62			197	
Cervical stroma invasion								
absent	130	92.2		55	90.2		185	0.41
present	11	7.8		6	9.8		17	
Total	141			61			202	
Adnexal involvement								
absent	131	92.3		59	95.2		190	0.33
present	11	7.7		3	4.8		14	
Total	142			62			204	
Lymphovascular invasion								
absent	107	77.5		42	66.7		149	0.07
present	31	22.5		21	33.3		52	
Total	138			63			201	
Tumor size (cm)								
≤2	87	69.6		48	80.0		135	0.09
> 2	38	30.4		12	20.0		50	
Total	125			60			185	
Lower uterine segment involvement								
absent	55	72.4		18	58.1		73	0.11
present	21	27.6		13	41.9		34	
Total	76			31			107	
Peritoneal cytology								
Negative	21	75.0		17	100.0		38	**0.026***
positive/suspicious	7	25.0		0	0.0		7	
Total	28			17			45	

* Fisher exact probability test (* significant difference)

Conclusions: We are reporting a relatively large number of endometrial carcinomas with intact and lost MMR proteins. In our cohort, tumors with deep myometrial invasion, high grade with positive peritoneal cytology of endometrioid or clear cell type in the older age group have a high probability of harboring an MSI-H.

587 Expression of ARID1A, BRG1 and INI1 in Undifferentiated Uterine Neoplasms: A Comprehensive Clinicopathologic Study

Dimitrios Korentzelos[1], Esther Elishaev[2], Chengquan Zhao[3], Mirka Jones[4], Thing Rinda Soong[4], Jamie Lesnock[2], Taylor Orellana[2], Alison Zeccola[2], Rohit Bhargava[2]
[1]University of Pittsburgh Medical Center, Pittsburgh, PA, [2]UPMC Magee-Womens Hospital, Pittsburgh, PA, [3]Magee-Womens Hospital, University of Pittsburgh Medical Center, Pittsburgh, PA, [4]University of Pittsburgh, Pittsburgh, PA

Disclosures: Dimitrios Korentzelos: None; Esther Elishaev: None; Chengquan Zhao: None; Mirka Jones: None; Thing Rinda Soong: None; Jamie Lesnock: None; Taylor Orellana: None; Alison Zeccola: None; Rohit Bhargava: *Advisory Board Member*, Eli Lilly & Company

Background: Undifferentiated/dedifferentiated endometrial carcinomas (CA-undiff and CA-dediff) and undifferentiated uterine sarcomas (SA-undiff) are aggressive uterine neoplasms of epithelial and mesenchymal origin respectively, with no specific line of differentiation. CA-dediff shows co-existence of a well to moderately differentiated carcinoma, but CA-undiff does not. A significant proportion of these cases feature mutations of members of the SWI/SNF chromatin remodeling complex, including ARID1A, SMARCA4 (BRG1) and SMARCB1 (INI1). We describe the clinical-pathological features of a cohort of these neoplasms as well as the immunohistochemical (IHC) expression of ARID1A, BRG1 and INI1.

Design: A total of 43 cases over a 15-year period were retrieved from our institutional archives, composed of 30 carcinomas (25 CA-dediff and 5 CA-undiff) and 13 SA-undiff based on original report. All cases classified as CA-undiff had some degree of cytokeratin AE1/AE3 and/or CAM5.2 reactivity. Not all information was available on all cases. Tissue was available on 17 carcinomas and 8 sarcoma cases. IHC for ARID1A, BRG1 and INI1 was performed on the undifferentiated tumor component. Progression-free (PFS) and overall survival (OS) were analyzed using Kaplan-Meier curves and log rank test.

Results: Patient/tumor characteristics and results of IHC stains are shown in table 1 and figure 1. CA-dediff and SA-undiff both showed poor PFS and OS compared to CA-undiff (figure 2), though the OS difference did not achieve statistical significance. However, 4 of 5 (80%) CA-undiff in this cohort were diagnosed with early stage disease.

Table 1:

	Carcinoma (dediff and undiff)	Sarcoma	p-value
Age in years	63.3	60.7	0.3616
Early stage (I & II)	12 of 24 (50%)*	4 of 6 (67%)	0.6567
Lymphovascular invasion	23 of 26 (88%)	7 of 7 (100%)	1.0
ARID1A Loss	13 of 17 (76%)	0 of 6 (0%)	0.0021
BRG1 Loss	3 of 17 (18%)	0 of 8 (0%)	0.5270
INI1 Loss	0 of 17 (0%)	0 of 7 (0%)	1.0

*Stage NA on 6 cases; 8 of 19 (42%) CA-dediff stage I/II and 4 of 5 (80%) CA-undiff stage I/II.

Figure 1 - 587

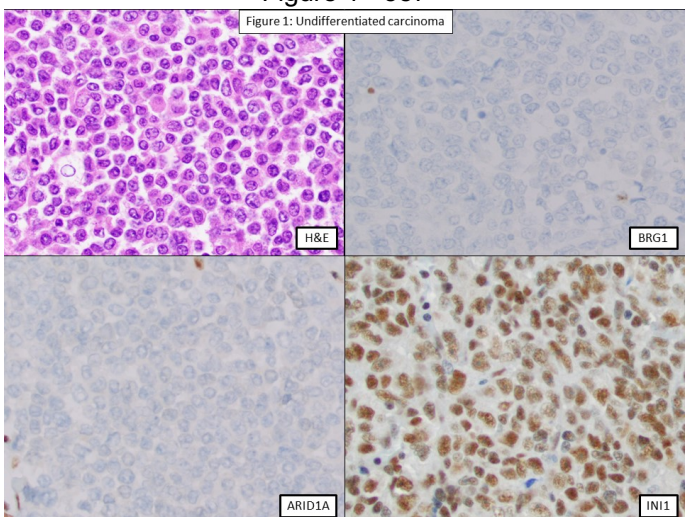

Figure 2 - 587

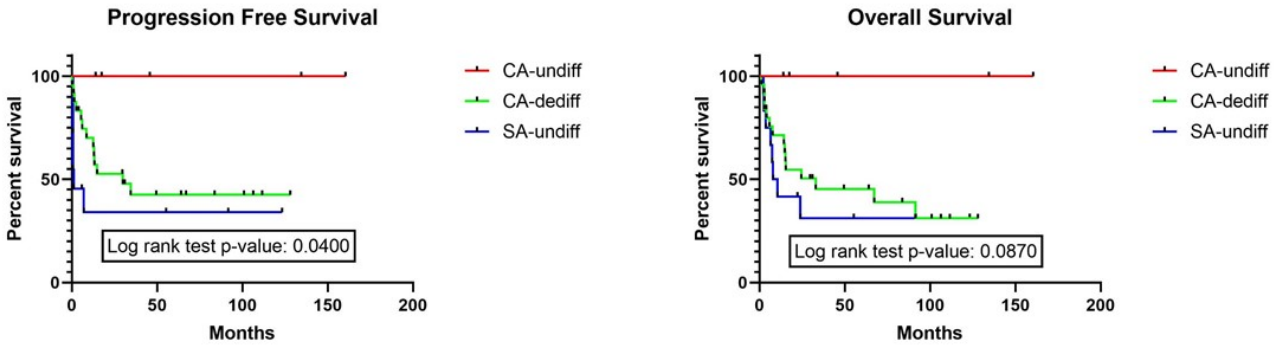

Conclusions: Similar to prior studies, our results indicate that loss of ARID1A and BRG1 expression is characteristic of a significant proportion of undifferentiated carcinomas. On the contrary, they do not represent a feature of SA-undiff. Given the overlapping morphology between the two neoplasms and the limited utility of traditional IHC, ARID1A and BRG1 could potentially assist in the differential diagnosis between the two, albeit validation in larger case series should be performed. The possible good prognosis of CA-undiff compared to CA-dediff should be further evaluated in larger studies. Moreover, due to the involvement of SWI/SNF in DNA repair, and the replicative stress being a hallmark of tumors bearing SWI/SNF genomic alterations, further studies looking at response to therapeutic options to target this pathway in undifferentiated carcinomas is warranted.

588 HER2 Expression And Amplification In p53 Aberrant Uterine High-Grade Endometrioid Carcinoma

Nicholas Ladwig[1], Walter Devine[1], James Grenert[1], Yunn-Yi Chen[1], Amy Joehlin-Price[2], Karuna Garg[1]
[1]University of California, San Francisco, San Francisco, CA, [2]Cleveland Clinic, Cleveland, OH

Disclosures: Nicholas Ladwig: None; Walter Devine: None; James Grenert: None; Yunn-Yi Chen: None; Amy Joehlin-Price: None; Karuna Garg: None

Background: *Her2* amplification and overexpression has been reported in up to one-third of uterine serous carcinomas (USC), and addition of trastuzumab to traditional chemotherapy has resulted in improved survival in patients with advanced stage or recurrent HER2 positive USC. There are currently no official guidelines for specimen type and algorithm for HER2 testing in gynecologic tumors but significant heterogeneity in HER-2 expression has been noted in USC. Recent TCGA molecular data has shown that high-grade endometrioid adenocarcinoma (FIGO 3 EEC) with *TP53* mutation cluster with USC into the copy number high or serous-like

group. We hypothesized that HER2 positivity could be seen in p53 aberrant FIGO 3 EEC given their similarity with USC, and this finding could have therapeutic and possibly prognostic significance.

Design: HER2 immunohistochemistry (IHC) and FISH was performed on 18 cases of p53 aberrant FIGO 3 EEC. HER2 IHC interpretation follows the CAP guideline for gastroesophageal adenocarcinoma (3+ = strong, complete basolateral or lateral membranous reactivity in ≥10% of tumor cells, 2+ = Weak to moderate, complete basolateral or lateral membranous reactivity in ≥10% of tumor cells, 1+ = Faint/barely perceptible membranous reactivity in ≥10% of tumor cells; cells reactive only in part of their membrane and 0 = No reactivity or membranous reactivity in <10% of tumor cells).

Results: Eleven tumors showed no HER2 expression (score = 0) and none of these showed amplification by FISH (1 case failed hybridization). Four tumors showed 1+ HER2 staining and all were negative by FISH. Three tumors showed at least focal 3+ staining with variable distribution: 100% of tumor cells in 1 case, 40% of tumor cells in the second case and less than 5% of tumor cells in the third case. HER-2 FISH showed amplification in the first two cases but was negative in the third tumor, perhaps representing a small subclone of amplified cells not evaluated by FISH.

HER-2 IHC and FISH results

HER-2 IHC score	# of cases	HER-2 FISH status (number of cases/concordance rate with IHC)
0	11	Negative (11/100%)
1+	4	Negative (4/100%)
3+	2 (=>10% cells)	Positive (2/100%)
	1 (<5% cells)	Negative (pending repeat analysis)

Conclusions: In this small cohort of p53 aberrant FIGO 3 EEC, the rate of HER2 positivity and amplification was 11%, with good concordance between IHC and FISH. We noted significant intratumoral heterogeneity in HER2 expression, which could have implications for selection of specimen type and interpretation.

589 Molecular Profiling Identifies Recurrent Alterations that Distinguish Uterine Serous Carcinoma from Pelvic High-Grade Serous Carcinoma

Nicholas Ladwig[1], Joseph Rabban[1], Karuna Garg[1]
[1]*University of California, San Francisco, San Francisco, CA*

Disclosures: Nicholas Ladwig: None; Joseph Rabban: None; Karuna Garg: None

Background: Pelvic high-grade serous carcinoma (pHGSC) and uterine serous carcinoma (USC) show near-identical morphologic features and can be difficult to distinguish, although separation of these entities has implications for tumor staging, considerations for targeted therapy (i.e. HER2 for USC and the homologous repair deficiency pathway for pHGSC), as well as for germline mutational testing for *BCRA1/2* mutations. Patient age, tumor distribution, and WT1 staining patterns are traditionally used to help separate these entities but there can be significant overlap. Both pHGSC and USC are driven by *TP53* mutations; however, there are other molecular alterations that appear to be exclusive or enriched in tumors of uterine versus pelvic origin. In this context, we compared the molecular profiles of surgically-resected pHGSC and USC using next generation DNA sequencing.

Design: Review of our archives identified 57 pHGSC and 15 USC, from which genomic DNA was purified from formalin-fixed, paraffin-embedded tumor tissue and capture based next-generation sequencing targeting 479 cancer genes was performed. WT1 immunohistochemical results were available for a subset of cases. This data was also compared to existing TCGA data to curate a cohort of genes with statistically significant rates of alteration between pHGSC and USC.

Results: pHGSC and USC demonstrated universal *TP53* mutations, but showed a distinct background of additional alterations in many cases (table). Alterations in *PIK3CA, PPP2R1A, FBXW7, SPOP, PIK3R1, and FGFR2* were more commonly identified in USC than pHGSC (p-value < 0.01). Alterations in *BRCA1* and *BRCA2* were exclusive to pHGSC, while alterations in *NF1* were more common in pHGSC than USC (p-value = 0.03). WT1 was positive in >90% of pHGSC and 10% of USC.

Diagnosis	n	USC-Related Genes								pHGSC-Related Genes		
		TP53	PIK3CA	PPP2R1A	FBXW7	SPOP	PIK3R1	FGFR2	ERBB2 amp.	BRCA1	BRCA2	NF1
USC	15	100%	33%	40%	33%	13%	7%	13%	20%	0%	0%	7%
pHGSC	57	100%	5%	0%	0%	2%	0%	2%	2%	18%	4%	14%

Diagnosis	n	Age (mean)	WT1 IHC+	Any USC-Related Gene Alteration	Any pHGSC-Related Gene Alteration
USC	15	69	10%	80%	7%
pHGSC	57	57	94%	9%	35%
				p value = <0.01	p value = 0.03

Conclusions: Although *TP53* mutations are universally identified in both USC and pHGSC, additional molecular alterations appear to be exclusive to the site of origin, and this information could be helpful in assigning site of origin in difficult cases. These results support the hypothesis that USC and pHGSC are biologically similar, yet distinct, tumors that in some cases can be separated from one another by molecular profiling.

590 Performance of p53 Immunohistochemistry as a Surrogate Marker for TP53 Mutations in the PORTEC-3 Endometrial Carcinoma Cohort

Alicia Leon-Castillo[1], Lisa Vermij[1], Stephanie de Boer[1], Naveena Singh[2], Anthony Fyles[3], C. Meg Mclachlin[4], Alexandra Leary[5], Hans Nijman[6], Vincent Smit[1], Remi Nout[7], Nanda Horeweg[1], Carien Creutzberg[1], Tjalling Bosse[1]

[1]Leiden University Medical Center, Leiden, Netherlands, [2]Barts Health NHS Trust, London, United Kingdom, [3]University of Toronto, Toronto, Canada, [4]London Health Sciences Centre, London, Canada, [5]Gustave Roussy, France, [6]University Medical Center Groningen, University of Groningen, Groningen, Netherlands, [7]Erasmus University Medical Center, Rotterdam, Netherlands

Disclosures: Alicia Leon-Castillo: None; Lisa Vermij: None; Stephanie de Boer: None; Naveena Singh: None; Anthony Fyles: None; C. Meg Mclachlin: None; Alexandra Leary: None; Hans Nijman: None; Vincent Smit: None; Remi Nout: *Grant or Research Support*, Elekta; *Grant or Research Support*, Varian; *Grant or Research Support*, Accuray; Nanda Horeweg: None; Carien Creutzberg: None; Tjalling Bosse: None

Background: *TP53* mutations are considered a surrogate marker for copy-number high endometrial cancers (EC). In EC biopsies, p53 immunohistochemistry (IHC) has been reported to be an accurate marker for these mutations. However, there have been no studies validating these results, particularly in the context of hysterectomy where poor fixation can hamper a correct interpretation of p53 staining. In this study we aim to describe the concordance between both methods in a large molecularly defined cohort of EC hysterectomy samples.

Design: EC of 423 consenting patients from the PORTEC-3 clinical trial were collected. P53-IHC was performed and scored abnormal (blinded for presence of *TP53* mutations) when the tumor showed overexpression, complete absence, cytoplasmic or subclonal expression. Subclonal abnormal p53 expression was defined as ≥10% of the tumoral volume showing an abrupt and complete regional abnormal p53 expression. *TP53* mutations were analyzed (blinded for IHC results) through next generation sequencing and assessed for pathogenicity.

P53 and mismatch repair (MMR) proteins IHC, as well as sequencing for *POLE* exonuclease domain mutations were used to molecularly classify EC following the diagnostic algorithm of the 2020 WHO Female Genital Tumor Classification (*POLE*mut, MMRd, NSMP and p53abn).

Sensitivity, specificity, and agreement between p53 IHC and *TP53* mutations were calculated. Categorical variables were compared with Fisher-Freeman-Halton test.

Results: *TP53* sequencing and p53-IHC were both successful in 320 EC (76%). There were 14 (4.3%) EC with multiple *TP53* pathogenic mutations (six *POLE*mut, five MMRd and three p53abn EC, p=0.104).

Concordance between p53-IHC and *TP53* mutations was 290/320 (90.6%), resulting in a sensitivity and specificity of 81.4% and 94.6% respectively (Table 1). Of the 20 discordant cases with a pathogenic *TP53* mutation and a p53 wildtype stain, six were *POLE*mut and eleven MMRd EC. Upon IHC review, five tumors (four MMRd and one NSMP EC) showed multiple discrete foci with abnormal p53 overexpression, representing far less than 10% of the tumor's volume. Ten samples had an abnormal p53 stain and no *TP53* mutations: two were MMRd EC with a subclonal abnormal p53 staining and eight were p53abn EC. After exclusion of *POLE*mut and MMRd EC, the concordance between p53-IHC and *TP53* mutations improved; 157/168 (93.5%).

p53 IHC scoring	*TP53* mutations				Total
	No/non-pathogenic *TP53* mutation		Pathogenic *TP53* mutation		
	All EC	*POLE* wildtype and MMRproficient EC	All EC	*POLE* wildtype and MMRproficient EC	
Wildtype	**211**	**93**	20	3	231
Abnormal-overexpression	6	6	**64**	**56**	70
Abnormal-complete absence	2	2	**5**	**5**	7
Abnormal-cytoplasmic	0	0	**1**	**1**	1
Abnormal-subclonal	2	0	**9**	**2**	11
Total	221	101	99	67	320

In bold, EC with concordant p53-IHC and TP53 mutational status results

Conclusions: Our results confirm the high concordance between p53-IHC interpretation and *TP53* mutations on EC hysterectomy samples. Most discrepancies between both techniques were identified in MMRd or *POLE*mut EC, resulting in an excellent concordance after exclusion of these molecular subgroups. This study further supports the use of p53-IHC as a near perfect surrogate for *TP53* mutations as part of the molecular EC classification.

591 P53 Pattern-Based Immunohistochemistry Classification in Primary Squamous Cell Vulvar Carcinoma Correlates with Prognosis and Can Change During Disease Progression

Sofia Lerias[1], Joana Ferreira[2], Fernanda Silva[3], Ana Felix[4]
[1]Instituto Português de Oncologia Francisco Gentil, Lisbon, Portugal, [2]Instituto Português de Oncologia de Lisboa Francisco Gentil, Lisbon, Portugal, [3]NOVA Medical School, Queijas, Portugal, [4]Instituto Portugues de Oncologia de Lisboa, Lisbon, Portugal

Disclosures: Sofia Lerias: None; Joana Ferreira: None; Fernanda Silva: None; Ana Felix: None

Background: Recent studies describe a pattern-based TP53 immunohistochemistry(IHC) interpretation, which can be used as a surrogate marker for TP53 mutational status in vulvar squamous cell carcinoma(VSCC). Our aim was to evaluate the TP53- IHC pattern-based approach in primary tumors, recurrences, and lymph-node metastasis of VSCC, and its correlation to HPV status, p16 expression and prognosis.

Design: Ninety-three cases of VSCC diagnosed between 2002-2018 with known HPV status(SPF-10PCR/ DEIA/LIPAv2 system) were included. IHC of p53(clone D07,Cell Marque) and p16(clone E6H4,Ventana Medical Systems) was performed on tissue microarrays(3 cores per sample). Eighty-four primary tumors, 41 recurrences(29 patients) and 31 lymph node metastases were included. TP53 expression was categorized into six IHC patterns: two wild-type patterns(TP53wt) and four mutant(TP53mut) patterns accordingly with Tessier-Cloutie et al. by three pathologists. A threshold of more than 70% positive tumor cells was used for p16 evaluation. Statistical analysis was performed.

Results: Mean patient age was 74 years(range 26–93). 47%, 10% and 43% of cases were diagnosed in FIGO stages I, II and III, respectively. Mean follow-up time was 47 months(42% A&W, 3% AWD, 38% DOD). Twenty-six tumors(31%) were HPVDNA-associated and CDKN2A was positive in 12(14%) primary tumors. TP53mut pattern was observed in 66(79%) primary tumors, 34(83%) recurrences and 26(84%) lymph node metastasis. The most frequent mutant pattern was the parabasal/diffuse overexpression(40%) and the mid-epithelial TP53wt pattern was exclusively observed in p16-positive lesions. TMA seems to be a reliable method for the evaluation of the TP53-IHC patterns. One of the lymph node metastases and 3 of the recurrences in TP53wt primary tumors became

TP53mut pattern. Three of the recurrences in TP53mut primary tumors became TP53wt. TP53mut pattern was associated with both HPVDNA- (86% vs 62% p<0.05) and absence of CDKN2A expression(86% vs 33%, p<0.01). After adjustment for stage and HPVDNA status, TP53mut pattern was associated with a worse prognosis(42% vs 57% OS; p<0.05).

Conclusions: Patients with TP53mut pattern had an inferior OS compared with TP53wt pattern adjusted to the FIGO stage and HPVDNA status. HPVDNA/CDKN2A-negative VSCC were associated with TP53mut pattern. The TP53-IHC pattern expression was heterogeneous between primary tumors, recurrences and lymph node metastases, suggesting that TP53 mutational status changes during the progression of the disease.

592 Aptima High-Risk HPV mRNA Assay of 939 Women with HSIL Cytology: Epidemiology and Histopathologic Outcomes

Aofei Li[1], Tiannan Wang[2], Jonee Matsko[3], Chengquan Zhao[4]
[1]University of Pittsburgh, UPMC, Pittsburgh, PA, [2]University of Southern California, Keck School of Medicine of USC, LAC+USC Medical Center, Los Angeles, CA, [3]UPMC Magee-Womens Hospital, Pittsburgh, PA, [4]Magee-Womens Hospital, University of Pittsburgh Medical Center, Pittsburgh, PA

Disclosures: Aofei Li: None; Tiannan Wang: None; Jonee Matsko: None; Chengquan Zhao: None

Background: The Aptima high-risk HPV(hrHPV) assay, which targets E6/E7 mRNA, has shown superior sensitivity and specificity in the literature. The present study aims to evaluate Aptima assay results in women with HSIL cytology and correlation with histopathologic outcomes.

Design: Cytology cases with HSIL diagnosis and co-testing of Aptima hrHPV assay were retrospectively reviewed from June 2015 to October 2020 in our archive. Cervical histopathology results within 6 months were also reviewed as follow-up for correlation. The results in 3 age groups (young: younger than 30, middle: 30 to 49; old: older than 50) were compared.

Results: 939 cytology HSIL cases with Aptima hrHPV assay were identified, of which 733 have six-month cervical histopathology for outcome correlation. Aptima HPV detection rate is similarly high among all age groups [96.6% (young) vs 95.6% (middle) vs 91.9% (old), p>0.4, chi-square test]. Histopathology outcome patterns are similar in the young and middle age groups (p>0.6), but are distinct in the old age group (p<0.001) with lower proportion of CIN2+ (CIN2 and above) cases [79.2% (young) vs 77.0% (middle) vs 55.4% (old)]. Aptima assay positivity shows additional predictive value for CIN2+ over CIN1- (less than CIN1) in the young and middle age group (odds ratio 6.32, p <0.0001), but less significant in the old age group (odds ratio 2.32, p>0.18). Of note, 2.4% (13/537) CIN2+ cases are Aptima hrHPV assay negative.

	hrHPV Positive			hrHPV Negative			Total		
Age (Positive %)	with F/U /all	CIN1- (%)	CIN2+ (%)	with F/U /all	CIN1- (%)	CIN2+ (%)	with F/U /all	CIN1- (%)	CIN2+ (%)
<30 (96.6)	103 /142	21 (20.4)	82 (79.6)	3 /5	1 (33.3)	2 (66.7)	106 /147	22 (20.8)	84 (79.2)
30-49 (95.6)	467 /603	98 (20.1)	369 (79.0)	21 /28	14 (66.7)	7 (33.3)	488 /631	112 (23.0)	376 (77.0)
≥50 (91.9)	128 /148	55 (43.0)	73 (57.0)	11 /13	7 (63.6)	4 (36.4)	139 /161	62 (44.6)	77 (55.4)
Total (95.1)	698 /893	174 (24.9)	524 (75.1)	35 /46	22 (62.9)	13 (37.1)	733 /939	196 (26.7)	537 (73.3)

Abbreviations: hrHPV, high-risk human papillomavirus; HSIL, high-grade squamous intraepithelial lesion; F/U, histopathology follow-up; CIN, cervical intraepithelial neoplasia; CIN1-: CIN1 or less than CIN1; CIN2+: CIN2 or above

Conclusions: Aptima hrHPV positive detection rate is high in HSIL women. It shows additional diagnostic value to cytopathology in women less than 50 years old. Importantly, however, a subpopulation (2.4%) of HSIL women who have developed CIN2+ lesions were not detected by Aptima hrHPV alone, highlighting the screening value of cytopathology in conjunction with HPV testing.

593 BCORL1-Driven High-Grade Endometrial Stromal Sarcomas and Uterine Adenosarcomas

Douglas Lin[1], Richard Huang[2], Douglas Mata[3], Brennan Decker[1], Natalie Danziger[1], Mirna Lechpammer[1], Matthew Hiemenz[1], Shakti Ramkissoon[4], Jeffrey Ross[5], Julia Elvin[1]
[1]Foundation Medicine, Inc., Cambridge, MA, [2]Foundation Medicine, Inc., Cary, NC, [3]Memorial Sloan Kettering Cancer Center, New York, NY, [4]Foundation Medicine, Inc., Morrisville, NC, [5]Upstate Medical University, Syracuse, NY

Disclosures: Douglas Lin: *Employee*, Foundation Medicine, Inc.; *Stock Ownership*, Roche; Richard Huang: None; Douglas Mata: *Employee*, Foundation Medicine, Inc.; Brennan Decker: *Employee*, Foundation Medicine; Natalie Danziger: *Employee*, Foundation Medicine Inc.; Mirna Lechpammer: *Stock Ownership*, GSK; Matthew Hiemenz: None; Shakti Ramkissoon: *Employee*, Foundation Medicine; Jeffrey Ross: *Employee*, Foundation Medicine; Julia Elvin: *Employee*, Foundation Medicine; *Stock Ownership*, Hoffmann-La Roche

Background: *BCORL1* is a transcriptional corepressor that is homologous to *BCOR*. Therefore, we hypothesized that molecular alterations of *BCORL1* may define a distinct subset of uterine sarcomas similarly to *BCOR*.

Design: We performed a retrospective search of our genomic testing database to identify *BCORL1*-altered uterine sarcomas. Clinicopathological and genomic data were re-reviewed, and both morphology and genomics were compared to previously described *BCOR*-altered endometrial stromal sarcomas (ESS).

Results: We identified 12 *BCORL1*-altered uterine sarcomas with striking resemblance to *BCOR*-ESS, including 5 cases with *BCORL1* rearrangements (*JAZF1-BCORL1, EP300-BCORL1,* or internal *BCORL1* rearrangement), 5 cases with inactivating *BCORL1* short variant mutations (T513fs*22, P600fs*1, R945*, R1196*, or R1265fs*4) and 2 cases with homozygous *BCORL1* deletion. The median age was 57.5 (range 33-79) years, and an association with aggressive clinical behavior (extrauterine spread and refractory recurrences) was identified. Diagnosis assigned prior to genomic testing varied: Seven patients were previously diagnosed as endometrial stromal sarcomas, two as high-grade uterine sarcomas, two as myxoid uterine leiomyosarcomas and one as a uterine spindle cell neoplasm consistent with leiomyosarcoma. Re-review demonstrated morphological overlap with *BCOR*-mutated ESS features, including high frequencies of both spindle (100%) and epithelioid (75%) components, myxoid stroma (83%) and collagen fibrosis (50%). High-grade nuclear atypia was present in 42% of cases. Similar to *BCOR*-ESS, 50% of *BCORL1*-altered sarcomas exhibited alterations in the targetable cyclin D1-CDK4 pathway via *CDK4* amplification or *CDKN2A* homozygous deletion. In contrast, 33% harbored *NF1* alterations; while 25% contained alterations in the *NF2-mTOR* pathway, thereby expanding potential therapeutic targets. In addition to ESS, *BCORL1* alterations (*JAZF1-BCORL1* fusions*, BCORL1* L461fs*5, or H1426fs*29*)* were identified in 6 cases of uterine adenosarcomas, whose sarcomatous component had high-grade atypia and prominent myxoid stroma, resembling *BCOR*- and *BCORL1*-altered ESS.

Conclusions: Inactivating *BCORL1* genomic alterations define a distinct subset of uterine sarcomas with biological overlap with *BCOR*-altered high-grade ESS, both of which may mimic myxoid leiomyosarcomas. *BCORL1*-driven uterine adenosarcomas with sarcomatous overgrowth should also be considered in the differential diagnosis of this group of tumors.

594 Pathologic Findings After Gender-Affirming Surgery: Evaluation of Cervical Pap Smears and Gynecological Tissue from Transmasculine Individuals

Lawrence Lin[1], Andrea Hernandez[1], Alan Marcus[1], Esther Adler[1]
[1]NYU Langone Health, New York, NY

Disclosures: Lawrence Lin: None; Esther Adler: None

Background: Gender affirming surgery is part of a multidisciplinary approach in the gender transition process, allowing patients to align their physical anatomy to their internal sense of identity. Our study evaluates the cytology and histopathology of transmasculine gynecological specimens. A deeper examination of the pathologic findings may strengthen care for transmasculine individuals and increase our understanding of the influence of hormonal therapy in specific organs.

Design: This is an IRB-approved retrospective study that included all transmasculine individuals undergoing a gender-affirming gynecological surgery from January 2015 to June 2020. All surgical pathology and cytology slides were reviewed. Clinical data were retrieved from electronic health records.

Results: Forty patients were identified with a median age of 26.5 years (range 17-56) and a median body mass index of 25.38 kg/m2 (range 18.9 - 43.4). The majority of patients were white (52%), were receiving androgen therapy for at least 6 months (95%) and had a previous bilateral mastectomy (92%). The histologic samples comprised of 40 uteri, 40 bilateral fallopian tubes and 36 bilateral ovaries. The overall findings are summarized in table 1. The majority of the endometria were inactive (75%) with significant stromal fibrosis (80%). Some patients showed evidence of cycling endometrium with proliferative (17.5%) and secretory (7.5%) patterns. The most common findings in the ovaries were the presence of multiple bilateral cystic follicles (50%), stromal hyperplasia (14%) and of corpora lutea (14%). The most common findings in the cervix was transitional metaplasia (42.5%). Of the 8 available cervical cytology specimens, 2 were unsatisfactory, 4 were negative for intraepithelial lesion or malignancy and 2 had atypical squamous cells of undetermined significance (ASC-US).

Table 1 – Findings in Cervical Pap Smears and Gynecological Tissue from Transmasculine Individuals

Findings	Cases / Total (Percentage)
Endometrium – menstrual cycle phase	
Inactive	30/40 (75%)
Proliferative	7/40 (17.5%)
Secretory	3/40 (7.5%)
Endometrium - other findings	
Stromal fibrosis	32/40 (80%)
Tubal metaplasia	23/40 (57.5%)
Myometrium	
Leiomyomata	5/40 (12.5%)
Smooth muscle cell atrophy	2/40 (5%)
Cervix	
Transitional metaplasia	17/40 (42.5%)
Parakeratosis	12/40 (12.5%)
Fallopian tubes	
Plical fibrosis	3/40 (7.5%)
Paratubal ectopic epididymis	3/40 (7.5%)
Ovaries	
Multiple bilateral cystic follicles	18/36 (50%)
Stromal hyperplasia	5/36 (14%)
Corpora lutea	5/36 (14%)
Follicular cyst	4/36 (11%)
Cervical Pap smears	
Negative for intraepithelial lesion or malignancy	4/8 (50%)
Unsatisfactory	2/8 (25%)
ASC-US	2/8 (25%)

Conclusions: Despite prolonged use of androgens, endometria in transmasculine individuals may show cycling activity with proliferative and secretory patterns. The presence of multiple bilateral cystic ovarian follicles provides evidence that androgens can result in abnormal follicular development, similar to polycystic ovary syndrome. The chronic use of androgens in young individuals seems to induce transitional metaplasia in the cervix, which can impact cervical cytology results including increase the percentage of unsatisfactory samples and ASC-US and has the potential to mimic high-grade squamous dysplasia.

595 Small Tumor Nests are Associated with Poor Clinical Outcome in Clear Cell Carcinoma of Ovary

Lawrence Lin[1], Ronaldo Zamuco[1], Pratibha Shukla[2]
[1]NYU Langone Health, New York, NY, [2]NYU School of Medicine, New York, NY

Disclosures: Lawrence Lin: None; Ronaldo Zamuco: None; Pratibha Shukla: None

Background: Clear cell carcinoma of ovary (CCCO) accounts for 5-25% of ovarian carcinomas. Considered a high-grade malignancy by default, the role of histological grading for assessing clinical outcome is not established in CCCO. We aimed to evaluate histopathological features predictive of clinical outcome in patients with CCCO.

Design: Pathology database was searched after IRB approval. A total of 69 cases of CCCO were studied. Slides from primary tumor resection were reviewed blinded to outcome. The original diagnosis of CCCO was confirmed and the following histopathologic features were recorded: percentage of solid component, degree of nuclear atypia, mitotic activity, intratumoral inflammation, presence of small tumor nests (intratumoral single cells or clusters of <5 cells in non-hyalinized stroma, Figure 1A-B), tumor budding (peritumoral single cells or clusters of <5 cells), lymph node involvement and endometriosis. Information regarding age at diagnosis, clinical stage, treatment and follow-up was obtained from medical charts. Kaplan-Meier survival curves with log rank test, Fisher's exact test and Mann-Whitney test were used for statistical analysis.

Results: Median patient age was 52 years (range 26-75 years). Forty-nine (71%) tumors were associated with endometriosis and 37 (53%) presented at stage I. Ten (15%) patients died of disease, 14 (20%) were alive with active disease and 45 (65%) had no evidence of disease at last follow-up (median follow-up: 34.2 months, range 1.2 – 230.6). Advanced stage, positive lymph nodes and presence of small tumor nests were significantly associated with shorter overall survival (p=0.006, p<0.001, p=0.004, respectively; Figure 2A-C) and recurrence/progression despite treatment (p<0.0001, p=0.0011, p=0.0003, respectively; table 1). Also, within the cohort of low stage patients (stage I and II), presence of small tumor nests was associated with recurrence/disease progression (p=0.0014; table 1). None of the other studied features reached statistical significance for assessment of prognosis.

Table 1. Clinicopathological features in clear cell carcinoma of ovary in relation to disease remission or recurrent/progressive disease

	Disease remission (overall cohort: n = 44; low-stage: n=39)	Recurrent / progressive disease (overall cohort: n = 25; low-stage: n=9)	p-value
Stage in the overall cohort (%)			***<0.0001****
I	32 (72%)	5 (20%)	
II	7 (16%)	4 (16%)	
III	4 (9%)	12 (48%)	
IV	1 (2%)	4 (16%)	
Lymph node involvement in the overall cohort (%)			***0.0011****
Absent	40 (95%)	12 (60%)	
Present	2 (5%)	8 (40%)	
Small tumor nests in the overall cohort (%)			***0.0003****
Absent	31 (70%)	6 (24%)	
Present	13 (30%)	19 (76%)	
Small tumor nests in low-stage disease (%)			***0.0014****
Absent	28 (72%)	1 (11%)	
Present	11 (28%)	8 (89%)	

* statistically significant

Figure 1 - 595

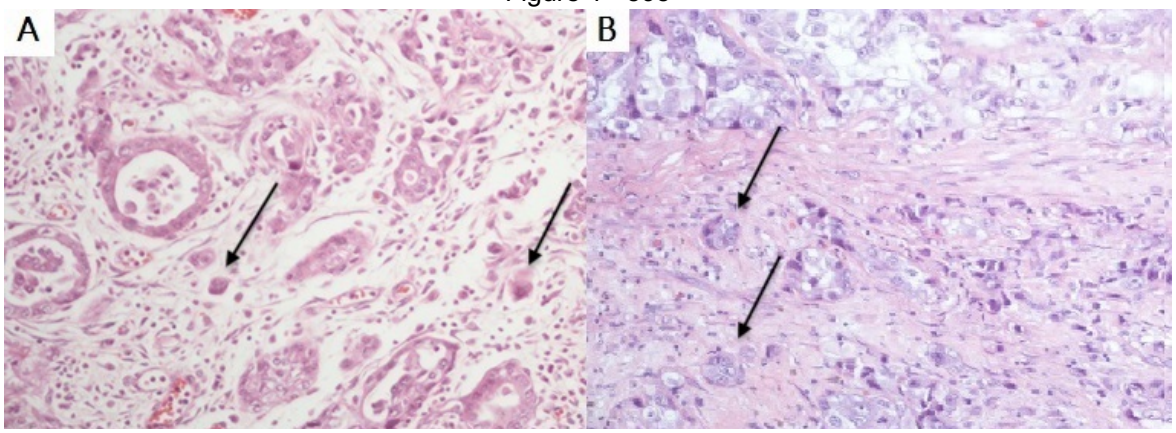

Figure 2 - 595

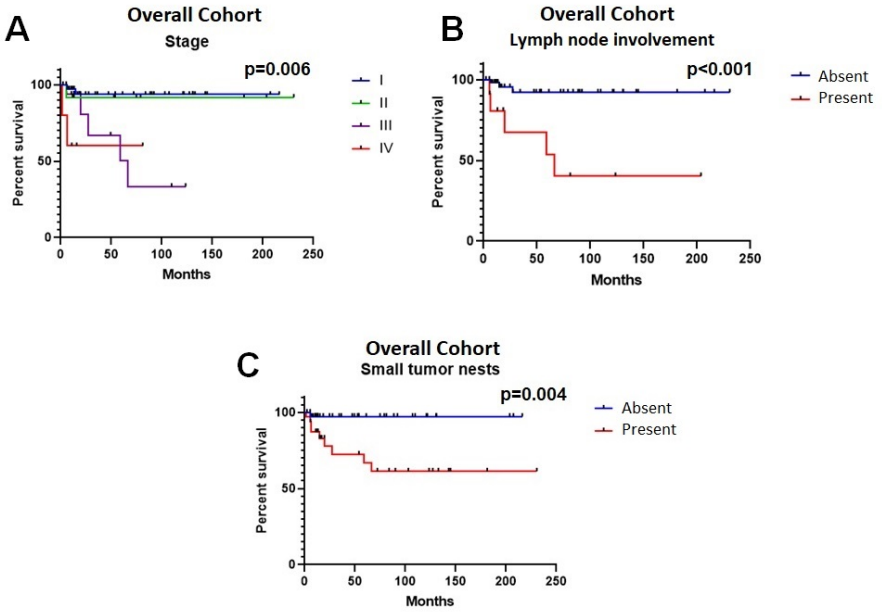

Conclusions: Besides the classic prognostic factors of stage and lymph node status, presence of small tumor nests seems to be associated with poorer outcome in patients with CCCO. Specifically, in patients with early stage disease, evaluation of small tumor nests may help to better determine prognosis. These findings should be further evaluated in larger studies.

596 Endometrial Cancer with Ambiguous Morphology Shows Diverse Immunohistochemistry and Molecular Profiles

Wanrun Lin[1], Yan Wang[1], Liying Zhang[2], Cyriac Kandoth[3], Ruby Chang[1], Hao Chen[1], Wenxin Zheng[1]
[1]UTSouthwestern Medical Center, Dallas, TX, [2]University of California, Los Angeles, Los Angeles, CA, [3]David Geffen School of Medicine at UCLA, Los Angeles, CA

Disclosures: Wanrun Lin: None; Yan Wang: None; Liying Zhang: *Stock Ownership*, Shanghai Genome Center; *Employee*, Shanghai Genome Center; Cyriac Kandoth: None; Ruby Chang: None; Hao Chen: None; Wenxin Zheng: None

Background: Endometrial cancers can be accurately diagnosed on the basis of morphology in most of the cases. However, it is known that high-grade endometrial endometrioid carcinomas (EEC) is difficult to differentiate from

endometrial serous carcinomas (ESC), albeit clinical outcome and management are clearly different from each other. International Society of Gynecologic Pathologists recently recommended a panel of immunohistochemistry (IHC) markers to be used to aid the diagnosis based on loss of PTEN or MMR protein immunoreactivity favoring high-grade EEC, while mutant p53 and block p16 sains occurring more commonly in ESC. Nevertheless, diagnostic problems remain since both mutant p53 and diffuse p16 stains are seen in a significant portion of high-grade EECs. This study aims to examine if IHC panels are able to accurately differentiate EEC from ESC by comparing the results of TCGA molecular classification of the endometrial cancers.

Design: Ten cases including 8 with ambiguous morphology (partial endometriod and partial serous) and 2 mixed EEC and ESC were studied. Representative areas of each case were stained with p53, p16, ER, PTEN, PAX-2, MMR panel, and WT-1 as well as genetically sequenced by using MSKCC-IMPACT analysis followed by TCGA molecular classifications (performed by CK, an original author of the TCGA article). Pathologic diagnosis was given to each case based on the results of IHC, then compared with the molecular classifications.

Results: Among the 10 cases, molecular classification shows 5 copy number high (CNH), 3 copy number low (CNL), 1 POLE-EDM, and 1 without specific mutation detected. Within the 5 CNH cases, 3 were morphologically diagnosed as ESC, 1 EEC, and 1 mixed EEC/ESC. One POLE-EDM and the other without particular mutation represented EEC G3 by morphology. Six cases with p53 mutant and p16 diffuse stains showed 3 ESC (CNH), 2 mixed EEC/ESC (1 CNL and 1 CNH) and 1 EEC G3 (CNH). Two cases with PTEN loss had 1 mixed EEC/ESC (CNH) and 1 EEC G3 (CNH). Three WT-1 positive cases showed 1 mixed EEC/ESC (CNH) and 1 ESC (CNH) 1 EEC (CNL). ER and PAX2 had no particular patterns. Detailed data is presented in Table 1.

*Diagnosis was made based on the combination of morphology and IHC findings; **P53: Mut, mutant type of expression; Multi, admised mutant and wild type of expression patterns; P16: DP, diffuse positive; ND, non-diffuse or patchy positive; N/A: not available; PL: partial loss; MSKCC-IMPACT: analyzed by IMPACT gene sequencing panel at Memorial Sloan-Katherine Cancer Center based on TCGA endometrial cancer data.

Table 1. Diagnostic utility with IHC panels for endometrial cancers with ambiguous or mixed morphology**

Case	P53	P16	ER (%)	PTEN	PAX-2	MMR	WT-1	Diagnosis*	MSKCC-IMPACT
1	Mut	DP	90	Intact	Loss	Intact	-	Mixed	Copy number low
2	Mut	DP	60	Loss	PL	Intact	+	Mixed	Copy number high
3	Multi	DP	85	N/A	PL	Intact	-	EEC G3	No mutation
4	Wild	DP	30	Intact	Intact	Intact	-	EEC G3	Copy number low
5	Mut	ND	60	Intact	Loss	PMS2-	-	EEC G3	POLE (p286R)
6	Mut	DP	90	Intact	Loss	Intact	-	ESC	Copy number high
7	Mut	DP	0	Intact	Intact	Intact	+	ESC	Copy number high
8	Mut	DP	50	Loss	Loss	Intact	-	EEC G3	Copy number high
9	Mut	DP	0	Intact	Intact	Intact	-	ESC	Copy number high
10	Wild	ND	85	Intact	Intact	Intact	+	EEC G3	Copy number low

Conclusions: Endometrial cancers with ambiguous morphology are heterogeneous and demonstrate diverse IHC and molecular profiles. Diagnostic utility of the IHC panel is limited. Mutant p53 with diffuse p16 is not specific for ESC. PTEN loss may occur in ESC. Both ER and WT-1 are non-specific. Accurate pathologic classification requires sequencing approach.

597 Predicting Risks of Tumor Recurrence and Nodal Metastasis for HPV Associated Endocervical Adenocarcinoma from Cervical Biopsies

Rongzhen Luo[1], M. Ruhul Quddus[2], Aijun Liu[3], Xianghong Yang[4], Wentao Yang[5], Xiaofei Zhang[6], Huiting Zhu[7], Ruijiao Zhao[8], Li Li[9], Qingping Jiang[10], Ruby Chang[11], Glorimar Rivera Colon[11], Jayanthi Lea[11], Wenxin Zheng[11]

[1]Sun Yat-sen University Cancer Center, Dallas, TX, [2]Women & Infants Hospital/Alpert Medical School of Brown University, Providence, RI, [3]Chinese PLA General Hospital, Beijing, China, [4]Shengjing Hospital of China Medical University, Shenyang, China, [5]Fudan University Shanghai Cancer Center, Shanghai, China, [6]Women's Hospital, School of Medicine, Zhejiang University, [7]Shanghai First Maternity and Infant Hospital, Shanghai, China, [8]Henan Provincial People's Hospital, Zhengzhou, China, [9]School of Basic Medical Sciences, Shandong University, Jinan, China, [10]Third Affiliated Hospital, Guangzhou Medical University, Guangzhou, China, [11]UTSouthwestern Medical Center, Dallas, TX

Disclosures: Rongzhen Luo: None; M. Ruhul Quddus: None; Aijun Liu: None; Xianghong Yang: None; Wentao Yang: None; Xiaofei Zhang: None; Huiting Zhu: None; Ruijiao Zhao: None; Li Li: None; Qingping Jiang: None; Ruby Chang: None; Glorimar Rivera Colon: None; Jayanthi Lea: None; Wenxin Zheng: None

Background: One of the major obstacles for patients with usual type endocervical adenocarcinoma (uEAC) receiving optimal surgical management is lack of predictive measures prior to radical surgery. Silva patterns of invasion (POI) is excellent to predict nodal metastasis (NM) from resections, but unclear if useful in biopsies. A very recent study about uEAC at UTSW showed necrotic tumor debris (NTD) and tumor nuclear grade (TNG) have a good prediction of NM from biopsy specimens. Such findings are promising since these microscopically identifiable features are part of routine pathology practice. The goal of this multi-institutional study is to investigate the values of Silva patterns of invasion, necrotic tumor debris and tumor nuclear grade in predicting risks of NM and tumor recurrence (TR) from cervical biopsies.

Design: This study included 397 paired biopsy-resection of uEACs. In every pair of cases, evaluability of POI, status of NTD, TNG and other pathologic parameters (tumor size, depth of invasion, lymphovascular invasion, and resection margins) were examined for the correlation with NM and TR. Standard statistical analyses were performed to examine if the tested pathologic parameters could predict the risks of NM and TR.

Results: Among 397 biopsies, only 144 (36%) were evaluable for POI. Cases with Pattern A invasion (n=37) had 3% NM and no TR, in comparison to 14% NM and 10% TR among cases with POI B or C (n=107). Cases NTD- (n=221) had 5% NM and TR, in contrast to 29% NM and 18% TR among cases with NTD+ (n=176). EACs with Grade 1 nuclei (n=86) had 3% NM and 2% TR, in contrast to 19% NM and 13% TR among cases with Grade 2 or 3 nuclei (n=311). Furthermore, when combining NTD and TNG, cases with grade 1 nuclei and negative NTD (n=73) had 0% NM and 1% TR, in contrast to the rest of cases with either NTG+ or grade 2-3 nuclei, which had significantly increased risks for NM (19%) and TR (13%) . Detailed data are summarized in Table 1.

* Fisher's Exact Test; NTD: necrotic tumor debris; TNG: tumor nuclear grade

Table 1. Risk predictions by evaluating pathologic features from biopsy specimens for patients with usual type endocervical adenocarcinoma.

		N	Nodal Metastasis (N/%)	p-value*	Tumor Recurrence (N/%)	p-value*
Growth Pattern	A	37	1 (3%)	0.0709	0 (0%)	0.0662
	B or C	107	15 (14%)		11 (10%)	
NTD	Absent	221	11 (5%)	<0.0001	11 (5%)	<0.0001
	Present	176	51 (29%)		31 (18%)	
TNG	1	86	3 (3%)	0.0002	2 (2%)	0.0027
	2 or 3	311	59 (19%)		40 (13%)	
NTD + TNG	Absent NTD and TNG 1	73	0 (0%)	<0.0001	1 (1%)	0.0025
	Others (Present NTD or TNG 2 or 3)	324	62 (19%)		41 (13%)	

Conclusions: Pathologic evaluation of uEAC with NTD and TNG on cervical biopsies has excellent predictive values. Evaluation of POI with Silva system is outstanding from resections, but limited on biopsies. Presence of either NTD+, TGN 2-3 or Silva POI B/C from biopsies are associated with a significantly higher risk of NM and TR. More importantly, NTD- together with TNG1 is associated with a negligible risk of NM and TR. Finding low risk patients from biopsy provides opportunities of fertility sparing management options for uEAC.

598 KRAS Mutation in Ovarian Serous Borderline Tumors and Extraovarian Implants Dictates an Unfavorable Prognosis

Austin McHenry[1], Pei Hui[2], Natalia Buza[3], Douglas Rottmann[4]
[1]Yale University, New Haven, CT, [2]Yale University School of Medicine, New Haven, CT, [3]Yale School of Medicine, New Haven, CT, [4]Yale-New Haven Hospital, New Haven, CT

Disclosures: Austin McHenry: None; Pei Hui: None; Natalia Buza: None; Douglas Rottmann: None

Background: Abnormal activation of mitogen-activated protein kinase (MAPK) pathway due to mutations in *KRAS* and *BRAF* are frequently found in ovarian serous borderline tumors (SBT). We investigated the mutation status of KRAS and BRAF in ovarian SBTs and their extraovarian implants in correlation with clinical outcome.

Design: Consecutive cases of SBT with extraovarian implants were retrieved from our institutional archives. Histological review was performed, followed by KRAS and BRAF mutation analyses on both the primary ovarian tumors and extraovarian implants. Clinical follow-up data were retrieved from the medical record.

Results: Among the 41 paired cases, there were 20 invasive implants and 21 non-invasive implants. KRAS analysis was informative in 36 primary tumors and 40 implants. Of these, 35 paired cases had KRAS data (19 non-invasive and 16 invasive-implants). KRAS mutations were found in 21 cases (60%), including 18 primary SBTs and 12 implants (5 non-invasive and 7 invasive). BRAF V600E mutations were found in 4 of 35 cases (4 primary tumors and 1 non-invasive implant) (11.4%). Concordant KRAS/BRAF mutational profiles were present in 18 paired tumors. A discordant profile was seen in 19 cases (10 non-invasive and 9 invasive implants), of which 11 were associated with endosalpingiosis (57.8%), in contrast to only 4 of 16 concordant cases with endosalpingiosis (25%). Of the 39 patients with available follow-up information, disease recurrence was seen in 34.8% (8/23) of patients with KRAS mutations, compared to none of 16 patients without KRAS mutations. High stage disease (IIIC or above) was seen in 47.8% (11/23) of patients with KRAS mutations, while only 37.5% (6/16) without KRAS mutations. Overall, patients with KRAS mutations in either the primary tumor or implant had a worse disease-free survival (P = 0.019, log-rank test, Figure 1). KRAS mutation of the primary tumors alone also predicted an adverse disease-free survival (Log-rank test, P = 0.037, Figure 2).

Figure 1 - 598

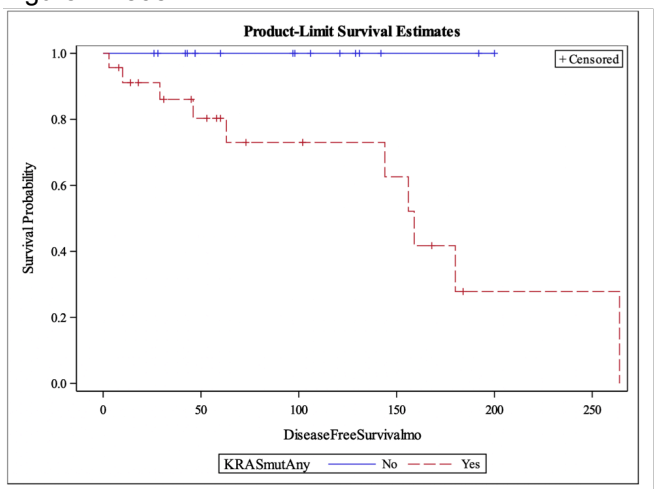

Figure 1: Patients with KRAS mutations in either primary tumor or implant had a worse disease-free survival (N= 39, Log-rank test, p-value = 0.019).

Figure 2 - 598

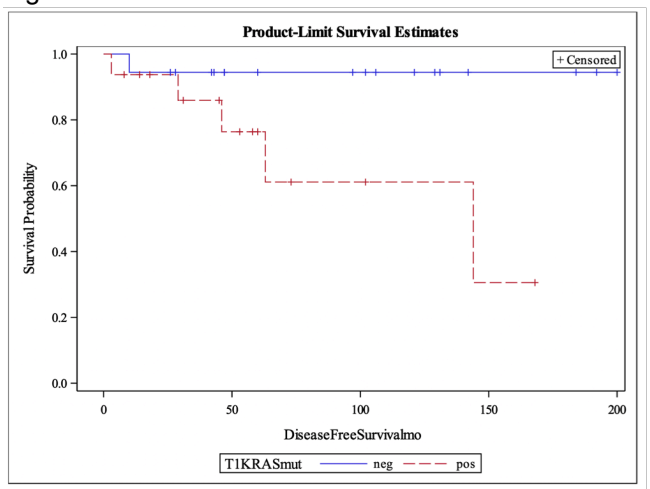

Figure 2: Patients with KRAS mutations evaluated only in the primary tumor predicated a worse disease-free survival (N= 34, Log-rank test, p-value = 0.037)

Conclusions: Significant discordance of KRAS mutation status exists between primary SBTs and their implants and KRAS mutated non-invasive implants are more frequently associated with endosalpingiosis, suggesting a different pathogenesis between invasive and non-invasive implants. KRAS mutation is a significant prognostic indicator for risk of tumor recurrence. KRAS mutation of either primary SBT or extraovarian implants may be used as an important prognostic biomarker.

599 Surface Prostatic Metaplasia of the Uterine Cervix: Prevalence in Gender Affirming Hysterectomies and Comparison to Benign Hysterectomies from Cis Women

Emily Mcmullen[1], Andrew Sciallis[1], Stephanie Skala[1]
[1]University of Michigan, Ann Arbor, MI

Disclosures: Andrew Sciallis: None; Stephanie Skala: None

Background: Ectopic prostate tissue (prostatic metaplasia) has been described as an uncommon incidental finding typically seen in the lamina propria of the uterine cervix. It is not well-understood whether prostatic-type glands in the cervix represent a developmental abnormality, teratomatous tissue, mesonephric remnants, or metaplasia of endocervical glands. There is a recently reported series of cases with prostatic-type glands involving surface squamous epithelium of the uterine cervix and/or vagina, usually in the setting of androgen excess (including therapy for gender dysphoria).

Design: The surgical pathology archives of a single large academic institution were searched for hysterectomies from male patients and/or with provided clinical history of gender dysphoria, resected between 2013 and 2020 (n=35). For comparison, 13 recent hysterectomies for prolapse and 13 recent hysterectomies for uterine fibroids were included. Study pathologists examined all submitted sections of cervix and stained representative slides with NKX3.1.

Results: Involvement of squamous epithelium by prostatic-type glands was seen in 34% (12/35) of gender-affirming hysterectomies, with 11 other cases showing scattered NKX3.1 positive basal keratinocytes without gland formation. One 37-year-old patient with prolapse demonstrated surface prostatic metaplasia, as did one 48-year-old perimenopausal woman (on progestin) undergoing hysterectomy for symptomatic fibroids. One additional prolapse hysterectomy from a 73-year-old woman on vaginal estrogen showed rare NKX3.1 positive basal keratinocytes.

Conclusions: In keeping with the literature, surface prostatic metaplasia was seen more often in hysterectomies performed for gender affirmation than for prolapse or symptomatic fibroids. However, our initial control cohort does include two cases with surface prostatic metaplasia and no known androgen excess. Staining of a more comprehensive control cohort is under way for further characterization of this process.

600 Overexpression of EZH2 in Ovarian Tumors is Associated with Advanced Stage and Tumor Recurrence

Rachelle Mendoza[1], Amir Dehghani[2], Elmer Gabutan[1], M. Haseeb[1], Raavi Gupta[1]
[1]SUNY Downstate Medical Center, Brooklyn, NY, [2]SUNY Downstate, Brooklyn, NY

Disclosures: Rachelle Mendoza: None; Amir Dehghani: None; M. Haseeb: None; Raavi Gupta: None

Background: Epithelial ovarian cancer (EOC) accounts for more deaths than any other gynecologic malignancy in the United States. Enhancer of zeste homolog 2 (EZH2) is often expressed at higher levels in human EOC cells compared to normal ovarian and tubal epithelial cells, and its expression positively correlates with proliferation in these cells. We investigated EZH2 expression in differentiating malignant and borderline serous and mucinous ovarian tumors.

Design: We identified 68 patients diagnosed with benign, borderline or malignant serous, mucinous or sero-mucinous ovarian tumors over a 10-year period at a tertiary care hospital.68 formalin-fixed paraffin-embedded representative tumor sections were selected. Immunohistochemical staining using a rabbit monoclonal antibody to EZH2 N-terminal (clone EPR9307; Abcam, Boston, USA) was performed. EZH2 nuclear expression was scored

based on the number of tumor cells expressing EZH2 and the intensity of staining. Patients were followed for tumor recurrence and survival for five years after initial diagnosis.

Results: Most of our patients were non-Hispanic Black (83.8%). 55 (80.9%) had serous, 11 (16.2%) had mucinous and 1 (1.5%) had sero-mucinous tumors. Most of the tumors were benign (41; 60.3%), 19 (27.9%) were malignant and 7 (10.3%) were borderline. Almost all of the malignant tumors were high grade (17/19; 89.5%). 5 years after diagnosis, 8 (11.8%) patients had recurrence, 2 (2.9%) died and 16 (23.5%) were lost to follow-up.

Compared to both benign and borderline, malignant ovarian tumors had significantly higher EZH2 nuclear expression, based on both quantity (Pearson Chi-Square=61.081, p=0.000) and intensity of staining (Pearson Chi-square=5.674, df=6, p=0.000). Among the malignant tumors, 84.2% had increased EZH2 expression (vs. 14.3% borderline tumors and 0.0% benign). Malignant cases with quantitatively increased EZH2 expression had significantly higher pathologic tumor staging (at least pT3; p=0.049; OR=0.167, 95% CI 0.026-1.088), higher FIGO stage at diagnosis (at least stage IIIa; p=0.047) and higher risk for recurrence (p=0.005). Among patients with malignant tumors, increased EZH2 expression was also predictive of shorter disease-free survival (log-rank p value=0.0008).

Characteristics	Categories	*n* (%)
Age (median, IQR), yrs		56 yrs (47.3-65.0)
Race	Non-Hispanic Black	57 (83.8)
	Other	11 (16.2)
Symptom	Pelvic mass	23 (33.8)
	Abdominal pain/distention	30 (44.1)
	Abnormal uterine bleeding	9 (13.2)
	Others	6 (8.8)
Tumor type	Benign	41 (61.2)
	Borderline	7 (10.4)
	Malignant	19 (28.4)
Tumor histology	Serous	55 (82.1)
	Mucinous	11 (16.4)
	Sero-mucinous	1 (1.5)
FIGO stage at diagnosis	Benign	42 (61.8)
	Early (stages I-II)	13 (19.1)
	Late (stages III-IV)	13 (19.1)
Recurrence	No recurrence	44 (84.6)
	With recurrence	8 (15.4)
Survival	Alive	51 (96.2)
	Deceased	2 (3.8)

Figure 1 - 600

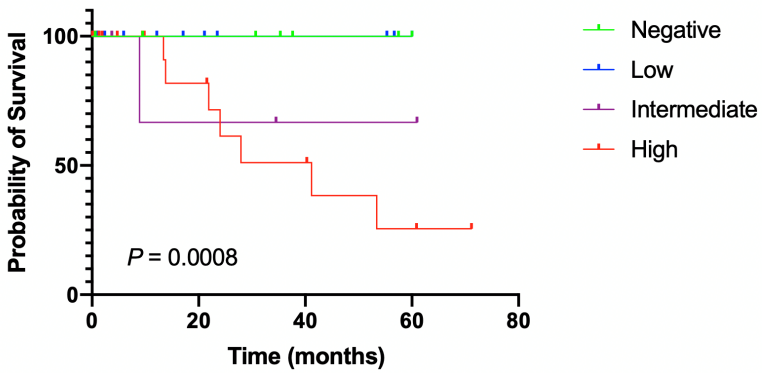

Conclusions: EZH2 expression can be utilized in differentiating borderline and malignant serous and mucinous tumors. EZH2 overexpression has prognostic significance in ovarian cancer, and should be included in the routine diagnostic workup.

601 PD-L1 Expression in Cervical Invasive Squamous Cell Carcinoma Is Associated with Poorer Outcomes: Analysis from an Urban Public Hospital

Ashley Monsrud[1], Vaidehi Avadhani[2], Marina Mosunjac[1], Lisa Flowers[1], Uma Krishnamurti[1]
[1]Emory University, Atlanta, GA, [2]Emory University Hospital, Atlanta, GA

Disclosures: Ashley Monsrud: None; Vaidehi Avadhani: None; Marina Mosunjac: None; Lisa Flowers: None; Uma Krishnamurti: None

Background: Upregulation of programmed death-ligand 1 (PD-L1), an immunoregulatory protein is associated with adverse outcome in several malignancies. Cervical cancer is one of the common gynecological malignancies. Therapy targeting the PD-L1 pathway offers options for better management of cervical invasive squamous cell carcinoma. This study aims to correlate PD-L1 expression with clinicopathologic factors and clinical outcomes in invasive cervical squamous cell carcinoma (ISCC).

Design: After IRB approval, formalin-fixed, paraffin embedded sections of 73 cases of ISCC at Grady Memorial Hospital, Atlanta, from 2010-2018 were immunostained for PD-L1 (Dako 22C3). Combined positive score (CPS= #of PD-L1 staining tumor cells, tumoral and peritumoral lymphocytes & macrophages x 100 / Total # of viable tumor cells) was evaluated. CPS of > 5 was interpreted as PD-L1 positive (PD-L1 +) for statistical analysis. We correlated PD-L1 expression with age, stage, and clinical outcomes. Kaplan-Meier curves for progression free survival (PFS) and overall survival (OS) were plotted and compared using the log rank test. Cox regression analysis was performed to identify significant prognostic factors (Two-tailed p< 0.05 was considered statistically significant).

Results: PD-L1 was positive in 30/73 (41.1%) of cases. A greater proportion of PD-L1 + cases (73.3%) presented in higher stages (stages 3 & 4) compared with PD-L1 negative cases (46.5%); p=0.03. All deaths were cancer related in our study. The mean disease specific survival (MDSS) was lower in PD-L1 + patients (24 months) compared with PD-L1 negative patients (36 months). PD-L1 + patients had a worse 5-year OS (40% vs. 60% for PD-L1 negative patients); p=0.04. PD-L1 + patients also had a worse 5-year PFS of 25% vs 50% in the PD-L1 negative group; p=0.04. Ten percent of patients were HIV positive and age distribution was similar in both groups. By Cox regression analysis, only stage appears to an independent prognostic indicator.

Table 1: PD-L1 expression and clinicopathologic characteristics and disease outcomes.

	PD-L1 negative 43/73(58.9%)	**PD-L1 positive 30/73 (41.1%)**	
Age			
Mean	48	47	
Median	47	47	
Range	28-67	29-69	
Stage			
High Stage (III/IV)	20(46.5%)	22(73.3%)*	p=0.03
Disease Specific Survival			
Mean (months)	36	24	
5- year PFS	50%	25%*	p=0.04
5- year OS	60%	40%*	p=0.04

Conclusions: The mean disease specific survival, 5-yr PFS, and 5-yr OS is significantly lower in PD-L1 positive patients. PD-L1 positive patients present at a higher stage of disease. By Cox regression analysis, only stage appears to an independent prognostic indicator. This study highlights the potential of PD-L1 targeted therapy in better management and treatment of cervical invasive squamous cell carcinoma.

602 Utility of EPM2AIP1 Immunohistochemistry as Surrogate Testing for MLH1 Promoter Methylation in Endometrial Cancer

Miralem Mrkonjic[1], Gulisa Turashvili[1]
[1]*Mount Sinai Hospital, University of Toronto, Toronto, Canada*

Disclosures: Miralem Mrkonjic: None; Gulisa Turashvili: None

Background: Immunohistochemistry for DNA mismatch repair (MMR) proteins has become routine practice in endometrial carcinomas for Lynch syndrome screening and/or part of diagnostic evaluation. Approximately 20-30% of endometrial carcinomas demonstrate microsatellite instability due to defective DNA mismatch repair. Vast majority of MLH1/PMS2-deficient tumors are sporadic and show *MLH1* promoter hypermethylation. MLH1 methylation testing by quantitative PCR-based technique is time, labor and tissue intensive with an average institutional turnaround time of two weeks. *MLH1* gene shares its promoter with *EPM2AIP1* gene, which is reported to be ubiquitously expressed. In vitro studies have demonstrated that *MLH1* promoter methylation also downregulates EPM2AIP1 transcription. We set out to assess whether immunohistochemistry (IHC) for EPM2AIP1 protein in combination with MMR proteins can serve as surrogate marker for *MLH1* promoter methylation.

Design: We performed a retrospective review of all MLH1/PMS2-deficient endometrial carcinomas that underwent *MLH1* promoter methylation testing from January 1, 2020 to October 18, 2020 at our institution. Microscopic slides were reviewed and IHC for EMP2AIP1 was performed. The results were correlated with MLH1 and PMS2 protein expression by immunohistochemistry (if available) and with *MLH1* promoter methylation status (percent methylated rate [PMR]).

Results: A total of 125 endometrial carcinomas were identified. To date, 16 cases have been successfully tested, including 15 endometrioid carcinomas and 1 dedifferentiated carcinoma. Of endometrioid carcinomas, 7 were FIGO grade 1, 5 were FIGO grade 2 and 3 were FIGO grade 3. Nuclear EPM2AIP1 protein expression was observed in benign endometrial epithelial and stromal cells, myometrial smooth muscle cells, and in one endometrioid adenocarcinoma with intact MMR protein expression. Loss of nuclear EPM2AIP1 staining was identified in 15/16 (94%) endometrial carcinomas with positive *MLH1* promoter methylation. Only one tumour demonstrated patchy and weak retained expression (PMR rate of 175%).

Conclusions: Based on these preliminary results, EMP2AIP1 immunohistochemistry is concordant with *MLH1* promoter methylation testing in 94% of cases and shows promise as a surrogate marker for *MLH1* promoter methylation in endometrial carcinomas.

603 HER2 Testing in High-grade Uterine Carcinoma: The Experience of an Academic Medical Center that Performs Primary HER2 FISH Testing

Kristen Muller[1], Jessica Dillon[1], Laura Tafe[1]
[1]*Dartmouth-Hitchcock Medical Center, Lebanon, NH*

Disclosures: Kristen Muller: None; Jessica Dillon: None; Laura Tafe: None

Background: HER2 testing is recommended for all advanced or recurrent endometrial serous carcinoma (EC) for the addition of HER2-targeted therapy to chemotherapy regimens. At our institution, we recently implemented HER2 testing for high-grade endometrial cancers with a serous component. In our laboratory, we perform fluorescence in situ hybridization (FISH) as the primary assay to identify HER2 amplification. At this time, there are still no best practice guidelines for assessing HER2 in EC although a modifying scoring system based on ASCO/CAP guidelines for breast cancer was recently proposed (PMID: 32649220). Here we report our experience with HER2 testing in EC.

Design: All EC cases analyzed for HER2 via dual-probe FISH (PathVysion) were included. Cases in which HER2 showed heterogeneity by FISH were also tested by HER2 immunohistochemistry (clone 4B5) in order to render a conclusive interpretation. HER2 was reported as positive when the HER2/CEP17 ratio was ≥2.0 and/or the IHC showed 3+ staining in >30% of the tumor cells (strong complete or basolateral/lateral pattern).

Results: To date, twenty EC cases were tested consisting of serous carcinoma (16), mixed serous and endometrioid carcinoma (2) and carcinosarcoma (2). Four cases were positive by FISH (20%), all of which were pure serous carcinomas. Corresponding HER2 IHC was performed in 10 cases, all of which collaborated the FISH results. Two cases were noted to have significant heterogeneity on FISH; HER2 IHC was utilized in these cases to assign a positive and negative result, respectively (Figure 1: HER2 positive case with heterogeneity). One case of (serous type), negative by FISH, showed marked cytoplasmic staining by IHC, a potential pitfall.

Figure 1 - 603

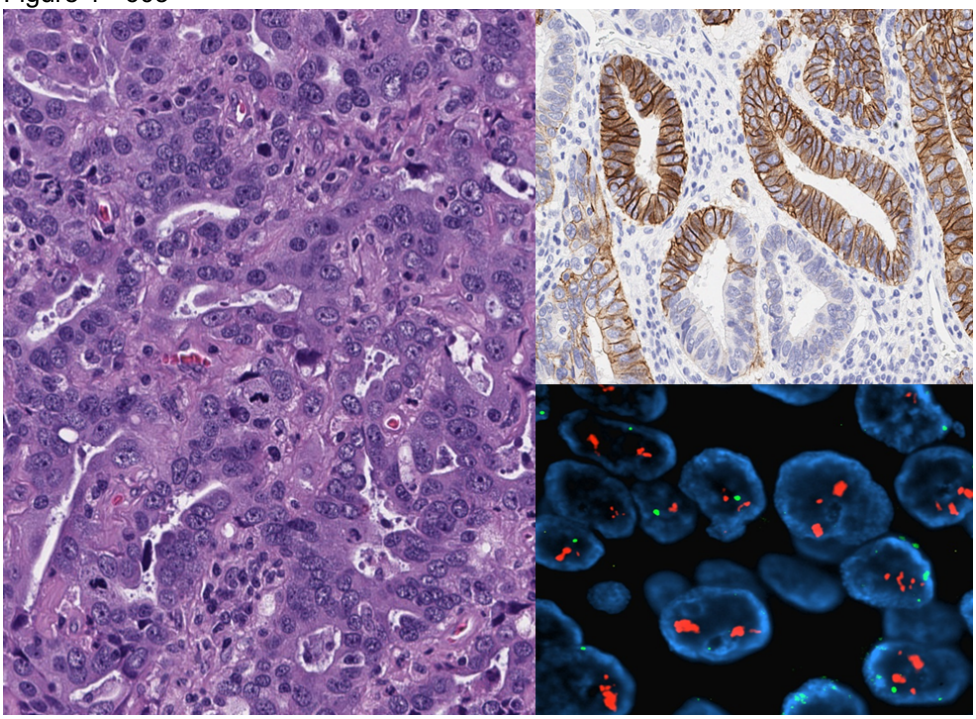

Conclusions: The NCCN guidelines now endorse HER2 testing for advanced and recurrent EC. However, guidelines for HER2 testing algorithms and cutoffs are still lacking. In our cohort, we showed 100% concordance between primary FISH testing and IHC. In instances of heterogeneity, IHC is helpful to further quantify the percentage of tumor cells with 3+ expression. Primary FISH testing is an acceptable approach to HER2 testing in EC.

604 Placental Evaluation in Symptomatic versus Asymptomatic Mothers with SARS-CoV-2 Infection

Parisa Najafzadeh[1], Nicole Gomez[2], Tiannan Wang[3], Richard Lee, Saloni Walia[4]
[1]Keck Hospital of USC, LAC+USC Medical Center, Los Angeles, CA, [2]LAC+USC Medical Center/Keck Medicine of USC, Los Angeles, CA, [3]University of Southern California, Keck School of Medicine of USC, LAC+USC Medical Center, Los Angeles, CA, [4]Keck School of Medicine of USC, Los Angeles, CA

Disclosures: Parisa Najafzadeh: None; Nicole Gomez: None; Tiannan Wang: None; Richard Lee: None; Saloni Walia: None

Background: This study was undertaken to understand the effects of SARS-CoV2 infection on human placenta and compare the histopathologic changes in placentas obtained from symptomatic vs asymptomatic patients with prenatal SARS-CoV2 infection.

Design: All placentas from patients with prenatal SARS-CoV2 infection obtained from April to Oct, 2020 at a single institution were evaluated for histopathologic changes. Data including gestational age at delivery, clinical symptoms of SARS-CoV2 infection, maternal/ obstetric outcomes, and neonatal outcomes were collected.

Results: A total of 33 placentas, gestational age from 21-41 weeks were included. There were nine preterm births. The most common findings were intervillous thrombi/ parenchymal infarcts (15/33, 45.4%) and maternal inflammatory response (18/33, 54.5%). Fetal inflammatory response was noted in 3/33 (9.1%) cases.

Five patients (15.1%) had clinically symptomatic SARS-CoV2 infection and 28 (84.8%) were asymptomatic. All 5 (100%) placentas from symptomatic patients had histopathologic abnormalities, acute chorioamnionitis in 4/5 (80%) and decidual arteriopathy in 2/5 (40%). In the asymptomatic group, 50% (14/28) showed significant abnormalities including chorioamnionitis (14/28, 50%), decidual arteriopathy (3/28, 10.7%), fetal vascular malperfusion (1/28, 3.6%), and funisitis (3/28, 10.7%).

Two pregnancies were from stillbirths: one from a symptomatic patient at 21 weeks' gestation and second from an asymptomatic patient at 32 weeks. Both placentas showed changes of maternal vascular malperfusion and maternal inflammatory response. The placenta of the fetal demise at 32 weeks demonstrated significant maternal and fetal vascular malperfusion with fibrinoid necrosis of decidual vessels, large foci of avascular villi, and significant infarction. The cause of stillbirth was attributed to trisomy 18 in the 21 weeks fetus and was likely related to placental insufficiency in the 32 weeks fetus.

Conclusions: Histopathologic findings of maternal inflammatory response and maternal vascular malperfusion are seen in placentas of pregnant patients infected by SARS-CoV2 in pregnancy. This is seen in both clinically symptomatic and asymptomatic pregnant patients. Further studies are needed to determine if these changes correlate with adverse perinatal outcome and, if so, to elucidate the mechanism by which SARS-CoV2 effect on the placenta manifests poor outcomes - both for the mother and the fetus.

605 Interobserver Reproducibility of Differentiated Exophytic Vulvar Intraepithelial Lesion (DEVIL) and the Distinction from its Mimickers in the Vulva

Grace Neville[1], David Chapel[2], Christopher Crum[2], Ju-Yoon Yoon[2], Sharon Song[2], Kenneth Lee[2], David Kolin[2], Michelle Hirsch[2], Marisa Nucci[1], Carlos Parra-Herran[1]
[1]Brigham and Women's Hospital, Harvard Medical School, Boston, MA, [2]Brigham and Women's Hospital, Boston, MA

Disclosures: Grace Neville: None; David Chapel: None; Christopher Crum: None; Ju-Yoon Yoon: None; Sharon Song: None; David Kolin: None; Michelle Hirsch: None; Marisa Nucci: None; Carlos Parra-Herran: None

Background: Most vulvar squamous cell carcinomas are HPV-associated or p53-abnormal. A third category of HPV-independent, p53 wild type lesions is uncommon and not fully understood. Differentiated Exophytic Vulvar Intraepithelial Lesion (DEVIL) has been characterized as a precursor of such tumors, including verrucous carcinoma. The diagnosis of DEVIL requires verruciform acanthosis, hyper/parakeratosis, hypogranulosis, cytoplasmic pallor and absence of atypia. The reproducibility of DEVIL as defined, and its distinction from lesions with overlapping morphology in the vulva, has not been studied.

Design: A set of 35 slides was evaluated by 9 reviewers (2 fellows, 7 practicing pathologists). The set was selected by two authors and included representation of the following categories: DEVIL, condyloma, verruciform vulvar intraepithelial neoplasia of usual (uVIN) or differentiated (dVIN) types, lichen simplex chronicus (LSC) and psoriasis. A tutorial with definitions and illustrations for each of the diagnostic categories was reviewed by each observer prior to evaluation. Kappa (κ) values were calculated and categorized as poor (0.01-0.2), fair (0.21-0.4), moderate (0.41-0.6), substantial (0.61-0.8) and strong (0.81-0.99).

Results: Overall, interobserver agreement was moderate (κ=0.55). Agreement was substantial for uVIN and condyloma, and moderate for DEVIL, dVIN, LSC and psoriasis (Table 1). Reproducibility increased when only practicing pathologists were included in the analysis (κ=0.7): diagnosis of DEVIL, dVIN and LSC reached substantial agreement, and diagnosis of uVIN and condyloma reached strong agreement. A total of 17% of cases reached perfect (9 / 9 observers) agreement, and 26% almost perfect (7 or 8 / 9 observers). When only practicing pathologists were analyzed, perfect agreement increased to 43% and almost perfect agreement to 37%.

Kappa	All observers (n=9)	Practicing pathologists only (n=7)
DEVIL	0.55	0.65
dVIN	0.48	0.61
uVIN	0.74	0.88
Condyloma	0.69	0.82
LSC	0.6	0.72
Psoriasis	0.42	0.53

Conclusions: The reproducibility in the diagnosis of exophytic and verruciform vulvar lesions, including the novel category of DEVIL, is acceptable overall. Reproducibility is higher in common and well-known lesions such as uVIN and condyloma, compared to rarer and more challenging diagnoses such as DEVIL, dVIN and psoriasis. Agreement is significantly better among practicing gynecologic pathologists, suggesting that training and experience improves reproducibility. Awareness of these lesions and their diagnostic criteria may increase agreement among pathologists. Our findings support the inclusion of DEVIL as a diagnostic entity in the spectrum of vulvar squamous intraepithelial neoplasia.

606 Isolated Lung Metastasis in Endometrial Carcinoma

Kelly Olson[1], Dandi Huang[2], Nhu Vu[3], Bradly Stelter[3], Ahmed Al-Niaimi[3], Stephanie McGregor[3]
[1]University of Wisconsin-Madison School of Medicine and Public Health, Madison, WI, [2]University of Wisconsin Hospital and Clinics, Madison, WI, [3]University of Wisconsin-Madison, Madison, WI

Disclosures: Nhu Vu: None; Bradly Stelter: None; Stephanie McGregor: None

Background: The incidence of endometrial cancer (EC) is increasing, and the prognosis of recurrent disease is poor. Recurrences are generally classified as pelvic or extrapelvic in the literature, with little emphasis on specific patterns of disease spread. We sought to characterize the recurrence patterns associated with EC in our institution.

Design: A clinical database of 1062 EC patients was interrogated and supplemented with chart review. Initial FIGO stage, histologic diagnosis, grade, treatment, time and site of first recurrence, and time to death or last follow-up were documented. Cases that initially presented as FIGO stage IVB were excluded.

Results: Among 120 cases of recurrence in patients with stage I-III disease (81 endometrioid, 27 serous, 12 other), biopsy-confirmed metastasis limited to the lung was present in 10 cases, all of which were reported to have at least a component of endometrioid carcinoma (4 FIGO grade 1, 5 FIGO grade 2, and 1 mixed endometrioid/serous). An additional 5 cases had lung involvement with concurrent lymph node recurrence and were all endometrioid (1 FIGO grade 1, 1 FIGO grade 2, and 3 FIGO grade 3). No serous carcinoma cases with recurrence had biopsy-proven disease with these patterns. Other sites of isolated recurrence were not associated with a specific histologic type. No consistent patterns were noted between initial FIGO stage and isolated lung recurrence (3 with IA, 3 with IB, 2 with II, and 2 with IIIC). Only 1/10 patients with isolated lung recurrence (initially stage IA) have succumbed to their disease to date (due to t-AML), with average follow-up of 4.7 years for living patients (range 3.4-14.9). In contrast, all 5 patients with both lung and lymph node involvement died due to EC (average 3.9 years, range 1.7-5.2).

Conclusions: Isolated lung metastasis may be more characteristic of endometrioid carcinoma than serous carcinoma, and it may also be associated with a better prognosis than that seen with concurrent lung and lymph node involvement. In this small series, cases with concurrent lymph node involvement also tended to be higher grade, indicating that isolated lung metastasis may be a feature of lower grade tumors. Larger studies are necessary to confirm these findings. Continued morphologic, immunophenotypic, and molecular characterization of tumors according to their recurrence patterns will improve our understanding of EC.

607 CNV Signature Model is Highly Accurate in the Distinction Between Primary Ovarian Mucinous Carcinoma and Gastrointestinal Adenocarcinoma

Carlos Parra-Herran[1], Fabien Lamaze[2], Sharon Nofech-Mozes[3], Tom Ouellette[2], Jasmina Uzunovic[2], Ilinca Lungu[2], Carolyn Ptak[2], Bernard Lam[2], Paul Krzyzanowski[2], Jane Bayani[2], Ekaterina Olkhov-Mitsel[4], Philip Awadalla[2], John Bartlett[2]

[1]Brigham and Women's Hospital, Harvard Medical School, Boston, MA, [2]Ontario Institute for Cancer Research, Toronto, Canada, [3]University of Toronto, Sunnybrook Health Sciences Centre, Toronto, Canada, [4]Sunnybrook Health Sciences Centre, Toronto, Canada

Disclosures: Carlos Parra-Herran: None; Fabien Lamaze: None; Sharon Nofech-Mozes: None; Tom Ouellette: None; Jasmina Uzunovic: None; Ilinca Lungu: None; Carolyn Ptak: None; Bernard Lam: None; Paul Krzyzanowski: None; Jane Bayani: None; Ekaterina Olkhov-Mitsel: None; Philip Awadalla: None; John Bartlett: *Consultant*, Insight Genetics, Inc., BioNTech AG, Biotheranostics Inc., Pfizer, Rna Diagnostics Inc., oncoXchange/MedcomXchange Communications Inc, Herbert Smith French Solicitors, OncoCyte Corporation; *Advisory Board Member*, MedcomXchange Communications Inc; *Speaker*, NanoString Technologies, Inc., Oncology Education, Biotheranostics, Inc., MedcomXchange Communications Inc; *Grant or Research Support*, Thermo Fisher Scientific, Genoptix, Agendia, NanoString Technologies, Inc., Stratifyer GmbH, Biotheranostics, Inc.; *Consultant*, Biotheranostics, Inc., NanoString Technologies, Inc., Breast Cancer Society of Canada

Background: Distinction between primary ovarian mucinous carcinoma from metastases to the ovary can be difficult. Immunohistochemistry (IHC) and single nucleotide variants such as *APC* mutations are useful in distinguishing primary ovarian mucinous from colorectal tumors. However, distinguishing between primary ovarian mucinous carcinoma and upper gastrointestinal carcinoma remains challenging since morphology and IHC have limited use. The value of copy number variation (CNV) profiles in this differential is still largely unexplored. Thus, we aimed to identify CNV-based signatures predictive of primary ovarian and gastrointestinal origin.

Design: We surveyed comprehensive sequencing sets including whole exome sequencing data from 40 institutional primary ovarian mucinous carcinomas and published public data from 84 primary ovarian mucinous carcinomas [PMID 31477716]. Whole exome sequencing data from The Cancer Genome Atlas repository was used to establish signatures for primary ovarian high-grade serous, colorectal, gastric, esophageal and pancreatobiliary carcinomas. Across 2670 samples, we screened 19273 genes with at least one CNV event coded as copy gain, loss or neutral. Using a recursive feature elimination selection algorithm, we identified 350 gene candidates and trained a random forest (RF) with 25 bootstrapping resampling steps on 3024 samples, representing 70% of the data set, with an up-sampling strategy to balance cancer type categories. The balanced 350-gene RF model was then applied to an independent testing set of 635 tumors (202 ovarian and 433 gastrointestinal).

Results: The generated RF model based on 350-gene CNV profiles achieved an overall 92% accuracy in the identification of primary ovarian carcinoma (mucinous and serous) vs gastrointestinal adenocarcinoma (sensitivity 96%, specificity 88%). When deconvoluting accuracy performance results between primary ovarian mucinous carcinoma and colorectal carcinoma, the model achieved 96% accuracy (sensitivity 93%, specificity 99%). Moreover, the model correctly predicted primary ovarian mucinous carcinoma vs upper gastrointestinal (esophageal, gastric, pancreatobiliary) adenocarcinoma with 96% accuracy (sensitivity 94%, specificity 98%).

Tumor category	350 gene CNV predictor model	
	# predicted - Ovarian	# predicted - Non-ovarian
Ovary - mucinous	87	7
Ovary - high-grade serous	109	21
Colon	0	124
Rectum	1	44
Esophagus	3	52
Pancreas	1	54
Stomach	1	131
Total	202	433

Conclusions: CNV signatures extracted from comprehensive next generation sequences accurately classified ovarian carcinomas, including primary ovarian mucinous carcinoma, from gastrointestinal carcinomas. Our model demonstrates significant genomic differences between primary ovarian mucinous carcinomas and upper gastrointestinal adenocarcinomas, which otherwise have great morphologic and IHC overlap. It is potentially an accurate tool to predict the origin of mucinous adenocarcinomas involving the ovary (primary vs metastatic).

608 Histopathology and Immunohistochemical Evaluation of 35 Placentas from SARS-CoV-2 Infected Patients

Filipa Pereira[1], Carolina Padrão[2], Maria Novo[1], Joaquim M. Tinoco[1], André Pereira[1], Maria Gabriela Gasparinho[1]
[1]Hospital Professor Doutor Fernando Fonseca, Amadora, Portugal, [2]Amadora, Portugal

Disclosures: Filipa Pereira: None; Carolina Padrão: None; Maria Novo: None; Joaquim M. Tinoco: None; André Pereira: None; Maria Gabriela Gasparinho: None

Background: The effects of severe acute respiratory syndrome coronavirus 2 (SARS-CoV-2) in the placenta are yet to be completely understood; mother-to-fetus transmission of SARS-CoV-2 infection is rare, with very few cases reported. Our goal is to describe the histopathologic findings in the placentas of women with SARS-CoV-2 infection at time-of-delivery.

Design: Delivered placentas of women with COVID-19 giving birth between April 1, 2020, and September 30, 2020, were screened. Clinical data (mothers' age, medical past history, maternal and fetoplacental complications in pregnancy, gestational age), macroscopic and histopathologic placental findings, fetus general condition and SARS-CoV-2 status were collected. Immunohistochemistry with SARS-CoV-2 N-protein antibody was performed in one representative slide of each placenta. SARS-CoV-2 RT PCR was performed in samples of all live births and in dead fetuses.

Results: A total of 212 placentas were received, from which, 35 parturient tested positive for SARS-CoV-2 RT-PCR between 15 days before labor and 10 days post-labor. The average age was 28 years-old, with an average gestational age of 37 weeks and 2 days. Ten patients had relevant past medical history. Eleven patients had maternal and fetal-placental complications (table). Ten placentas were histologically normal; 20 had pathologic findings, including maternal and/or fetal vascular malperfusion, ascending intrauterine infection and villitis of unknown etiology, while 5 had only minor alterations. Immunohistochemistry for detection of SARS-CoV-2 N-protein was positive in only one case, with strong and diffuse expression in villous syncytiotrophoblast, associated with extensive placental infarcts; this case resulted in fetal death and the fetus tested positive for SARS-CoV-2 RT-PCR in a lung sample collected by fine-needle aspiration biopsy). The 33 live fetuses and 1 other case of fetal death, all were negative to SARS-CoV-2 infection.

Maternal and fetal-placental complications:	Number of cases
Preeclampsia	3
Hypertension-related liver disease	1
Gestational diabetes	2
Diabetic ketoacidosis	1
Premature rupture of membranes	1
Intrauterine growth restriction	1
Fetal deaths	2

Conclusions: Placental infection by SARS-CoV-2 appears to be a very rare occurrence, despite the presence of morphological alterations in placentas delivered from COVID-19 patients. The absence of SARS-CoV-2 detection by immunohistochemistry doesn't allow to establish a causal effect between infection and placental alterations. Nevertheless, the only case positive by immunohistochemistry constitutes per se evidence of maternal-fetal transmission of SARS-CoV-2, with associated pathological placental findings, as well as fatal consequences for the fetuses.

609 Defining Substantial Lymphovascular Space Invasion in Endometrial Cancer

Elke Peters[1], Alicia Leon-Castillo[2], Vincent Smit[2], Marie Boennelycke[3], Estrid Hogdall[4], Claus Hogdall[5], Carien Creutzberg[2], Ina Jürgenliemk-Schulz[6], Jan Jobsen[7], Jan Willem Mens[8], Ludy Lutgens[9], Elzbieta van der Steen-Banasik[10], Gitte Ortoft[5], Tjalling Bosse[2], Remi Nout[11]

[1]Haaglanden Medical Center, The Hague, Netherlands, [2]Leiden University Medical Center, Leiden, Netherlands, [3]Diagnostic Centre Rigshospitalet, Copenhagen University Hospital, Denmark, [4]University Hospital of Copenhagen, Copenhagen, Denmark, [5]Rigshospitalet, Copenhagen University Hospital, Copenhagen, Denmark, [6]University Medical Center Utrecht, Utrecht, Netherlands, [7]Medisch Spectrum Twente, Enschede, Netherlands, [8]Erasmus MC, Rotterdam, Netherlands, [9]Maastricht UMC+, Maastricht, Netherlands, [10]Radiotherapiegroep, Arnhem, Netherlands, [11]Erasmus University Medical Center, Rotterdam, Netherlands

Disclosures: Elke Peters: None; Alicia Leon-Castillo: None; Vincent Smit: None; Marie Boennelycke: None; Estrid Hogdall: None; Claus Hogdall: None; Carien Creutzberg: None; Ina Jürgenliemk-Schulz: None; Jan Jobsen: None; Jan Willem Mens: None; Ludy Lutgens: None; Elzbieta van der Steen-Banasik: None; Gitte Ortoft: None; Tjalling Bosse: None; Remi Nout: *Grant or Research Support*, Elekta; *Grant or Research Support*, Varian; *Grant or Research Support*, Accuray

Background: Lymphovascular space invasion (LVSI) occurs in a minority of endometrial cancer (EC) cases, and the extent of LVSI is an important risk factor for recurrence and/or metastases. A three-tiered, semi-quantitative LVSI assessment (no LVSI and focal LVSI versus substantial LVSI) is recommended, however differentiation between focal and substantial LVSI remains challenging. In this study we aimed to improve the reproducibility of identifying clinically meaningful LVSI by performing quantitative analyses of LVSI in relation to the risk of pelvic lymph node recurrence (PLNR) in EC patients who did not receive adjuvant external beam radiotherapy (EBRT).

Design: H&E slides from ECs with reported LVSI positivity (any) from the PORTEC-1 and -2 trials were retrieved and used to assess quantitative data, including the number of LVSI-positive vessels per H&E slide, average number of tumor cells in the largest embolus and the number of LVSI-positive H&E slides. The extent of LVSI has clinical relevance when the associated risk of recurrence is sufficient to justify adjuvant treatment despite the associated risk of side effects. A PLNR risk of >15% was considered a clinically relevant increase for recommending EBRT. The risk of PLNR risk was calculated (Kaplan-Meier method, with Cox regression) using a stepwise adjustment for the number of LVSI-positive vessels (table 1). This analysis was then repeated in the DGCD (Danish Gynecological Cancer Database) cohort.

Results: 502 EC patients in the PORTEC-1/-2 trials did not receive EBRT. 38 patients had focal LVSI and 21 had substantial LVSI. There were significant differences in the mean number of LVSI positive vessels (1,9 (SD 2,5) versus 5,6 (SD 6,4), p<0,001) embolus size (31 cells (SD 32) versus 55 (SD 53), p=0,002) and number of H&E positive slides (1,19 (SD 0,46) versus 1,5 (SD 0,73), p=0,019). The 5-year PLNR risk was 3.3%, 6.7% (p=0.51), and 26.3% (p<0.001) when 0, 1-3, or ≥4 vessels had LVSI involvement; similar results were obtained for the DGCD cohort.

PORTEC-1 and PORTEC-2

N emboli	patients	events	*p*	HR	95% CI			KM 5-year
No LVSI	443	18	*NA*	*NA*		*NA*		3,30
focal	38	3	0,256	2,03	0.60	-	6.90	8,30
substantial	21	5	< 0,001	8,17	3.00	-	22,20	30,20
< 2	12	0	0,978	0,00	0,00			0,00
≥ 2	47	8	< 0,001	5,06	2,20	-	11,67	19,80
< 3	20	1	0,822	1,26	0,17	-	9,44	5,30
≥ 3	39	7	< 0,001	5,37	2,24	-	12,90	20,80
< 4	32	2	0,513	1,63	0,38	-	7,02	6,70
≥ 4	27	6	< 0,001	6,92	2,74	-	17,51	26,30

< 5	36	3	0,193	2,25	0,66	-	7,65	9,00
≥ 5	23	5	< 0,001	6,53	2,42	-	17,64	25,80

< 6	42	4	0,091	2,55	0,86	-	7,53	10,20
≥ 6	17	4	< 0,001	7,62	2,42	-	22,67	30,40

DGCD

N emboli	**patients**	**events**	***p***	**HR**	**95% CI**			**KM 5-year**
No LVSI	321	13	*NA*	*NA*		*NA*		4.7
focal	37	4	0,015	4.1	1.3	-	12.8	14.5
substantial	43	8	0,001	6.7	2.6	-	16.8	24.3
< 3	21	2	0,173	2.8	0.6	-	12.5	11.6
≥ 3	59	10	0,001	5.7	2.5	-	13.0	22.8
< 4	27	2	0,242	2.5	0.6	-	11.1	8.9
≥ 4	53	10	0,001	7.4	3.1	-	17.8	26.1
< 5	29	3	0,05	3.6	1.0	-	12.9	12.1
≥ 5	51	9	0,001	6.7	2.7	-	16.4	24.7
< 6	38	4	0,017	4.0	1.3	-	12.4	14.0
≥ 6	42	8	0.001	6.9	2.7	-	17.4	25.1

Conclusions: Clinically relevant LVSI in EC was reached when applying a numeric threshold (≥4 LVSI-involved vessels). This threshold may be applied in cases in which focal versus substantial LVSI is not obvious and thereby will improve reproducibility.

610 Patterns of MHC Class I Immunohistochemical Expression in Gynecologic Malignancies and its Potential Implication in Susceptibility to Immune Checkpoint Inhibitor Therapy

Tip Pongsuvareeyakul[1], Renan Ribeiro e Ribeiro[2], K M Islam[1], Kamaljeet Singh[2], C. James Sung[1], Katrine Hansen[2], M. Ruhul Quddus[1]

[1]Women & Infants Hospital/Alpert Medical School of Brown University, Providence, RI, [2]Women and Infants Hospital, Providence, RI

Disclosures: Tip Pongsuvareeyakul: None; Renan Ribeiro e Ribeiro: None; K M Islam: None; Kamaljeet Singh: None; C. James Sung: None; M. Ruhul Quddus: None

Background: Immune checkpoint inhibitors have been increasingly utilized for the treatment of gynecologic cancer. Even in the appropriate molecular context, some patients fail to respond.

The loss of major histocompatibility complex (MHC) class I immunohistochemical (IHC) expression was recently proposed as a mechanism for therapeutic resistance, diminishing neoantigen presentation and providing a route for tumor cells to "escape" the immune system.

The IHC antibody targets the MHC Class I heavy chain, which joins the beta2-microglobulin light chain in the endoplasmic reticulum. This unit is then bonded to an antigen, after which the trimer is relocated to the cell membrane. These steps are reflected in the expression patterns seen by IHC, but little is known about the relationship between IHC expression pattern and actual neoantigen bioavailability *in vivo*.

Design: Whole tissue sections of different endometrial and vulvar lesions were stained with anti-HLA class 1 ABC antibody [EMR8-5], cat# ab70328, Abcam, dilution 1:2000. Membranous and cytoplasmic staining were computed

separately. Heterogeneity was also noted, defined as notable variation in staining intensity/distribution throughout the tumor sample.

Staining pattern was labeled "preserved" when greater than 90% of tumor cells showed membranous and/or cytoplasmic expression of MHC class I, "focal loss" when staining ranged from 10-90% and "complete loss" when less than 10% of tumor cells showed consistent expression.

A comparison between interpretation methods (membranous and cytoplasmic versus membranous only) was made.

Results: A total of 134 whole tissue sections were stained, including 40 samples of serous carcinoma (29.9%), 35 of endometrioid adenocarcinoma (26.1%), 10 cases of carcinosarcoma (7.5%) and 2 cases of clear cell carcinoma (1.5%). Differentiated vulvar intraepithelial neoplasia (dVIN) and squamous cell carcinoma (SCC) represented 32 (23.9%) and 15 (11.2%) samples, respectively.

Membranous staining (Fig. 1A, 1D) was found in 104 cases (77.6%). Cytoplasmic staining (Fig. 1B, 1C) was found in 113 cases (84.3%). Heterogeneous expression was present in 97 cases (72.4%).

Staining interpretation differed greatly depending on whether membranous expression was considered alone or both membranous and cytoplasmic expression were considered together. Table 1 and Figure 2 summarize these findings. A kappa coefficient of agreement between both methods resulted in 0.333.

		MHC expression (membranous and cytoplasmic)			Total
		Preserved	Focal loss	Complete loss	
MHC expression (only membranous)	Preserved	34	0	0	34
	Focal loss	37	33	0	70
	Complete loss	11	11	8	30
Total		82	44	8	134

Figure 1 – 610

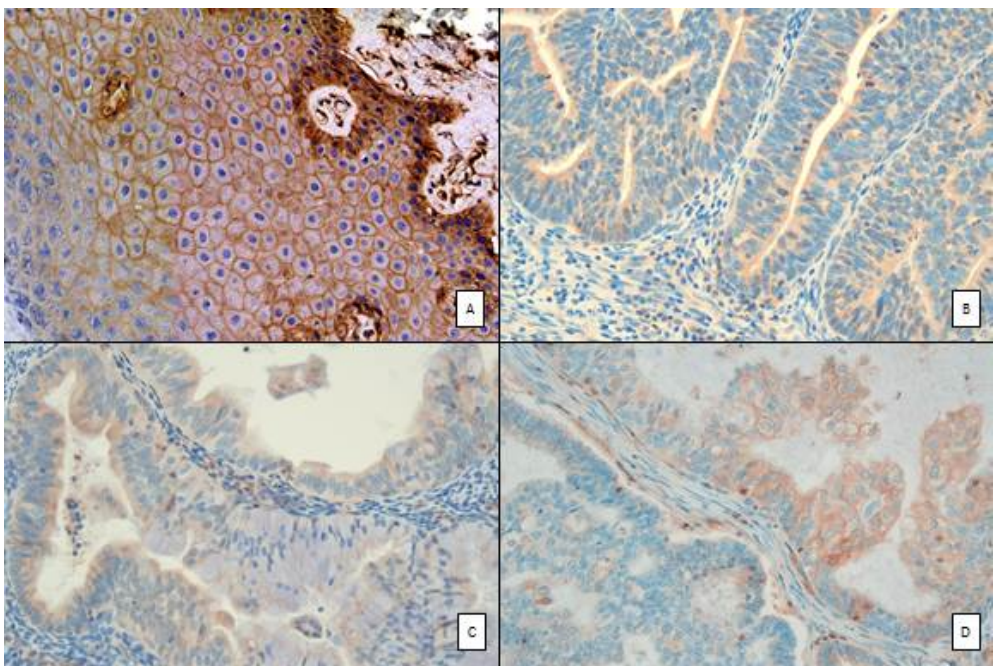

Figure 2 - 610

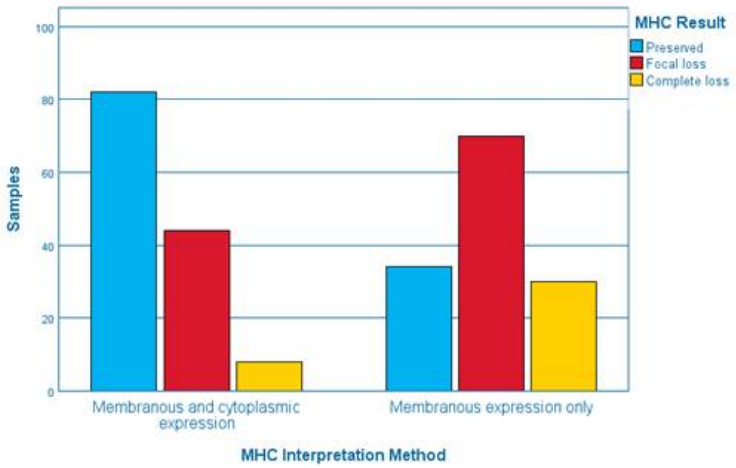

Conclusions: MHC Class I IHC expression is variable among gynecologic malignancies. Membranous and/or cytoplasmic expression may reflect functional differences between tumor cells, with different biological meanings.

Further studies and standardization of the IHC interpretation method are required if this marker is to be introduced in clinical practice as a biomarker for susceptibility to immune checkpoint inhibitor therapy.

611 Complex Endometrial Hyperplasia with Corded and Hyalinized Pattern: A Distinct Form of Endometrial Hyperplasia Resembling Corded and Hyalinized Endometrial Adenocarcinoma

Jennifer Pors[1], Kevin Kolahi[2], Teri Longacre[2]
[1]Stanford University School of Medicine, Stanford, CA, [2]Stanford University, Stanford, CA

Disclosures: Jennifer Pors: None; Kevin Kolahi: None; Teri Longacre: None

Background: The evolving classification of endometrial adenocarcinoma includes numerous histologic variants, including corded and hyalinized endometrioid carcinoma (CHEC). From the archives of our gynecologic pathology consultation service, we identified 10 endometrial samplings with a distinct corded and hyalinized pattern, for which the diagnosis of CHEC was considered. By morphology, these lesions showed crowded gland clusters and cords of cells embedded in a hyalinized stroma, reminiscent of CHEC, but with insufficient architectural complexity or cytologic atypia for the diagnosis of endometrioid adenocarcinoma. We propose that the presence of a corded and hyalinized stromal pattern is not limited to endometrioid carcinoma, but may also occur in association with endometrial hyperplasia and likely reflects the protean appearance that may be exhibited by precursor endometrioid proliferations in the female genital tract.

Design: Files from our gynecologic pathology consultation service were searched for uterine endometrial proliferations that demonstrated complex glandular formations and epithelioid cells, spindled cells, and/or fusiform cells often associated with the production of a dense hyaline matrix, for which the diagnosis of CHEC was considered.

Results: Ten patients were identified (mean age 36 yr; range 23 to 57 yr). The majority presented with abnormal uterine bleeding (8/9 [89%]). By immunohistochemistry (IHC), the majority showed at least focal keratin (5/7 [56%]), and ER expression (3/4 [75%]), but no expression of inhibin (0/3 [0%]), CD10 (0/7 [0%]), HMB45 (0/1 [0%]) or GATA3 (0/1 [0%]) (additional IHC data pending). One patient (1/10 [10%]) had a co-existent endometrioid adenocarcinoma that was not associated with a CHEC pattern. Follow up was available for 3 patients (mean 45 mos; range 44 to 47 mos) (additional follow-up data pending). No patient developed endometrial adenocarcinoma.

One patient had persistent endometrial hyperplasia (1/3 [33%]), while the two others were free of disease at follow-up (2/3 [67%]).

Conclusions: The bland morphologic features and the favorable clinical follow-up in this limited series, suggests that complex glandular formations in absence of significant cytologic atypia represent a unique endometrial precursor lesion. We propose that the presence of a corded and hyalinized stromal pattern is not limited to endometrioid carcinoma, but may also occur in association with endometrial hyperplasia. The diagnosis “complex hyperplasia with a corded and hyalinized pattern” seems warranted to describe this precursor lesion.

612 Unmethylated Mismatch Repair Deficiency in the Combined PORTEC-1,-2 and -3 Endometrial Cancer Trials: Underlying Causes and Survival Analysis

Cathalijne Post[1], Ellen Stelloo[2], Vincent Smit[1], Dina Ruano[1], Carli Tops[1], Lisa Vermij[1], Tessa Rutten[1], Ina Jürgenliemk-Schulz[2], Ludy Lutgens[3], Jan Jobsen[4], Remi Nout[5], Emma Crosbie[6], Alexandra Leary[7], Linda Mileshkin[8], Stephanie de Boer[1], Nanda Horeweg[1], Tom van Wezel[9], Carien Creutzberg[1], Tjalling Bosse[1]
[1]Leiden University Medical Center, Leiden, Netherlands, [2]University Medical Center Utrecht, Utrecht, Netherlands, [3]Maastricht UMC+, Maastricht, Netherlands, [4]Medisch Spectrum Twente, Enschede, Netherlands, [5]Erasmus University Medical Center, Rotterdam, Netherlands, [6]University of Manchester, Manchester, United Kingdom, [7]Gustave Roussy, France, [8]Peter MacCallum Cancer Centre, Mt Stuart, Australia, [9]LUMC, Leiden, Netherlands

Disclosures: Cathalijne Post: None; Ellen Stelloo: None; Vincent Smit: None; Dina Ruano: None; Carli Tops: *Consultant*, none; Lisa Vermij: None; Tessa Rutten: None; Ina Jürgenliemk-Schulz: None; Ludy Lutgens: None; Jan Jobsen: None; Remi Nout: *Grant or Research Support*, Elekta; *Grant or Research Support*, Varian; *Grant or Research Support*, Accuray; Emma Crosbie: None; Alexandra Leary: None; Linda Mileshkin: None; Stephanie de Boer: None; Nanda Horeweg: None; Tom van Wezel: None; Carien Creutzberg: None; Tjalling Bosse: None

Background: In a comprehensive analysis of mismatch repair deficiency (MMRd) in the combined PORTEC-1,-2 and 3 trials 410 out of 1336 endometrial cancers (EC) were MMRd; 74% of MMRd cases were caused by *MLH1* promotor hypermethylation ('methylated'). In the present study we aimed to evaluate the causes of MMRd in the remaining 101 unmethylated cases.

Design: Next-generation sequencing (NGS) was performed on paired tumour and normal tissues of all unmethylated cases to identify germline or somatic MMR gene variants affecting function and loss of heterozygosity (LOH). Recurrence-free survival (RFS) for the three unmethylated groups (germline, somatic and unexplained) were estimated and compared to methylated MMRd-ECs using Kaplan-Meier method and pairwise log-rank test. MMRd-ECs with a concurrent *POLE* exonuclease domain variant affecting function (*POLE*mut-MMRd) were excluded form the analysis.

Results: Of the 101 unmethylated MMRd-ECs 35 were caused by an MMR germline variant (18x *path_MSH6*, 10x *path_PMS2*, 5x *path_MSH2*, 1x *path_MLH1*, 1x unknown variant), 32 by somatic MMR alterations (18x double somatic variants, 8x somatic variant + LOH, 6x one somatic variant), in 14 cases no somatic alteration was found in the MMR genes (‘unexplained’), 17 cases had insufficient material for tumour NGS and 3 for normal tissue NGS. Additionally, one methylated MMRd-EC harboured a *path_MLH1* germline variant. Within the germline group, *path_MLH1* and *path_MSH2* carriers were younger than *path_PMS2* and *path_MSH6* carriers (median age of 50, 52, 62 and 63 years respectively; p=0.02). No statistically significant difference in clinicopathological characteristics between germline, somatic and unexplained MMRd-ECs were found; *POLE*mut was identified in 2 (6%), 5 (16%) and 2 (14%) tumours respectively (p=0.40). Five-year RFS was 91% (95%CI 82-100; p=0.32), 92% (83-100; p=0.26), and 100% (100-100; p=0.26) respectively for germline, somatic and unexplained MMRd-EC, compared to 78% (74-84) for methylated MMRd-EC.

Figure 1 - 612

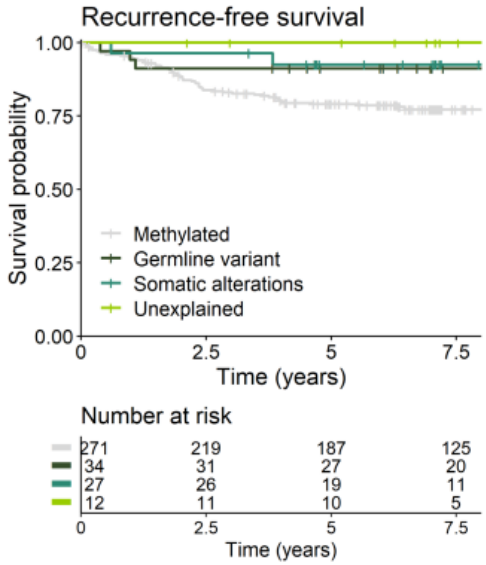

Conclusions: Among MMRd-ECs with neither *MLH1* methylation nor a MMR germline variant, 70% (32/46) could be explained by somatic alterations. Among sentinel EC caused by a germline variant, *path_MSH6* and *path_PMS2* were most commonly observed. Unmethylated MMRd-ECs, independent of underlying MMRd cause, showed a better RFS than methylated MMRd-ECs.

613 Early Stage Placenta Accreta Spectrum Disorder Is Clinically Under-Recognized in Women with Uterine Atony: Implications for Pathologic Management of Hysterectomy Specimens

Joseph Rabban[1], Arianna Cassidy[1], Liina Poder[1], Nasim Sobhani[1], Joanne Gras[1]
[1]University of California, San Francisco, San Francisco, CA

Disclosures: Joseph Rabban: None; Arianna Cassidy: None; Nasim Sobhani: None; Joanne Gras: None

Background: The etiology and pathologic features of uterine atony requiring emergent hysterectomy are poorly understood, and there are no specific guidelines for pathologic handling of such specimens. This study hypothesized that 1) clinically unrecognized focal early stage placenta accreta spectrum disorder (PASD) may account for subset of such cases but that 2) pathologic detection may be limited by the extent of tissue sampling.

Design: This study included hysterectomies performed for uterine atony following placental delivery in pregnancies > 24 weeks' gestation at a single high-risk obstetric referral center. Those with pre-delivery clinical suspicion for PASD were excluded. Hysterectomy specimens were retrospectively evaluated to determine the prevalence of pathologically-defined PASD. Extent of tissue sampling and clinical factors were compared between those with and without PASD.

Results: Of 36 hysterectomy specimens that met inclusion criteria, PASD was identified in 13 (36%) with 11 demonstrating focal accreta and 2 demonstrating increta. PASD was observed in the uterus alone in 10 specimens, the placenta alone in 1 specimen, and the uterus and placenta in 2 specimens. Macroscopic features suspicious for adherent foci of placenta were seen in 6 cases. Among the remaining cases, those with PASD had a higher median number of endomyometrial tissue sections examined than those without PASD (9 sections vs 4 sections). Those with histopathologic PASD were more likely to have clinical risk factors for PASD than those without (100% vs 65%, p=0.03). There were no differences in risk factors for uterine atony between the two groups (39% vs 38%, p>0.99). Those with histopathologic PASD were more likely to require manual placental extraction than those without (100% vs 50%, p=0.004).

Conclusions: Early stage PASD was clinically under-recognized in at least 36% of patients with uterine atony, although this may be an underestimate, since some specimens were minimally sampled. Guidelines are merited for enhanced examination and targeted sampling of the endomyometrium and placental maternal surface to evaluate for focal PASD in hysterectomies performed for uterine atony. Clinical characteristics may be useful in determining which specimens to prioritize for histopathologic enhanced examination.

614 Uterine and Vulvar STUMP, But Not Leiomyosarcoma, Should Be Included in Morphology-Based Screening for Hereditary Leiomyomatosis Renal Cell Carcinoma Syndrome: A Single Institutional Study Integrating Morphology with Tumor and Germline Sequencing

Joseph Rabban[1], Julie Mak[1], Nicholas Ladwig[1], Walter Devine[1], Karuna Garg[1]
[1]University of California, San Francisco, San Francisco, CA

Disclosures: Joseph Rabban: None; Julie Mak: None; Nicholas Ladwig: None; Walter Devine: None; Karuna Garg: None

Background: Morphology-based screening for fumarate hydratase deficiency (FH-d) in uterine leiomyomas is effective for triaging patients to genetic counseling for formal risk assessment for hereditary leiomyomatosis renal cell carcinoma syndrome (HLRCC). Whether uterine leiomyosarcoma (LMS) or smooth muscle tumor of uncertain malignant potential (STUMP) should be included in such morphologic screening has not been fully elucidated. Therefore, this study utilized a dual strategy of interrogating 1.) the genetic testing database of our cancer referral center for pathologic diagnoses of uterine LMS or STUMP among women with germline FH pathogenic variant and 2.) the next generation sequencing (NGS) database of all women with uterine LMS or STUMP who underwent tumor testing in our institution.

Design: Our institutional genetic counseling database was queried for all women with personal and/or family risk factors for any inherited syndrome warranting germline testing using a multi-gene panel that included FH. We then searched our institutional cancer registry and our pathology database for a diagnosis of uterine LMS or STUMP in the women with germline FH pathogenic variant. Separately, we reviewed the slides of all women with uterine LMS or STUMP who underwent NGS tumor testing using our institution's 500 gene panel for morphologic features of FH-d (alveolar edema, staghorn vessels, chain-like tumor cell growth, macronucleoli and cytoplasmic eosinophilic globules).

Results: A pathogenic or likely pathogenic germline variant in FH was detected in 54 (0.87%) of the 6208 women tested at our institution. While none of these patients had a uterine LMS or STUMP, 10 women with a germline FH pathogenic or likely pathogenic variant had a leiomyoma with FH-d morphology. Among 19 uterine LMS that underwent NGS tumor testing, none had a FH pathogenic or likely pathogenic variant though macronucleoli were present in 12 and eosinophilic globules were in 2. Among 3 STUMP (2 uterine, 1 vulvar) that underwent NGS tumor testing, 2 (1 uterine, 1 vulvar) had an FH deep deletion as well as classic FH-d morphology; neither patient pursued genetic testing.

Conclusions: Uterine and vulvar STUMP should be included with leiomyomas in morphology-based screening strategies to identify women at increased risk for HLRCC who would benefit from genetic counseling and germline genetic testing. Uterine LMS does not appear to be associated with increased risk for HLRCC, though some tumors may exhibit macronucleoli that simulate those of FH-deficient leiomyomas and STUMP.

615 Evaluation of Pathologic Features in Trachelectomy Specimens and Correlation with Outcomes-A Single Institution Experience

Preetha Ramalingam[1], Elizabeth Euscher[1], Mario Marques-Piubelli[1], Anais Malpica[1]
[1]The University of Texas MD Anderson Cancer Center, Houston, TX

Disclosures: Preetha Ramalingam: None; Elizabeth Euscher: None; Mario Marques-Piubelli: None; Anais Malpica: None

Background: Trachelectomy, either radical or simple (RTR or STR), is a fertility sparing surgical option for patients (pts) with early-stage cervical carcinoma (Ca). In this study, we present the clinicopathologic features of TR cases obtained in a single institution.

Design: 56 TR cases were identified from our files (2004-2020). Pts' age, clinical presentation, FIGO stage, treatment, outcome, tumor size, histotype, lymphovascualr invasion (LVI), frozen section findings, parametrial tissue and lymph node (LN) status were evaluated. Kaplan-Meier curve was used for overall survival.

Results: Median age was 32 yrs (range 21-49yrs). Clinical presentation: abnormal (abn) pap smear (42), abn uterine bleeding (9), mass seen during pregnancy (3), mass during annual check-up (1), unknown (1). 52 were RTR, 4 were STR. 24 had bilateral pelvic LNs (BPLNs), 10 bilateral sentinel LNs (BSLNs), 20 BSLNs and BPLNs, 1 right SLN and left PLN, 1 had no LN dissection. Median tumor size: 2.4cm (range 1.7 to 4cm). Histotype: 26/56 (46%) adenocarcinoma (ACa), 21/56 (38%) squamous carcinoma (SCa), 3/56 (5%) Aca and SCa, 5/56 (9%) adenosquamous ca 1/56 (2%) cervical ca, NOS. Invasive ca was present in the TR in 27/56 (48%), absent in 29/56 (52%) [2 had residual adenocarcinoma in situ (AIS) and one had CIN-3]. Endocervical margin (EM) at frozen section (FS) was negative (neg) in 49/54 (91%) and positive (pos) in 5/54 (9%). 11/29 (37.9%) with pos/indeterminate margins on cone/LEEP had residual tumor in RTR. 32/56 (57%) cases had no LVI. Parametria were neg in all RTR; LN status: 49/55 (89%) neg, 5/55 (9%) pos, isolated keratin pos cell 1/55 (2%). FIGO stage was available in all cases: IA1 9 (16%), IA2: 13 (23%), IB1: 32 (57%), IB2: 1 (2%), IIIC (2%). 39/56 (69%) had no additional therapy; 11 had total abdominal hysterectomy (TAH) either for: pos (4)/close(1) EM in FS, completion (5) or pregnancy related complication (1); 1 had TAH and chemotherapy (CT); 1 had TAH and radiation (RT); 2 had CT; 1 had RT. 4/4 immediate TAH for pos EM on FS had residual AIS (1) or invasive Ca (3). Median follow-up 61.5 months (mos) (range 3-159). 50/54 (92%) pts were alive (A) without disease (dis), 1/54 (2%) A with dis, 2/54 (4%) died of dis (DOD) and 1/56 (2%) died of other causes. The 2 pts who DOD had neg RTR. 2 pts recurred at 15 mos and 82 mos. 6/36 (17%) pts had pregnancy post RTR. 3yr overall survival (OS): 98%, 5yr OS 98%. OS did not correlate with FIGO stage, LVI, or LN status.

Conclusions: The outcome of pts treated with TR is excellent. Residual AIS or invasive Ca was seen in all cases with pos EM at FS. For 2 pts that DOD, no pathologic findings could predict outcome, raising the possibility of constitutional factors.

616 Pandemic Related Delay of Care is Not Associated with Diagnostic Discrepancy

Madeline Reganis[1], Dan DeCotiis[2], Connie Cao[1], Allison Goldberg[1], Joanna Chan[1]
[1]Thomas Jefferson University Hospital, Philadelphia, PA, [2]Einstein Medical Center, Philadelphia, PA

Disclosures: Madeline Reganis: None; Allison Goldberg: None; Joanna Chan: None

Background: The COVID-19 pandemic resulted in clinical closures for non-emergent procedures, including cervical excisions prompted by high grade biopsies or Pap tests. This led to an unusually long time period between diagnosis of high grade squamous intraepithelial lesions (HSIL) and excision. The natural history of HSIL lesions is that up to 30% of HSILs regress and 10% progress to cancer. The few studies that look at timing of progress and evaluation are indefinite as to the time period necessary for progression or regression. This study examines whether the pandemic induced delay between diagnosis of HSIL and excision of lesion shows a discrepancy between the biopsy and excision, representing either regression or progression of cervical dysplasia.

Design: IRB approval was obtained. Data from 48 cervical excision samples accessed as 24 sequential cases prior to 24 cases following the institutional hold on non-emergent procedures (3/18/2020 to 6/8/2020) were evaluated. Data was tabulated and analyzed in Microsoft excel with additional statistical testing performed using the R programming language.

Results: Average time between biopsy and excision was 41.8 days prior to, and 88.7 days during the pandemic (p=0.002). Diagnostic discrepancy between biopsy and excision was 25% prior to and 37% during the pandemic (p=0.53). Discordant diagnoses between biopsy and excision were more likely to be a downgrade from HSIL to LSIL regardless of length of time between biopsy and excision. Average number of days between biopsy and excision was 59.15 days in accordant diagnoses and 79.5 days in discordant diagnoses (p=0.42).

Conclusions: The institutional pause on procedures correlates with increase in time between biopsy and excision. There is no statistical defined relationship between the institutional pause and discrepancy in diagnosis. Furthermore, there is no clear relationship between length of time between biopsy and excision and discrepancy in diagnosis. The data does show that in cases of a discrepant diagnosis between biopsy and excisional procedure, it is more likely to be a change from high grade diagnosis to either benign or low grade lesion. Future directions include evaluating the initial biopsies in discordant cases for features that may better predict regression. In addition, this study may have implications as to the benefit of doing clinical surveillance with biopsies for a longer time period before having an excisional procedure.

617 MHC Class I Expression in Uterine Serous Carcinoma With and Without Human Epidermal Growth Factor Receptor 2 (HER2) Amplification

Renan Ribeiro e Ribeiro[1], Katrine Hansen[1], C. James Sung[2], M. Ruhul Quddus[2]
[1]Women and Infants Hospital, Providence, RI, [2]Women & Infants Hospital/Alpert Medical School of Brown University, Providence, RI

Disclosures: Renan Ribeiro e Ribeiro: None; Katrine Hansen: None; C. James Sung: None; M. Ruhul Quddus: None

Background: Immune checkpoint inhibitors for the treatment of gynecologic cancer have been increasingly adopted. Recently, the loss of major histocompatibility complex (MHC) class I IHC expression has been proposed as a possible mechanism of therapeutic resistance.

Uterine Serous Carcinoma (USC) is a relatively rare and aggressive endometrial cancer. A subset of USC shows HER2 overexpression and can be detected by immunohistochemistry (IHC) or gene amplification by fluorescent in situ hybridization (FISH). Tumors with HER2 amplification may be amenable to targeted therapy.

Little is known about MHC class I IHC expression in USC and its relationship with other biomarkers. We aimed to investigate MHC expression patterns in a subset of USC with known HER2 status by IHC and confirmed by FISH.

Design: After approval by the Institutional Review Board, 29 cases of serous uterine carcinoma, with known HER2 status by IHC and confirmed by FISH, were selected.

MHC Class I was analyzed by staining with anti-HLA class 1 ABC antibody [EMR8-5], cat# ab70328, Abcam, dilution 1:2000. Staining was interpreted as "preserved" when greater than 90% of tumor cells showed membranous and/or cytoplasmic expression of MHC class I; "focal loss" when staining ranged from 10-90%; and "complete loss" when less than 10% of tumor cells showed consistent expression.

The data abstraction was performed using Microsoft Excel and data analysis on SPSS 26.

Results: By IHC, 23 USC cases (89.6%) were HER2 negative, and 3 cases (10.3%) were HER2 equivocal. HER2 amplification was detected by FISH in 6 cases (20.7%), while the remaining 23 (82.8%) were negative.

MHC Class I expression was preserved (Figure 1A) in 8 USC (27.6%). Seventeen cases (58,6%) showed "focal loss" of expression (Figure 1B and 1C), whereas only 4 cases (13,8%) showed a complete absence of expression (Figure 1D). All cases with complete loss were negative for HER2 amplification via FISH.

Table 1. HER2 status by FISH and MHC Class I IHC expression in uterine serous carcinomas.

	MHC expression			Total
	Preserved	Focal loss	Complete loss	
HER2 FISH Negative	7	12	4	23
Positive	1	5	0	6
Total	8	17	4	

Figure 1 - 617

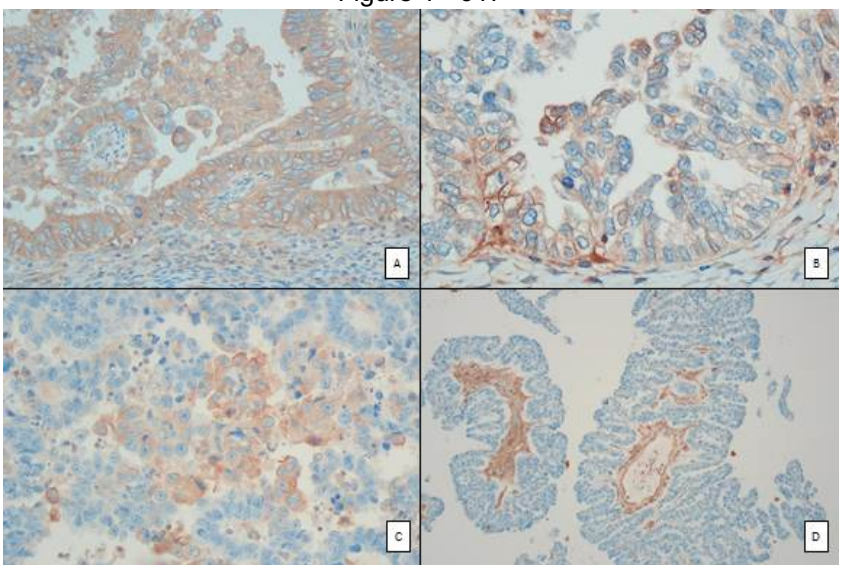

Conclusions: A complete loss of MHC class I IHC expression was only found among USC negative for HER2 amplification. These cases may not be suitable for treatment with immune checkpoint inhibitors or Her2/neu receptor inhibitor. Further studies are necessary to understand the susceptibility of USC to current targeted therapy options, and for the identification of novel potential targets.

618 NF-1 Mutated Pelvic High Grade Serous Carcinoma Exhibits Morphology More Aligned with Low Grade Serous Neoplasia than with BRCA Mutated Cancers: Implications for Identifying Tumors That Merit Molecular Testing for Potential Response to RAS Pathway Inhibitors

Lara Richer[1], Nicholas Ladwig[1], Walter Devine[1], Joseph Rabban[1]
[1]*University of California, San Francisco, San Francisco, CA*

Disclosures: Lara Richer: None; Nicholas Ladwig: None; Walter Devine: None; Joseph Rabban: None

Background: *NF1* is a tumor suppressor and negative regulator of the RAS/MAPK pathway. Biallelic loss of *NF1* has been shown to lead to overactivity of the RAS/MAPK pathway and clinical trials evaluating the use of MEK inhibitors in *NF1*-mutated low-grade gliomas and plexiform neurofibromas have shown encouraging results. *NF1* is also mutated in approximately 5% of pelvic high grade serous carcinoma (pHGSC). We hypothesized that *NF1* mutations in pHGSC may be mutually exclusive with *BRCA* mutations, which can confer response to PARP inhibitor therapy, and that *NF1*-mutated pHGSC may exhibit specific morphology that distinguishes it from *BRCA*-mutated pHGSC.

Design: Our institutional database of pHGSC tested using a 500 gene next generation sequencing panel was queried for cases with *NF1* mutations between 2016 and 2020. The prevalence of *BRCA*-associated SET morphology, including growth patterns, geographic necrosis, mitotic count, tumor infiltrating lymphocytes, as well as fallopian tube involvement, was defined by review of glass slides. Clinical demographics and outcome were retrieved from the electronic medical records.

Results: Nine pHGSC with pathogenic *NF1* mutations were identified, all of which carried a pathogenic *TP53* mutation and showed aberrant p53 immunoexpression. None of the cases harbored *BRCA1* mutation though one tumor had a somatic *BRCA2* mutation. No mutation in any other homologous recombination (HRD) pathway related genes were identified. 8/9 presented at FIGO stage III/IV and 5 underwent neoadjuvant therapy, of whom 2 showed a chemotherapy response score of 2 or 3. Classical SET morphology was present in only 1/7 cases with adequate slides available for review and only 2 cases contained serous tubal intraepithelial carcinoma. In contrast, adenofibromatous architecture, serous borderline tumor-like

growth, and LGSC-like buds and nests were present in 4/7. Three patients died of disease at 8, 28 and 63 months after initial presentation. The remainder were without evidence of disease at most recent follow-up (average 17.5 months).

Conclusions: The morphology of *NF1*-mutated pHGSC shows more overlap with the architecture of pLGSC than with *BRCA*-related SET morphology. Such morphology, if validated in larger studies, could serve as a trigger to test for *NF1* mutations as a marker of potential consideration for targeted inhibition of the RAS/MAPK pathway.

619 Challenging Mismatch Repair Protein Expression Patterns in Endometrial Carcinoma

Douglas Rottmann[1], Padmini Manrai[2], Austin McHenry[2], Pei Hui[3], Natalia Buza[4]
[1]Yale-New Haven Hospital, New Haven, CT, [2]Yale University, New Haven, CT, [3]Yale University School of Medicine, New Haven, CT, [4]Yale School of Medicine, New Haven, CT

Disclosures: Douglas Rottmann: None; Padmini Manrai: None; Austin McHenry: None; Pei Hui: None; Natalia Buza: None

Background: The TCGA molecular classification of endometrial carcinomas (ECs) identified a subgroup of ECs with mismatch repair (MMR) deficiency, with a high mutation burden and better prognosis. These tumors can be identified by loss of MMR protein expression by immunohistochemistry (IHC), which typically follows one of four patterns: MLH1/PMS2 loss, PMS2 loss, MSH2/MSH6 loss, or MSH6 loss. However, unusual MMR expression patterns have been reported in colorectal carcinoma and rarely in EC, complicating the pathology interpretation.

Design: All ECs diagnosed between 2015 and 2020 with available MMR IHC slides were retrieved from our departmental archives. Cases with either 1) MMR deficiency by IHC or 2) microsatellite instability (MSI-High or MSI-Low) by PCR were selected for the study. Results of MLH1 promoter methylation, tumor and germline genetic analysis, and follow-up information were collected from the electronic medical records. H&E and MMR IHC-stained slides were reviewed to confirm the diagnosis and determine the pattern of MMR expression. Each MMR protein was assigned to one of several patterns: completely retained, complete loss, retained with focal decreased staining, loss with focal weak retained staining, mostly retained with subclonal loss, or mostly lost with subclonal retained staining. Tumors with suboptimal staining quality due to pre-analytical variables were excluded. However, presence of cytoplasmic staining with retained or lost nuclear staining was recorded.

Results: A total of 104 ECs were included in the study: 73 endometrioid, 9 dedifferentiated, 6 serous, 3 clear cell, 1 undifferentiated, 10 mixed carcinomas, and 2 carcinosarcomas. Unusual pattern of expression for at least one MMR protein was seen in 58 cases (56%) and 6 cases showed retained staining for all proteins despite MSI-Low by PCR. Three cases showed complete loss of 3 MMR proteins (MLH1, PMS2, MSH6), 5 tumors had subclonal loss of MSH6 in addition to MLH1/PMS2 loss, and 4 tumors had subclonal retained staining, with one case of subclonal loss of MSH6 and subclonal retention of MLH1 and PMS2 (Table 1). Focal decreased MSH6 staining intensity was observed in 36 tumors, 24 of which also showed loss of MLH1/PMS2 with MLH1 promoter hypermethylation.

MMR IHC Pattern	MLH1	PMS2	MSH2	MSH6	Total cases
Subclonal loss	0	0	0	5	5
Subclonal retained	4	3	0	0	4
Retained with focal decreased staining	6	2	7	36	40
Loss with focal weak staining	15	5	0	5	19

Table 1. Patterns of expression/loss for each MMR protein by IHC. The total cases column shows the total number of cases with at least one MMR protein showing that pattern.

Conclusions: More than half of 104 MMR deficient ECs (56%) demonstrated an atypical pattern of expression of at least one MMR protein, most frequently MSH6. Focal decrease in MSH6 staining intensity was most often associated with MLH1/PMS2 loss in the setting of MLH1 promoter hypermethylation. Unusual MMR protein expression patterns present a diagnostic challenge in ECs with potential clinical implications related to Lynch syndrome screening, prognosis, and immunotherapy.

620 HPV-Independent, p53-Independent Non-Invasive Verruciform Lesions of the Vulva: A Comparison of Clinical, Histological and Recurrence Parameters

Simon Roy[1], Vincent Quoc-Huy Trinh[2], Kurosh Rahimi[1]
[1]Université de Montréal, Montreal, Canada, [2]Vanderbilt University Medical Center, Nashville, TN

Disclosures: Simon Roy: None; Vincent Quoc-Huy Trinh: None; Kurosh Rahimi: None

Background: Non-invasive, p53 and HPV-independent lesions each display verruciform architecture and have been classified as “vulvar acanthosis with altered differentiation” (VAAD), “differentiated exophytic vulvar intraepithelial lesion” (DEVIL) and “verruciform lichen simplex chronicus” (vLSC). We aimed to better characterize the clinical, histological and follow-up parameters of a larger cohort.

Design: Cases were first identified retrospectively using the search term “verruciform” and “verrucous” from 2008 until 2020 (*n*=71). 35 cases were excluded since pathology slides (*n*=8) or clinical information (*n*=8) were not available and when an alternative diagnosis was favored upon microscopic examination (*n*=19). A literature review was performed to extract diagnostic features of VAAD, DEVIL and vLSC and cases were classified by two pathologists. Criteria for VAAD included epithelial eosinophilic change, hypogranulosis and hyperkeratosis. (Figure 1). For vLSC, hypergranulosis, hyperkeratosis and absence of epithelial eosinophilic change were required. Cases classified as DEVIL did not satisfy criteria for neither VAAD nor vLSC and displayed an exophytic architecture. Cumulative survival from initial diagnosis to first recurrence of a verruciform lesion was assessed using the Kaplan-Meier procedure and Log-Rank testing (SPSS version 26).

Results: We identified 36 eligible patients with verruciform non-invasive lesions (*n*=36) which occurred at a median age of 60.5 years with a median follow-up of 33.5 months. (Table 1) Clinically, pruritus was only reported in patients with VAAD (*n*=3, 21%). Lesion color was significantly different across verruciform categories (p=0.028). Histologically, the three features that significantly differed between groups were hypogranulosis (p=0.004), epithelial eosinophilic change (p=0.005) and the low-power architecture (acanthotic versus exophytic, p=0.006). Apart from these criteria already known to distinguish these entities, no other significant criteria were discovered and significant overlap was observed, particularly between VAAD and DEVIL. Using Log-Rank testing, patients without invasive carcinoma at presentation, with vLSC, had a longer survival without recurrence compared to VAAD and DEVIL (P=0.056) and longer survival without invasive carcinoma (P=0.083) (Figure 2).

TABLE 1. Clinical and histologic datapoints between categories of non-invasive verruciform lesions of the vulva

	VAAD (n=14)	DEVIL (n=10)	VLSC (n=12)	Total (n=36)	P-value
Median age (years, IQR)	76 (61-87)	69 (56.5-82)	68 (59-76)	60.5 (59.3-80.8)	0.176
Cancer history	8 (57%)	2 (20%)	4 (33%)	14 (39%)	0.452
Vulvar large cell keratinizing SCC	1 (7%)	1 (10%)	1 (8%)	3 (8%)	
Non-Gynecological Cancer	5 (36%)	7 (70%)	7 (58%)	19 (53%)	
None					
Prior treatment	8 (57%)	2 (20%)	4 (33%)	14 (39%)	0.164
Surgery	2 (14%)	0 (0%)	0 (0%)	2 (6%)	0.189
Vulvar or pelvic radiotherapy	1 (7%)	1 (10%)	0 (0%)	2 (6%)	0.563
Chemotherapy					
Previous diagnosis of dysplasia	6 (43%)	2 (20%)	5 (42%)	13 (36%)	0.458
Any history	4 (29%)	0 (0%)	4 (33%)	8 (22%)	0.133
LSIL	3 (21%)	0 (0%)	2 (17%)	5 (14%)	0.308
uVIN	1 (7%)	2 (20%)	2 (17%)	4 (14%)	0.631
dVIN					
Previous diagnosis of vulvar inflammation	6 (43%)	3 (30%)	4 (33%)	13 (36%)	0.787
	6 (43%)	3 (30%)	3 (25%)	12 (33%)	0.608
Any history	0 (0%)	0 (0%)	1 (8%)	1 (3%)	0.358
LSA	2 (14%)	1 (10%)	1 (8%)	4 (11%)	0.883
LP					
LSC					
Clinical symptoms	3 (21%)	0 (0%)	0 (0%)	3 (8%)	0.076
Pruritus	3 (21%)	1 (10%)	3 (25%)	7 (19%)	0.657
Pain	5 (36%)	5 (50%)	2 (17%)	12 (33%)	0.248
Lump or plaque	5 (36%)	5 (50%)	7 (58%)	17 (47%)	0.485
None or unreported					
Clinical appearance	5 (35%)	0 (0%)	0 (0%)	5 (14%)	**0.028**
Erythematous	2 (14%)	5 (50%)	6 (50%)	13 (36%)	

White Unreported	7 (50%)	(50%)	6 (50%)	18 (50%)	
Median follow-up (months)	39 (29-67.6)	28 (13-42,7)	42.2 (33.7-123.7)	33.5 (14.4-66.1)	0.483
Lesion origin Vulva Periclitoral Vagina or vestibule	12 (86%) 1 (7%) 1 (7%)	7 (70%) 2 (20%) 1 (10%)	12 (100%) 0 (0%) 0 (0%)	31 (86%) 3 (8%) 2 (6%)	0.365
Largest specimen type Biopsy Resection	10 (71%) 4 (29%)	9 (90%) 1 (10%)	5 (42%) 7 (58%)	24 (67%) 12 (33%)	0.051
Parakeratosis Absent Plaque-like Multi-layered tiers Only focal	2 (14%) 5 (36%) 5 (36%) 2 (14%)	3 (30%) 3 (30%) 10 (10%) 3 (30%)	7 (58%) 0 (0%) 1 (8%) 4 (33%)	12 (33%) 8 (22%) 7 (19%) 9 (25%)	0.060
Slate grey lamina lucida, presence	0 (0%)	1 (10%)	2 (17%)	3 (9%)	0.325
Anucleate corneocytes in the stratum corneum, presence	12 (86%)	8 (80%)	9 (75%)	29 (81%)	0.788
Granular layer Absent hypergranulosis Thickened, focal Thickened, mostly continuous	6 (43%) 7 (50%) 1 (7%)	4 (40%) 4 (40%) 2 (20%)	0 (0%) 8 (67%) 4 (33%)	10 (28%) 19 (53%) 7 (19%)	0.089
Hypo-granulosis Absent Present, focal Present, mostly continuous	1 (7%) 5 (36%) 8 (57%)	2 (20%) 5 (50%) 3 (30%)	8 (67%) 4 (33%) 0 (0%)	11 (31%) 14 (39%) 11 (31%)	**0.004**
Epithelial eosinophilic change Absent Present, alternating Present, mostly continuous	2 (14%) 7 (50%) 5 (36%)	6 (60%) 1 (10%) 3 (30%)	10 (83%) 2 (17%) 0 (0%)	18 (50%) 10 (28%) 8 (22%)	**0.005**
Architecture, profile Acanthotic alone Exophytic Exophytic and endophytic	13 (93%) 1 (7%) 0 (0%)	3 (30%) 2 (20%) 5 (50%)	8 (67%) 3 (25%) 1 (8%)	24 (67%) 6 (17%) 6 (17%)	**0.006**
Architecture, rete In-ward bending of rete Broad-based rete Narrow rete	1 (7%) 8 (57%) 5 (36%)	1 (10%) 7 (70%) 2 (20%)	0 (0%) 6 (50%) 6 (50%)	2 (6%) 6 (50%) 6 (50%)	0.587
Basal layer Mitoses, presence Spongiosis Dyskeratosis	4 (29%) 8 (57%) 0 (0%)	3 (30%) 2 (20%) 0 (0%)	3 (25%) 4 (33%) 2 (17%)	10 (28%) 14 (39%) 2 (6%)	0.963 0.164 0.120
Neutrophilic microabcesses, presence	3 (21%)	2 (20%)	0 (0%)	5 (14%)	0.233
Stromal fibrosis	1 (7%)	2 (20%)	2 (17%)	5 (14%)	0.631
Inflammatory infiltrate Present, band-like Present, discontinuous Absent	0 (0%) 7 (50%) 7 (50%)	4 (40%) 2 (20%) 4 (40%)	2 (17%) 3 (25%) 7 (58%)	6 (17%) 12 (33%) 18 (50%)	0.095
Inflammatory infiltrate None Lymphocyte-Predominant	7 (50%) 7 (50%)	5 (50%) 5 (50%)	7 (58%) 5 (42%)	19 (53%) 17 (47%)	0.895
Background non-invasive dVIN uVIN vLSC LSA Conventional LSC Lichen planus	0 (0%) 0 (0%) 7 (50%) 1 (7%) 1 (7%) 1 (7%)	0 (0%) 0 (0%) 6 (60%) 2 (20%) 1 (10%) 2 (20%)	1 (8%) 0 (0%) 5 (42%) 3 (25%) 0 (0%) 3 (25%)	1 (3%) 0 (0%) 18 (50%) 6 (17%) 2 (6%) 6 (17%)	0.358 1.000 0.693 0.451 0.563 0.451
Margins in contact with the lesion	12 (86%)	9 (90%)	7 (58%)	28 (78%)	0.135
Immunohistochemistry P53, wild-type P53 not performed P16, wild-type P16, not performed	5 (36%) 9 (64%) 4 (29%) 10 (71%)	7 (70%) 3 (30%) 5 (50%) 5 (50%)	4 (33%) 8 (67%) 3 (25%) 9 (75%)	16 (44%) 20 (56%) 12 (33%) 24 (67%)	0.159 0.413

Figure 1 - 620

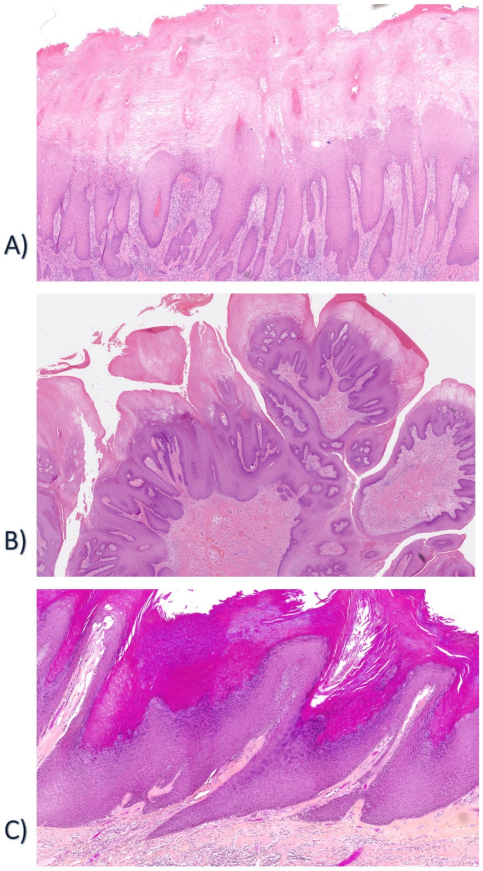

Figure 2 - 620

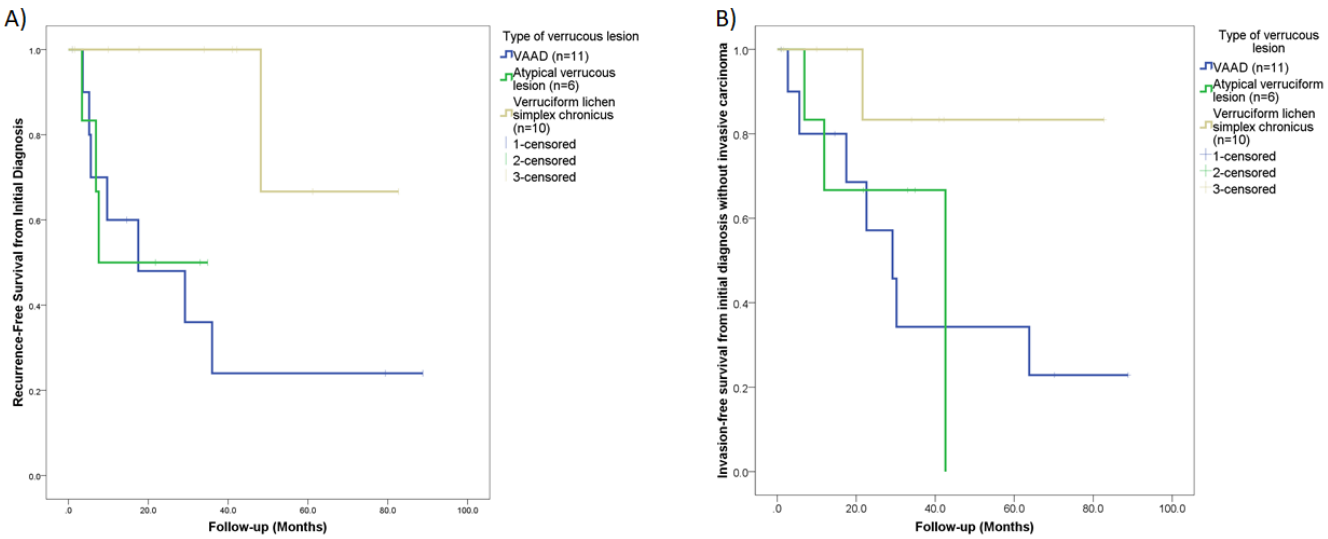

Conclusions: Our results suggest significant histological overlap of verruciform lesions of the vulva, yet differences in recurrence and progression-free survival amongst lesions. This highlights the significance of categorizing each subtype in the most accurate way possible.

621 High BRD4 Expression is an Independent Prognostic Factor in Endometrial Carcinoma

Ozlen Saglam[1], Biwei Cao[1], Xuefeng Wang[1], Gokce Toruner[2], José Conejo-Garcia[1]
[1]H. Lee Moffitt Cancer Center & Research Institute, Tampa, FL, [2]The University of Texas MD Anderson Cancer Center, Houston, TX

Disclosures: Ozlen Saglam: None; Biwei Cao: None; Xuefeng Wang: None; Gokce Toruner: None; José Conejo-Garcia: *Stock Ownership*, Compass Therapeutics, Anixa Biosciences; *Consultant*, Anixa Biosciences, Compass Therapeutics; *Grant or Research Support*, Compass Therapeutics, Anixa Biosciences; *Consultant*, Leidos; *Grant or Research Support*, Compass therapeutics

Background: Epigenetic pathway-related genes and PD-L1 expression by immunohistochemistry were explored in endometrial cancer (EC) pathogenesis. The expression levels of BRD4, DNMT3b, HDAC9, KAT6A, ER and PgR in EC subtypes were correlated with PD-L1 and clinicopathologic parameters.

Design: A tissue microarray (TMA) was constructed using 106 tumor samples. TMA included 30 FIGO grade 1&2 endometrioid, 28 FIGO grade 3 endometrioid, 31 serous and 17 clear cell carcinomas. All epigenetic markers were evaluated by multiplying the percentage of positively stained cells with nuclear staining intensity (1+, 2+, 3+) (H-score). Qualitatively, the combined positive score (CPC) of 1% or higher was considered as “expressed” for PD-L1. Wilcoxon test and Kruskal-Wallis test were used to explore the association between marker expression and tumor subtypes. Cox proportional-hazard regression model was further employed to investigate marker expression against overall survival (OS).

Results: The epigenetic marker expression differed among subtypes of EC. Serous-type cancer had the highest BRD4, DNMT3b, HDAC9, and KAT6A expression levels. PD-L1 expression was positively associated with the H-scores of KAT6A and BRD4, and negatively with PgR. PD-L1 expression levels did not show any difference among tumor subtypes. In the multivariable Cox proportional-hazards model adjusted with age, disease stage, tumor subtype, and lymphovascular invasion the median H-score of BRD4 was negatively associated with OS (p=0.030) (figure 1). PD-L1 expression had borderline significance for better disease outcomes (p=0.052).

Figure 1 - 621

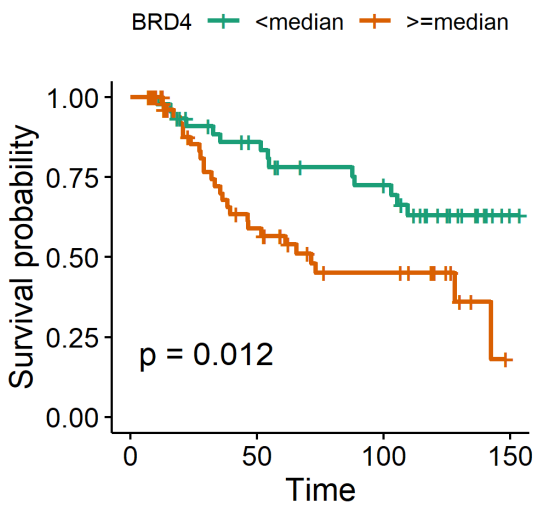

Conclusions: Among the EC subtypes, serous-type cancers have the highest epigenetic biomarker expression. Combination therapy with BRD4 or KAT6A inhibitors is a potential treatment option against PD-L1 resistance. BRD4 is an independent prognostic factor in EC.

622 Integrated Molecular and Clinicopathologic Study of Tubo-Ovarian High-Grade Serous Carcinoma

Giacomo Santandrea[1], Claudio Ceccarelli[1], Donatella Santini[1], Daniela Turchetti[1], Claudio Zamagni[2], Anna Myriam Perrone[1], Pierandrea De Iaco[1], Antonio De Leo[3]
[1]S.Orsola-Malpighi Hospital, University of Bologna, Bologna, Italy, [2]Sant'Orsola-Malpighi Academic Hospital of Bologna, Italy, Bologna, Italy, [3]University of Bologna, Bologna, Italy

Disclosures: Giacomo Santandrea: None; Antonio De Leo: None

Background: High-Grade Serous Carcinoma (HGSC) of tubo-ovarian origin is characterized by two main morphologic patterns: classic histotype and SET variant. A number of clinical and histopathologic parameters have been studied to better predict the clinical outcome and BRCA status. The aim of this study was to investigate the correlation of HGSC tumor morphology, BRCA mutational status, and clinicopathologic features to identify parameters predictive of biological behavior and molecular features.

Design: 105 HGSC cases were included in the present study. Extensive macroscopic observation regarding tumor origin, site of the lesions, tumor extension and growth pattern have been assessed. The tubo-ovarian site was sampled and examined via SEE-FIM protocol. All cases have been subsequently reviewed according to the new 2020 WHO diagnostic criteria. Complete anamnestic and clinical parameters have been collected. *BRCA1* and *BRCA2* analysis was performed on DNA extracted from formalin-fixed paraffin-embedded (FFPE) cancer tissue through Next Generation Sequencing (NGS). Any variants were then validated in constitutional DNA by targeted Sanger sequencing. BRCA germline deletions/duplication were also investigated via MLPA analysis on constitutional DNA.

Results: *BRCA1/2* mutations have been identified in 44% of cases and was significantly correlated with SET morphology ($p<0.0001$), higher Peritoneal Cancer Index (PCI) score ($p=0.05$) and better clinical outcome. SET tumors showed a statistically significant association with pushing pattern of invasion ($p=0.0001$), high number intraepithelial TILs ($p=0.0001$), higher mitotic index ($p=0.05$) and lower CA-125 levels ($p=0.002$). 80% of cases have been classified as tubo-ovarian origin and 20% as pure ovarian. No correlation has been observed between site of origin and BRCA status or tumor morphology. Positive anamnesis for breast cancer, tumor morphology, iTILs and PCI index have been implemented to create a “clinicopathologic BRCAness predictive algorithm” which resulted in better sensitivity, specificity, positive predictive value and negative predictive value compared with a pure morphology-based algorithm.

Conclusions: *BRCA* mutational status was associated with SET morphology, higher PCI score and better clinical outcome. SET morphology was associate with high TILs, high mitotic index and pushing pattern of peritoneal invasion, but not with the tumor site of origin. A “clinicopathologic BRCAness predictive algorithm” has been implement with better performance compared with a pure histological approach based on SET morphology alone. This further highlights the evidence for a multidisplinary approach to better characterize tubo-ovarian HGSCs.

623 Exploring Molecular Predictors of Malignancy in Ovarian Steroid Cell Tumors as a Complement to Morphology

Heather Smith[1], Peng Wang[2], Carrie Fitzpatrick[2], Pankhuri Wanjari[1], W. Glenn McCluggage[3], Robert Young[4], Esther Oliva[5], Jennifer Bennett[2]
[1]University of Chicago Medical Center, Chicago, IL, [2]University of Chicago, Chicago, IL, [3]The Royal Hospitals/Queen’s University of Belfast, Birmingham, United Kingdom, [4]Harvard Medical School, Boston, MA, [5]Massachusetts General Hospital, Harvard Medical School, Boston, MA

Disclosures: Heather Smith: None; Peng Wang: None; Pankhuri Wanjari: None; W. Glenn McCluggage: None; Robert Young: None; Esther Oliva: None; Jennifer Bennett: None

Background: Ovarian steroid cell tumors (SCT) can be divided into two groups—SCT NOS and Leydig cell tumor (LCT). SCT NOS is considered a neoplasm of uncertain malignant potential while LCT is benign. For SCT NOS there are several pathologic features suggestive of malignancy (m) including size > 7 cm, necrosis, hemorrhage, moderate to severe nuclear atypia, and > 2 mitoses/10 HPF. However, their molecular phenotype has not been

explored to determine whether specific gene alterations are predictive of aggressive behavior, which may help complement morphological analysis.

Design: We evaluated the clinicopathologic features of 25 SCT (17 NOS, 4 mSCT, 4 LCT) and performed next-generation sequencing (NGS) using a 1213 gene panel on 5 (2 mSCT, 2 NOS, 1 LCT).

Results: Patients ranged from 16 to 79 (mean 50) years and 13/22 (59%; unknown in 3) presented with hormonal manifestations. All were confined to the ovary except 2 mSCTs that were stage II and III. No recurrences occurred with SCT NOS or LCTs, while 3 (75%) mSCTs recurred (no follow-up in fourth). Features suggestive of malignancy were noted in 4 (100%) mSCT, 6 (35%) SCT NOS, and 1 LCT (25%) (Figure 1). As nearly all SCTs showed at least focal hemorrhage, this finding was favored to represent procedural change and was excluded from analysis.

NGS detected *MDM2* and *CDK4* amplification in both mSCTs, but not in the SCTs NOS or LCTs. Aside from a *CTNNB1* missense mutation in 1 SCT NOS, no other mutations or copy number variations were identified. Based on this finding, we performed MDM2 immunohistochemistry (IHC) on all 25 tumors. IHC was scored for both intensity (0=negative, 1+=weak, 2+=moderate, 3+=strong) and extent. mSCT showed 3+ nuclear staining in 20 to 70% (mean 30%) of cells. It was positive in 15 (88%) SCTs NOS (intensity: 1+ to 3+, range: 10 to 90%, mean: 38%) and in 2 (50%) LCTs (2+, 25% and 60%). Interestingly, the two sequenced SCTs NOS showed strikingly different MDM2 expression patterns: one was strongly positive in >90% of cells, while the other was weakly positive in 10% of cells. The sequenced LCT was moderately positive in 25% of cells.

Figure 1 - 623

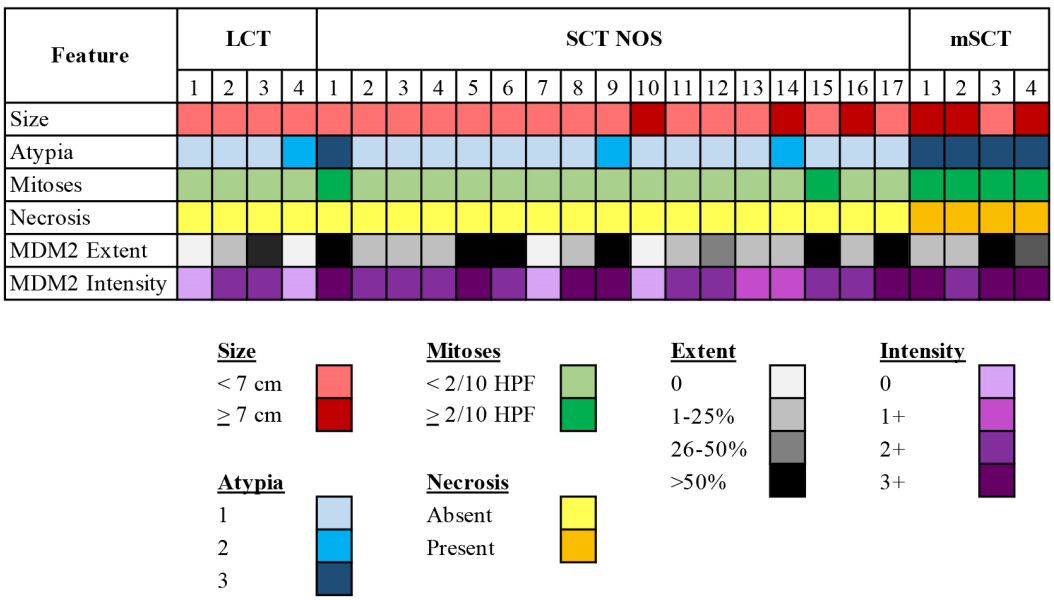

Conclusions: *MDM2* amplification was only detected in mSCTs, although the number of cases sequenced is small. As MDM2 IHC does not appear to show a direct correlation between intensity/extent of staining and presence of amplification, FISH for *MDM2* is currently underway in all tumors. If FISH is negative in SCTs NOS and LCTs, then it may be a useful adjunct to morphology in predicting SCT behavior.

624 Targeted RNA Sequencing Highlights a Diverse Genomic Landscape in High Grade, Undifferentiated, and Difficult to Classify Uterine Sarcomas

Sharon Song[1], Marisa Nucci[2], Christopher Crum[1], Bradley Quade[1], Beth Harrison[1], Brendan Dickson[3], David Kolin[1]

[1]Brigham and Women's Hospital, Boston, MA, [2]Brigham and Women's Hospital, Harvard Medical School, Boston, MA, [3]Mount Sinai Health System, Toronto, Canada

Disclosures: Sharon Song: None; Marisa Nucci: None; Christopher Crum: None; Bradley Quade: None; Beth Harrison: None; Brendan Dickson: *Grant or Research Support*, Illumina; David Kolin: None

Background: High-grade and undifferentiated uterine sarcomas represent morphologically and genetically heterogeneous uterine mesenchymal neoplasms. Recent molecular studies have uncovered distinct molecular alterations, occasionally associated with unique clinicopathologic features, expanding our understanding of the spectrum of findings in uterine sarcomas. The aim of this study was to characterize the genetic landscape of a cohort of morphologically high-grade uterine sarcomas by targeted RNA sequencing (RNA-Seq).

Design: A retrospective archival review from a single institution was performed for high-grade endometrial stromal sarcoma, monomorphic undifferentiated uterine sarcoma, and morphologically high-grade uterine sarcomas which were difficult to classify based on morphology and immunohistochemistry. Slides were reviewed to confirm the diagnosis, and representative sections were submitted for RNA-Seq.

Results: 21 uterine sarcomas were identified and successfully sequenced. The average patient age was 50 years (range 20-74). The fusions detected by RNA-Seq are summarized in Table 1. The most common fusion was *ZC3H7B-BCOR*, identified in 3 cases (14.3%), with the reciprocal fusion, *BCOR-ZC3H7B,* also seen (4.8%). Single instances of the following fusions were detected: *YWHAE-NUTM2B* (4.8%), *YWHAE-CD109* (4.8%), *EPC1-BCORL1* (4.8%), *COL1A1-PDGFB* (4.8%), and *EWSR1-WT1* (4.8%). 12 cases (57%) did not have any detectable fusions.

Table 1. Gene fusions detected by RNA-Seq in a cohort of 21 cases of morphologically high grade uterine sarcomas.

Fusion	Age (mean)	n (%)
ZC3H7B-BCOR	42.3	3 (14.3%)
BCOR-ZC3H7B	49	1 (4.8%)
YWHAE-NUTM2B	56	1 (4.8%)
YWHAE-CD109	64	1 (4.8%)
EPC1-BCORL1	65	1 (4.8%)
COL1A1-PDGFB	52	1 (4.8%)
EWSR1-WT1	20	1 (4.8%)
Negative	50.8	12 (57%)

Conclusions: High-grade and undifferentiated uterine sarcomas can be difficult to classify, but detection of a fusion gene can facilitate classification. Further study is required to determine the prognostic significance of these translocations and better characterize their morphologic attributes. The significant number of cases lacking detectable fusions with this panel is presumed to be the result of alternate driving events, emphasizing the need for more active investigation in this area.

625 Clinical Correlation of Silva Patterns of Invasion and 2019 FIGO Low-Stage (IA and IB1) in Endocervical Adenocarcinoma (ECA)

Simona Stolnicu[1], Monica Boros[2], Lynn Hoang[3], Noorah Almadani[4], Louise De Brot[5], Glauco Baiocchi[5], Graziele Bovolim[5], Maria Jose Brito[6], Georgia Karpathiou[7], Antonio Ieni[8], Esther Guerra[9], Takako Kiyokawa[10], Pavel Dundr[11], Carlos Parra-Herran[12], Sofia Lerias[13], Ana Felix[14], Andres Roma[15], Anna Pesci[16], Esther Oliva[17], Kay Park[18], Robert Soslow[19], Nadeem Abu-Rustum[18]

[1]University of Medicine, Pharmacy, Sciences and Technology, Targu Mures, Romania, [2]University of Oradea, Oradea, New Zealand, [3]The University of British Columbia, Vancouver, Canada, [4]The University of British Columbia, Vancouver General Hospital, Vancouver, Canada, [5]A.C.Camargo Cancer Center, São Paulo, Brazil, [6]Hospital Garcia de Orta, Almada, Portugal, [7]University Hospital of Saint-Etienne, Saint-Etienne, France, [8]Messina, Italy, [9]Hospital Universitari de Bellvitge, Hospitalet de Llobregat, Spain, [10]The Jikei University School of Medicine, Tokyo, Japan, [11]Charles University, Prague, Czech Republic, [12]Brigham and Women's Hospital, Harvard Medical School, Boston, MA, [13]Instituto Português de Oncologia Francisco Gentil, Lisbon, Portugal, [14]Instituto Portugues de Oncologia de Lisboa, Lisbon, Portugal, [15]University of California, San Diego, San Diego, CA, [16]IRCCS Ospedale Sacro Cuore Don Calabria, Negrar, Verona, Italy, [17]Massachusetts General Hospital, Harvard Medical School, Boston, MA, [18]Memorial Sloan Kettering Cancer Center, New York, NY, [19]Memorial Sloan Kettering Cancer Center/Weill Medical College of Cornell University, New York, NY

Disclosures: Simona Stolnicu: None; Monica Boros: None; Louise De Brot: None; Glauco Baiocchi: None; Graziele Bovolim: None; Maria Jose Brito: None; Georgia Karpathiou: None; Esther Guerra: None; Takako Kiyokawa: None; Pavel Dundr: None; Carlos Parra-Herran: None; Sofia Lerias: None; Ana Felix: None; Andres Roma: None; Anna Pesci: None; Esther Oliva: None; Kay Park: None; Robert Soslow: None; Nadeem Abu-Rustum: None

Background: The Silva pattern of invasion can detect which patients with ECA are at risk of lymph node metastases (LNM). It may be most relevant for small and low-stage carcinomas such as FIGO stage IA and IB1 rather than IB2/IB3. The aim of the present study was to analyze Silva patterns of invasion and presence of lympho-vascular invasion (LVI) as they relate to clinical outcomes in stages IA and IB1 ECAs.

Design: Slides from 399 FIGO stage IA and IB1 ECAs were collected from 15 international institutions. Hematoxylin and eosin slides containing tumor were examined for Silva (A, B, C) patterns and presence of lympho-vascular invasion (LVI). 2019 FIGO stage, presence of LNM, local/distant recurrences and survival data were retrieved from the clinical data files of each institution. Cross-tabulation analyses (χ^2 and Anova test), regression binary logistic tests, Kaplan-Meier test, log-rank Mantel Cox test were used for statistical analysis.

Results: 152 (38.1%) were staged IA (77 cases (19.3%) IA1 and 75 cases (18.8%) IA2) and 247 (61.9%) were staged IB1.Stage IA ECAs were more likely to have pattern Silva A than IB1 (p=0.00001). Univariate analysis (cross-tabulation test) showed a higher frequency of Silva pattern B/C in IB1 ECAs compared to IA (p=0.00001, OR=7.114, 95%CI= 3.983-12.708). Multivariate analysis (binary logistic regression) showed that the only statistically significant factors for stage IA versus IB1 ECAs were LVI (p=0.008) and Silva pattern (p=0.00001), while among IA substages LVI remained significant (p=0.0006). The 5-year and 10-year OS and RFS rates were better for stage IA versus IB1 patients (p=0.002; p= 0.007). Outcome (OS and RFS; Kaplan Meier analysis) at 5 and 10 year were similar in stage I/Silva A cases versus Silva B cases without LVI (p=0.001) (log rank test). In Silva C cases, OS and RFS; (Kaplan Meier analysis) appeared better for stage IA than for Stage IB1/Silva (p=0.083; p=0.622) (log rank test), although not significantly.

Conclusions: Silva pattern and LVI are important prognostic factors among stage IA1-IB1 ECAs and should be included in pathology reports. Furthermore, since Silva B without LVI had a similar prognosis to Silva A, we propose a binary Silva system, grouping together lower-risk cases (pattern A and B without LVI) versus high risk cases (pattern B with LVI and pattern C). Silva C IA should not be considered IB1 based on clinical outcomes.

626 Endometrial Carcinomas: Exploring the Concordance Between ARID1A Immunohistochemistry and ARID1A Mutational Status

Tanner Storozuk[1], Peng Wang[2], Ricardo Lastra[2], Jennifer Bennett[2]
[1]*University of Chicago Medical Center, Chicago, IL,* [2]*University of Chicago, Chicago, IL*

Disclosures: Tanner Storozuk: None; Peng Wang: None; Ricardo Lastra: None; Jennifer Bennett: None

Background: *ARID1A* mutations have been reported in ~40% of copy number low endometrial carcinomas (EC). In the ovary, a correlation between ARID1A immunohistochemistry (IHC) and mutational status has been reported, but this association has only received limited attention in ECs.

Design: We evaluated the clinical and morphological features of 52 ECs with known *ARID1A* mutational status. ARID1A IHC was performed on the same slide used in molecular testing, and classified as intact, diffuse complete loss (Figure 1A), diffuse partial diminution (Figure 1B), heterogeneous complete loss (Figure 1C), or heterogeneous partial diminution (Figure 1D).

Results: Most tumors (44; 85%) were endometrioid (27 grade 1; 14 grade 2; 3 grade 3), while the remainder were serous (n=3), clear cell (n=2), mixed (n=1), carcinosarcoma (n=1), and dedifferentiated (n=1). FIGO stage was as follows (biopsy only in 2): 44 (88%) stage I, 2 (4%) stage II, 3 (6%) stage III, and 1 (2%) stage IV. Follow-up was available for 51 patients with 33 (65%) alive and well, 11 (22%) alive with disease, and 7 (14%) dead of disease.

Abnormal IHC was observed in 32 (62%) tumors (Table). Pathogenic *ARID1A* mutations were identified in 32 (62%) tumors, all of which were frameshift (21; 66%), nonsense (6; 19%), or both (5; 16%). No *ARID1A* copy number variations were detected. Evidence of biallelic inactivation (presence of two mutations) was noted in 6 (12%) tumors. Concordance between IHC and mutational status was seen in 40 (77%) tumors (p=0.0004) with a sensitivity of 70% and specificity of 81%.

Progression-free survival (PFS) versus IHC and mutational status was calculated for the 43 endometrioid carcinomas with follow-up. No correlation was identified for IHC (p=0.442), but *ARID1A*-mutant tumors showed a trend toward decreased PFS (p=0.127).

Clinicopathological and molecular features are summarized in Figure 2.

	Immunohistochemistry					
Mutational Status	Intact	Abnormal	Diffuse Complete Loss	Diffuse Partial Diminution	Heterogeneous Complete Loss	Heterogeneous Partial Diminution
Wildtype	14	6	1	0	4	1
Mutant	6	26	8	4	8	6

Figure 1 - 626

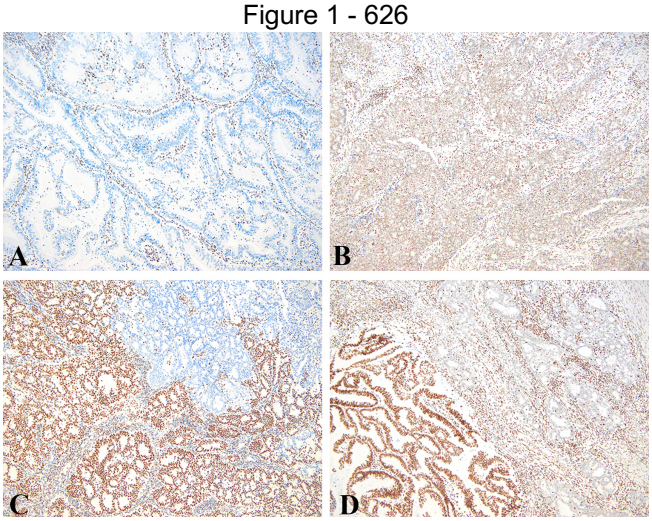

Figure 2 - 626

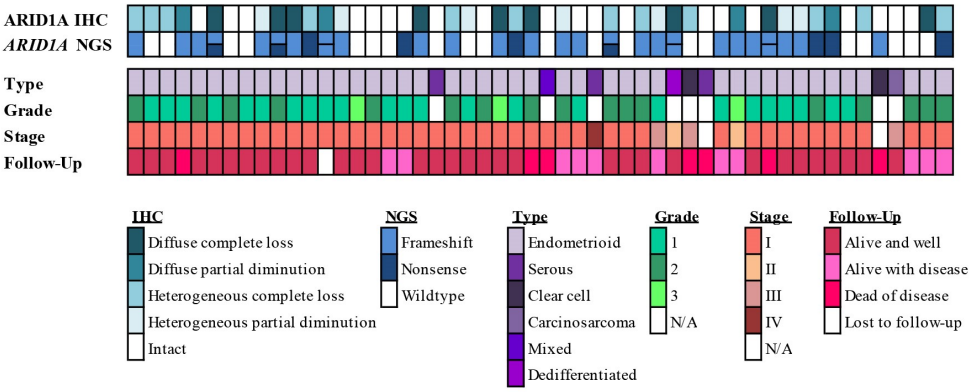

Conclusions: Overall, ARID1A IHC can serve as a surrogate marker for *ARID1A* mutational status in ECs. However, as 6 (19%) *ARID1A*-mutant tumors exhibited intact ARID1A expression, follow-up molecular testing is necessary in those patients with metastatic/recurrent disease since EZH2 inhibitors are currently being explored in tumors with SWI/SNF deficiency. Conversely, 6 (30%) of *ARID1A*-wildtype ECs demonstrated abnormal IHC expression. Whether EZH2 inhibitors are effective in this group of tumors (similar to PD-L1 inhibitors in MMR-deficient tumors) remains to be explored.

627 Clinical, Pathological and Molecular Correlates of Recurrent/Metastatic Low Grade Endometrial Endometrioid Carcinoma

Jana Suresh[1], Rajni Chibbar[2], Raymond Lai[3], Cheng-Han Lee[4], Sabrina Förstner[5], Richa Chibbar[5], Anita Agrawal[6], Rani Kanthan[2], Vijayananda Kundapur[2]
[1]University of Saskatchewan, Saskatoon, Canada, [2]University of Saskatchewan, Saskatchewan Health Authority, Saskatoon, Canada, [3]Dyna life Medical Labs, Edmonton, Canada, [4]BC Cancer, Vancouver, Canada, [5]University of Alberta, Edmonton, Canada, [6]Kingston General Hospital, Queen's University, Kingston, Canada

Disclosures: Jana Suresh: None; Rajni Chibbar: None; Raymond Lai: None; Cheng-Han Lee: None; Sabrina Förstner: None; Richa Chibbar: None; Anita Agrawal: None; Rani Kanthan: None; Vijayananda Kundapur: None

Background: The Cancer Genome Atlas (TCGA) stratified endometrial carcinoma into four clinically significant molecular groups. It has been suggested that molecular and immunohistochemical markers should be preferably applied to biopsy specimen for prognostic classification. The low –somatic copy number tumors includes Type I endometrial carcinoma, associated with unopposed estrogen, occurs in younger age group and has relatively better survival. However 7-10% of patients with low grade endometrial endometrioid carcinoma (LGEEC) tend to recur locally, distally or present with metastatic disease. Currently, we do not have markers to better stratify or identify low grade EEC that will recur. Exon -3 mutations of β- catenin gene has been suggested to occur at a higher frequency in recurrent LGEEC. Estrogen and progesterone receptors are expressed in approximately 95% of LGEEC. The objective of our study was to determine whether ER, PR, and exon 3 b-catenin mutation analysis can be used to refine risk stratification in LGEEC.

Design: We retrospectively searched our institutional database from 2008 to 2018, for biopsy proven cases of recurrent LGEEC, FIGO grade I and II. As controls cases of EEC, FIGO grade I and II without recurrence were included. Chart review and clinicalpathological data was collected. Immunohistochemistry was performed on selected blocks for estrogen (ER) and progesterone (PR) receptors, MMR and p53. Mutation analysis for exon 3 b-catenin (CTNNB1) and KRAS was performed.

Results: We identified a total of 662 cases of endometrioid carcinoma of which 47 cases had recurrence (22 with local and 25 with distant metastases). We selected 47 cases as control group without recurrence. Eight cases were microsatellite unstable by IHC. Of the remaining 39 cases, 9 (23%) were ER/PR receptor negative. Interestingly, of the 9 ER/PR negative cases, upon work up five were identified to be mesonephric like

adenocarcinomas (MLA). A 40% of the local and 5% of the distant metastasis group had mutation in exon 3 of CTNNB1 gene. Likewise, KRAS mutation was seen in 6% local and 50% distant metastasis.

Conclusions: Recurrence/metastasis rate for LGEEC was 8% in our institution. Our preliminary data demonstrate that further risk stratification can be achieved by ER and PR receptor immunohistochemical analysis on biopsy specimens to identify patients at risk of recurrence or metastasis for adequate work up and surgery.

628 Comprehensive Tissue Testing For BRCA1/2 Gene Mutations Is An Integral Tool In The Management Of High Grade Serous Carcinoma Patients – A Single Cancer Center Experience With 252 Cases

Cornelia Thoeni[1], Andrea Vaags[2], Lilian Gien[3], Sharon Nofech-Mozes[4], Bojana Djordjevic[5]
[1]University of Toronto, Toronto, Canada, [2]Trillium Health Partners, Mississuga, Canada, [3]Sunnybrook Health Sciences Centre, Odette Cancer Centre, Toronto, Canada, [4]University of Toronto, Sunnybrook Health Sciences Centre, Toronto, Canada, [5]University of Toronto, Sunnybrook Health Sciences Centre, Toronto, Canada

Disclosures: Cornelia Thoeni: None; Andrea Vaags: None; Lilian Gien: *Advisory Board Member*, Myriad; Sharon Nofech-Mozes: None; Bojana Djordjevic: None

Background: Recommendation for referral of patients with upper Müllerian tract High Grade Serous Carcinoma (HGSC) for genetic counseling and germline *BRCA1/2* mutation testing has existed for over a decade with variable referral rates and often prolonged turnaround time (TAT). In Nov. 2018, tumor *BRCA1/2* mutation testing became provincially funded in Ontario, Canada, based on the approval of Poly (ADP-ribose) polymerase inhibitor (PARPi) therapy (Olaparib) as maintenance therapy in newly diagnosed and recurrent platinum sensitive HGSC patients with *BRCA1/2* germline and somatic mutations. This is a summary of a single cancer center's institutional experience with the clinical introduction of this process.

Design: Between Nov. 2018 and Oct. 2020 HGSC patients underwent tissue, germline or combined *BRCA1/2* mutation testing at external accredited molecular laboratories in the greater Toronto area. We performed comprehensive chart reviews including PARPi therapy eligibility and planning.

Results: All (252) patients with HGSC were tested for pathogenic *BRCA1/2* gene variants using tumor tissue and/or peripheral blood cells with 240 successful tests. 133 (55%) patients underwent tissue testing only, 18 (7.5%) germline testing only and 89 (37%) combined testing (Figure 1). Initial TATs were variable, however, workflow readjustments achieved a TAT of 21 days or less. Out of 240 HGSC patients, 40 (16%) demonstrated pathogenic *BRCA1/2* mutations (12 somatic, 11 germline and 17 somatic-germline status undetermined). Consistent with literature, the majority - 30 (75%) - of pathogenic variants were within the *BRCA1* gene and mainly entailed exon losses, frame-shift mutations or introduction of a premature stop codon. All 40 patients were further evaluated for PARPi maintenance: 10 received Olaparib or Niraparib (also recently approved), 1 showed platinum-resistance and was excluded, and 29 patients are currently planned for therapy if shown to be clinically eligible.

Figure 1 - 628

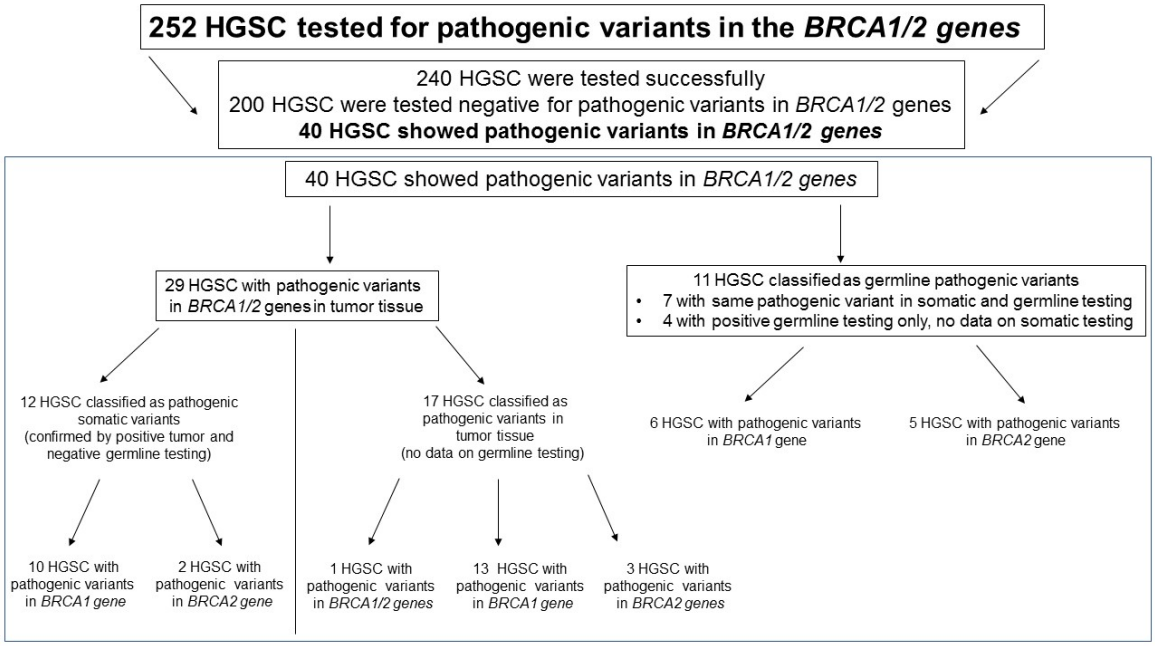

Conclusions: Uptake of newly available *BRCA1/2* mutation tumor testing occurred in over 90 % of HGSC patients at our institution. Genetic counseling with germline and reflex tumor testing are two parallel processes serving complementary aspects of care. While germline testing is important for assessing overall cancer risk for patients and their relatives, tumor testing is an assay predicting eligibility for PARPi in an expedited manner and is readily accessible at the time of pathological diagnosis.

629 Ewing Sarcoma of the Gynecologic Tract: A Rare Entity to be Considered in the Differential Diagnosis of Spindle and Round Cell Sarcomas Occurring in the Female Genital Tract

Cindy Wepy[1], Marisa Nucci[2], Christopher Crum[1], Christopher Fletcher[1], David Kolin[1]
[1]Brigham and Women's Hospital, Boston, MA, [2]Brigham and Women's Hospital, Harvard Medical School, Boston, MA

Disclosures: Cindy Wepy: None; Marisa Nucci: None; Christopher Crum: None; Christopher Fletcher: None; David Kolin: None

Background: Ewing sarcoma is characterized by small round cell morphology and translocations involving the *EWSR1* gene. It rarely occurs in the gynecologic tract, where the potential for misdiagnosis exists due to its rarity and morphologic and immunophenotypic overlap with other more commonly encountered gynecologic sarcomas. This study explored the range of clinical, morphologic, and immunophenotypic features of a series of Ewing sarcomas occurring in the female genital tract.

Design: Cases were identified from 2009-2019 in departmental and consult archives (n=8). They were reviewed for patient demographics and clinical, morphologic, immunohistochemical, and molecular features.

Results: A total of 8 cases were included, summarized in Table 1. Median patient age was 35.5 (range 19-56) years. Tumor sites included uterus (n=4), cervix (n=2), vagina (n=1), and pelvis (n=1). Two cases demonstrated variant ovoid/spindle cell morphology (Figure 1), with the remainder demonstrating round cell morphology. Tumors were positive for CD99 (7/7) and NKX2.2 (2/2), and negative for ER (2/2), PR (4/4), and CD10 (2/2). Four cases were initially classified as other entities prior to the diagnosis being revised to Ewing sarcoma, including high grade endometrial stromal sarcoma (n=2), undifferentiated uterine sarcoma (n=1), and unclassifiable spindle and epithelioid sarcoma (n=1). Six of eight cases had molecular confirmation: FISH demonstrated *EWSR1* gene

rearrangements (6/6) and targeted next generation DNA sequencing revealed *EWSR1-FLI1* fusions (2/3) and an *EWSR1-ERG* fusion (1/3). The two cases without molecular confirmation were positive for both CD99 and NKX2.2. Of four patients with available follow up so far, two died of disease and two developed persistent/metastatic disease.

Table 1. Clinicopathologic features of Ewing sarcoma of the female genital tract (n=8). — not available/performed.

Case	Age (yrs)	Site	Initial Diagnosis	Morphology	FISH	NGS	Follow Up
1	22	Pelvis	Undifferentiated uterine sarcoma	Ovoid/spindle cell	*EWSR1* rearrangement	*EWSR1-ERG* fusion	Died of disease 10 months after presentation
2	31	Cervix	Unclassifiable spindle and epithelioid sarcoma	Round cell	*EWSR1* rearrangement	*EWSR1-FLI1* fusion	Disease metastatic to lungs at 3 and 11 years after presentation
3	56	Vagina	Ewing sarcoma	Round cell	*EWSR1* rearrangement	—	Died two weeks after initial surgery
4	24	Uterus	Ewing sarcoma	Round cell	*EWSR1* rearrangement	—	—
5	40	Uterus	High-grade endometrial stromal sarcoma	Round cell	*EWSR1* rearrangement	—	—
6	46	Uterus	High-grade endometrial stromal sarcoma	Ovoid/spindle cell	*EWSR1* rearrangement	*EWSR1-FLI1* fusion	Disease metastatic to lungs at presentation
7	19	Cervix	Ewing sarcoma	Round cell	—	—	—
8	47	Uterus	Ewing sarcoma	Round cell	—	—	—

Figure 1 - 629

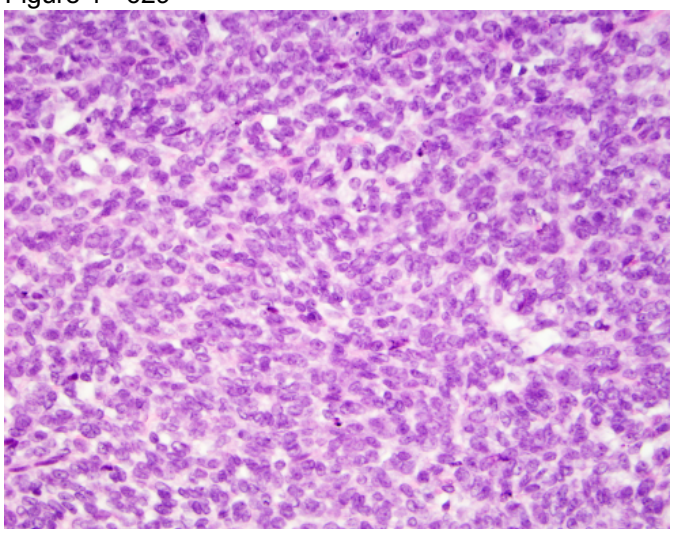

Conclusions: Ewing sarcoma of the gynecologic tract is a rare, aggressive entity that should be considered in the differential with other gynecologic sarcomas. In addition to classic round cell morphology, variant spindled/ovoid to epithelioid morphology may also be present. Young patient age, in combination with negative immunohistochemical staining for ER, PR, and CD10 should prompt consideration of this entity with the appropriate immunohistochemical

workup and/or molecular confirmation. Targeted molecular profiling of “unclassifiable” gynecologic sarcomas can help establish the diagnosis, especially in cases with variant morphology or arising at unusual sites, with potential treatment implications.

630 Cervical Biopsies Diagnosed as “At Least High Grade Squamous Intraepithelial Lesion (HSIL)” or “At Least Adenocarcinoma In Situ (AIS)” and Morphologic Predictors of Invasive Carcinoma

Rebecca Wolsky[1], Daniel Reiter[2]
[1]University of Colorado, Denver, CO, [2]University of Colorado, Aurora, CO

Disclosures: Rebecca Wolsky: None; Daniel Reiter: None

Background: Biopsies of cervical dysplasia are common, with the ultimate goal of reducing the incidence of invasive squamous cell carcinoma (invSCC) as well as endocervical adenocarcinoma (EAC). It is well known that some biopsies show features suspicious for invasion, so-called "at least HSIL" or "at least AIS," but these features have not been well defined, nor have they been correlated with outcomes of invasion. Recently, the Silva system of EAC pattern of invasion has been incorporated into the CAP cancer protocol, yet there is no objective method for distinguishing “at least AIS” from minimal pattern A invasion. As the Silva patterns begin to inform clinical management, examining and defining the liminal space between AIS and pattern A invasion may have management implications and bearing on clinical outcomes studies of pattern A patients.

Design: After IRB approval, cervical biopsies (1999-2019) at one academic institution were searched for diagnoses of HSIL or AIS, “at least,” “suspicious for,” or “worrisome for” invasion. Subsequent/concurrent pathology reports were reviewed for the presence of invSCC or EAC. Morphologic patterns of “at least” biopsies were described and calculated for risk of subsequent invasion.

Results: 22 cases of “at least HSIL” (of which 18 had subsequent reports available) and 11 cases of “at least AIS” (8 subsequent reports available) were identified. Risk of invasion on subsequent pathology was 11 of 18 (61%) for invasive SCC and 3 of 8 (38%) for EAC. Morphologic patterns in cervical biopsies with "at least HSIL" and "at least AIS" are described (see Table 1).

Morphologic pattern	# biopsies with pattern (%)	Risk of invasion on subsequent pathology (# invasion present/# subsequent report available) (%)
At least HSIL		
Complex bands of HSIL	11 (50)	5/7 (71)
HSIL with pushing border	5 (23)	1/3 (33)
HSIL with irregular border	3 (14)	1 /2 (50)
Necrosis	2 (9)	1/1 (100)
At least AIS		
Poor orientation	8 (73)	3/6 (50)
Complex AIS	7 (64)	3/5 (60)
Increased quantity of AIS	2 (18)	0/1 (0)
Deep AIS	1 (9)	0/1 (0)
Stromal reaction	1 (9)	Subsequent report not available
Possible infiltration	1 (9)	0/1 (0)
Extends to edge of biopsy	1 (9)	0/1 (0)

Conclusions: Overall, the risk of subsequent invSCC for cervical biopsies diagnosed at a single academic institution as "at least HSIL" or equivalent was 61%. The risk of EAC after "at least AIS" was 38%. The practice of diagnosing a subset of cervical biopsies as suspicious for invasion is widespread, yet little has been formally published on this topic. Knowledge of the risk of subsequent invasive carcinoma may be useful for clinical practice

at our institution, and a larger, multi-institutional study would be beneficial. We further sought to describe the morphologic patterns that prompt a diagnosis of “at least” and to correlate each with risk of invasion. For squamous lesions, the most common pattern was bands of HSIL with architectural complexity such as folding and looping; 71% of such biopsies showed subsequent invSCC. Regarding glandular lesions, patterns leading to a diagnosis of “at least AIS” included poor orientation and complex AIS (ex. glandular anastomosis) with 50% and 60% respectively showing subsequent invasion. These morphologic patterns likely stem from the knowledge that it is difficult, and sometimes impossible, to distinguish AIS from minimal Silva pattern A EAC. As Silva patterns integrate into clinical practice, understanding of the sometimes nebulous line between pattern A and AIS will be important.

631 Genetic Heterogeneity of Mullerian Carcinosarcomas Revealed by Molecular Profiling

Ju-Yoon Yoon[1], Fei Dong[1], Ursula Matulonis[2], Marisa Nucci[3], David Kolin[1]
[1]Brigham and Women's Hospital, Boston, MA, [2]Dana-Farber Cancer Institute, Boston, MA, [3]Brigham and Women's Hospital, Harvard Medical School, Boston, MA

Disclosures: Ju-Yoon Yoon: None; Fei Dong: None; Ursula Matulonis: None; Marisa Nucci: None; David Kolin: None

Background: Carcinosarcoma is a biphasic tumor defined by presence of malignant epithelial and mesenchymal components, the latter of which is thought to arise by epithelial mesenchymal transition (EMT) from the carcinomatous component. *TP53* gene mutations are found in most and are thought to be important driver of tumorigenesis. However, a minor subset are *TP53*-wildtype, and several studies have demonstrated relative genetic heterogeneity in these tumors.

Design: Carcinosarcomas (n=142) of the female genital tract which had undergone targeted molecular profiling were retrospectively identified, comprising 94 endometrial, 42 tubo-ovarian, 4 primary peritoneal, 1 endometriosis-associated, and 1 cervical. The NGS assay used hybrid capture to target 447 tumor suppressor and oncogenes for point mutations and copy number changes. Microsatellite status was assessed from sequencing data or mismatch repair (MMR) immunohistochemistry. High tumor mutational burden (TMB) was defined as ≥10 mutations/megabase (≥10/MB). Kaplan-Meier survival analyses were performed using the survfit R package.

Results: *TP53* mutations were identified in 120/142 cases (84.5%). TMBs ranged from 1.2/MB to 114.8/MB (median 6.1, n=141), and TMB was significantly higher in *TP53*-wildtype cases (Mann-Whitney p = 0.0064), with 9/21 (42.8%) cases having high TMB (vs. 13/120 in *TP53*-mutant). Among the *TP53*-wildtype cases, eight were predicted to harbor p53 dysfunction based on *MDM2* and/or *MDM4* copy gain. In the 14 tumors without predicted p53 dysfunction, *POLE* mutation, MMR deficiency, or epigenetic dysfunction (eg. *ARID1A* mutations) were predicted as potential driver events. Neither *TP53* status nor TMB was associated with differences in overall survival. Among those with high TMB and known MMR/MSI status, nine were noted to be MMR proficient and POLE wildtype. Besides high TMB (22/141), other genomic findings of potential therapeutic interest included MMR deficiency (3/86), *ERBB2* gene amplification (3/142) and *BRCA2* mutation (3/142).

Conclusions: Several genomic findings of potential therapeutic interest were identified, including high TMB, which was more common in *TP53*-wildtype cases. Genetic mechanisms for high TMB included MMR and POLE dysfunction, however some cases lack a clear mechanism. Perhaps related to this heterogeneity, high TMB was not prognostic in our cohort, even though MMR and POLE dysfunction have been associated with better survival in various GYN cancers.

632 Clear Cell Papillary Cystadenoma of the Ovary and Pelvic Cavity: A Clinicopathological, Immunohistochemical and Molecular Study of Five New Cases

Lin Yu[1], Meng-yuan Shao[2], Rui Bi[2], Xiaoyu Tu[3], Bin Chang[2], Qianming Bai[3], Xiaoyan Zhou[3], Wentao Yang[3]
[1]Fudan University Shanghai Cancer Center, Fudan University, Shanghai, China, [2]Fudan University Shanghai Cancer Center, Shanghai Medical College, Fudan University, Shanghai, China, [3]Fudan University Shanghai Cancer Center, Shanghai, China

Disclosures: Lin Yu: None; Meng-yuan Shao: None; Rui Bi: None; Xiaoyu Tu: None; Bin Chang: None; Qianming Bai: None; Xiaoyan Zhou: None; Wentao Yang: None

Background: Clear cell papillary cystadenoma (CCPC) is associated with von Hippel-Lindau disease (VHLD) but rarely involves the ovary. Until now, Only one case of ovarian CCPC has been reported in the English literature. Because of its rarity and unexpected occurrence in the ovary, the tumor is likely to be misdiagnosed

both clinically and pathologically. This diagnostic pitfall may lead to inappropriate treatment. We report five additional cases of CCPC primarily occurring in the ovary and pelvic cavity, in order to further characterize this rare but distinctive entity.

Design: The clinicopathological data of 5 cases of CCPC were collected; immunohistochemical staining, interphase fluorescence in situ hybridization (FISH), Sanger sequencing and next-generation sequencing (NGS) were performed.

Results: The tumors occurred in the ovary (n=4) and pelvic cavity (n=1) of adult women aged 29 to 57 years, with a mean age of 43.6 years. Preoperative duration ranged from 3 months to 2 years. Clinically, 4 tumors presented as pelvic masses with abdominal pain and discomfort in 2 cases; and another 1 tumor was detected accidentally by routine physical examination. The tumor size ranged from 4 to 9 cm (mean, 5.9 cm). Histologically, the tumor was mainly composed of complex broad to finely branching papillary structures. Their cores showed hyalinized or edematous, with rich vascular plexus and haemorrhage. The papillae were lined by a uniform cuboidal epithelium with round, centrally placed nuclei and clear or eosinophillic cytoplasm. No mitoses or atypia were identified in all 5 cases. Cases 2 and 3 had solid and tubular areas. Immunohistochemically, all tumors displayed coexpression of AE1/AE3,CK7, vimentin,CD10 and WT-1, with variable positivity for EMA(4/5), PAX8 (4/5),PAX2 (3/3),D2-40 (5/5) and CK5/6 (5/5). ER, PR, Napsin-A,HNF-1βand TTF1 were all negative. Ki-67 proliferation index was approximately 5%. Genetically, loss of heterozygosity at VHL gene was detected by interphase FISH in cases 5; Point mutation(C.445G>C: P.A 149 P) of exon 2 of VHL gene was found by Sanger sequencing and NGS in case 2. Five cases all underwent surgical excisions. Follow-up data (range, 1 to 41 mo; mean, 20.6 mo) showed all 5 patients had no recurrences and were alive without disease.

Table 1. Clinicopathological and molecular features of 5 cases of clear cell papillary cystadenoma

Case	Sex	Age	Location	Tumor size（cm）	Signs and symptoms	Duration	VHL disease	Others	Referring diagnosis	Treatment	Follow-up(m)	Alteration of VHL gene
1	F	39	Left ovary	NA	Pelvic mass with abdominal pain	NA	No	No	CCS	TC	NED,6	LOH-;No mutation of exon1,2,3
2	F	41	Left ovary	9	Pelvic mass	3 months	Cy(R-P),He(C)	Le(U)	CCS	TC	NED,38	Mutation(C.445G>C: P.A 149 P) of exon 2
3	F	52	Right ovary	4	Pelvic mass	2 years	Cy(R-L)	No	Epithelial tumor,unclassified	TAH-BSO+PL	NED,41	No mutation of exon1,2,3
4	F	57	Left ovary	6	Ovarian cysts revealed by physical examination	/	No	No	Adenocarcinoma	TC	NED,1	NA
5	F	29	Pelvic cavity	4.5	Pelvic mass,abdominal discomfort	6 months	No	Restless leg syndrome	Low-grade mesothelioma	TC	NED,17	LOH+

CCD indicates clear cell carcinoma;C,cerebellum;Cy,cysts;He,hemangioblastoma;L,liver;L,leiomyoma;NA,not available; NED,no evidence of disease;O,omentectomy;PL,pelvic lymphadencetomy;R,renal;RLS,Restless leg syndrome;TC,tumourectomy;TAH-BSO,total abdominal hysterectomy with bilateral salpingo-oophorectomy;U,uterus;VHL,Von Hippel Lindau disease;LOH,loss of heterozygosity.

Figure 1 - 632

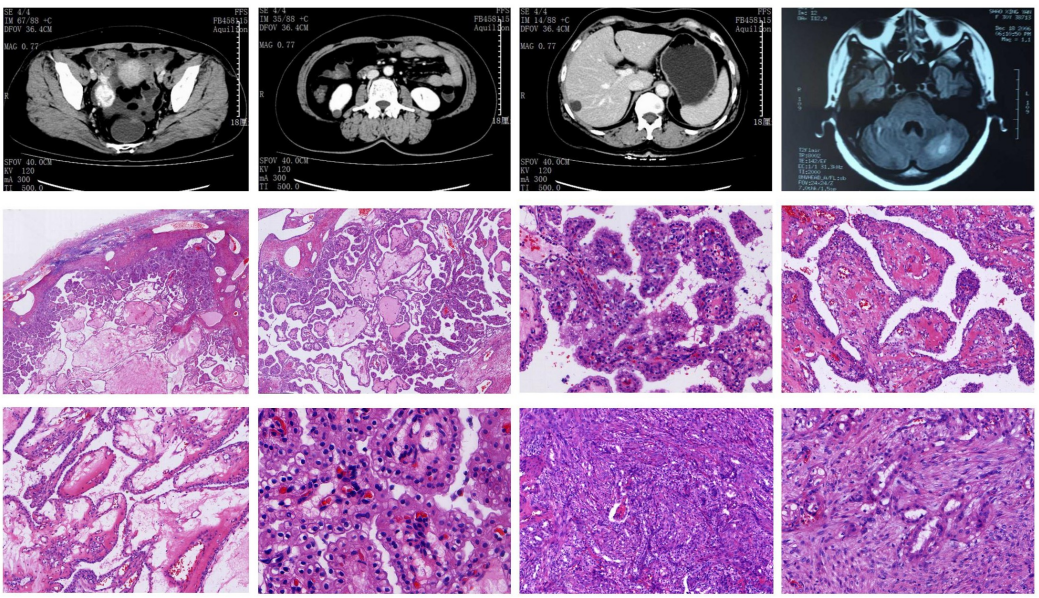

Figure 2 - 632

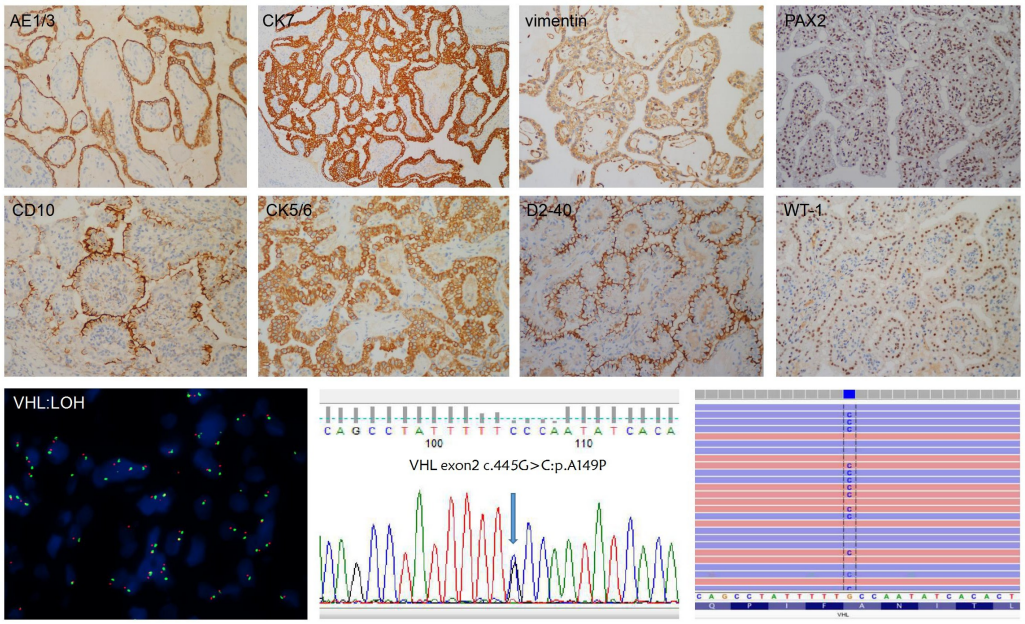

Conclusions: CCPC represents an uncommon neoplasm associated with VHLD, which is characteristic of complex tubulopapillary architecture lined by a uniform cuboidal epithelium, with characteristic bland clear or eosinophillic cells and distinctive sub-epithelial vascular pattern. It can occur in the ovary, although very rarely. Familiarity with its clinicopathological, immunohistochemical and molecular features is helpful in avoiding confusion with a variety of ovarian epithelial tumors with overlapping features, especially clear cell carcinoma.

633 Tumor Budding Activity Is an Independent Prognostic Factor in Squamous Cell Carcinoma of the Vulva

Somaye Zare[1], Andreas Ciscato[1], Oluwole Fadare[2]
[1]University of California, San Diego, La Jolla, CA, [2]UC San Diego School of Medicine, La Jolla, CA

Disclosures: Somaye Zare: None; Andreas Ciscato: None; Oluwole Fadare: None

Background: Tumor budding is recognized as a potential prognostic factor in carcinomas from several anatomic sites. Tumor budding is defined as clusters of ≤5 tumor cells that appear to be detached from the invasive tumoral front and which infiltrate into surrounding stroma. In this study, we evaluate the prognostic value of tumor budding in a single-institutional cohort of squamous cell carcinoma (SCC) of the vulva.

Design: Our cohort included 64 cases of surgically excised vulvar SCC (TNM stage pT1b or higher) with clinical follow-up whose slides were available for review. Tumor budding activity were assessed in 10 HPFs, resulting in each case being classified into one of 3 groups: no budding, low budding activity (1 to 14 foci), and high budding activity (≥15 foci). In addition, a variety of other histomorphologic parameters were reviewed and correlated with clinicopathologic factors and outcome data. In a subset of 60 cases with evaluable material and definitive results, tumors were stratified into HPV-associated (n=31) and HPV-independent (n=29) subgroups based on immunohistochemical studies for p16 and p53.

Results: High tumor budding was strongly associated with poor prognosis, including reduced overall, disease-specific, and disease-free survival (p<.01 for all). Multivariate analysis showed that the prognostic significance of tumor budding was independent of TNM stage and p53 status, with a hazard ratio of 1.2 for low tumor budding and 6.7 for high tumor budding, in comparison to tumors with no budding activity (p=.004). Among the other potentially prognostic factors, higher stage, advanced age, and p53 mutation-type staining were significantly associated with decreased overall survival (p<.05). Tumors with mutant p53 status had higher budding activity compared to HPV-associated cases (p< .001). The co-existence of high tumor budding and p53 mutation-type staining defined a

subset with the worst outcomes relative to other subgroupings (p= .001). Other features, including keratinization, nuclear size, and mitotic count were not significantly associated with survival.

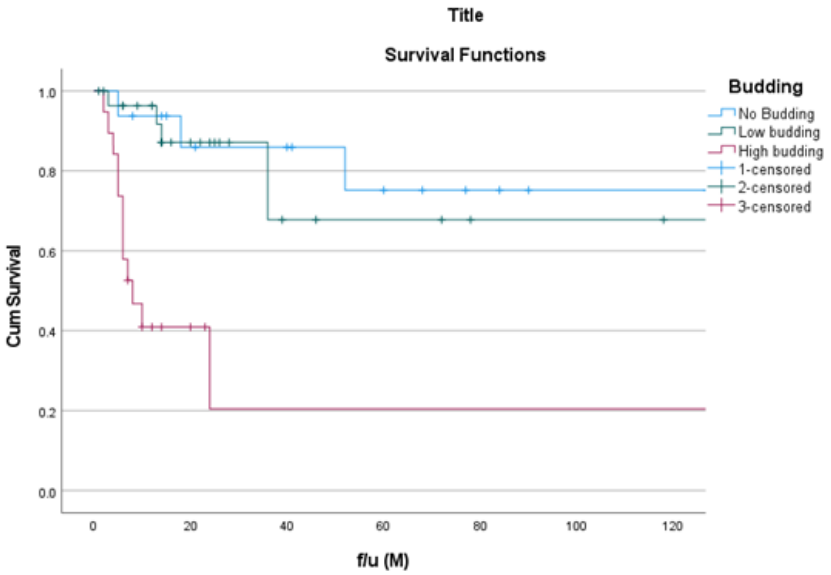

Conclusions: Tumor budding is an independent prognostic indicator in vulvar SCC, with high budding activity being associated with worse outcomes. Vulvar SCCs with p53 mutation-type staining show more budding activity compared to HPV- associated tumors, and the concurrent presence of p53 mutation-type staining and high budding activity is associated with notably poor outcomes.

634 Necrosis of Uncertain Type Confers a Low Rate of Recurrence in Uterine Smooth Muscle Neoplasms

Roman Zyla[1], Gulisa Turashvili[2]
[1]University of Toronto, Toronto, Canada, [2]Mount Sinai Hospital, University of Toronto, Toronto, Canada

Disclosures: Roman Zyla: None; Gulisa Turashvili: None

Background: Necrosis is a common finding in uterine smooth muscle neoplasms. While infarct-type necrosis is often identified in leiomyomas, the presence of coagulative tumor cell necrosis or necrosis of uncertain type warrants classification as either smooth muscle neoplasm of uncertain malignant potential (STUMP) or leiomyosarcoma, depending on the presence or absence of other histologic features of malignancy. However, the prognostic significance of necrosis of uncertain type or coagulative necrosis in otherwise benign-appearing uterine smooth muscle neoplasms remains controversial.

Design: Archival cases of uterine smooth muscle tumors with necrosis (excluding leiomyosarcomas) were reviewed retrospectively. The type of necrosis was classified as infarct-type, uncertain-type or coagulative. Parameters used to categorize necrosis included the presence or absence of a hyaline/inflammatory border, the retention of 'ghost' nuclei, the presence of significant inflammation and preservation of neoplastic cells around vessels in the necrotic focus. Tumor size, cytologic atypia, maximal mitotic rate, tumor border and radiologic tumor appearance were also recorded. Post-operative clinical data was reviewed to identify patients experiencing tumor recurrence or metastasis.

Results: A total of 34 patients were identified, with a mean age of 41 years (range 29-57). The mean follow-up time in the cohort was 25 months (range 0-233). On initial diagnosis, 26 tumors were diagnosed as leiomyoma and 8 as STUMP. On histologic review, necrosis was classified as infarct-type in 26 cases, uncertain-type in 6 cases and coagulative in 2 cases. The mean tumor size was 8.3 cm (range 2.6-18). All tumors had at most mild cytologic atypia and a mean mitotic rate of 1.6 per 10 high-powered fields (range 0-13). All tumors in which the borders could

be histologically assessed were well-circumscribed. Where available, the radiologic tumor appearance was in keeping with a benign process in 11 patients and suspicious in 1 patient. Only 1 patient experienced possible recurrence at 173 months; the tumor was initially diagnosed as leiomyoma with 'red degeneration' but the necrosis was re-classified as being of uncertain type. The recurrent tumor was histologically distinct and while it was positive for smooth muscle actin by immunohistochemistry, definitive lineage classification could not be made.

Conclusions: In the absence of other histologic features of malignancy, necrosis of uncertain type or unequivocal coagulative necrosis alone confers a low rate of recurrence in uterine smooth muscle tumors. Further research is needed to assess the optimal follow-up and treatment of tumors in which these types of necrosis are the sole feature suggestive of malignant potential.